TECHNICAL MEMORANDUM

Stantec **FORMATION ENVIRONMENTAL** **M2 Resource Consulting**

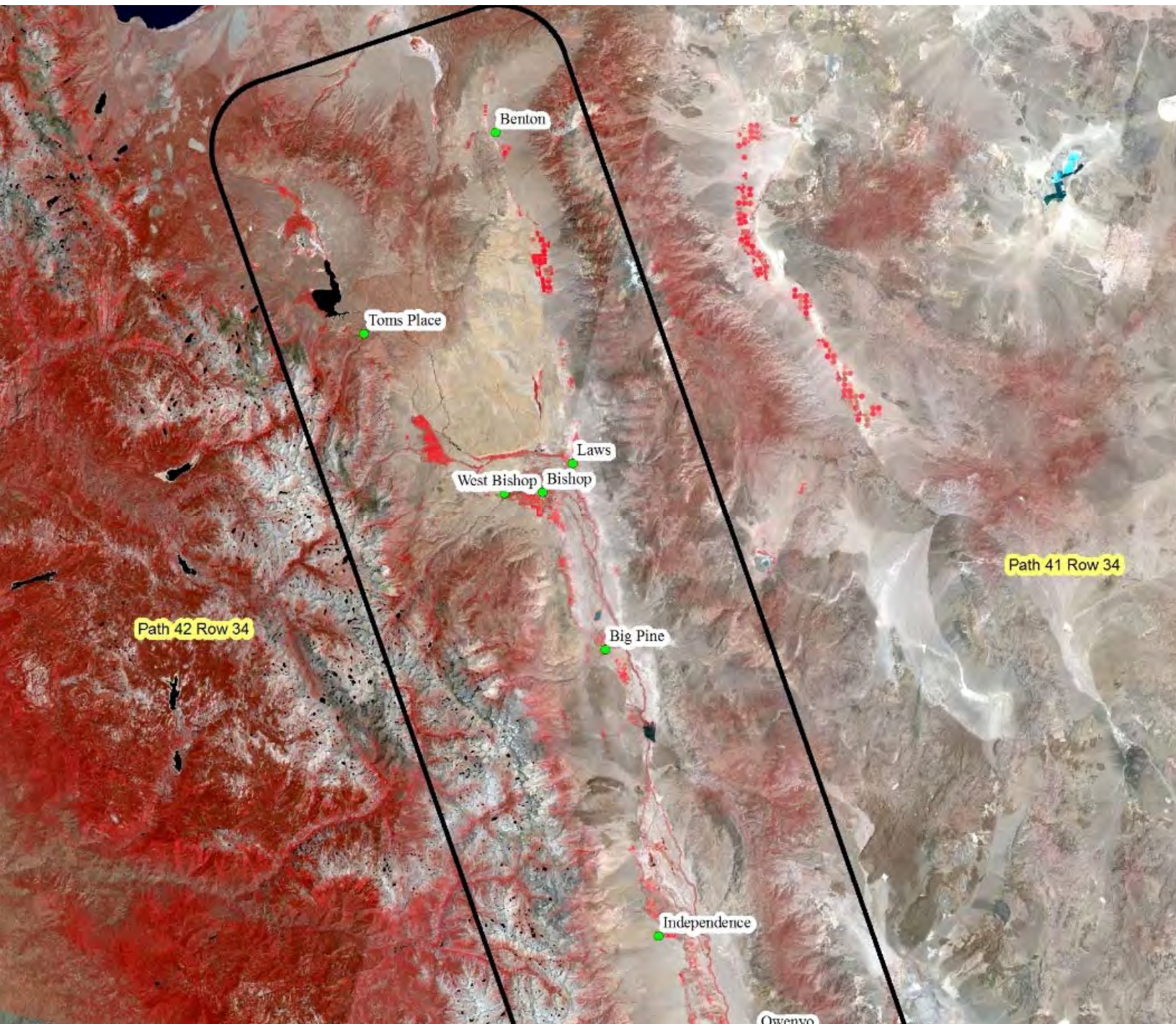|	
Title:	Final Report on Remote Sensing Pilot Project Implementation
Project:	Task Order 008 – Remote Sensing Pilot Project Implementation
Client:	Los Angeles Department of Water and Power
Date:	March 2018

LADWP

TABLE OF CONTENTS

LIST OF TABLES

LIST OF ACRONYMS

Acronym	Definition
AF/yr	Acre-Feet per Year
DSS	Decision Support System
ET	Evapotranspiration
ETa	Actual Evapotranspiration
GIS	Geographical Information System
ICWD	Inyo County Water Department
LADWP	Los Angeles Department of Water & Power
LAI	Leaf Area Index
TM	Technical Memorandum

LIST OF APPENDICES

A – TM 8.1 - Imagery Download, Preparation, and Preprocessing

B – TM 8.2 - Leaf Area Index-Image Analysis

C – TM 8.3.1 – Evapotranspiration Mapping

D – TM 8.3.2 - Integration of Spatial Evapotranspiration into the Bishop/Laws Groundwater Model

E – TM 8.3.3 - Estimation of Historical ETa from Agriculture in the Chalfant and Benton Valleys

1.0   BACKGROUND AND INTRODUCTION

Since the 1990s, Los Angeles Department of Water and Power (LADWP) resource specialists and vegetation scientists from the Inyo County Water Department (ICWD) have been monitoring vegetation in the Owens Valley in accordance with the Inyo/LA Long-Term Water Agreement (1991). This monitoring is used to guide management of groundwater pumping and involves line point transects and other labor-intensive field methods.

Recently, LADWP has employed remote sensing as a tool to evaluate groundwater- and surface water-dependent vegetation on and around Owens Lake in the southern portion of the Owens Valley. Remote sensing technology provides significant advantages, including the ability to evaluate large geographic areas at relatively low cost, compare historical images with current conditions, and utilize standardized algorithms that are not affected by subjective interpretation. At the same time, the type and quality of images available, and the technology for processing those images is advancing at a rapid pace.

For these reasons, there is a need to evaluate the possibility of augmenting or even potentially replacing current methods of vegetation monitoring in the Owens Valley using remote sensing technology. Additionally, there is the possibility that remote sensing can be used to improve existing groundwater models associated with individual well fields, especially in the simulation of evapotranspiration.

The purpose of the Remote Sensing Pilot Project (Task Order 008 of Agreement No. 47381-6) was to evaluate the applicability of remote sensing both for improvement of existing groundwater modeling and potentially monitoring vegetation associated with the Inyo/LA Long-Term Water Agreement (1991). This Final Report represents the final deliverable for the project.

As conceived in the Remote Sensing Work Plan (MWH, 2016), key findings from the Pilot Project were documented in brief periodic technical memoranda (TM). These TMs were not intended to contain extensive introductory material, but instead focused on results from individual work areas. A listing of the key TMs delivered is summarized in **Table 1**, and a summary of each included in this Final Report. In addition, each TM is included as an appendix to this Final Report.

2.0   ORGANIZATION OF FINAL REPORT

This Final Report is organized as follows:

- Section 1 – Introduction and Background
- Section 2 – Organization of Final Report
- Section 3 – Summary of Technical Memoranda
- Section 4 – Summary and Recommendations

Table 1
Summary of Technical Memoranda

Task	TM Number	Subject	Date	Appendix
1 - Imagery Download, Preparation, and Preprocessing	TM 8.1	Imagery Download, Preparation, and Preprocessing	Jan. 2017	A
2 - Leaf Area Index Image Analysis	TM 8.2	Leaf Area Index-Image Analysis	May 2017	B
3 - Evapotranspiration (ET) Mapping and Options for Integration	TM 8.3.1	Evapotranspiration Mapping	May 2017	C
	TM 8.3.2	Integration of Spatial Evapotranspiration into the Bishop/Laws Groundwater Model	March 2018	D
	TM 8.3.3	Estimation of Historical ETa from Agriculture in the Chalfant and Benton Valleys	March 2018	E

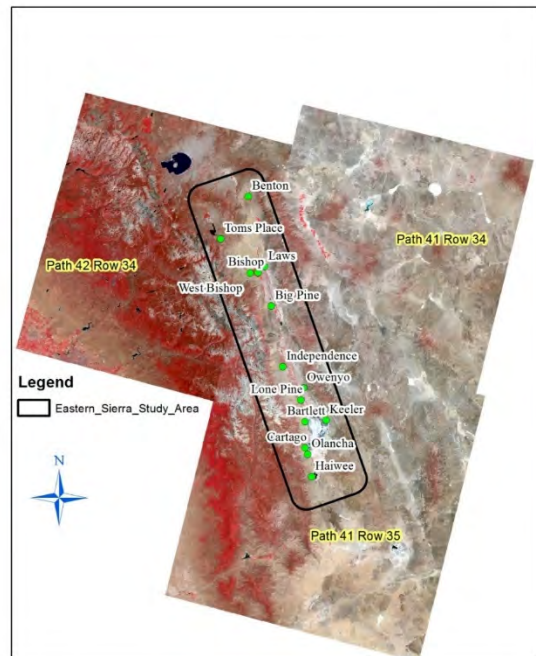## 3.0   SUMMARY OF TECHNICAL MEMORANDA

A summary of each TM is provided in this section.

3.1 TM 8.1 - Imagery Download, Preparation, and Preprocessing

The objective of this TM and associated work was to conduct imagery downloading and preprocessing, which is a prerequisite for performing any remote sensing analysis. In turn, this imagery provided the base dataset for analysis of vegetation trends within the pilot study area.

Satellite data from the Landsat program was used, which provides accurate, routine, and repeat measurements of Earth's land cover[1]. Landsat imagery from 1985 to 2016 (32 years) were acquired; details of processing methodologies and data products used were documented in this TM.


The Landsat images identified as "Good" from the data quality assessment were imported into an ESRI ArcGIS image mosaic dataset. The acquisition date and other metadata (scene, band, sensor information, derivative product calculation, etc.) are documented. The mosaic dataset allows analysts to quickly scroll through the historical Landsat archive and derivative products sequentially for quick spatial-temporal trend analysis. This tool only works on an ArcGIS software platform and requires accompanying imagery dataset. The image quality assessment tool and all the processed Landsat dataset are

---

[1] More details on the Landsat program, onboard sensors and data products are available at https://landsat.usgs.gov/

available to the project team. The imagery database developed is approximately 8 TB and was used for developing Leaf Area Index (LAI) and Evapotranspiration (ET).

3.2 TM 8.2 - Leaf Area Index-Image Analysis
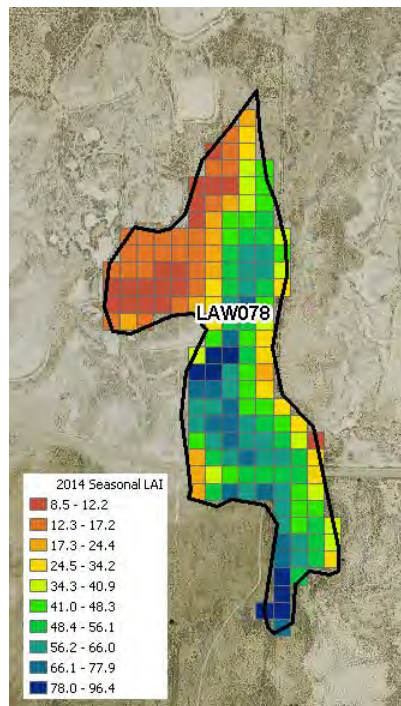
TM 8.2 describes the steps involved in the development and validation of long term satellite-derived LAI dataset. The objective of this work was to analyze temporal trends of LAI to quantify the historical variability of LAI per pixel and use this information to isolate relevant change as compared to the baseline period (1984 to 1987). All pre-processed Landsat imagery from TM 8.1 was used in the canopy reflectance model to build a time series LAI dataset.

Over 30+ years of observed and estimated dataset of vegetation cover and LAI was analyzed. Comparisons show strong relationship between satellite-derived LAI dataset and ground observations of vegetation cover.

The long term (1985-2016) LAI dataset development from canopy reflectance model using Landsat imagery was completed. The LADWP and ICWD vegetation cover monitoring dataset collected in the Owens Valley over the last 30+ years was processed and used for comparison against the developed LAI dataset. Parcel level comparisons show excellent agreement between the two datasets. These results indicate that remote sensing techniques for estimating LAI is an effective tool for spatial and temporal monitoring of vegetation across Owens Valley.

3.3 TM 8.3.1 - Evapotranspiration Mapping

TM 8.3 describes the steps involved in the development of remote sensing based actual evapotranspiration (ETa) dataset and its validation. Validation of spatial ETa estimates against eddy covariance data shows good agreement. Results suggest that the remote sensing-based spatial ETa mapping has the potential to be developed as an operational tool for managing water resource and monitoring vegetation in the groundwater-dependent ecosystem of Owens Valley.
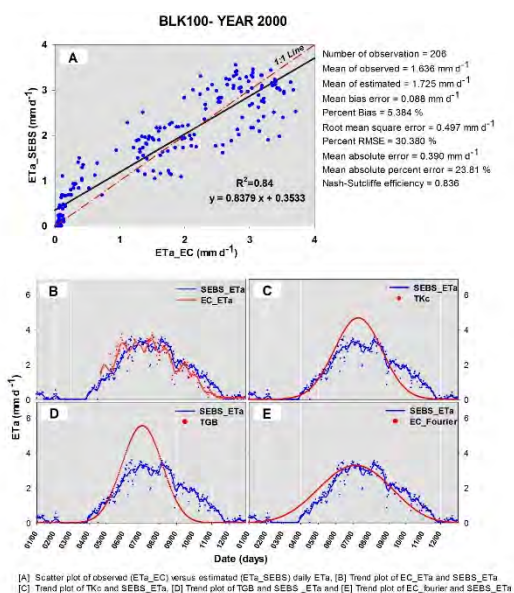
3.4 TM 8.3.2 - Integration of Spatial Evapotranspiration into the Bishop/Laws Groundwater Model
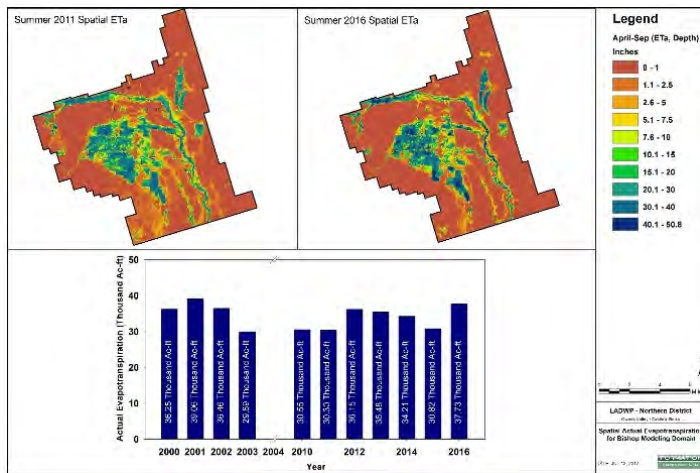
The depth to groundwater at 34 monitoring well sites was compared to ETa data from remote sensing for the surrounding 100-meter radius circle around the monitoring well. Results from this work demonstrate that the strength and behavior of the trend is dependent on complex interactions. This includes (but is not limited to) well location, groundwater depth, plant community composition, soil profile characteristics, precipitation, runoff, and adjacency to irrigated land, rivers, intermittent streams, and irrigation ditches. Results from this work indicate the following apparent time series trends:

- **Connected Trends:** A connected trend was defined (for this analysis) as a consistent qualitative relationship where ETa was connected to summer depth to groundwater measurements. Specifically, as groundwater depth decreases, there is a corresponding increase in ETa and vice versa. This trend was apparent for 14 of the 34 (41%) wells evaluated.

- **Disconnected Trends:** A disconnected trend was defined as a relationship where ETa was inversely related to summer depth to groundwater measurements. Specifically, as groundwater depth increased, there was a corresponding increase or stabilization of ETa and plant biomass. This relationship was most prevalent for wells near irrigated agriculture and irrigated urban areas and occurred in 5 of the 34 wells (15%) with valid time series. In these conditions, vegetation growth and ETa is unaffected (due to irrigation) from changes in depth to groundwater.

- **No Trends:** Several wells exhibited no relationship with depth to groundwater and ETa. These wells were in barren or sparsely-vegetated upland areas where the depth to groundwater was greater than 25 feet (outside of the root zone). Seasonal summer ETa was generally 2 inches or less, indicating minimal vegetation on the landscape.

Factors such as plant communities, soil profile characteristics, applied water, precipitation events, runoff magnitude and proximity to streams are some of the external factor besides the well characteristics, impacting the ETa and groundwater trends.

A more quantitative relationship between ETa and groundwater depth was also evaluated for the 34 wells in the Bishop/Laws model domain using regression analysis. The analysis shows apparent relationship between ETa and groundwater depth; however, the relationship is by no means consistent. A method of analyzing the regression of monthly ETa data was developed to provide suggestions for the variables of maximum ET, maximum ET elevation, and extinction depth using the MODFLOW ET package. It is recommended that modeling in the Bishop/Laws area be initiated using these variables, modifying them as necessary during calibration efforts. Future studies focusing on quantifying this relationship should use a high-resolution dataset and further investigate the interactions of various factors.

3.5 TM 8.3.3 - Estimation of Historical ETa from Agriculture in the Chalfant, and Benton Valleys
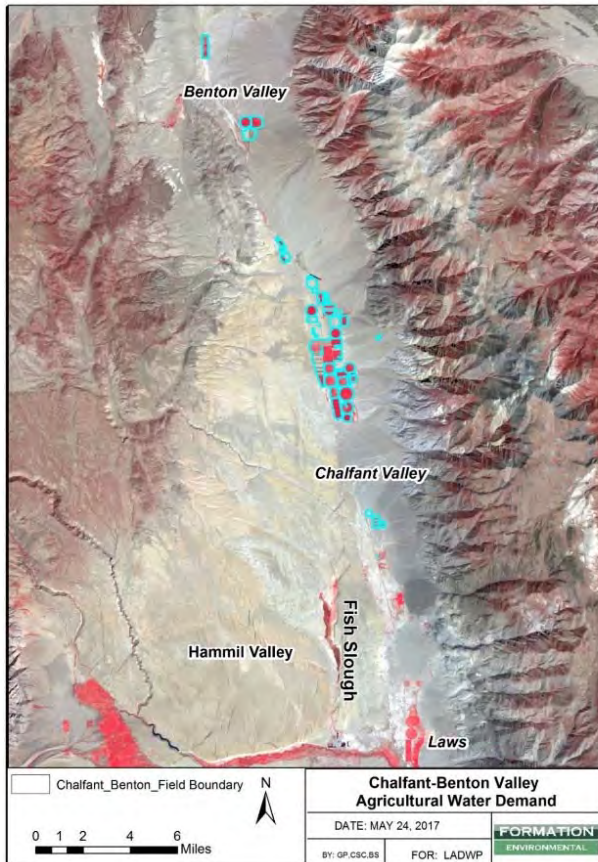
Remote sensing (Landsat) was used to estimate the total agricultural demands in the Chalfant and Benton Valleys during the times in which ETa are currently available from Landsat data. These data were compared to flow data from Fish Slough to evaluate a potential relationship between pumping in Chalfant/Benton Valleys, and the observed decrease in flows over time.

Fish Slough, located to the north of the Bishop/Laws model boundary, southwest of Chalfant Valley, and east of Hammil Valley, is an area of groundwater discharge with sensitive habitat and critical environmental concern. There has been a long-term reduction in flow at Fish Slough from 6,000 – 7,000 acre-feet per year (AF/yr) in the 1960's to 3,000 AF/yr currently. As a result, there is a need to identify the reason for reduced flows (i.e., pumping from the Bishop/Laws area, pumping in the Chalfant area, or some other factor).

The purpose of this subtask was to investigate one potential reason for reduced flows at Fish Slough through time in support of the Bishop/Laws model update being performed for LADWP. It is hypothesized that the groundwater withdrawal in Chalfant and Benton Valleys for agriculture consumptive use has contributed to the reduction in flow at Fish Slough.

This analysis shows that consumptive use by agriculture is a significant and increasing component of the water budget in the Chalfant/Benton Valleys, which could easily result in decreased flows to Fish Slough. It also suggests that groundwater flow through the alluvium north of Laws into the Owens Valley has decreased through time. Results of this analysis are being incorporated into the Bishop/Laws model update, such that flow on the northern boundary of the model is not necessarily fixed, but may also decrease with time.

4.0   SUMMARY AND RECOMMENDATIONS

Leaf Area Index. The LAI (leaf area index) dataset developed from remote sensing provided exhaustive information on vegetation dynamics across Owens Valley from 1985 through present. The time period from 1985 also marks the starting of vegetation monitoring by LADWP and ICWD. A comparison of the observed vegetation cover with the remote sensing-LAI dataset indicated that remote sensing techniques can be effective in capturing the spatial and temporal dynamics of vegetation growth across Owens Valley. Ground truth efforts conducted to validate LAI showed excellent performance of the modeled/estimated LAI value. As a next step to this task, it is recommended that:

1. The observed vegetation cover data collected by LADWP and ICWD should be quality checked and organized in a GIS (Geographical Information System) framework for easy access and analysis.

2. The developed remote sensing-LAI dataset should be compiled into a GIS framework and hosted through a web/local application for easy viewing, querying and downloading.

3. A rigorous validation of the remote sensing-LAI dataset by (i) ground truth verification and (ii) generating peer reviewed scientific publication should be performed. These are critical steps in the adoption of this technology.

4. Based on the above, a decision support system could be built utilizing developed data that can be used as a tool to inform the performance of vegetation across the Owens Valley and its relationship to annual pumping plans.

Evapotranspiration. Evapotranspiration is used as an indicator in the Green Book for assessing the vegetation type that leads to larger decisions on pump operations. The ETa (Actual Evapotranspiration) dataset developed for the two discrete time periods, 2000 through 2003 and 2010 through 2016, were used for the validation study, and options were explored for its integration into various work-flows. The validation study indicated good agreement, and the depth to groundwater and ETa relationship showed promising trends. The ETa dataset was found to be an excellent tool for monitoring agricultural water use in Chalfant and Benton Valleys which in turn could be used to study water balance. As next steps to this task it is recommended that:

1. An ETa dataset for the remaining 20 years should be developed to have a complete and continuous data from 1985.

2. Additional focused studies should be conducted to investigate the depth to groundwater and ETa relationship in selected areas.

3. A queryable platform should be built for accessing bi-weekly, monthly, bi-annual and yearly raster layers of ETa.

Based on the preceding recommendations, the following tasks are recommended for the next phase of remote sensing work in the Owens Valley.

Task 1: Review and expand the Remote Sensing - LAI dataset

1. Develop a concept document for review by an external expert on the approach used for ground truth and validation of the remote sensing LAI dataset.

2. Develop a viewer or dashboard for viewing and querying the LAI dataset.

3. As mandated in the Green Book a GIS framework would be developed and populated with observed datasets. This would be integrated with the viewer/dashboard (see next task) dynamic comparison and analysis. Collaborative effort with all stakeholders would be required to bring quality checked data into the framework.

4. Expand ground truth approach to all the LADWP permanent point frame transects (35 transects).

5. Prepare peer-reviewed scientific manuscripts for publications in journals.

Task 2: Expand and Analyze the Remote Sensing - ETa dataset

1. Analyze depth-to-groundwater and ETa relationship for selected wells across Owens valley

2. Develop ETa dataset for the remaining 20 years starting from 1985 and integrate all ETa outputs into the view or dashboard application.

3. Provide support to groundwater modeling team for integrating ETa into their work flow.

4. Develop a manuscript on ETa validation study for publication in peer reviewed journal.

Task 3: Develop a Decision Support System (DSS)

A large amount of spatial and tabular datasets was developed as part of this project. These datasets could be converted into information that can be used for decision making. The DSS would be developed to analyze and rate the performance of the ecosystem. A set of indices based on LAI and ET would be developed to compare the performance of vegetation against baseline observations. The viewer/dashboard discussed in Tasks 1 and 2 and the DSS framework discussed herein, would be developed as a secure web application available for authorized users only.

APPENDIX A

TM 8.1 - Imagery Download, Preparation, and Preprocessing

TECHNICAL MEMORANDUM

Title: TM 8.1 – Imagery Download, Preparation, and Preprocessing

Project: Task Order 008 – Remote Sensing Pilot Project Implementation

Client: Los Angeles Department of Water and Power
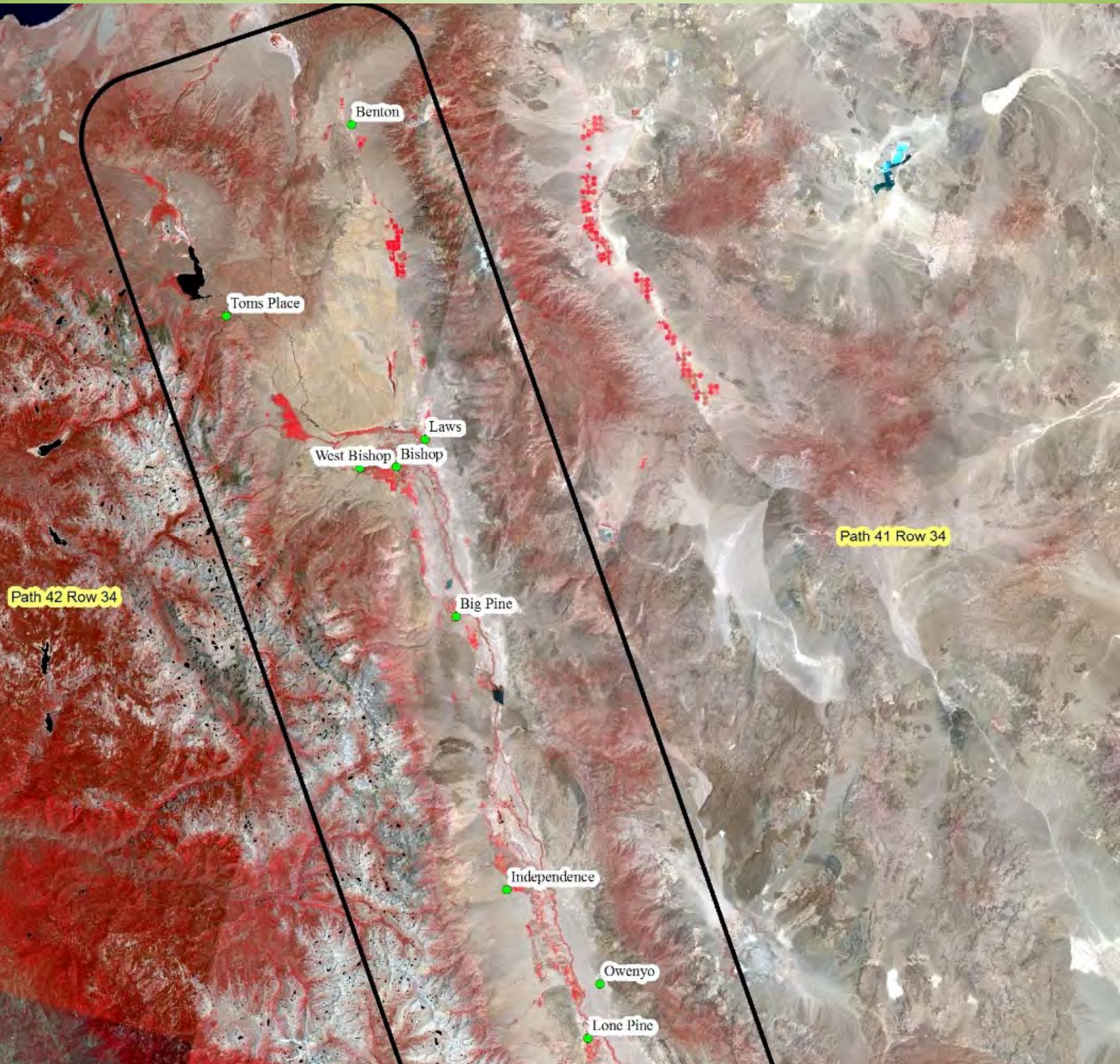
Date: January 17, 2017

TABLE OF CONTENTS

LIST OF FIGURES

LIST OF TABLES

ACRONYMS / ABBREVIATIONS

AOI	Area of Interest
CDR	Landsat Surface Reflectance Climate Data Records
CSV	Comma Separated Value
DN	Digital Number
ETa	Evapotranspiration actual
ESRI	Environmental Systems Research Institute
FCC	False Color Composite
ICWD	Inyo County Water Department
LADWP	Los Angeles Department of Water and Power
LAI	Leaf Area Index
LEDAPS	Landsat Ecosystem Disturbance Adaptive Processing System
MODIS	Moderate Resolution Imaging Spectroradiometer
NASA	National Aeronautics and Space Administration
REGFLEC	REGularized canopy reFLECtance
SEBS	Surface Energy Balance System
TB	Terabytes
TM	Technical Memorandum
USGS	United States Geological Survey
WRS	World Reference System

1.0   INTRODUCTION

This Technical Memorandum (TM) has been prepared in support of the Remote Sensing Pilot Project Implementation for the Owens Valley area. This TM represents the deliverable for Subtask 008.1 of Task Order 008 of Agreement No. 47381-6. As conceived in the Work Plan for this effort (MWH, 2016), key findings from the Pilot Project are documented in brief periodic TMs. These TMs are not intended to contain extensive introductory material, but are intended instead to focus on the results of specific portions of the work. A listing of the key TMs associated with this work is summarized in **Table 1**, with the highlighted TM 1.1 presented in this document.

Table 1
Summary of Technical Memoranda

Task	TM Number	Subject
1 - Imagery Download, Preparation, and Preprocessing	TM 8.1	Imagery, cloud screening results, and radiometrically corrected imagery
2 - Leaf Area Index Image Analysis	TM 8.2	Leaf area index (LAI) image analysis, comparison of LADWP and ICWD historical data with remote sensing results, sampling scheme for collecting ground truth data
3 - Evapotranspiration (ET) Mapping and Options for Integration	TM 8.3.1	Surface Energy Balance System (SEBS) actual Evapotranspiration (Eta) delivery, SEBS ET development and validation
	TM 8.3.2	Integration of Spatial ETa into the Bishop/Laws groundwater model
	TM 8.3.3	Estimation of historical ETa from agriculture in the Chalfant, Hammil, and Benton Valleys
	TM 8.3.4	Evaluation of existing northern boundary conditions

2.0   PURPOSE AND OBJECTIVES OF TM

As part of water resources and vegetation management related to the Inyo/LA Water Agreement, both the Los Angeles Department of Water and Power (LADWP) and the Inyo County Water Department (ICWD) conduct vegetation monitoring in the Owens Valley. This type of monitoring began in 1985 and has continued to present day. The overarching purpose of the current work is to evaluate the possibility of augmenting or even potentially replacing current methods of vegetation monitoring in the Owens Valley using remote sensing technology. The objective of Task 8.1 was to conduct imagery downloading and preprocessing, which is a prerequisite for performing any remote sensing analysis. In turn, this imagery will provide the base dataset for analysis of vegetation trends within the pilot study area (Tasks 2 and 3).

3.0   SUMMARY OF WORK CONDUCTED

For this task, satellite data from the Landsat program was used, which provides accurate, routine, and repeat measurements of Earth's land cover[1]. Landsat 5, 7 and 8 satellites collect data following a near-polar sun synchronous orbit on the world reference system (WRS-2). Each satellite has a 16-day revisit cycle; however, for the majority of the study duration, at least two satellites were available with orbits offset to provide an 8-day repeat coverage. Landsat imagery from 1985 to 2016 (32 years) were acquired; details of processing methodologies and data products used are documented in this TM.

Landsat imagery for Path 41 Row 34, Path 41 Row 35, and Path 42 Row 34 (Figure 1) were acquired from the U.S. Geological Survey (USGS) data archive (https://earthexplorer.usgs.gov/). Since the data acquisition was started in November 2016, only imagery from January 1985 until October 2016 was considered in the acquisition. Imagery from November to December 2016 will be acquired in later phases of this project. The acquired imagery product included Landsat Surface Reflectance Climate Data Records (CDR). CDRs are high level Landsat data products that support land surface change studies. This is an atmospherically corrected surface reflectance product generated by USGS using Landsat Ecosystem Disturbance Adaptive Processing System (LEDAPS) software developed by NASA, which applies Moderate Resolution Imaging Spectroradiometer (MODIS) atmospheric correction routines to Landsat Level-1 scenes. Landsat Level-1 standard data products were also acquired, these are processed to standard parameters, and distributed as scaled and calibrated digital numbers (DN). The DN's can be scaled to absolutely calibrated radiance or reflectance values using metadata distributed with the product. Three (3) Landsat scenes were required to completely cover the study area. A total of 5,990 images were acquired which includes 2995 CDR product and an equal number of Level-1 product, occupying approximately 8 TB of disk space. Figure 2 shows the number of images available for each path-row of Landsat satellites during the study period.

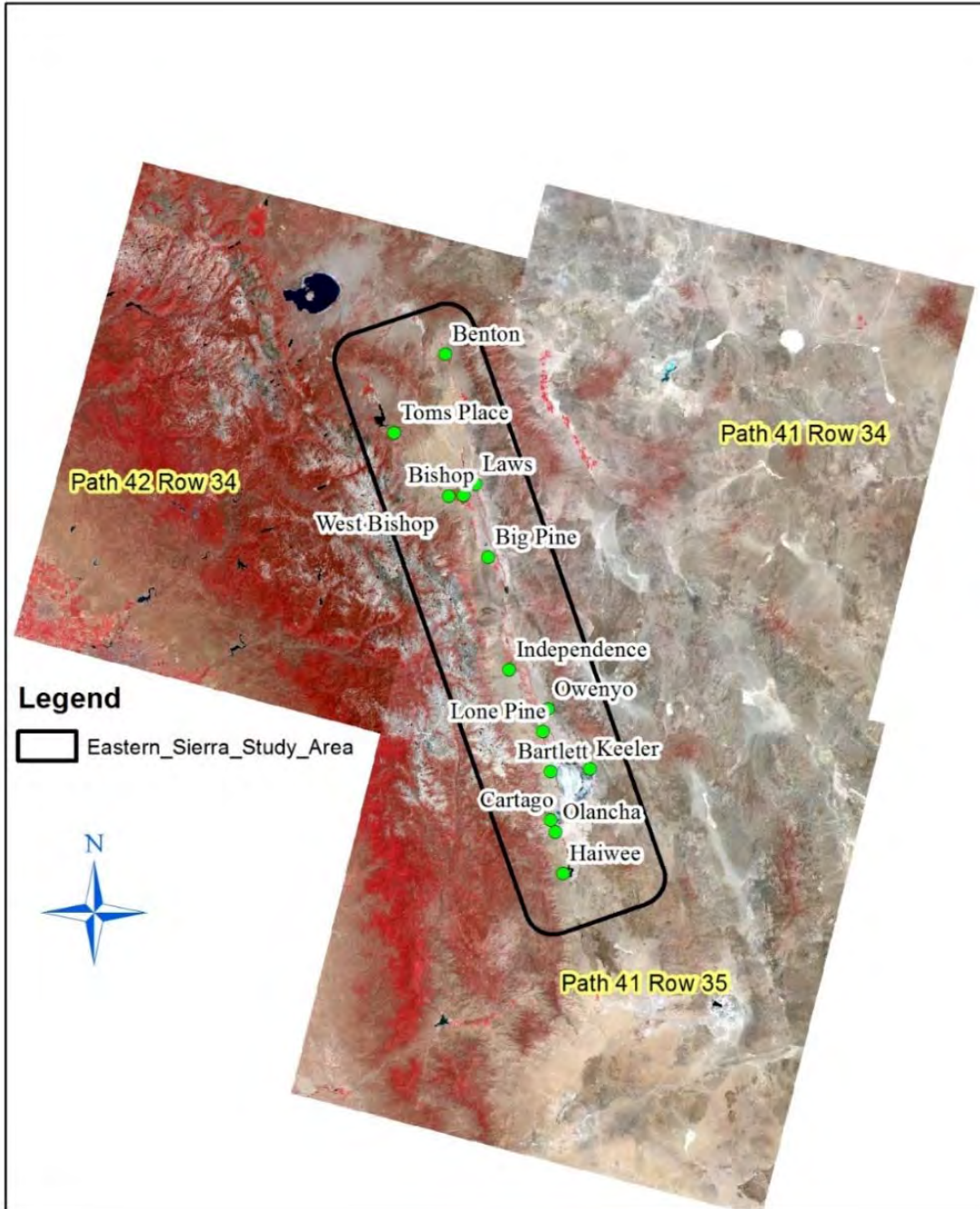[1] More details on the Landsat program, onboard sensors and data products are available at https://landsat.usgs.gov/

Figure 1
Landsat Scenes Path-Row 41-35, 42-34, and 41-34 False Color Composite Showing the Study Area in the Highlighted Boundary
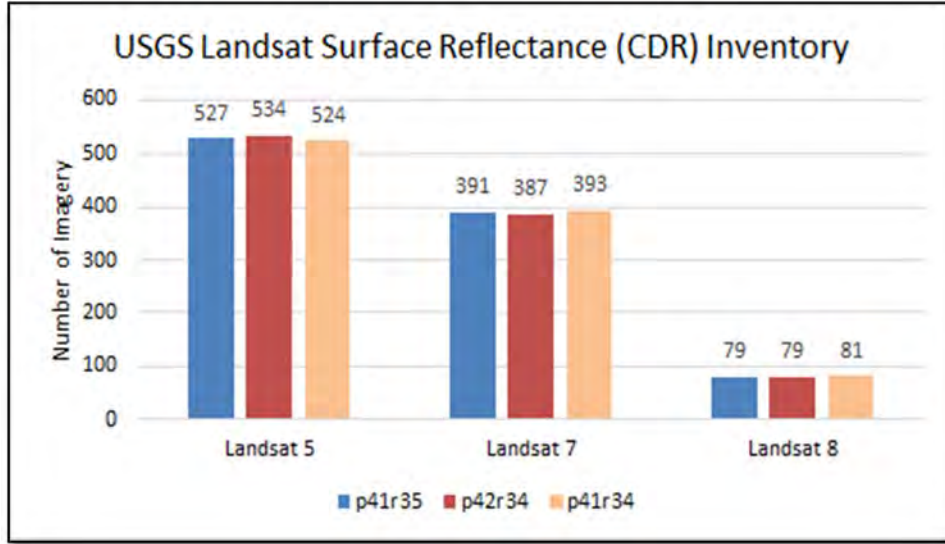
Figure 2
Available Imagery Dataset from Landsat Program during 1982 to 2016

All images were preprocessed and prepared for the analysis. The preprocessing included data uncompressing, data sub-setting, data scaling and data quality assessment. An image quality assessment tool was developed using Microsoft Access (Figure 3). This tool provided an efficient and accurate way to access the large imagery database and perform visual inspection for presence of clouds, snow, saturated pixels, spatial shifting and any other defects. The quality of each scene was tagged and stored in an Access database; this database could be exported as CSV or excel file for further analysis and decision making.
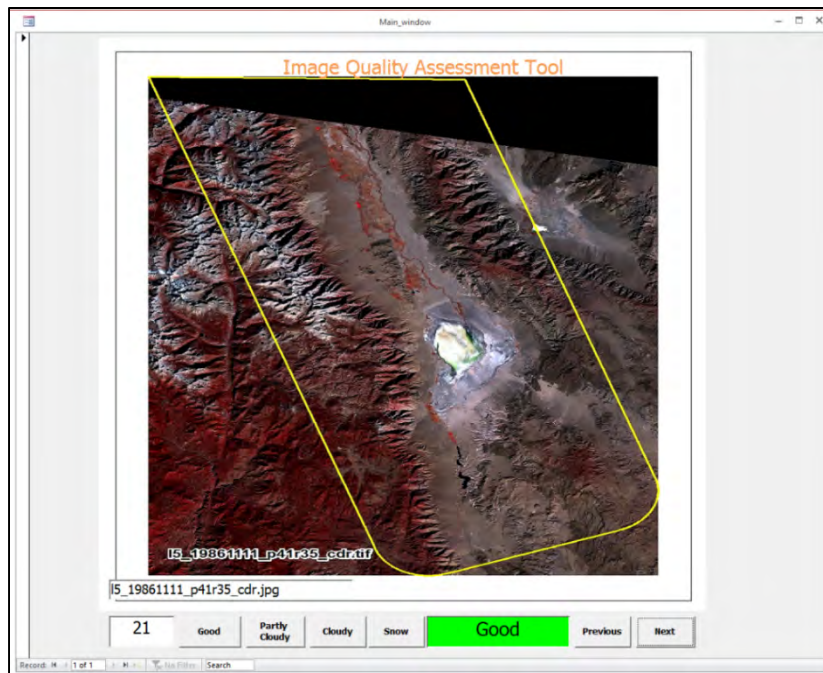
Figure 3
Image Quality Assessment Tool

Images were tagged based on presence of cloud, haze, cloud shadow and saturated pixels. An example of the various criteria used for tagging the images in shown in Figure 4. Of the total 2,995 acquired CDR images, 1,727 images were identified as good for analysis. These images had no cloud cover, haze, cloud shadow, geospatial shift and distorted pixels within the Area of Interest (AOI). The screening performed using the CDR product is applicable for the Level 1 data products also. Figure 5 shows the final tally on imagery quality after screening for each path-row and for the different Landsat satellites.

Obscured by thin layer of haze

Obscured by thick layer of clouds.

Obscured by cloud, haze and shadow

Image defect detected
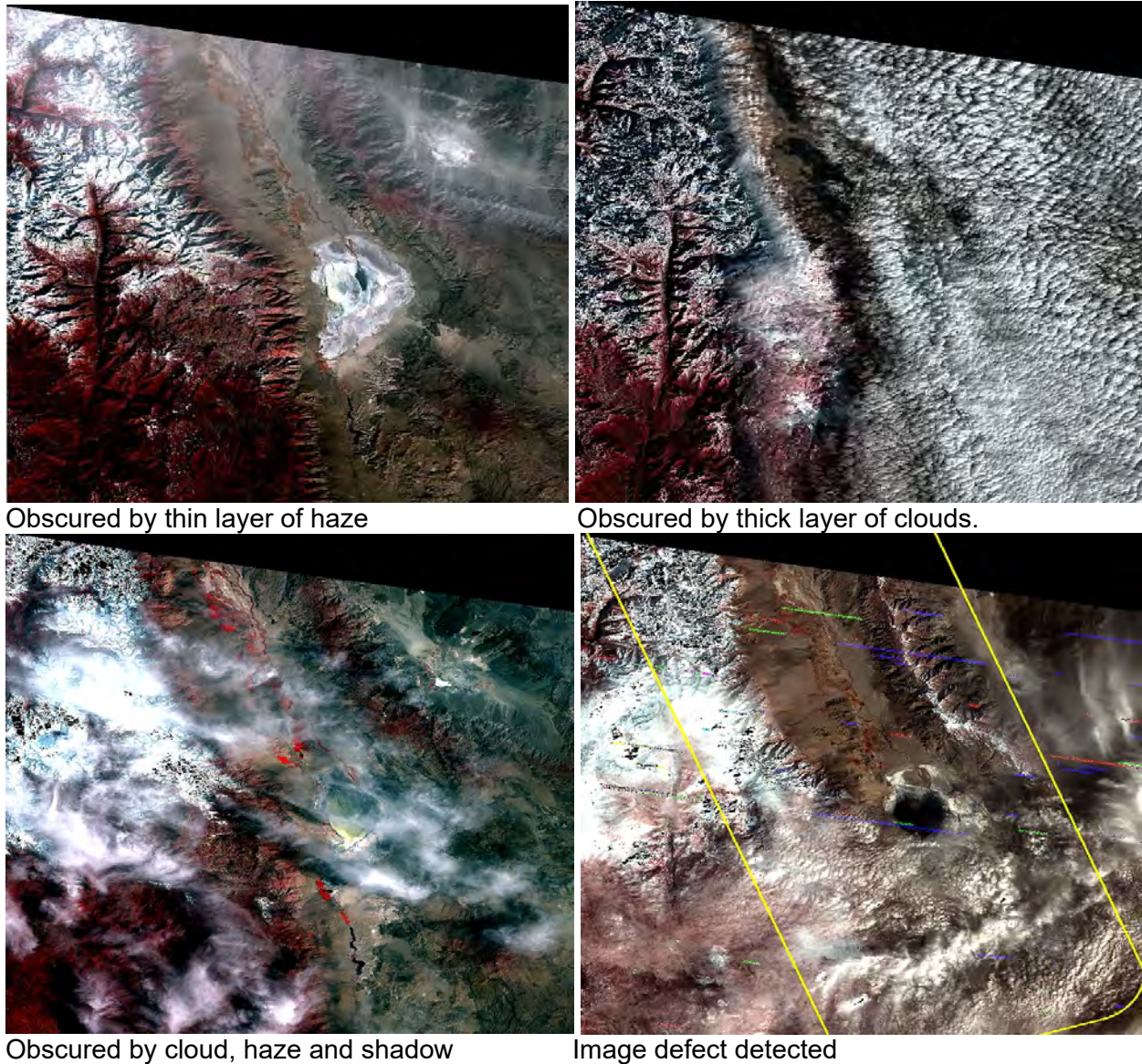
Figure 4
Tagging Criteria for Image Quality Assessment
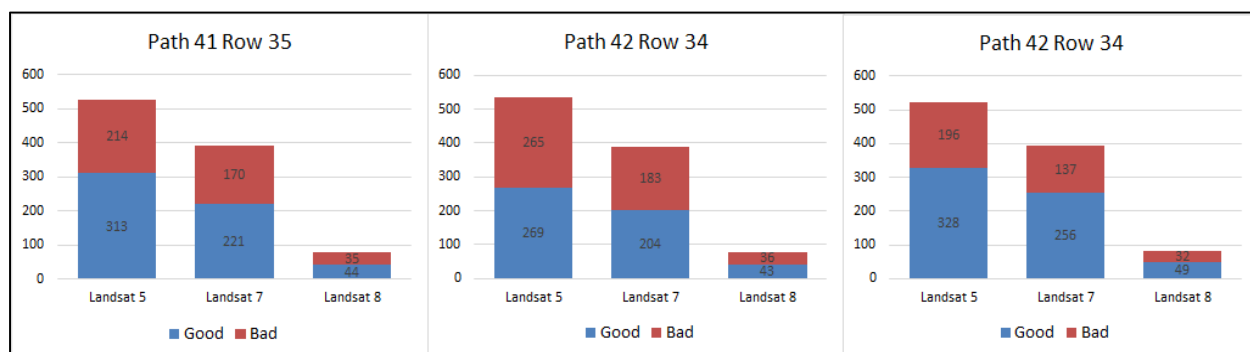
Figure 5
Results of Image Quality Assessment

All of the atmospheric corrected surface reflectance imagery will be ingested into the REGularized canopy reFLECtance program (REGFLEC) for development of leaf area index estimation. The Level-1 standard product is being used in the SEBS image analysis framework for developing ETa dataset. The SEBS image analysis framework uses calibration coefficients in the metadata to convert DN into land surface reflectance and temperature. An atmospheric correction module is built into the SEBS framework for correcting atmospheric attenuations.

4.0   RESULTS AND FINDINGS

The Landsat images identified as "Good" from the data quality assessment were imported into an ESRI ArcGIS image mosaic dataset. The acquisition date and other metadata (scene, band, sensor information, derivative product calculation, etc.) are documented. The mosaic dataset allows analysts to quickly scroll through the historical Landsat archive and derivative products sequentially for quick spatio-temporal trend analysis. This tool only works on an ArcGIS software platform and requires accompanying imagery dataset. The image quality assessment tool and all the processed Landsat dataset are available to the project team. The imagery database developed is approximately 8 TB and is being used for developing LAI (Task 2) and ET (Task 3) information.

5.0   REFERENCES

MWH, 2016. Final Work Plan: Remote Sensing Pilot Project (Task Order 002 of Agreement 47381-6). September.

APPENDIX B

TM 8.2 – LEAF AREA INDEX-IMAGE ANALYSIS

TECHNICAL MEMORANDUM

Title: TM 8.2 – Leaf Area Index-Image Analysis

Project: Task Order 008 – Remote Sensing Pilot Project Implementation

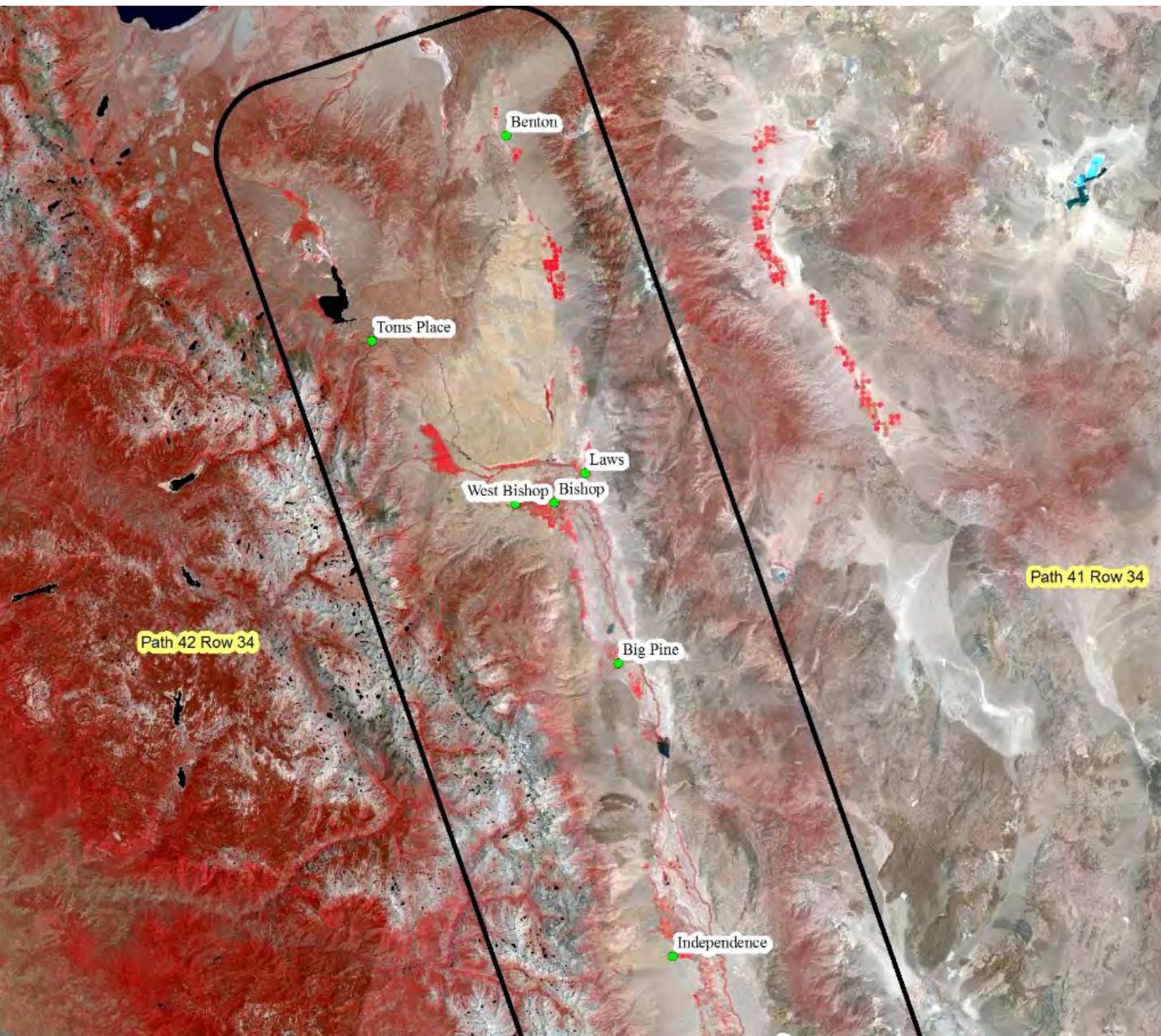**Client:** Los Angeles Department of Water and Power

Date: May 2017

TABLE OF CONTENTS

LIST OF FIGURES

LIST OF TABLES

ACRONYMS / ABBREVIATIONS

AOI	Area of Interest
CDR	Landsat Surface Reflectance Climate Data Records
CSV	Comma Separated Value
DEM	Digital Elevation Model
DN	Digital Number
ET	Evapotranspiration
ESRI	Environmental Systems Research Institute
FCC	False Color Composite
GNDVI	Green Normalized Difference Vegetation Index
ICWD	Inyo County Water Department
LADWP	Los Angeles Department of Water and Power
LAI	Leaf Area Index
NDVI	Normalized Difference Vegetation Index
NASA	National Aeronautics and Space Administration
NAIP	National Agricultural Imagery Program
REGFLEC	REGularized canopy reFLECtance
SEBS	Surface Energy Balance System
SLAI	Seasonal Leaf Area Index
TM	Technical Memorandum
USGS	United States Geological Survey
WRS	World Reference System
LUT	Look-Up-Table Generation
LPGS	Level-1 Product Generation System
REGFLEC	REGularized canopy reFLECtance program
VI	Vegetation Index

1.0   INTRODUCTION

This Technical Memorandum (TM) has been prepared in support of the Remote Sensing Pilot Project Implementation for the Owens Valley area. This TM represents the deliverable for Subtask 8.2 of Task Order 008 of Agreement No. 47381-6. As described in the Work Plan for this effort (MWH, 2016), key findings from the Pilot Project are documented in brief periodic TMs. These TMs are not intended to contain extensive introductory material, but are intended instead to focus on the results of specific portions of the work. A listing of the key TMs associated with this work is summarized in **Table 1**, with the highlighted TM 8.2 presented in this document. TM8.2 describes the steps involved in the development and validation of long term satellite-derived LAI (Leaf Area Index) dataset. Over 30+ years of observed and estimated dataset of vegetation cover and LAI was analyzed. Comparisons show strong relationship between satellite-derived LAI dataset and ground observations of vegetation cover. These results indicate that remote sensing techniques for estimating LAI is an effective tool for spatial and temporal monitoring of vegetation across Owens Valley.

Table 1
Summary of Technical Memoranda

Task	TM Number	Subject
1 - Imagery Download, Preparation, and Preprocessing	TM 8.1	Imagery, cloud screening results, and radiometrically corrected imagery
2 - Leaf Area Index Image Analysis	TM 8.2	Leaf area index (LAI) image analysis, comparison of LADWP and ICWD historical data with remote sensing results, sampling scheme for collecting ground truth data
3 - Evapotranspiration (ET) Mapping and Options for Integration	TM 8.3	Surface Energy Balance System (SEBS) ET delivery, SEBS ET development and validation
	TM 8.4	Integration of Spatial ETa into the Bishop/Laws groundwater model
	TM 8.5	Estimation of historical Eta from agriculture in the Chalfant, Hammil, and Benton Valleys
	TM 8.6	Evaluation of existing northern boundary conditions

2.0   PURPOSE AND OBJECTIVES OF TM

As part of water resources and vegetation management related to the Inyo/LA Water Agreement, both the Los Angeles Department of Water and Power (LADWP) and the Inyo County Water Department (ICWD) conduct vegetation monitoring in the Owens Valley. This type of monitoring began in 1985 and has continued to present day.

The overarching purpose of this remote sensing work is to evaluate the possibility of augmenting or even potentially replacing current methods of vegetation monitoring in the Owens Valley using remote sensing technology. More specifically, the objective of Subtask 8.2 was to analyze temporal trends of Leaf Area Index (LAI) to quantify the historical variability of LAI per pixel and use this information to isolate relevant change as compared to the baseline period (1984 to 1987).

All pre-processed Landsat imagery from Subtask 8.1 was used in the canopy reflectance model to build a time series LAI dataset.

3.0   REVIEW OF SUBTASK 8.1

This section will be discussing the updated information in subtask 8.1. All imagery identified for download (from Landsat 5, 7, and 8 for Path 41, Row 34, Path 41, Row 35, and Path 42, Row 34, from 1985 to 2016) has been completed. As detailed in TM 8.1 (January, 2017), all the data were acquired from the U.S. Geological Survey (USGS) data archive (https://earthexplorer.usgs.gov/). The chosen processing level for the data acquisition was Level-1 Product Generation System (LPGS) with standard terrain correction L1T. At this level, all of the imagery was radiometrically calibrated and orthorectifed using ground control points. The imagery was also corrected for relief displacement using a digital elevation model (DEM). This level of processing produced the highest quality product suitable for pixel-level time series analysis.

Landsat 5 was launched on March 1, 1984, but the first images available from the USGS data archive only include the latter part of 1984. As a result, imagery from 1984 is not included in the acquisition window due to the limited number of available images. The data acquisition window for the analysis ranges from 1985 to 2016. The total number of downloaded imagery files is 3016. **Figure 1** shows the number of downloaded imagery, by sensor and by Path/Row. All post-processing and quality assessment of downloaded imagery were completed, resulting in 56% of the imagery considered acceptable for analysis (**Figure 2**). The remaining images were considered unacceptable for use because of cloud cover or other factors.
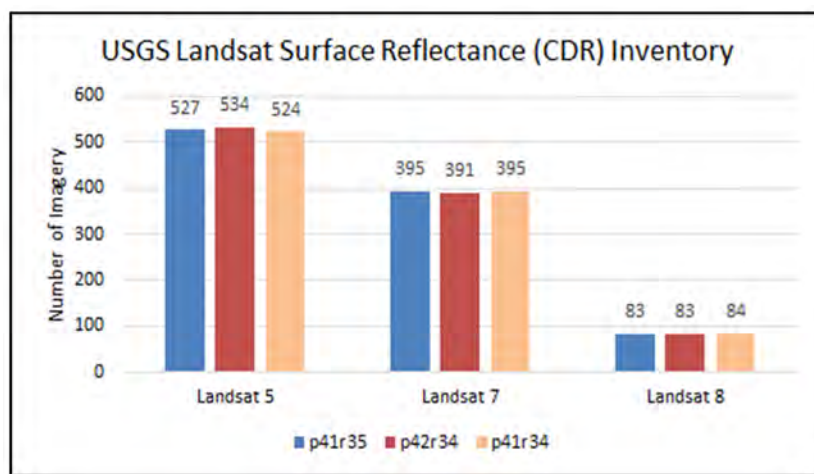

Figure 1
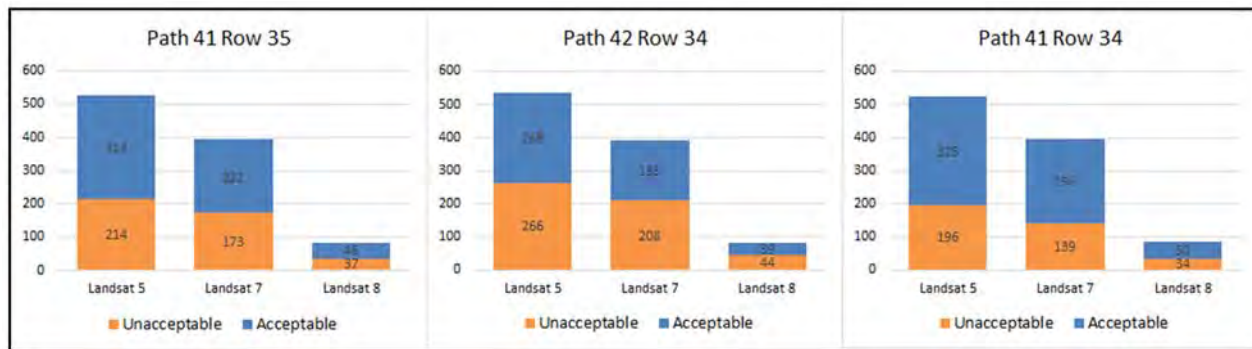**Available Imagery Dataset from Landsat Program, 1985 to 2016**

Figure 2 Results of Image Quality Assessment

4.0   SUMMARY OF WORK CONDUCTED

Leaf Area Index (LAI) represents an important vegetation-specific biophysical parameter that can be monitored with Landsat imagery to quantify changes in photosynthetic leaf material over time. LAI is sensitive to photosynthetic activity and is an important metric for assessing historical growth, biomass, and vigor of vegetation. LAI (m^2/m^2) represents the amount of green leaf material in an ecosystem and is geometrically defined as the total one-sided area of photosynthetic tissue per unit of ground surface area. Under conditions of stress, leaf area growth, leaf area duration, and leaf photosynthesis are affected at different spatial and temporal scales. In natural vegetation systems, stress will modify many of the canopy characteristics. Hence, LAI is a biophysical parameter which characterizes plant growth and development, and can be computed using satellite imagery to monitor vegetation performance over long term.

There are numerous reasons to select LAI as the choice of Vegetation Index (VI) over the more common Normalized Difference Vegetation Index (NDVI). Normalized Difference Vegetation Index (NDVI) is a simple ratio of two spectral bands expressed as Near-Infrared reflectance minus Red reflectance over Near-Infrared reflectance plus Red reflectance. NDVI is widely used, given its simplistic formulation and that it can be created quickly with minimal computing resources. Despite being widely used, NDVI has significant limitations. NDVI is appropriate for medium density vegetation, but approaches saturation at low and high ranges of LAI. It is therefore not recommended for highly dense vegetation areas or very sparse vegetation areas (**Figure 3**).
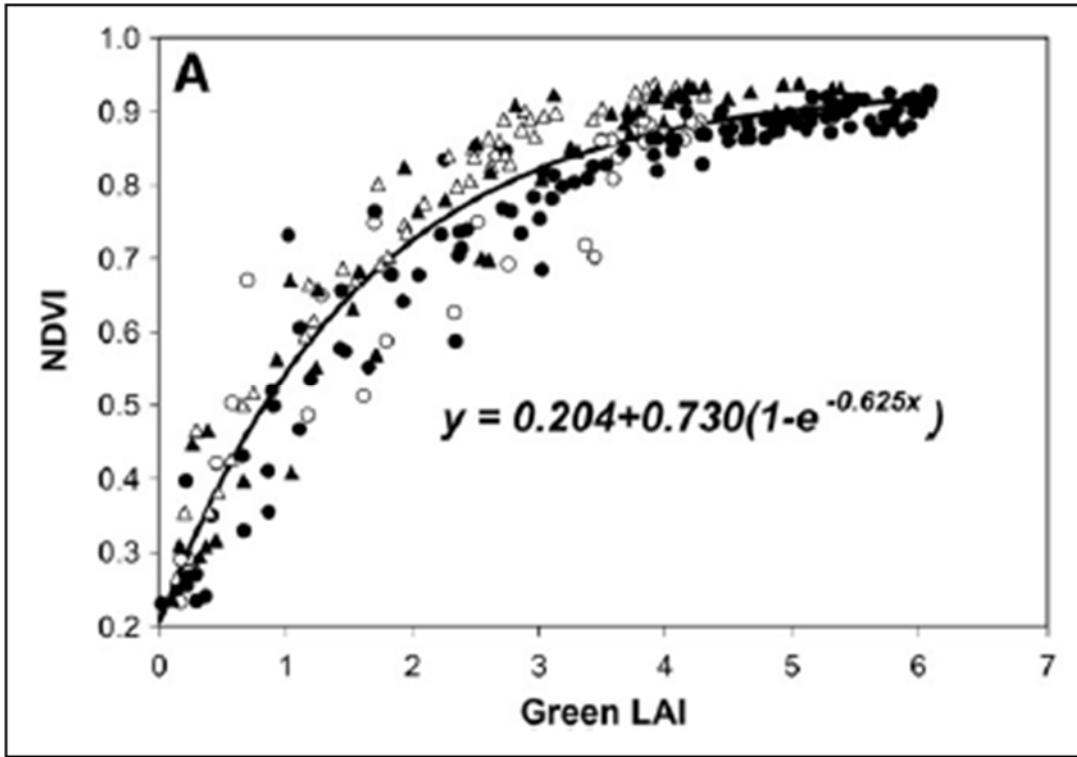
(Reproduced from Vinna, 2011)

Figure 3
Relationship between NDVI vs LAI

Previous project experience in the Owens Lake region shows additional differences between NDVI and LAI analyses. The charts shown on Figure 4 illustrate the NDVI and LAI trend for three different types of alkaline meadows (Dry, Mixed, and Saturated). NDVI reaches a plateau at high LAI or peak of the growing season and is less sensitive in the off growing season (NDVI values are abnormally high in off growing season).
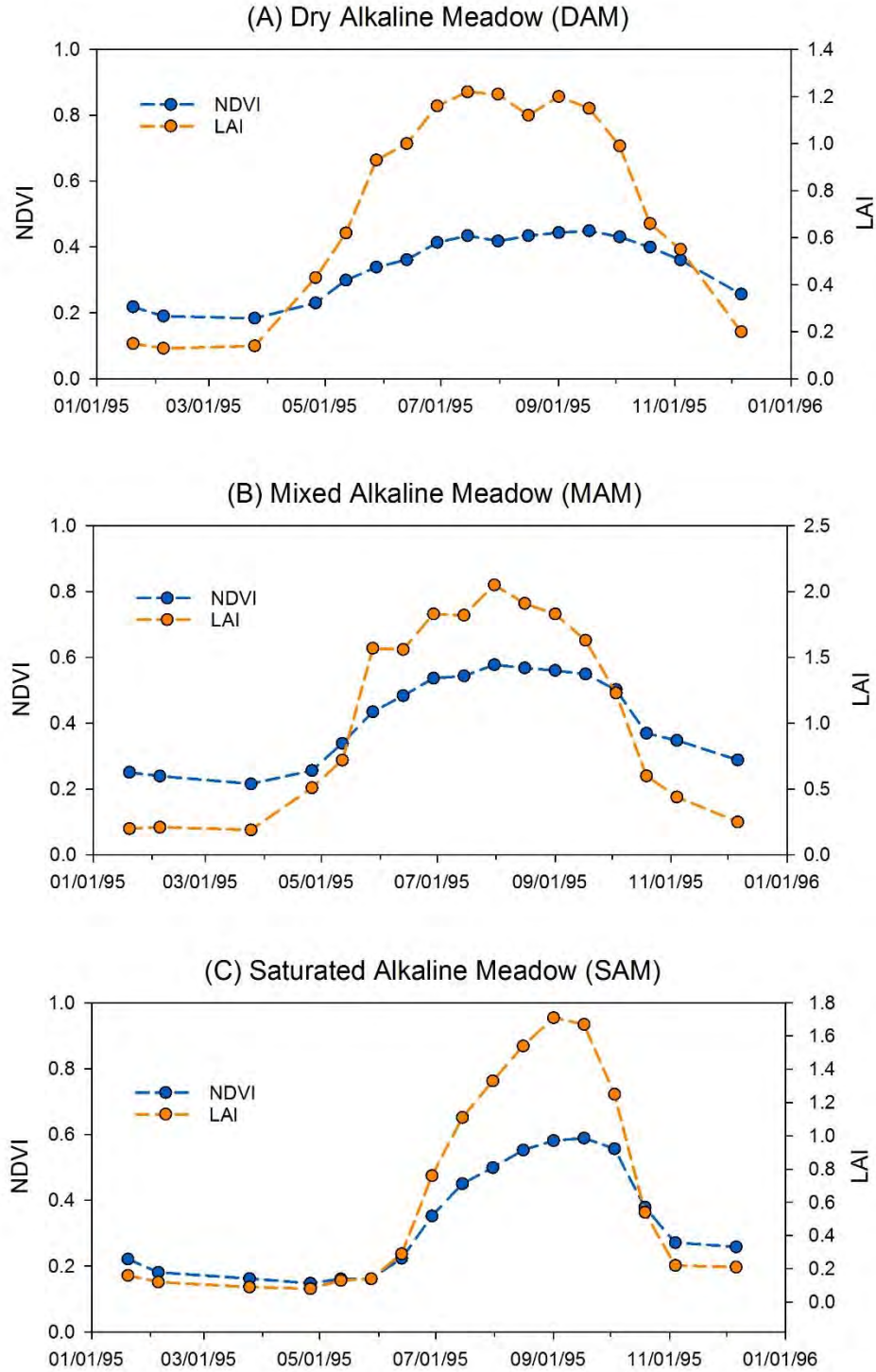
Figure 4
NDVI and LAI Annual Trend for (A) Dry Alkaline Meadow (B) Saturated Alkaline Meadow and (C) Mixed Alkaline Meadow

LAI was chosen as the vegetation index for this analysis because most of the vegetation in the study area are in the low range of LAI. Overall, LAI will provide a more accurate representation of the vegetation areas in Eastern Sierra.

4.1 Development of Leaf Area Index (LAI)

The program used in the analysis to produce LAI was the REGularized canopy reFLECtance program (Houborg 2009). The program was built using Interactive Data Language (IDL) and was run on the ENVI/IDL platform. This program couples leaf optics (PROSPECT) and canopy reflectance (ACRM) model components, facilitating the direct use of reflectance in green, red, and near-infrared wavelengths for the inverse retrieval of total one-sided green leaf area per unit ground area (LAI). PROSPECT and ACRM implements a physically-based reflectance model at leaf and canopy level. Both methods provide an explicit connection between the biophysical variables and the reflectance measured from the satellite.

One of the major steps in the program is to generate a database of a wide range of leaf biochemical and canopy biophysical properties (**Figure 5**: Look-Up-Table Generation) and the associated spectral response by running the coupled model in forward mode using the parameters listed. This database enables the generation of curves of LAI as functions of near-infrared (NIR) reflectance, NDVI and Green Normalized Difference Vegetation Index (GNDVI) for various combinations of plant parameters (N, S_z, θ_l, C_{ab}, S_1, f_B). These relationships are the stored in a multi-dimensional Look-Up-Table Generation (LUT) for the next step. The next step is LUT-based iterative inversion technique for retrievals of key biophysical properties of interest, in this study, LAI. Using the relationships generated in the previous step, the observed NIR reflectance, NDVI and GNDVI from satellite data are used to generate separate LAI maps for a large number of plant-community-specific parameter combinations (N, S_z, θ_l, C_{ab}, S_1, f_B). The selection of the optimal values for the parameter combinations is done by an iterative search and guided by minimizing the LAI difference (Fig 7: ΔLAI; inversion procedure, where L1, L2, L3 are LAI values estimated using NIR reflectance, NDVI, GNDVI, respectively). With the determination of these parameters, the dimension of the LUT to compute LAI is reduced and LAI values can be determined for each of the pixels within the plant community.
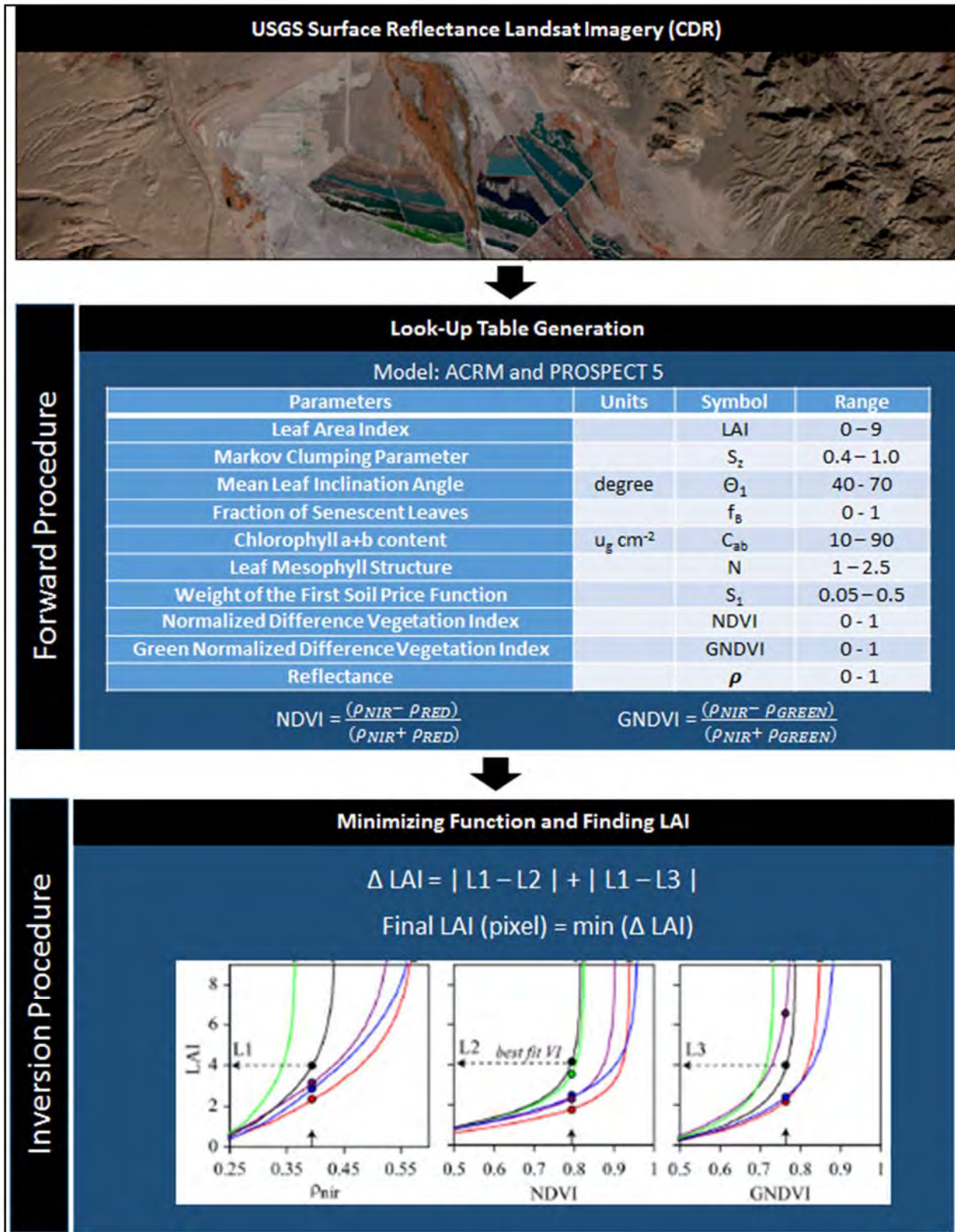
Figure 5
Flow Chart of REGFLEC Program

Figure 6 shows an example of false color composite (FCC) Landsat imagery (**Figure 6A**) and the corresponding LAI data (**Figure 6B**) for the Bishop/Laws region. The red tone in the Landsat imagery corresponds to vegetated area. In the LAI data, the blue/green tone indicates higher LAI value, whereas brown/yellow color denotes lower value of LAI. Note the agriculture fields in the northeast portion of the image shows higher LAI values compared to other vegetated areas. The LAI dataset is developed at 30x30m pixel for all the included images from 1985-2016 for the entire study area.
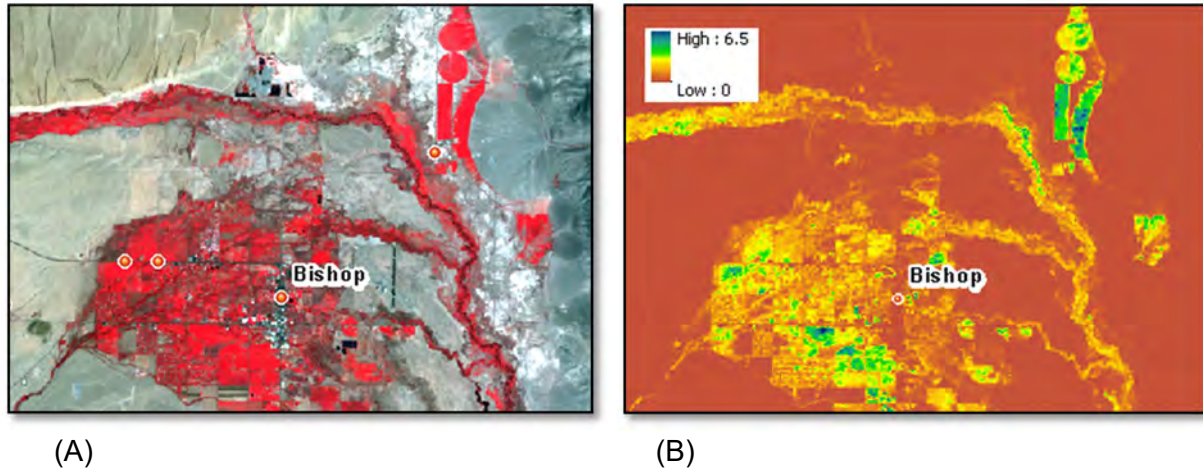

(A)   (B)

Figure 6
(A) Landsat Imagery in False Color Composite (Aug 16, 2016) and
(B) LAI for the Same Region (Aug 16, 2016)

LAI values can be extracted for any pixel through 1985 to 2016 and plotted as a time series to monitor the performance of vegetation over time. **Figure 7** is an example of a time series LAI plot for the highlighted pixel (yellow pixel pointed by the arrow) in the image. The annual growth and senescence cycle (phenology) of vegetation is captured through multiple estimates over a year and can be plotted to assess the vegetation growth over time. The natural range of variability in vegetation performance for any pixel could be analyzed for last 30 plus years.
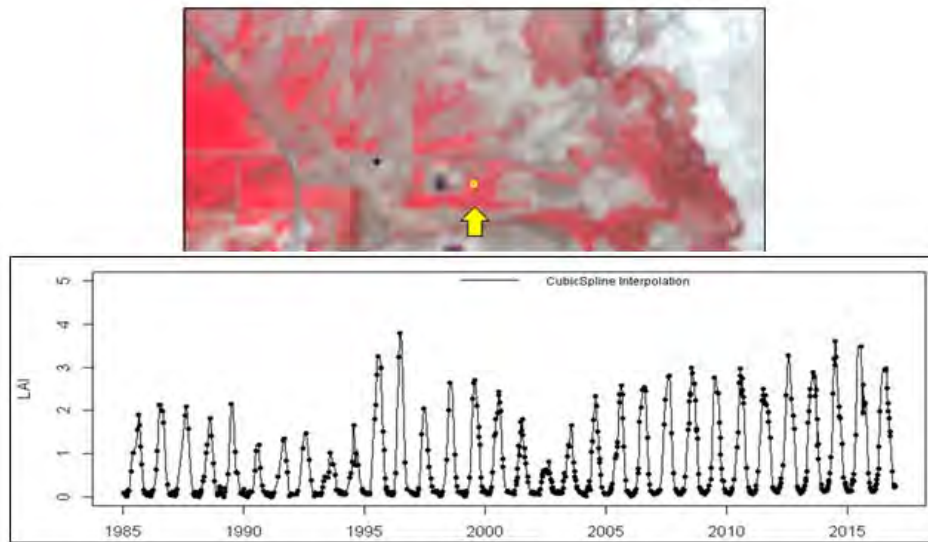

Figure 7
Time Series Plot of LAI for a Highlighted Pixel in the Image

In the time series LAI chart, each data point is a LAI value of a specific date. The peak and the length of the growing season varies from year to year. If only one date is picked, the LAI value might not represent the condition of the vegetation of that entire year. A value is needed to capture the productivity of the vegetation for entire phenology. Seasonal LAI (SLAI) is the area integral for the line curve from January 1 until December 31. Seasonal LAI not only captures the peak but also the length of the season (**Figure 8**).
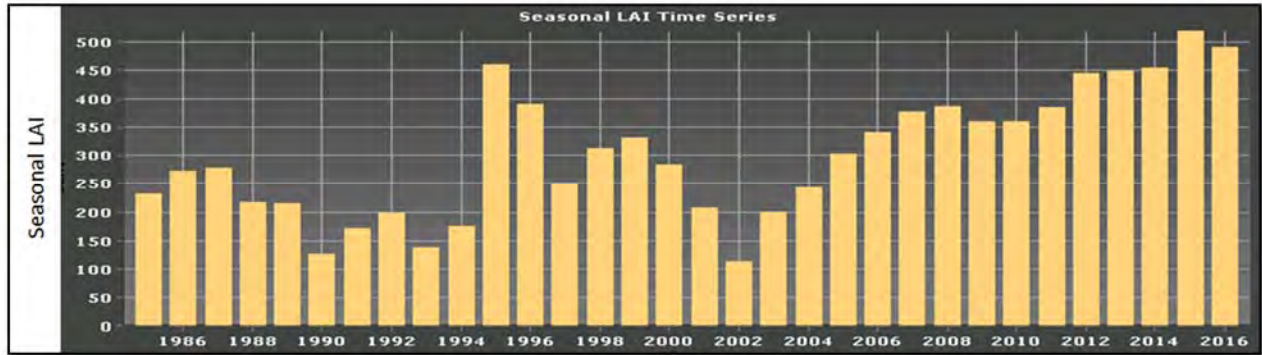

Figure 8
Seasonal LAI Calculated from the Time Series LAI Values

The study area from Benton Hot Springs to Owens Valley is approximately 1.5 million acres and the total number of pixels within this region is more than 10 million. A polygon layer (**Figure 9**) was generated to define the size and shape of each pixel within the study area. This pixel polygon layer was used to store the large LAI dataset and retrieve it for analysis, where each polygon includes LAI and SLAI values for all analyzed imagery.
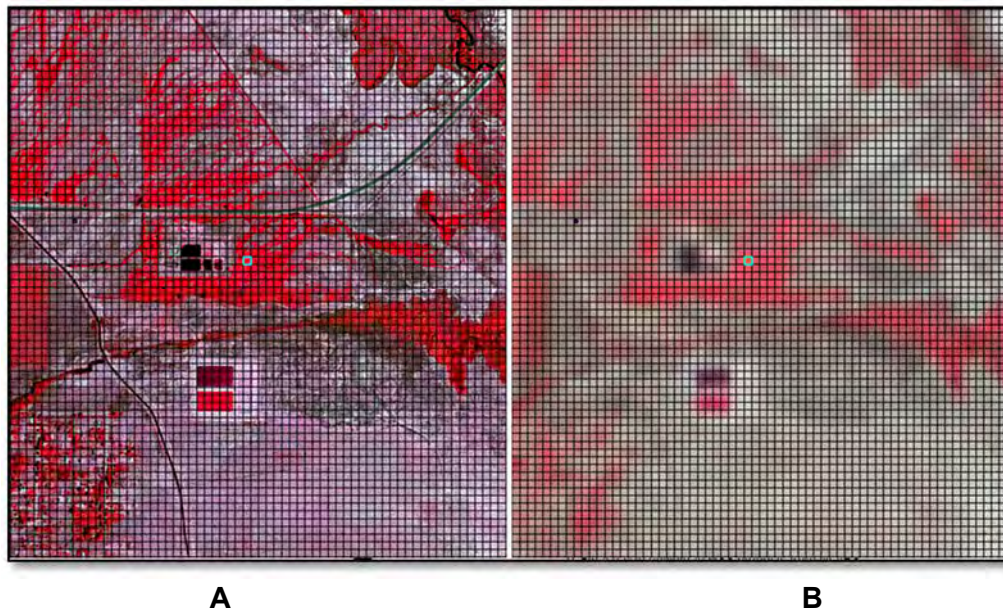

A   B

Figure 9
**(A) Pixel Polygon (black lines) Overlaid over NAIP Imagery and (B) Pixel Polygon
Overlaid over Landsat Imagery**

4.2 Field Observation Data

LADWP and the ICWD have collected long-term vegetation cover information in the Owens Valley over the last 30⁺ years. This observation dataset will be compared with the LAI dataset generated from remote sensing model. While the observed vegetation cover datasets correspond to various timeframes and spatial extents, they would still be used to develop inferential relationships to historical estimates of LAI. The long-term vegetation cover information collected by LADWP and ICWD can be categorized into five data groups:

  (1) ICWD Line Point Transect

  (2) LADWP Line Point Transect

  (3) LADWP Permanent Transect

  (4) LADWP Baseline Transect, and

  (5) ICWD Baseline Transect

These groups are summarized on **Table 2** and described in more detail below.

Group 1: ICWD Line Point Transect – ICWD line point transect data is available from 1991 to present. During this time, sampling has been done once a year with transect locations randomly selected within the parcel every year. Approximately 90-135 parcels were sampled each year, and the transects within each parcel averaged approximately 10 per parcel. The length of each transect is 50m, and the distance between two sampling points along transects is 0.5m. At each sampling point, a pin was dropped, and an observation was recorded. If the pin touched a leaf, then it was recorded as "hit". Sum of all the hits along the transect provide vegetation percent cover.

Group 2: LADWP Line Point Transect – LADWP line point transect data has been collected starting in 2004 using similar field layout as the ICWD line point transect approach. A major difference is in the location of transect within the parcel, which remains fixed from year to year. LADWP line point transect data samples transects at most of the 154 permanent parcels every year.

Group 3: LADWP Permanent Point Frame Transect – LADWP permanent point frame data has been collected from 35 transects across the Owens Valley and is available starting from 1988. Each transect is 100m and sampled every 30cm. A pin is dropped at every sampling locations along the transect. Besides recording the observation of "hit" or "no hit" (this attribute is called FIRST), the number of times the pin touches the leaves before hitting the ground is also recorded (this attribute is called MULTIPLE).

Group 4: LADWP Baseline Transect – This line point transect data was for the "Baseline" period of 1985-1987. The transects were 100m long each, and the location of transects were never recorded. The closest this data can be located spatially is at the "parcel" level. Although baseline data took three seasons to gather (1985-1987), it is considered as a single year collection. The LADWP baseline transect measured vegetation across approximately 189 parcels.

Group 5: ICWD Baseline Transect – This dataset overlaps LADWP baseline data because of common data set. Approximately 153 parcels were monitored, of which 143 overlapped and had exactly same data as DWP baseline.

Figure 10 is an example of vegetation monitoring transects locations within a single parcel. The blue points denote ICWD line point transect (Group 1), pink points are the LADWP line point transect (Group 2), while the yellow points are the LADWP permanent point frame transect (Group 3). ICWD line point transect appear more on the figure because each point represents only one year whereas LADWP line point and permanent point surveys the same location every year; therefore, each point contains multiple year data.

The vegetation cover monitoring dataset includes plant species information, per transect. Approximately 925 plant species are identified in the LADWP and ICWD datasets. All the dataset was quality checked and imported into access database for analysis. The plant species were further classified according to habitat groups (forb, shrub, grass, tree and vine) and life cycle (annual, biennial, and perennial).

Table 2
Summary of Different Groups of Field Observation of Vegetation Cover Data

| Name	Transect Length	Distance Between Two Points	Same Location Annually	Attributes	Time Frame
ICWD Line Point	50 m	0.5 m	No	First (Percent Cover)	1991-2014
DWP Line Point	50 m	0.5 m	Yes	First (Percent Cover)	2004-2015
DWP Permanent Transect	100 m	30 cm	Yes	First (Percent Cover) Multiple	1987-2016
DWP Baseline Transect	100 m	-	Location never recorded	First (Percent Cover)	1 year (1985-1987)
ICWD Baseline Transect	100 m	-	Location never recorded	First (Percent Cover)	1 year (1985-1987)
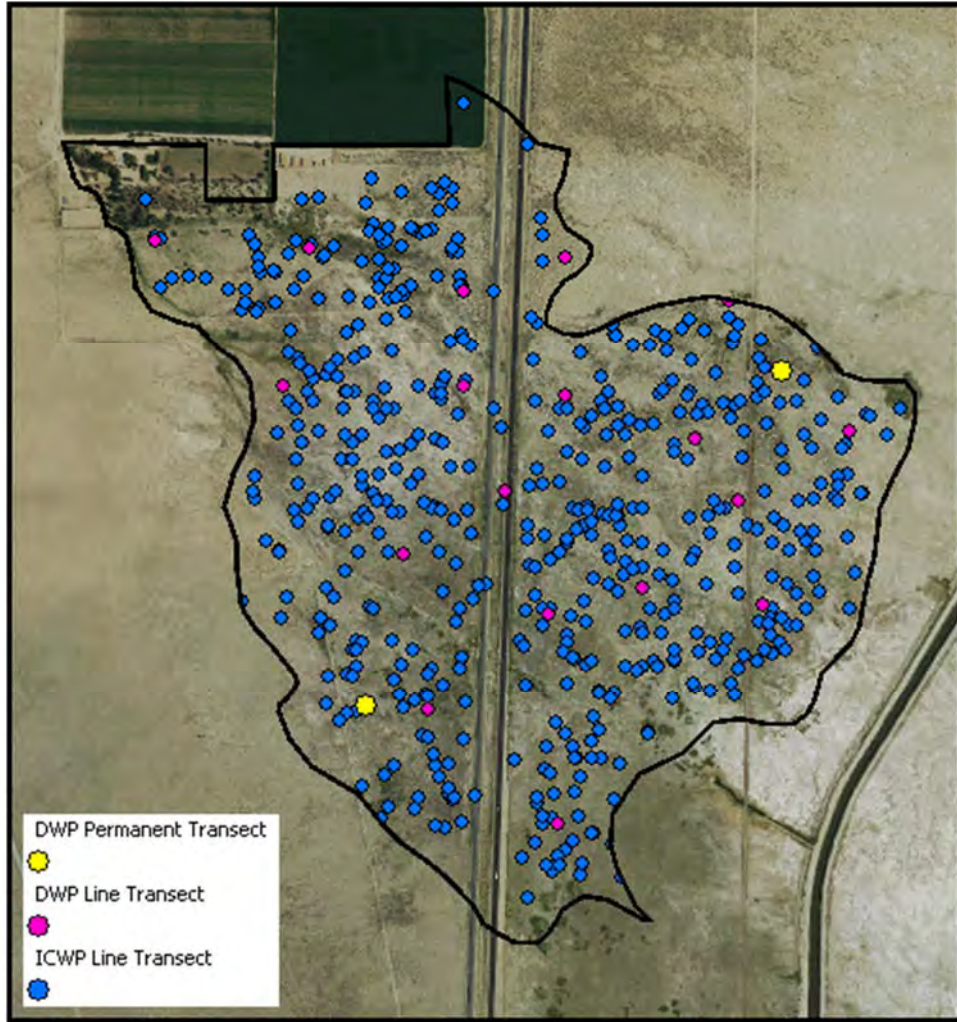
Figure 10
Sampling Locations for Three Different Categories of Field Data within a Single Parcel (BLK094) Boundary located in the South of Aberdeen

The effect of random selection of transect in the ICWD dataset (Group 1) as compared to fixed transect in LADWP dataset (Group 2) was evaluated by aggregating both the datasets to the parcel level. The average of all the transect data within a parcel provided the aggregated vegetation cover value for the parcel.

Figure 11 shows the correlation between the ICWD and LADWP line point transect data at the parcel scale. The ICWD samples different locations every year within the parcel whereas LADWP has fixed sampling location. The high correlation (R-Square~ 0.80) between the two datasets at the parcel scale shows that the two datasets are consistent at parcel level. It can also be inferred that the parcels have homogeneous vegetation, and therefore the location of sampling does not influence the vegetation cover values. . The long-term LAI dataset developed from REGFLEC model using remote Landsat imagery is compared against parcel and transect vegetation cover observations and presented in the following section.
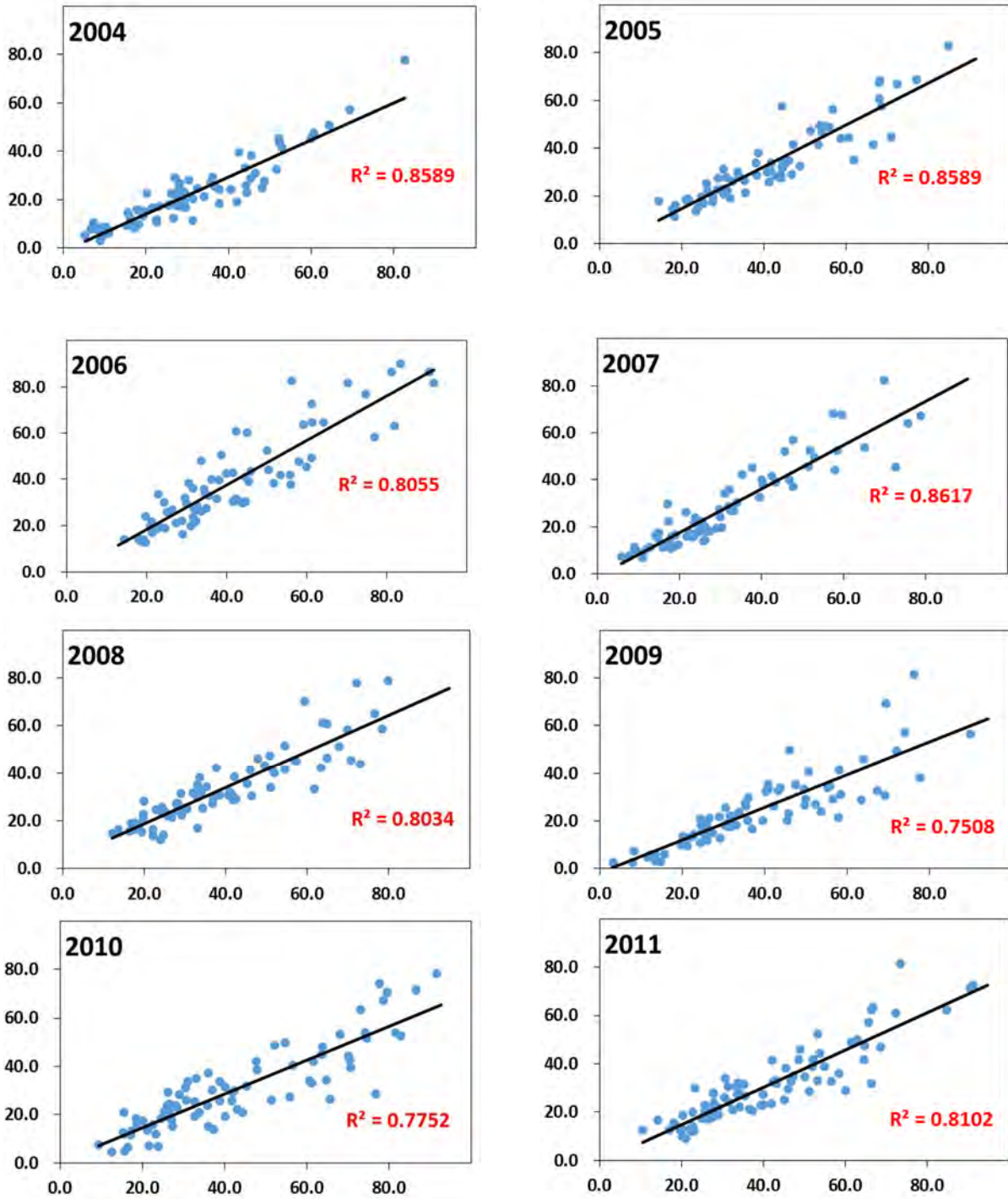
Note - X-axis is LADWP cover data and Y-axis is ICWD cover data, both aggregated to parcel level

Figure 11
Comparing LADWP Line Point Transect Data with ICWD Line Point Transect Data at Parcel Level
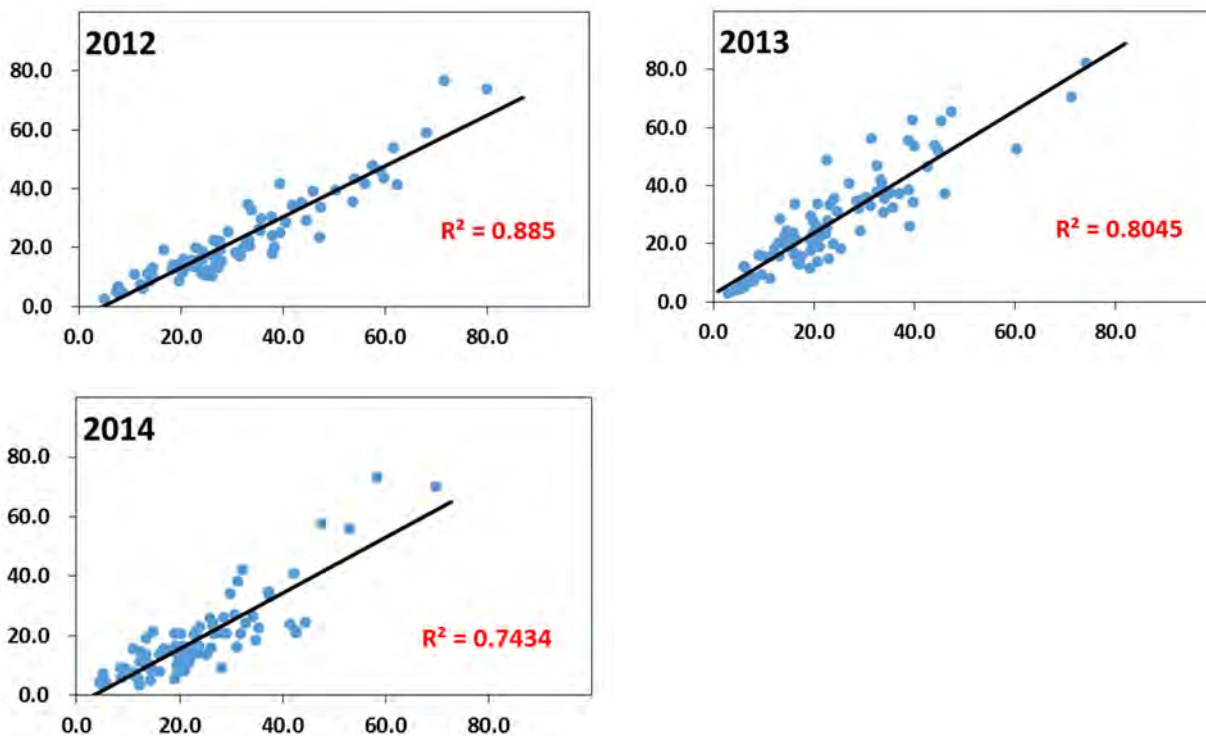
Note - X-axis is LADWP cover data and Y-axis is ICWD cover data, both aggregated to parcel level

Figure 11 Cont.

Comparing LADWP Line Point Transect Data with ICWD Line Point Transect Data at Parcel Level

4.3 Comparisons and Validations

Comparisons of satellite model-derived long-term LAI estimates against the different vegetation cover monitoring datasets is presented in this section. There is a strong relationship between LAI and vegetation cover, however there are many challenges when comparing the observed line point transect vegetation cover against satellite derived LAI values. Some of the differences between the observed (line point vegetation cover) and estimated (pixel LAI & SLAI) values which could contribute to uncertainty are:

1. LAI and SLAI estimates are generated for pixels with an area of 30 m^2, whereas the observed vegetation cover dataset is a line point transect spanning 50 to 100m.

2. LAI is estimated for all the dates with good available images (quality checked) in a year, whereas vegetation cover is a one-time observation during the peak growing season.

To circumvent some of these spatial-temporal differences in the dataset, several levels of comparisons were undertaken. In addition, field campaigns are planned for collection of LAI measurements which would be the part of more comprehensive validation.

4.3.1   Parcel Level Comparison with SLAI

The LADWP and ICWD line point transect data (Group 1 & 2) aggregated to the parcel level were compared to SLAI. SLAI aggregates the year-long LAI values for the pixel into one value which could be compared to observed vegetation cover. Average SLAI was extracted for the 154 permanent parcels and compared to the parcel-average vegetation cover. **Figure 12** shows an example of vegetation monitoring data and SLAI data. Appendix 1 and Appendix 2 shows the comparison with LADWP and ICWD dataset respectively. The comparison at the parcel level shows that the satellite-model derived SLAI has a very strong relationship with the observed vegetation cover information. The baseline dataset (Group 4 & 5) also shows good agreement with satellite-model derived SLAI at parcel level.
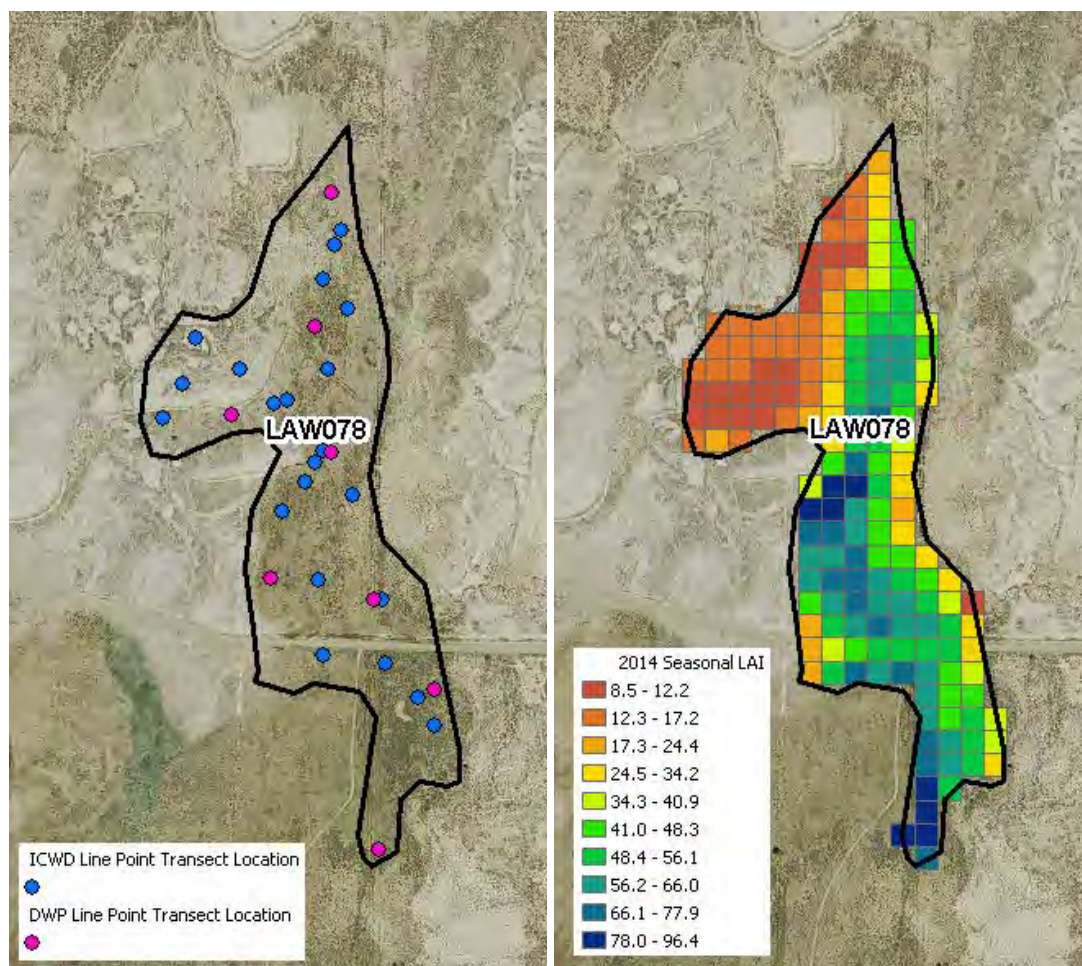
Figure 12 Example of parcel data comparison with SLAI

Figure (left) shows the 2014 transect locations for DWP and ICWD. Average percent cover for Parcel LAW078 is calculated by summing all percent cover for all transect locations within the parcel and dividing the sum by number of transect locations. Figure (right) shows the seasonal LAI in pixel polygon. Average seasonal LAI for Parcel LAW078 is calculated by summing all seasonal LAI pixel values and dividing by number of pixels within the parcel. The background image is 2014 NAIP (National Agricultural Imagery Program).

4.3.2   Transect Level Comparison with SLAI

The LADWP and ICWD line point transect data (Group 1 and 2) were aggregated to the transect level and compared to SLAI. The sum of all the species cover data within the transect provided the aggregated vegetation cover value for the transect. Approximately 1,700 transects from

LADWP and 2,000 transects from ICWD were available for comparison. All the pixels intersected by the transects were used to extract the average SLAI. The results of this analysis is not presented in this TM but would be included in the final project report.

4.3.3 Transect Level Comparison with LAI estimate from image closest to observation data.

The observed vegetation cover information is collected once a year during the peak vegetation growth period. In this analysis the LAI value from image closest to the observation date is used for comparison. It is assumed that peak vegetation growth period is 21st June and all vegetation cover observations are taken on this data. The Group 1, and 2 observation datasets at the transect level were compared against LAI estimate from single imagery acquired around the observation period. Vegetation cover of the transect were compared to the average LAI value from all the pixels intersected by the transect. Approximately 1,700 transects from LADWP and 2,000 transects from ICWD were available for comparison. The results of this analysis is not presented in this TM but would be included in the final project report.

4.3.4 LADWP Permanent Point Frame Transect Comparison with SLAI and LAI

The LADWP permanent point frame transect (Group 3) data available for 35 transects is a consistent dataset available from 1988. The transect location BP1 has been chosen as an example to compare the SLAI dataset calculated using Landsat satellite imagery (**Figure 13**). More examples of transects are illustrated in **Appendix 3**.
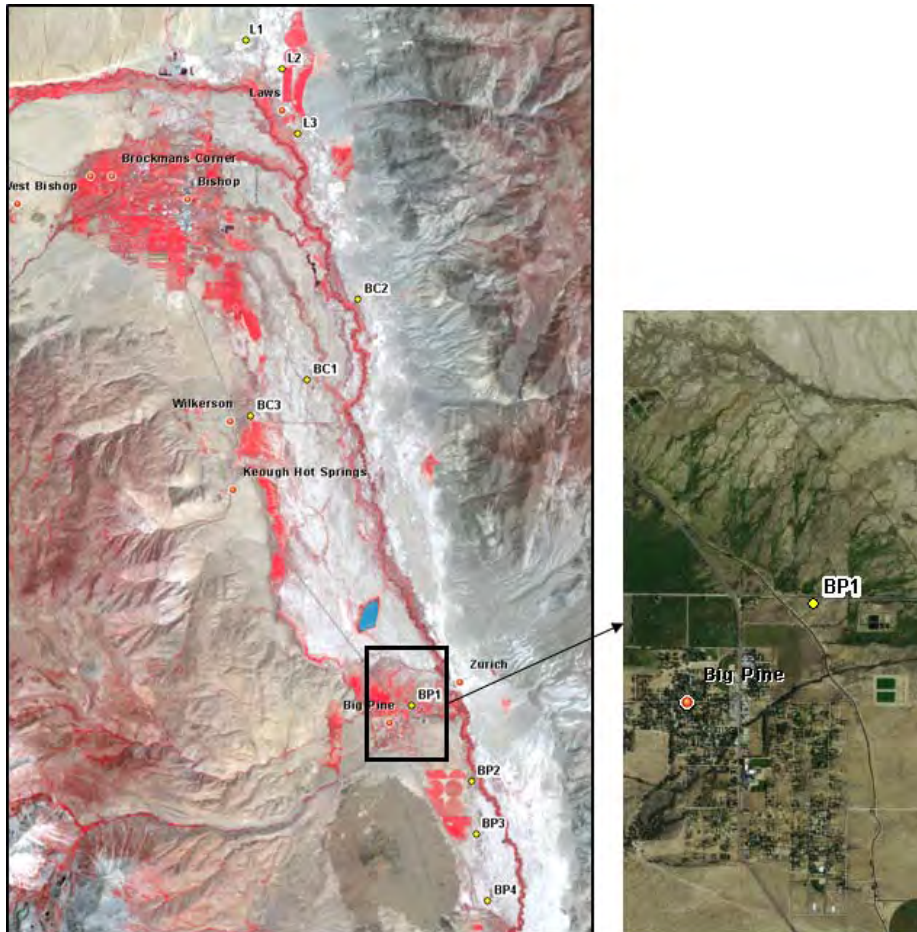
Figure 13
Location of BP1 Transect in LADWP Permanent Point Frame Observation Dataset,
Selected for Comparison to LAI & SLAI Dataset

Table 3 shows the summary of the field data collected at transect BP1. There was no data collected in 1996 at this transect. The species column shows the predominant species at this transect were Atriplex Torreyi (ATTO, Torrey's Saltbush), and Sarcobatus Vermiculatus (SAVE4).

Table 3
MULTIPLE Hit Vegetation Cover Observation Dataset for Permanent Transect BP1

Species	1989	1990	1991	1992	1993	1994	1995	1996	1997	1998	1999	2000	2001	2002
ATTO	47	14	69	19	91	63	47		246	91	161	108	108	51
SAVE4	11	0	18	11	28	26	38		58	32	33	23	22	6
SPAI	10	0	7	0	4	2	3		5	6	7	8	4	6
BAHY	0	0	0	1	6	0	0		0	17	0	0	0	0
AAFF	0	0	0	0	0	0	35		8	0	0	0	0	0
ERNA10	7	0	1	0	0	0	0		2	2	4	7	6	2
ANAT	0	0	0	0	7	0	0		0	0	0	0	0	0
SATR12	0	0	0	0	0	2	0		0	0	0	0	0	0
DESO2	0	0	0	0	0	0	0		0	0	0	0	0	0
STPA4	0	0	0	0	0	0	0		0	0	0	0	0	0
Total	75	14	95	31	136	93	123		319	148	205	146	140	65

Species	2003	2004	2005	2006	2007	2008	2009	2010	2011	2012	2013	2014	2015	2016
ATTO	81	41	62	69	82	78	121	156	109	65	9	12	10	9
SAVE4	8	3	14	16	16	27	32	27	35	33	8	14	4	9
SPAI	9	1	4	12	9	4	21	9	15	6	12	4	2	3
BAHY	3	0	8	27	0	5	2	3	5	0	0			
AAFF	0	0	2	0	0	0	0	0	1	0	0	0		
ERNA10	0	0	0	0	0	0	2	1	0	7	0			
ANAT	0	0	0	0	0	0	0	0	0	0	0			
SATR12	0	0	0	2	0	0	0	0	0	0	0		0	
DESO2	0	0	0	0	0	0	0	1	0	0	0			
STPA4	0	0	0	0	0	0	0	0	0	0	0	0	0	
Total	101	45	90	126	107	114	178	197	165	111	29	30	16	21
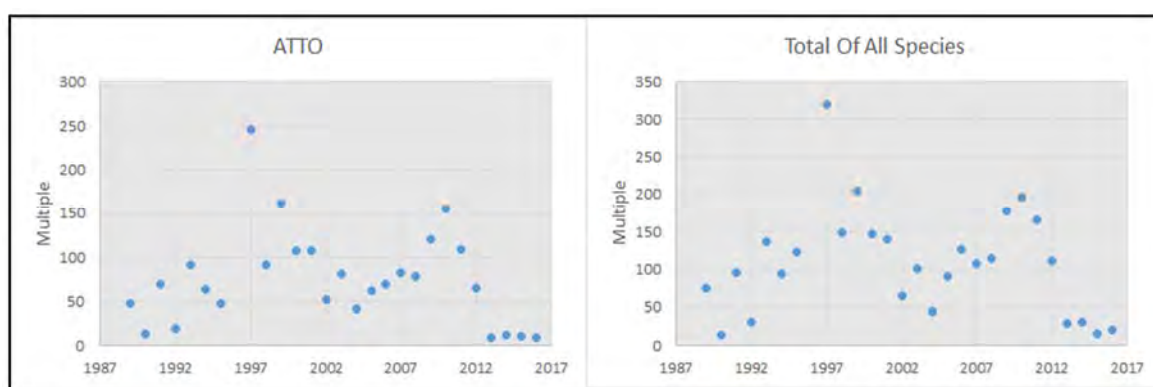
Figure 14
MULTIPLE Values Plotted for ATTO and Total of All Species

From the field data, two peaks were observed from the time series charts (**Figure 14**) either using data of the major species or sum of all species. These peaks occur around years 1997 and 2010. During these two years, vegetation density is estimated to be the highest. A similar trend is also observed in the LAI and SLAI time series charts (**Figure 15**). The trend (**Figure16**) of observed vegetation cover and estimated SLAI shows good performance of the model in estimating LAI. Transect level comparison provides the most rigorous comparison and hence the relationship is expected to be lower than comparisons made at parcel level. The pixels intersected by the transects have a much larger footprint therefore the average value of the computed LAI or SLAI will include the noise from the surroundings. The transect level comparisons were performed with contextual information from the transect surrounding for better interpretation of the results (see Appendix 3).

(A)
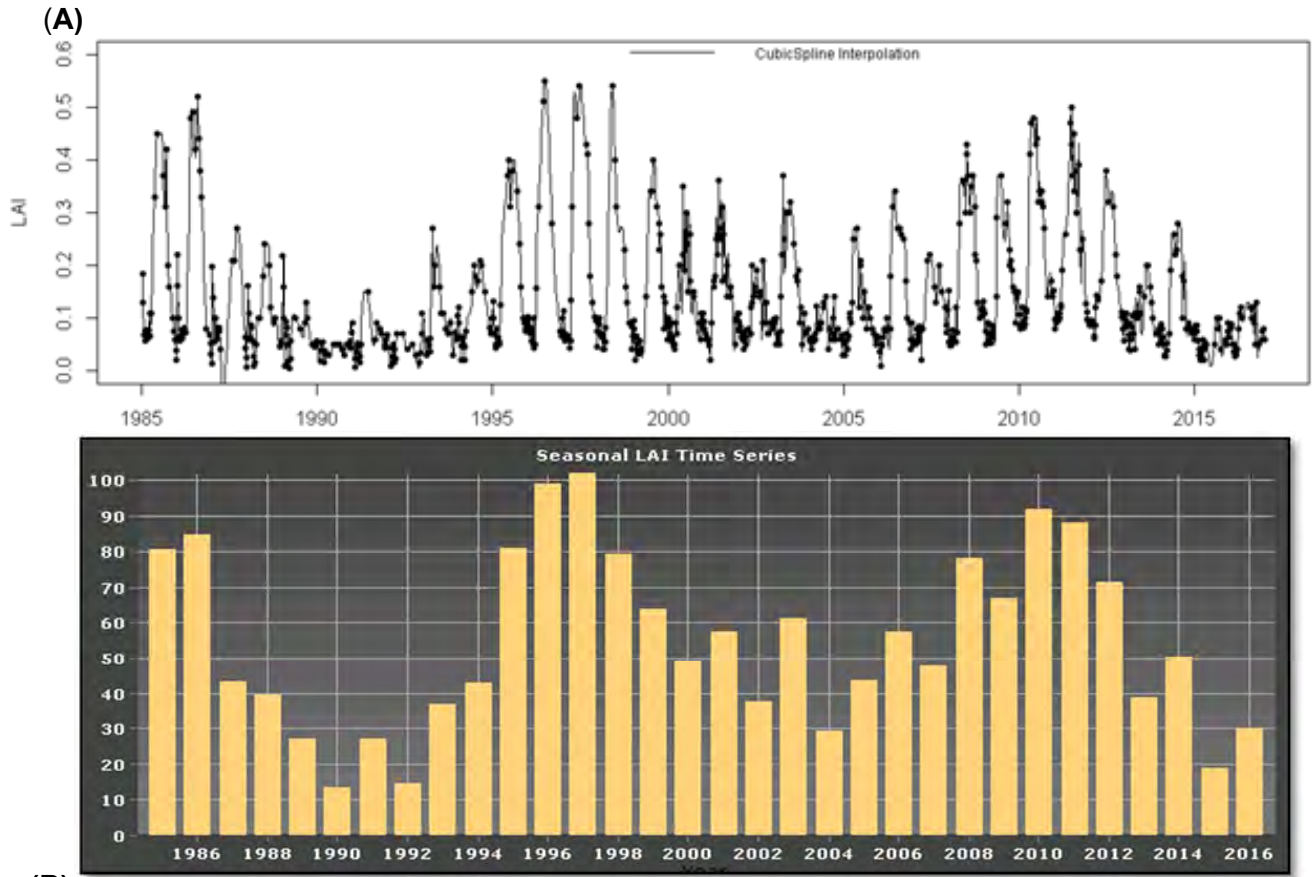
(B)

Figure 15
(A) LAI Time Series and (B) Seasonal LAI (SLAI) for Transect BP1
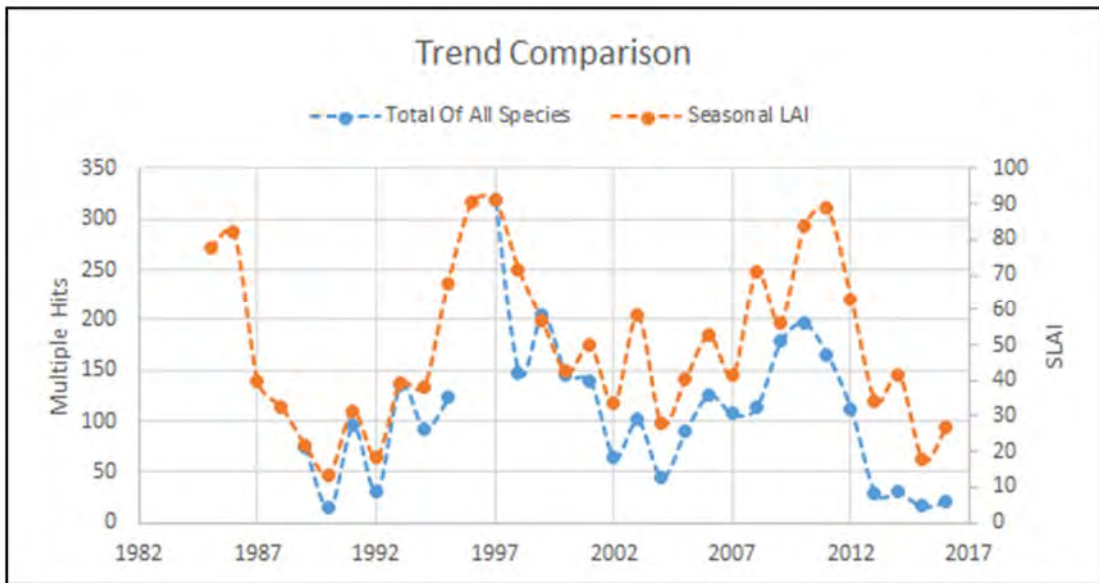
Note the missing observation value in 1996.

Figure 16
Estimated SLAI and Observed Cover (MULTIPLE hit field observations) for Transect BP1
Note the missing observation value in 1996

5.0   RESULTS AND FINDINGS

The long term (1985-2016) LAI dataset development from canopy reflectance model using Landsat imagery is completed for two path-row. The LADWP and ICWD vegetation cover monitoring dataset collected in the Owens Valley over the last 30+ years was processed and used for comparison against the developed LAI dataset. Several level of comparisons of developed LAI dataset against observed vegetation cover were undertaken, however not all of them are presented in this TM. All the remaining comparison analysis will be quality checked and provided in final project report. Parcel level comparisons (Appendix 1 and 2) shows excellent agreement between the two datasets. The LAI and SLAI follows the trend of observed vegetation cover at transect level (Appendix 3). These results indicate that remote sensing techniques for estimating LAI is an effective tool for spatial and temporal monitoring of vegetation across Owens Valley.

A field expedition for ground truth collection of LAI data would be part of the validation analysis and would be included in the final report.

6.0   REFERENCES

Gitelson, A. A., Viña, A., Arkebauer, T. J., Rundquist, D. C., Keydan, G., & Leavitt, B. (2003). Remote estimation of leaf area index and green leaf biomass in maize canopies. Geophysical Research Letters, 30, 1248.

Glenn E. P., Huete A. R., Nagler P. L., Nelson S. G. (2008). Relationship Between Remotely-sensed Vegetation Indices, Canopy Attributes and Plant Physiological Processes: What Vegetation Indices Can and Cannot Tell Us About the Landscape. Sensors (2008), 8, 2136 – 2160.

Hourborg, R., Anderson, M. C., (2009). Utility of an image-based canopy reflectance modeling tool for remote estimation of LAI and leaf chlorophyll content at regional scales. Journal of Applied Remote Sensing, Vol. 3, 033529 (7 May 2009).

MWH, 2016. Final Work Plan: Remote Sensing Pilot Project (Task Order 002 of Agreement 47381-6). September

Myneni, R. B., Nemani, R. R., & Running, S. W. (1997). Estimation of global leaf area index and absorbed PAR using radiative transfer models. IEEE Transactions on Geoscience and Remote Sensing, 35, 1380–1393.

Sellers, P. J., Mintz, Y., Sud, Y. C., & Dalcher, A. (1986). A simple biosphere model (SiB) for use within general-circulation models. Journal of the Atmospheric Sciences, 43, 505–531.

Stantec/Formation Environmental, 2017. TM 8.1 – Imagery Download, Preparation, and Preprocessing. January 17.

Viña, A., & Gitelson, A. A., Nguy-Robertson A., Peng Y. (2011). Comparison of different vegetation indices for the remote assessment of green leaf area index of crops. Remote Sensing of Environment 115 (2011) 3468–3478.

APPENDIX 1: LADWP LINE POINT TRANSECT DATA AGGREGATED TO PARCEL LEVEL AND COMPARED TO AVERAGE SLAI OF THE PARCEL
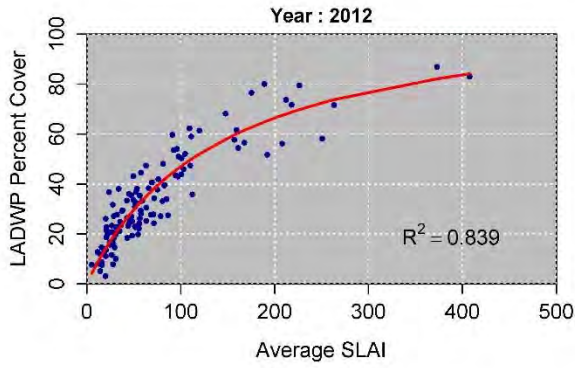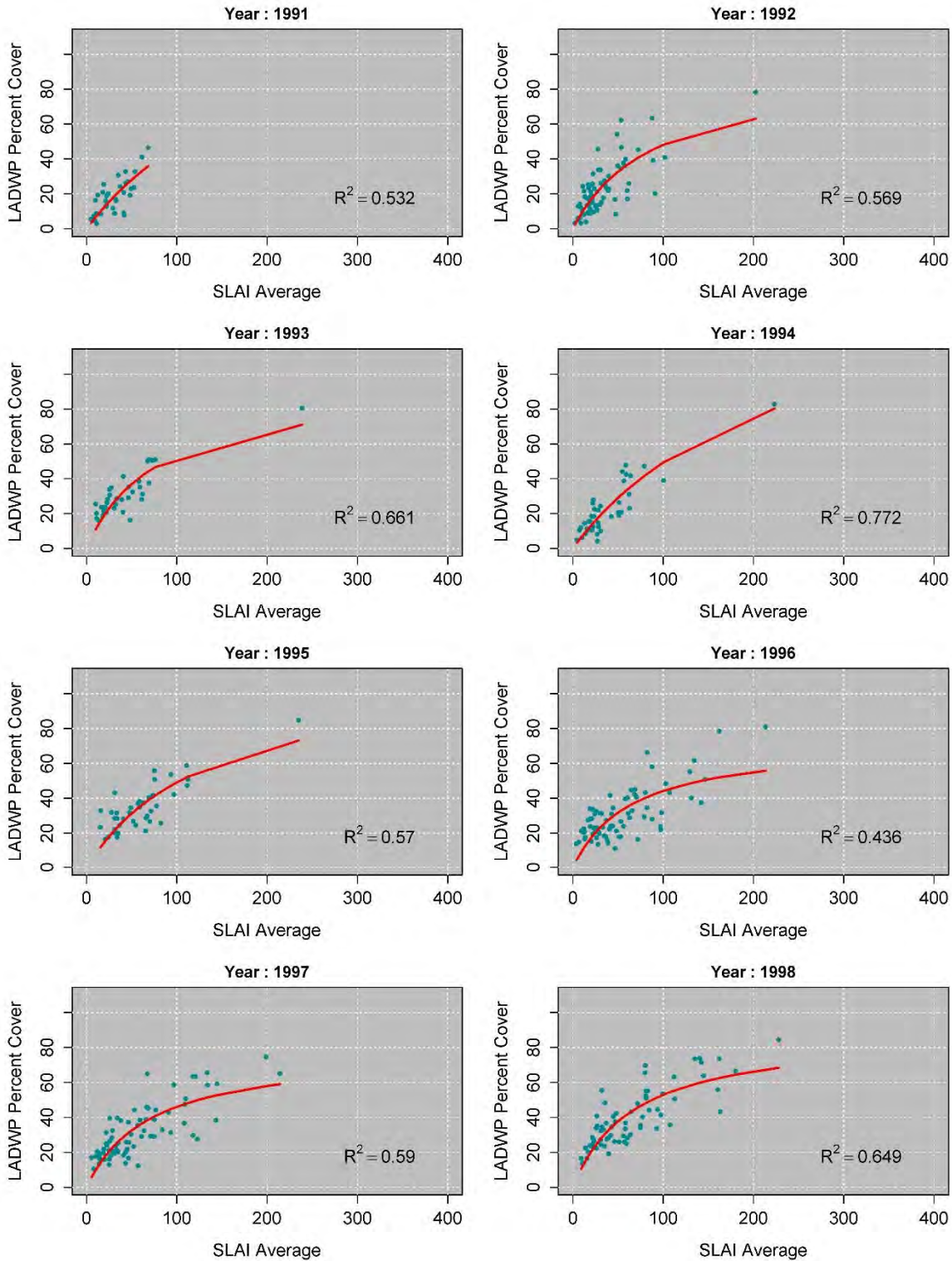
Field Dataset: DWP Line Point Percent Cover (Y-axis)
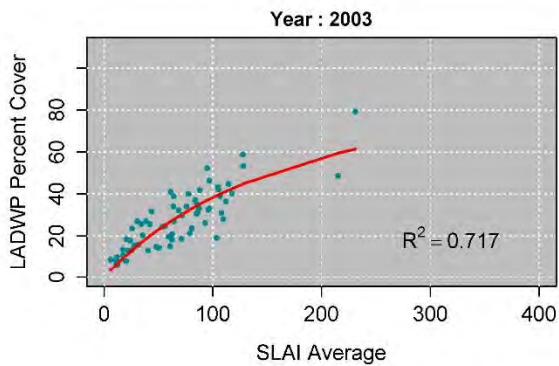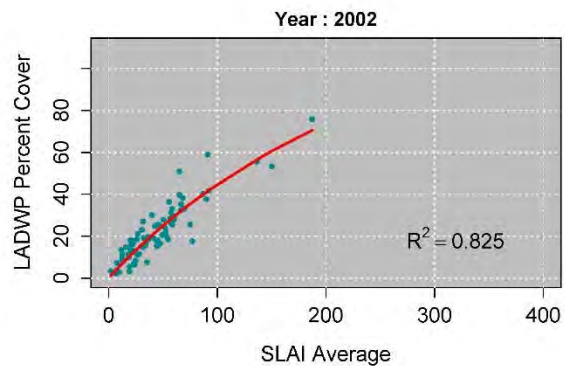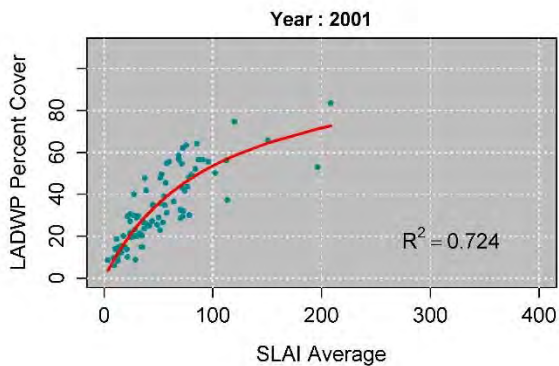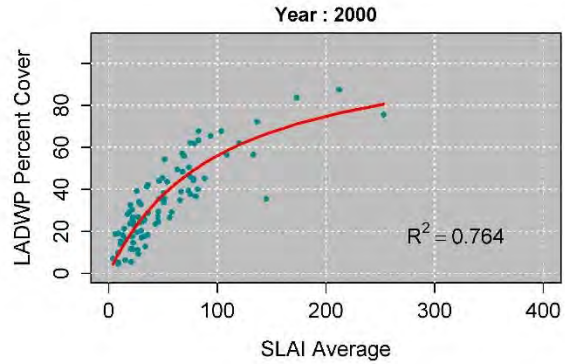Remote Sensing Dataset: Average Seasonal LAI of parcels (X-axis)

Figure below shows the relationship between DWP Percent Cover and Average Seasonal LAI for entire dataset from 1991 to 2014.
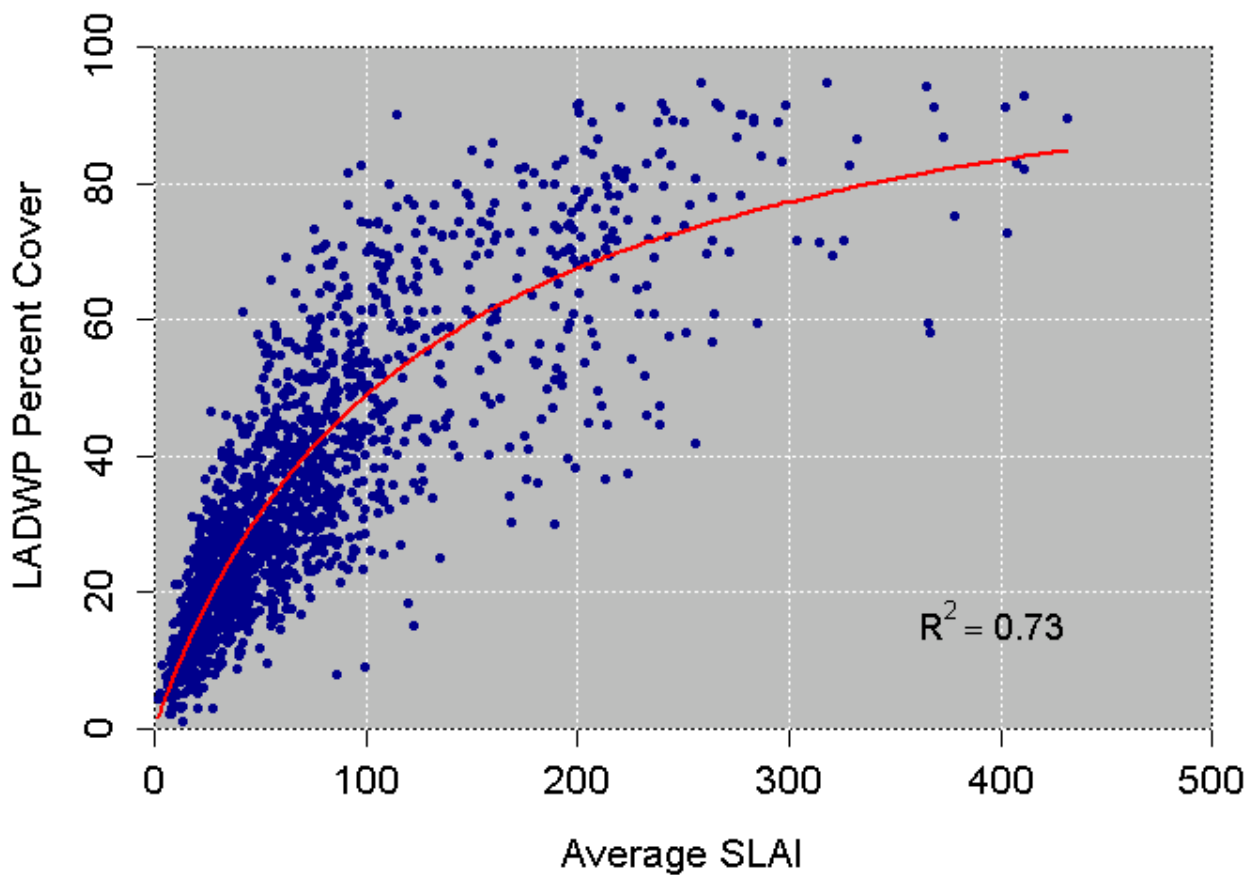
Figures below show the relationship between DWP Percent Cover and Average Seasonal LAI segregated by year from 2004 to 2015.
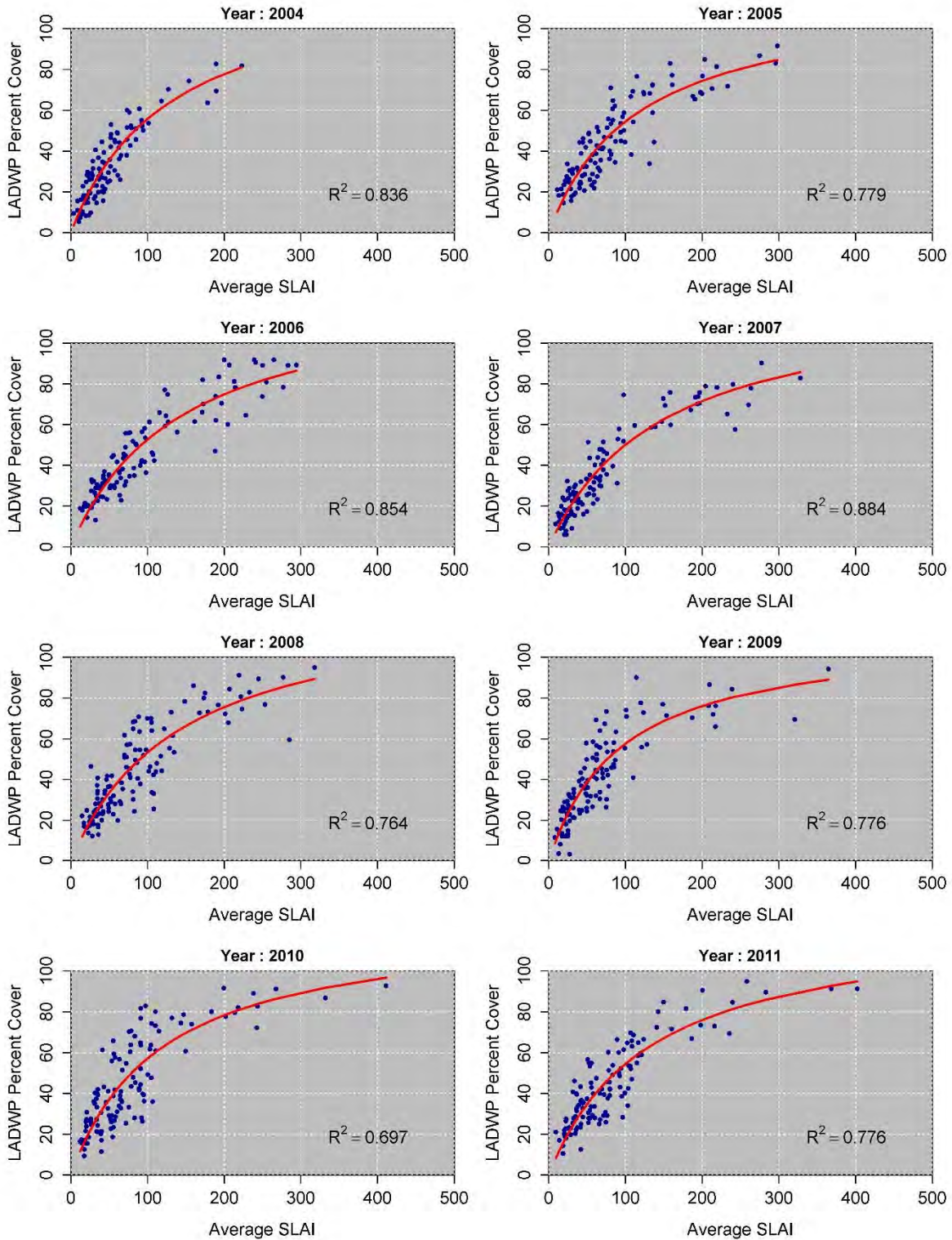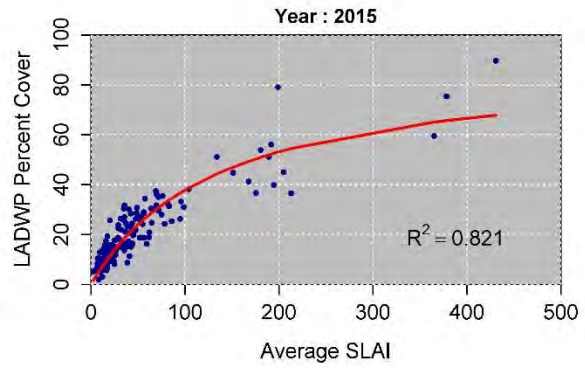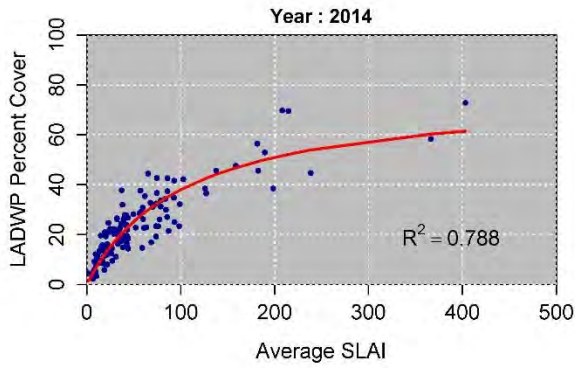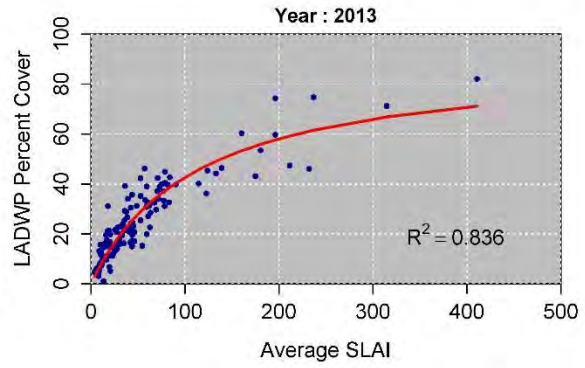
APPENDIX 2: ICWD LINE POINT TRANSECT DATA AGGREGATED TO PARCEL LEVEL AND COMPARED TO AVERAGE SLAI OF THE PARCEL
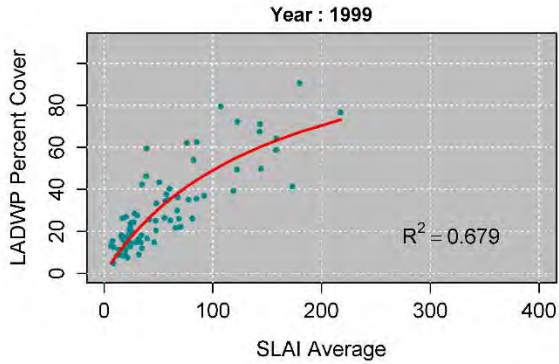
Field Dataset: ICWD Line Point Percent Cover (Y-axis)
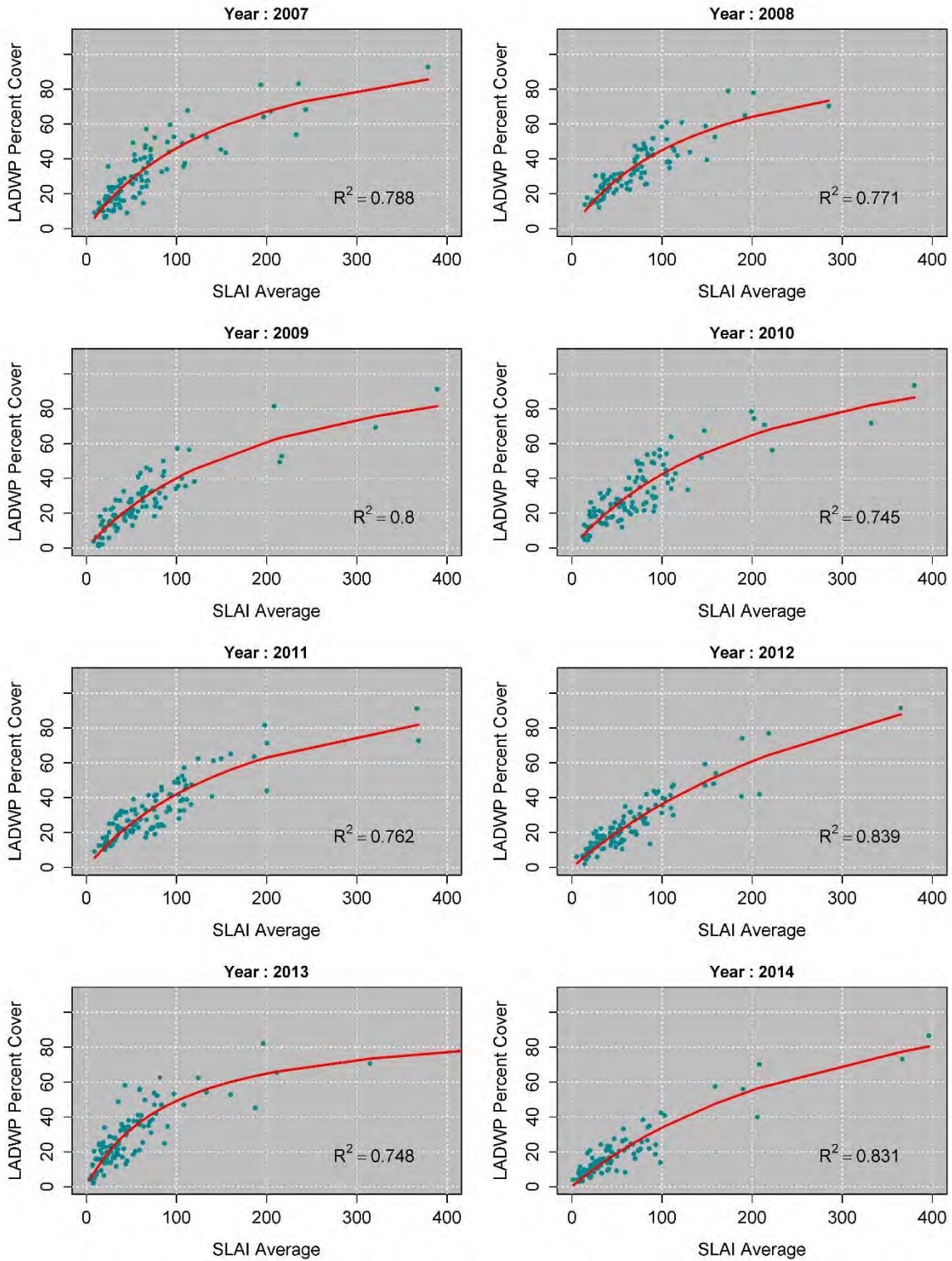Remote Sensing Dataset: Average Seasonal LAI of parcels (X-axis)

Figure below shows the relationship between ICWD Percent Cover and Average Seasonal LAI for entire dataset from 1991 to 2014.
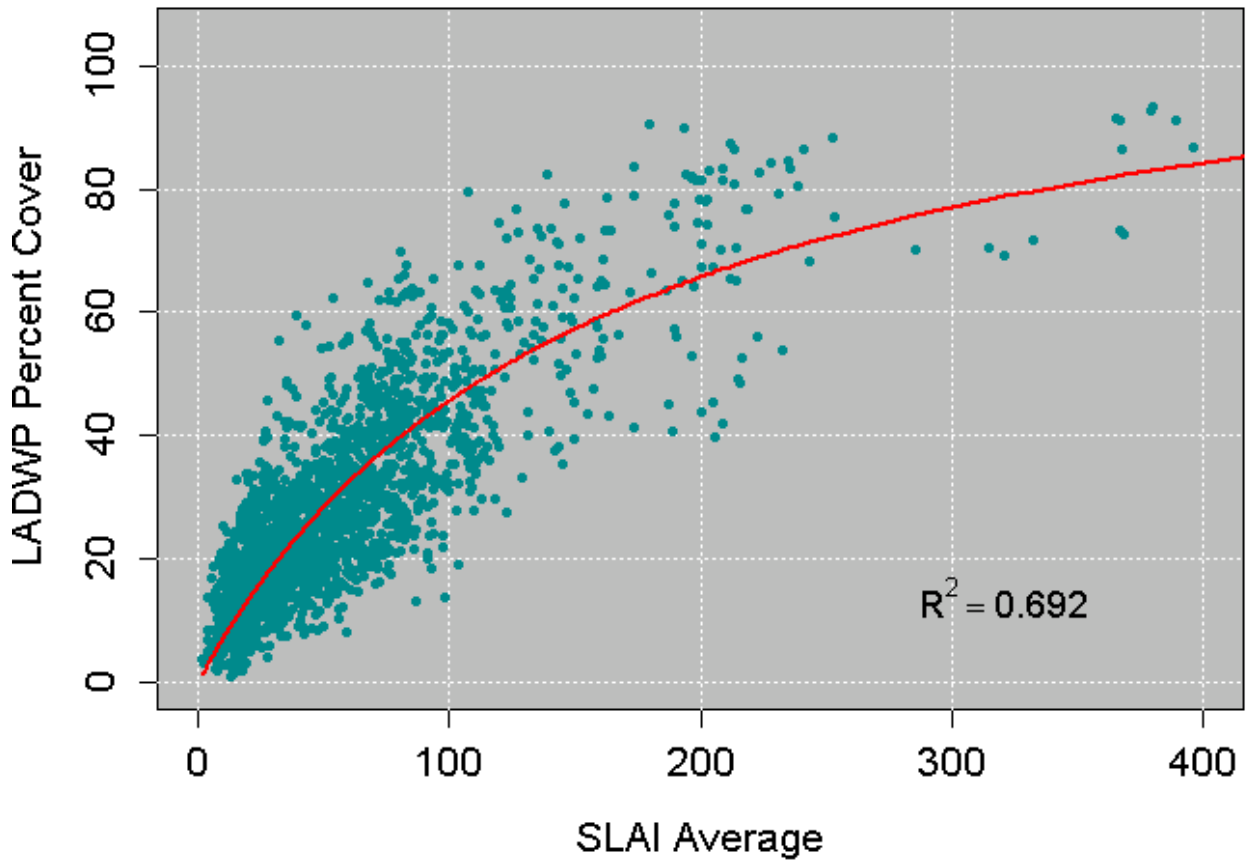
Figures below show the relationship between ICWD Percent Cover and Average Seasonal LAI segregated by year from 1991 to 2014.

Year : 1999

LADWP Percent Cover

$R^2 = 0.679$

SLAI Average

Year : 2000

LADWP Percent Cover

$R^2 = 0.764$

SLAI Average

Year : 2001

LADWP Percent Cover

$R^2 = 0.724$

SLAI Average

Year : 2002

LADWP Percent Cover

$R^2 = 0.825$

SLAI Average

Year : 2003

LADWP Percent Cover

$R^2 = 0.717$

SLAI Average

Year : 2004

LADWP Percent Cover

$R^2 = 0.838$

SLAI Average

Year : 2005

LADWP Percent Cover

$R^2 = 0.733$

SLAI Average

Year : 2006

LADWP Percent Cover

$R^2 = 0.804$

SLAI Average

Appendix 3: TRANSECT LEVEL COMPARISON OF LADWP PERMANENT TRANSECT VEGETATION COVER TO LAI AND SLAI

LADWP has approximately 35 permanent transects, below is plots for 9 transects. Remaining would be provided in the final report.

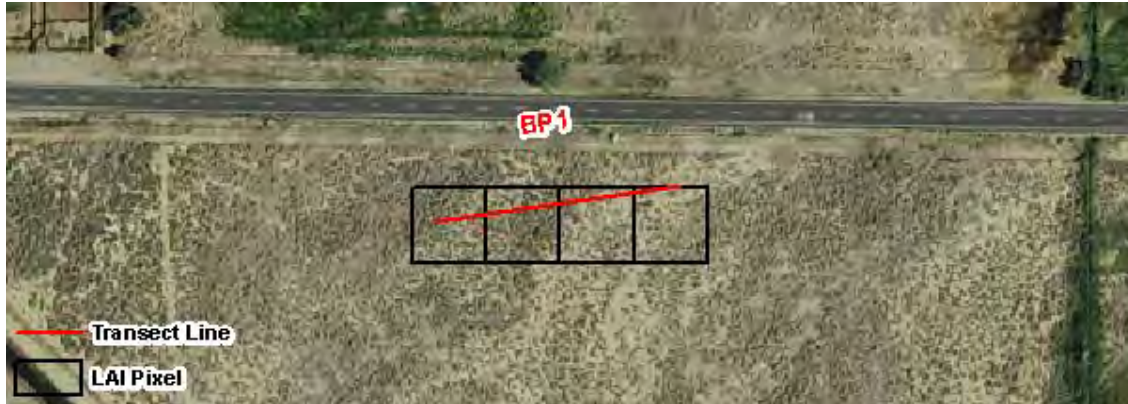*DWP Permanent Transect Name: BP1*

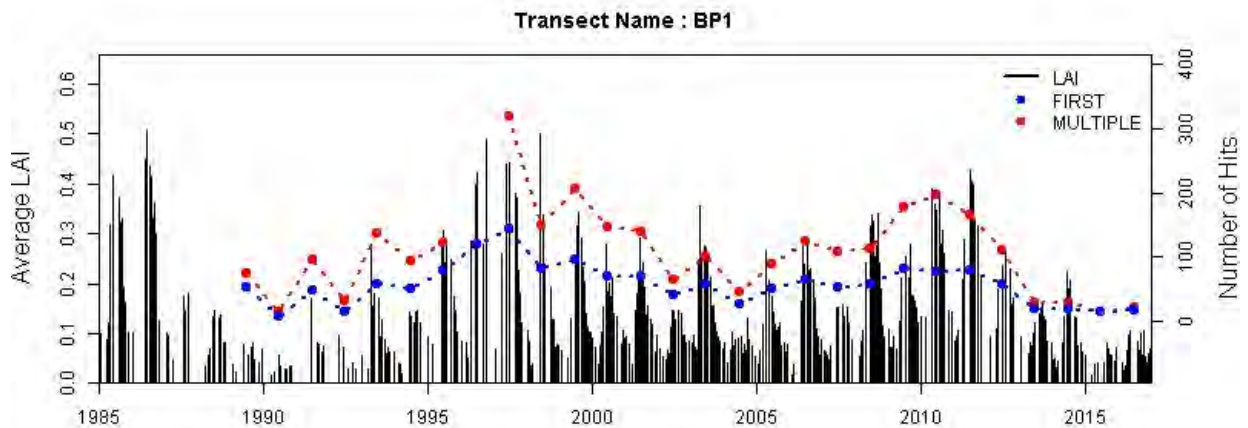Figure above shows the transect line and LAI pixels on 2014 NAIP imagery

Chart above shows the trend of average LAI of all the pixels (black polygon) and FIRST Hit DWP Line Point Field dataset
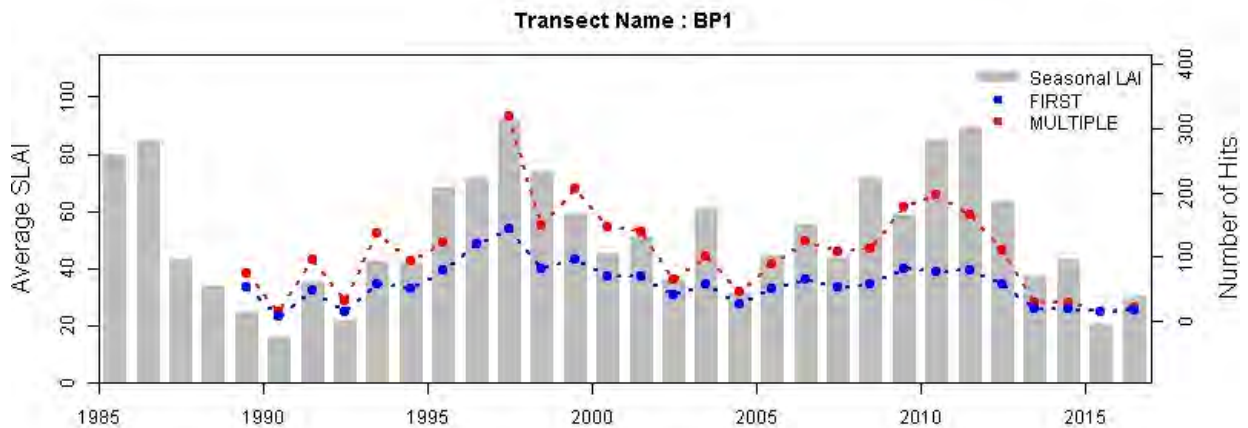

Chart above shows the trend of average Seasonal LAI of all the pixels (black polygon) and MULTIPLE Hit DWP Line Point Field dataset
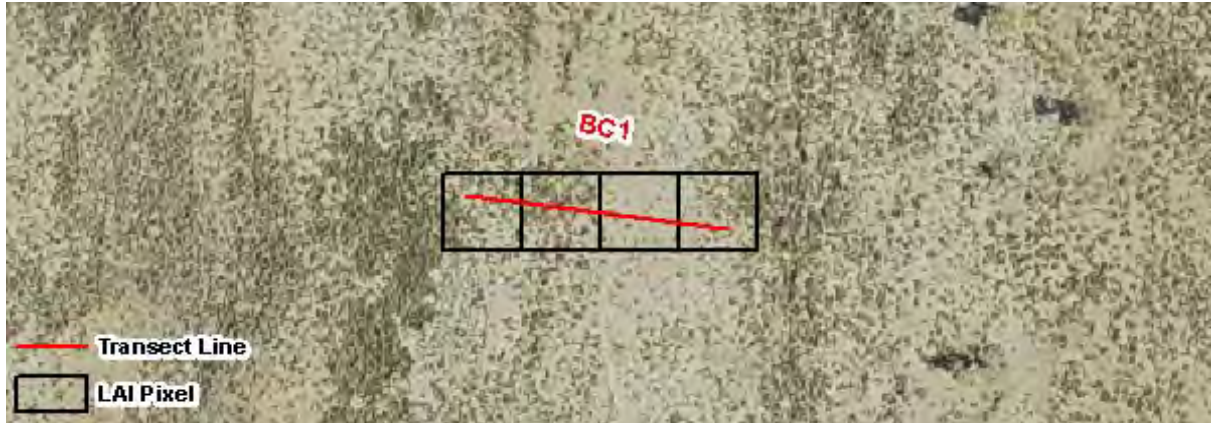
DWP Permanent Transect Name: BC1

Figure above shows the transect line and LAI pixels on 2014 NAIP imagery
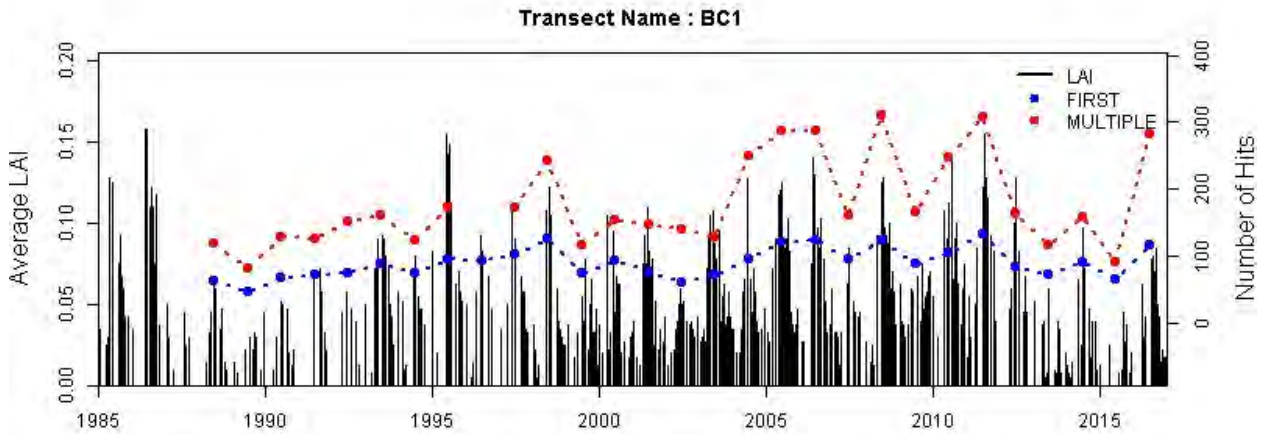

Chart above shows the trend of average LAI of all the pixels (black polygon) and FIRST Hit DWP Line Point Field dataset

Chart above shows the trend of average Seasonal LAI of all the pixels (black polygon) and MULTIPLE Hit DWP Line Point Field dataset

DWP Permanent Transect Name: BC2

Figure above shows the transect line and LAI pixels on 2014 NAIP imagery

Chart above shows the trend of average LAI of all the pixels (black polygon) and FIRST Hit DWP Line Point Field dataset
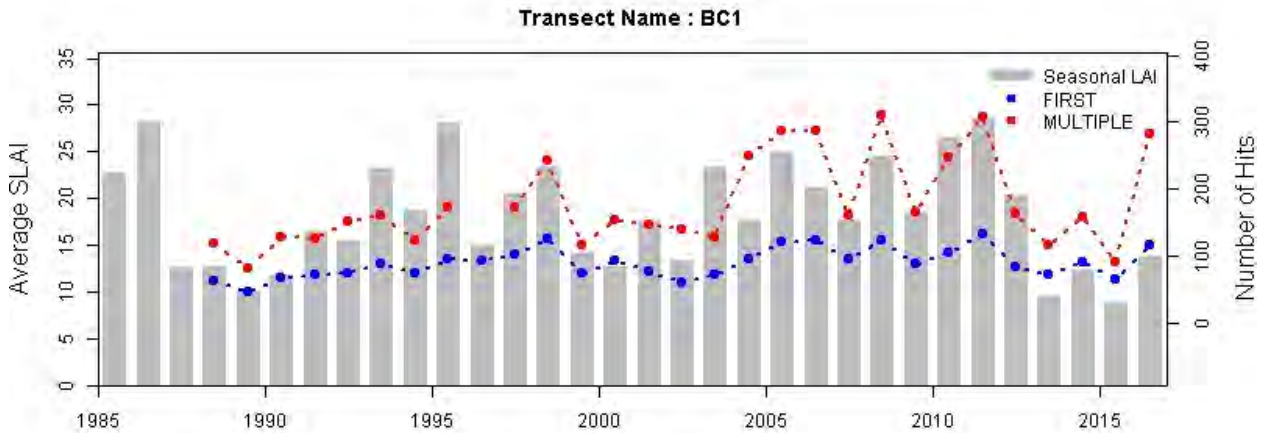

Chart above shows the trend of average Seasonal LAI of all the pixels (black polygon) and MULTIPLE Hit DWP Line Point Field dataset
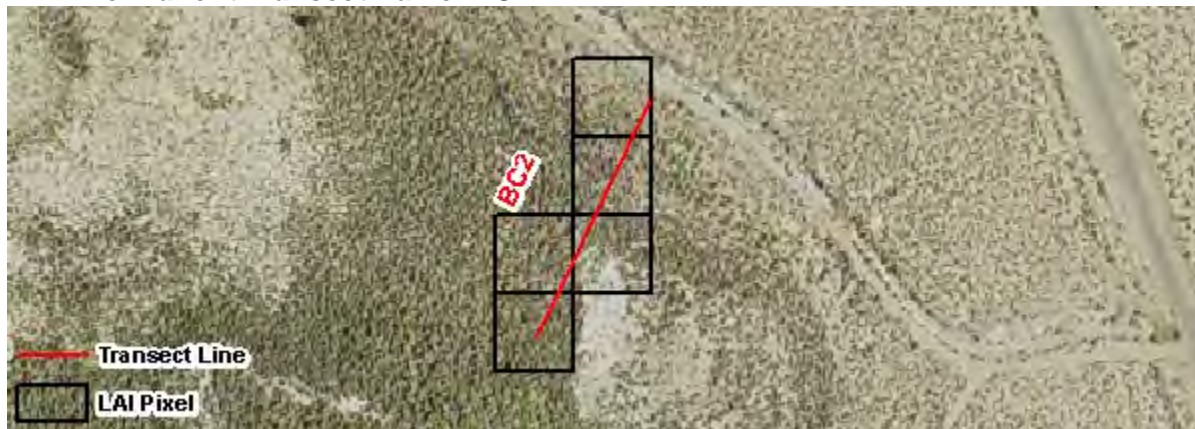
DWP Permanent Transect Name: BC3

Figure above shows the transect line and LAI pixels on 2014 NAIP imagery
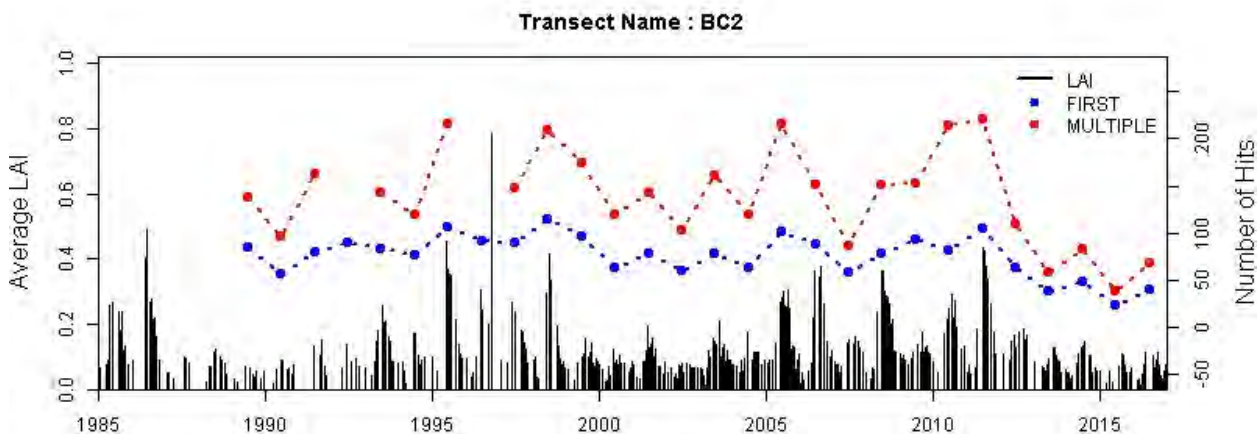

Chart above shows the trend of average LAI of all the pixels (black polygon) and FIRST Hit DWP Line Point Field dataset

Chart above shows the trend of average Seasonal LAI of all the pixels (black polygon) and MULTIPLE Hit DWP Line Point Field dataset

DWP Permanent Transect Name: BP2

Figure above shows the transect line and LAI pixels on 2014 NAIP imagery

Chart above shows the trend of average LAI of all the pixels (black polygon) and FIRST Hit DWP Line Point Field dataset
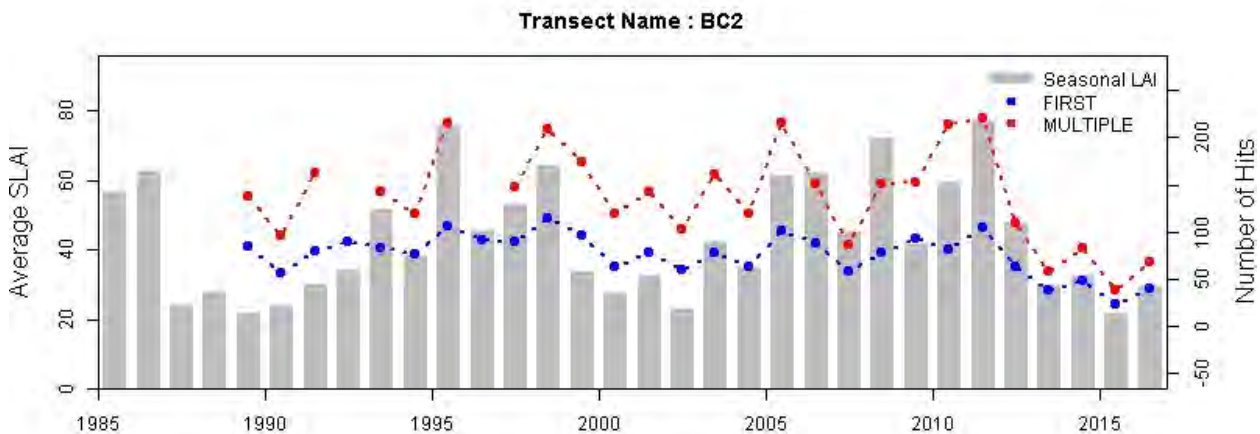

Chart above shows the trend of average Seasonal LAI of all the pixels (black polygon) and MULTIPLE Hit DWP Line Point Field dataset
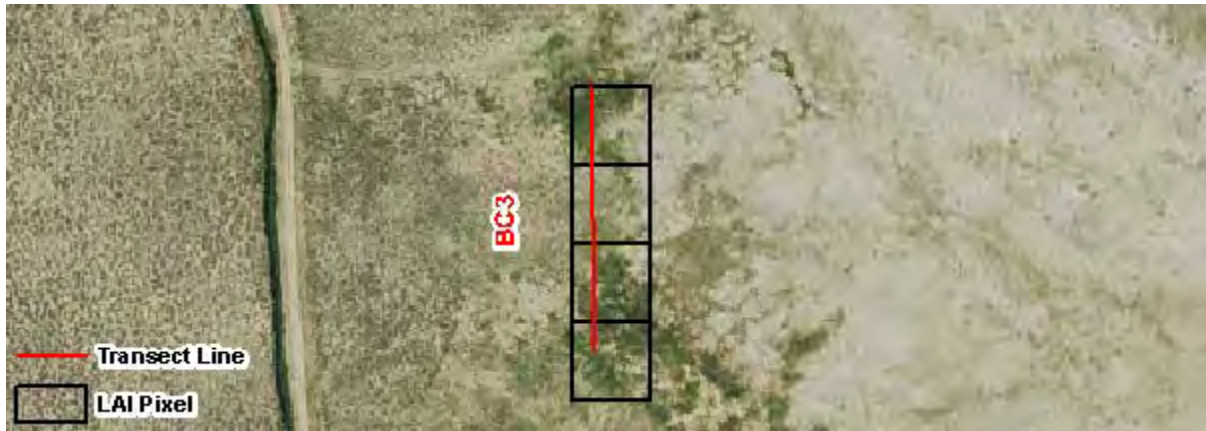
DWP Permanent Transect Name: BP3

Figure above shows the transect line and LAI pixels on 2014 NAIP imagery
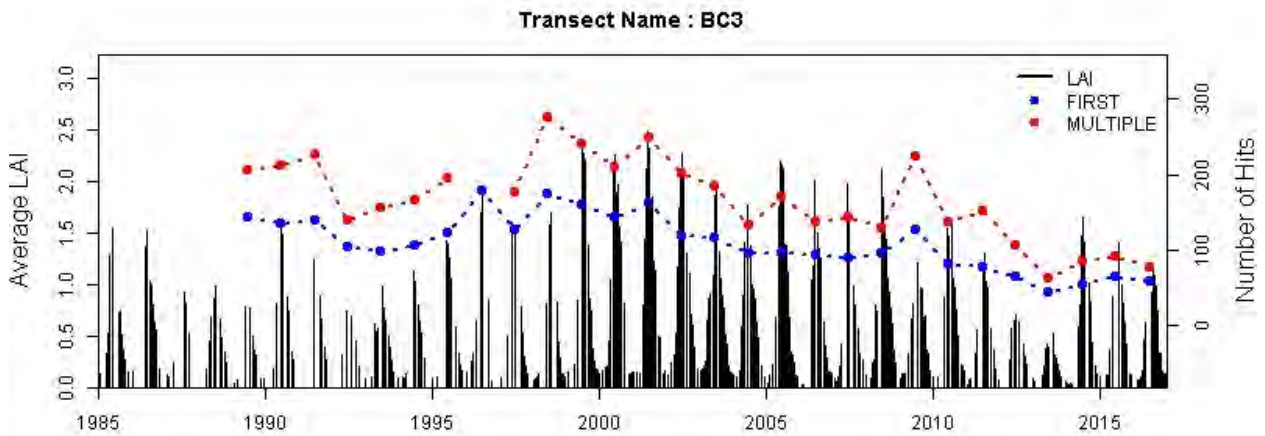

Chart above shows the trend of average LAI of all the pixels (black polygon) and FIRST Hit DWP Line Point Field dataset

Chart above shows the trend of average Seasonal LAI of all the pixels (black polygon) and MULTIPLE Hit DWP Line Point Field dataset

DWP Permanent Transect Name: BP4

Figure above shows the transect line and LAI pixels on 2014 NAIP imagery
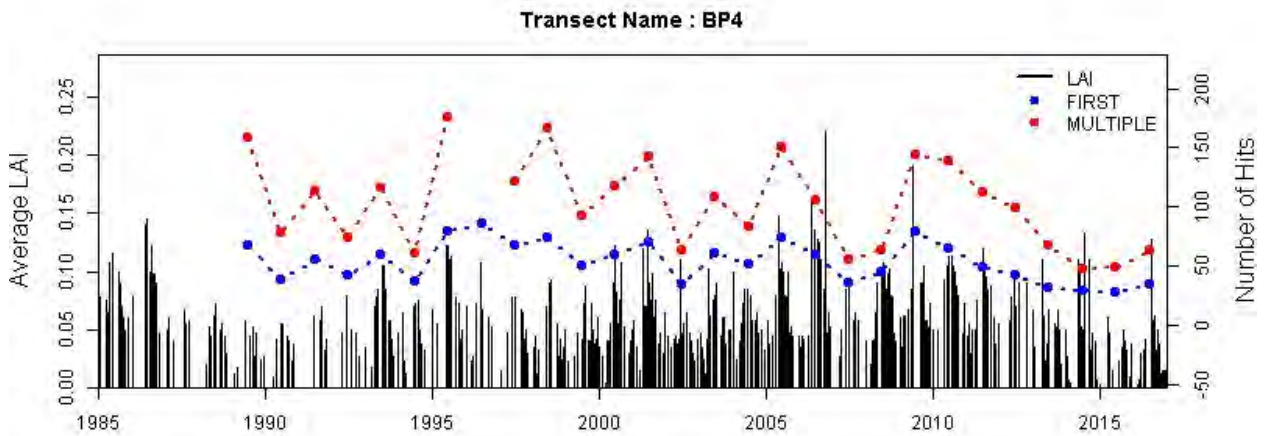
Chart above shows the trend of average LAI of all the pixels (black polygon) and FIRST Hit DWP Line Point Field dataset
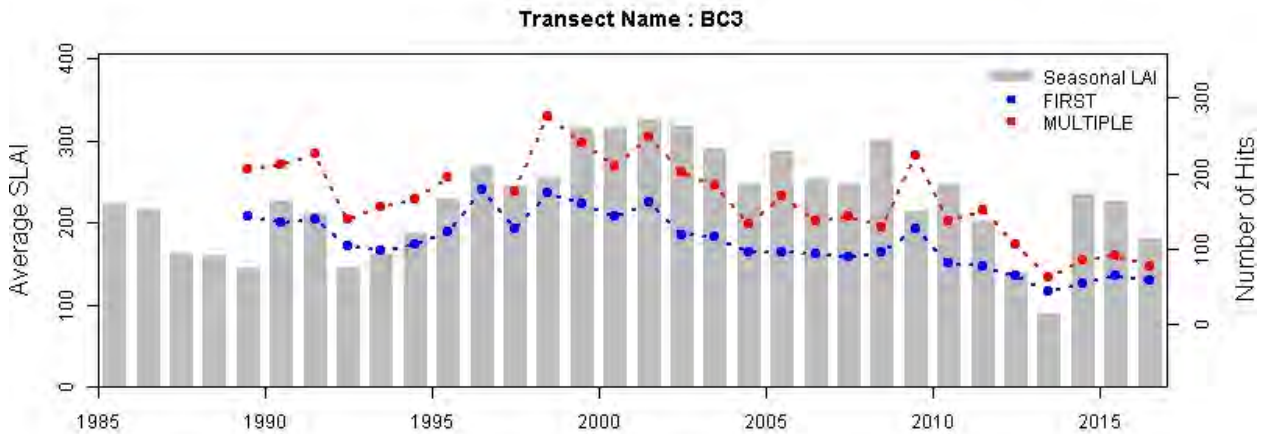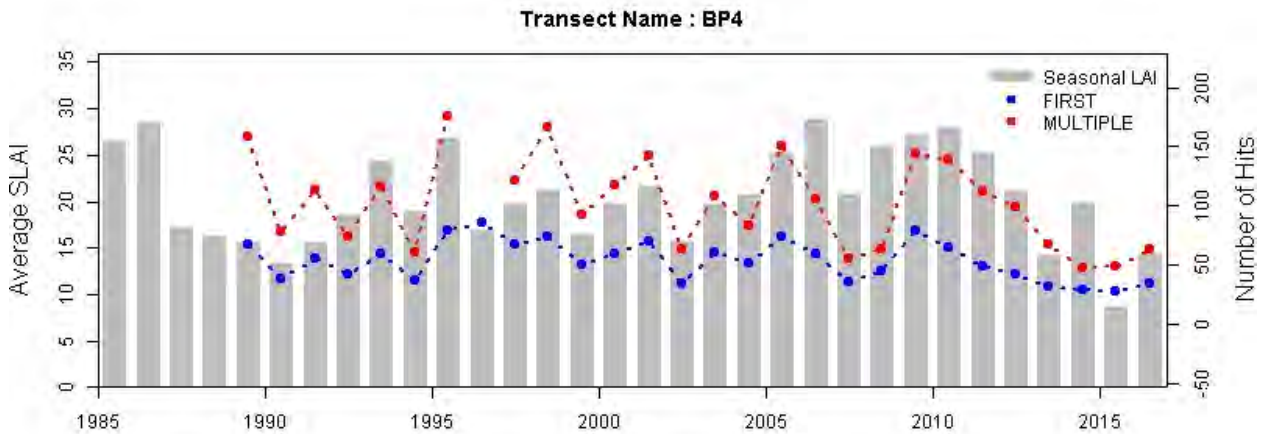

Chart above shows the trend of average Seasonal LAI of all the pixels (black polygon) and MULTIPLE Hit DWP Line Point Field dataset

DWP Permanent Transect Name: L1
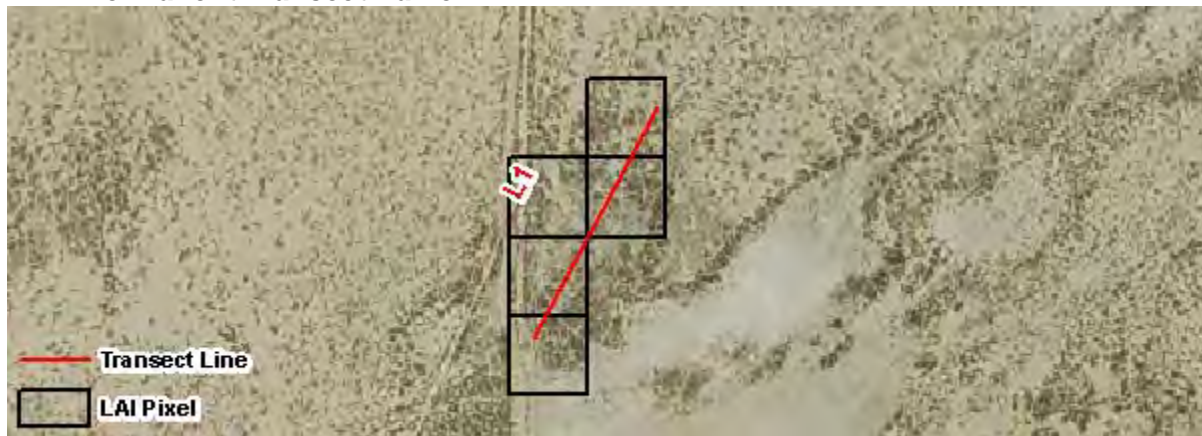
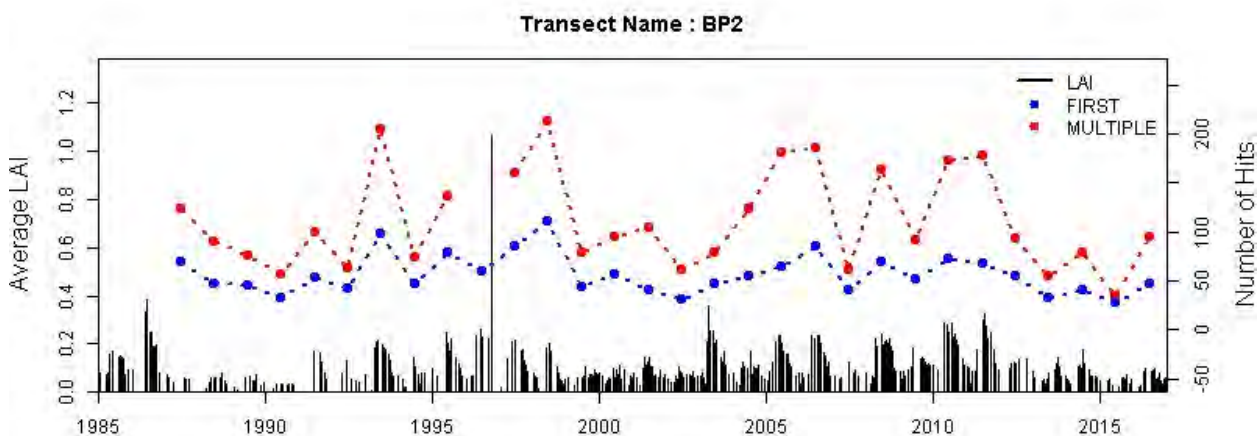Figure above shows the transect line and LAI pixels on 2014 NAIP imagery
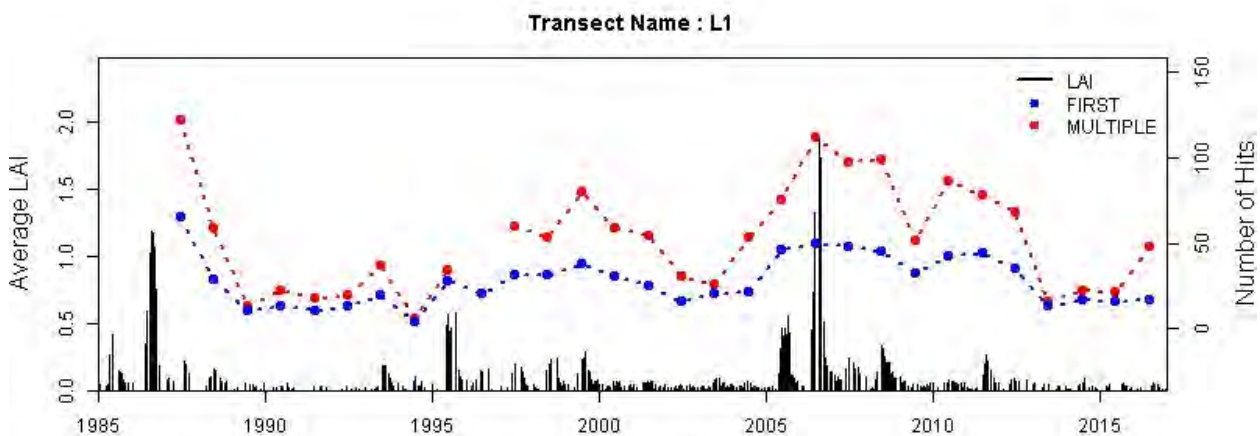
Chart above shows the trend of average LAI of all the pixels (black polygon) and FIRST Hit DWP Line Point Field dataset
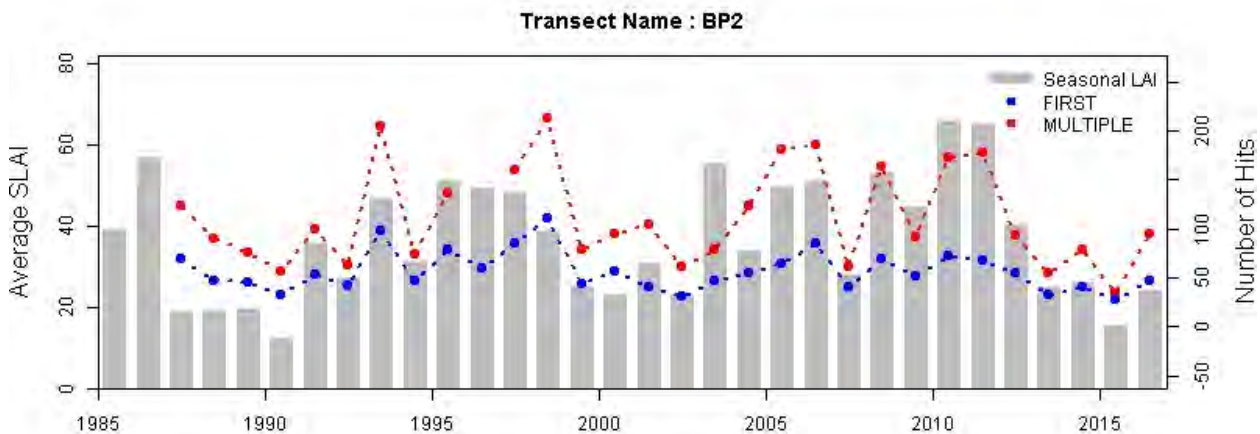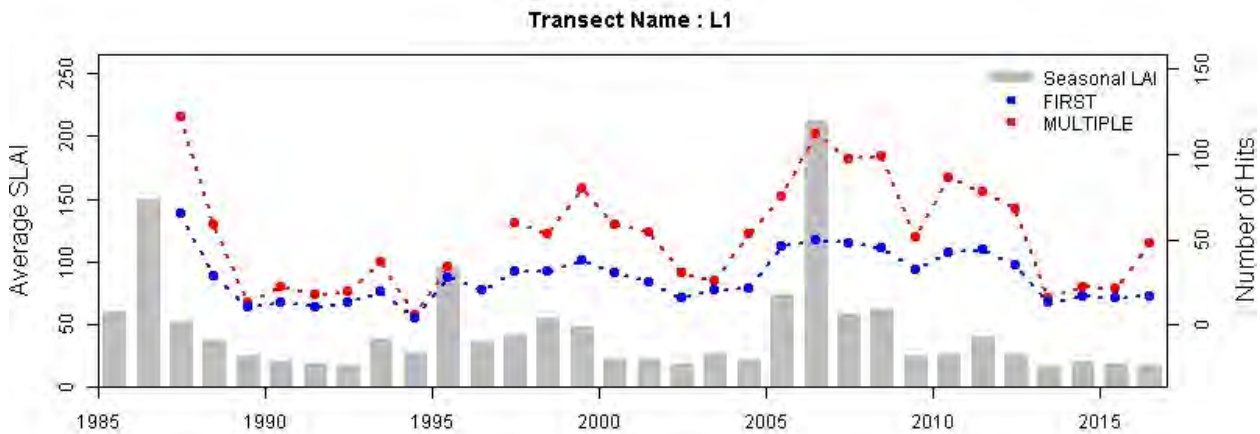

Chart above shows the trend of average Seasonal LAI of all the pixels (black polygon) and MULTIPLE Hit DWP Line Point Field dataset
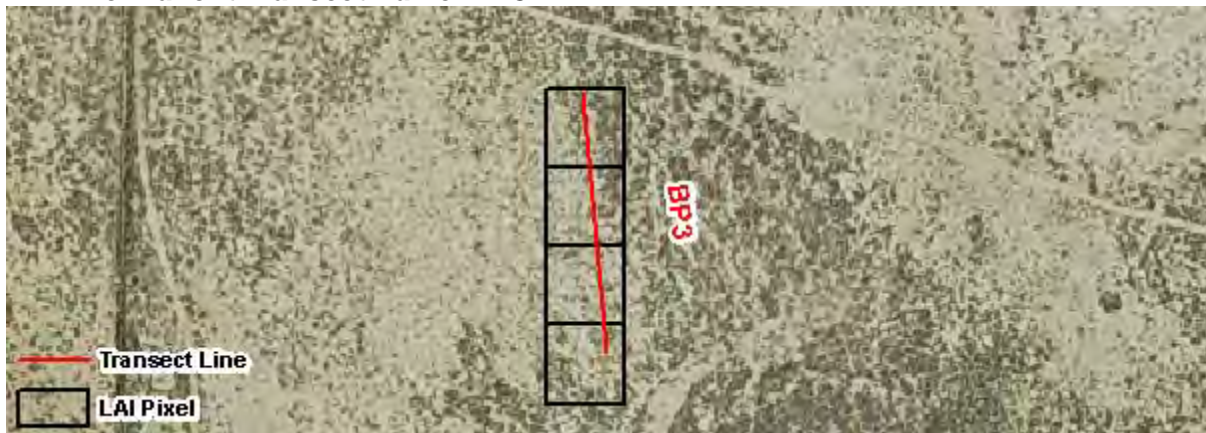
DWP Permanent Transect Name: L2
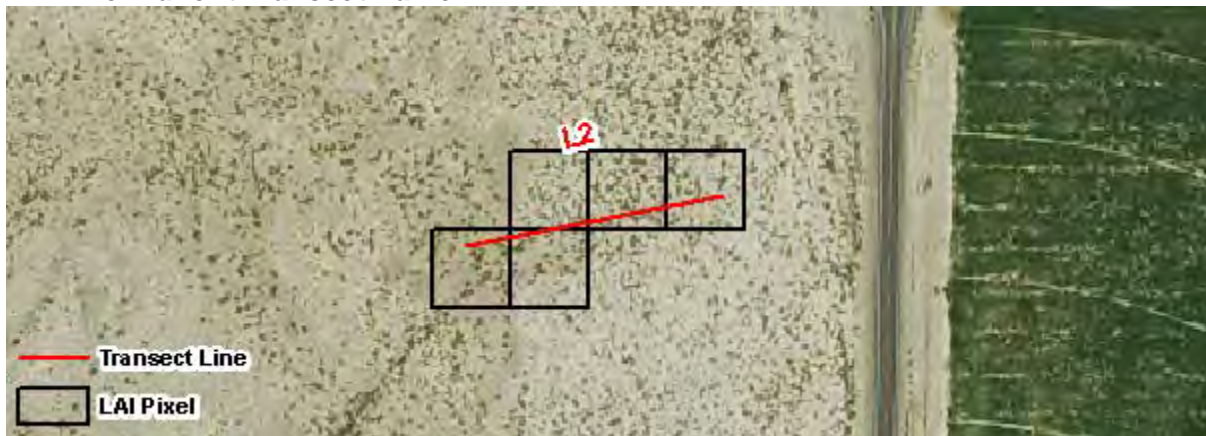
Figure above shows the transect line and LAI pixels on 2014 NAIP imagery
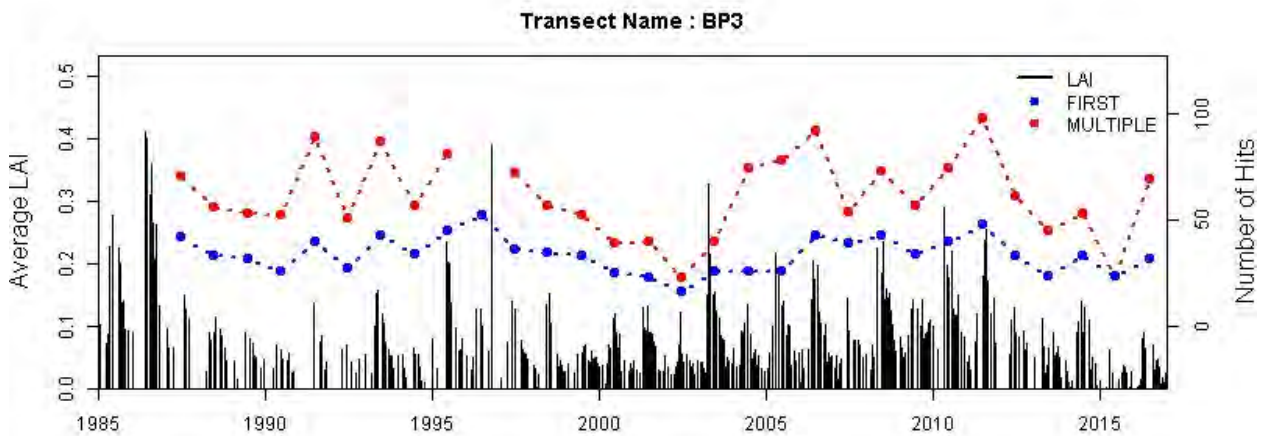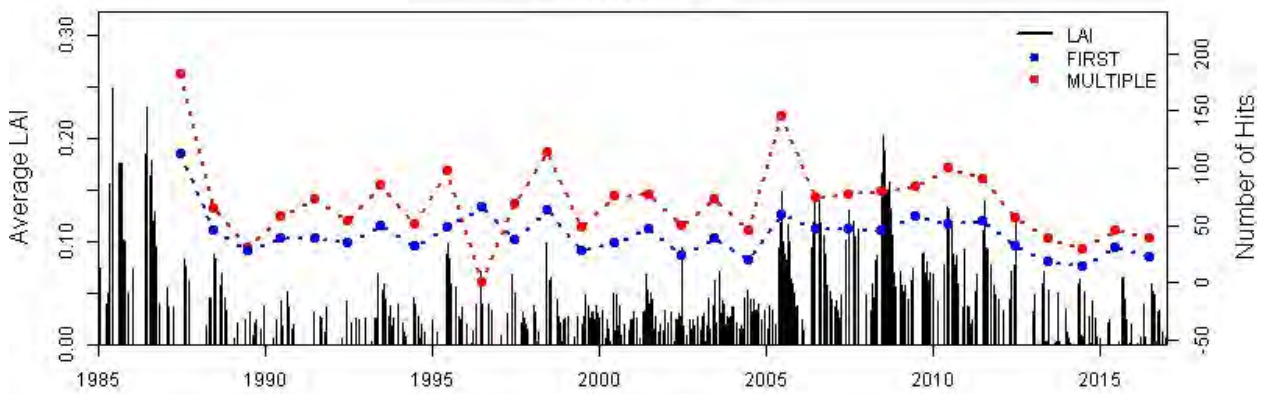

Chart above shows the trend of average LAI of all the pixels (black polygon) and FIRST Hit DWP Line Point Field dataset
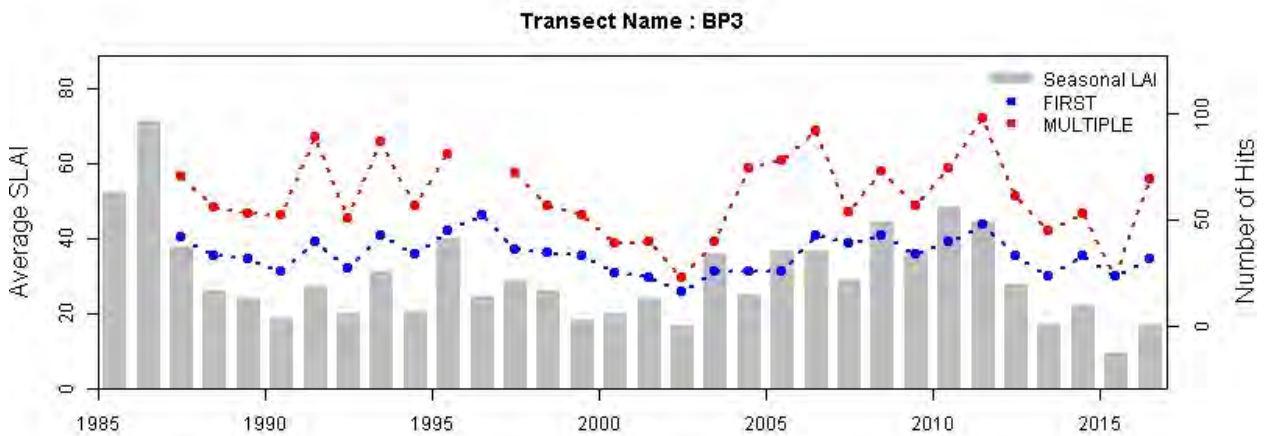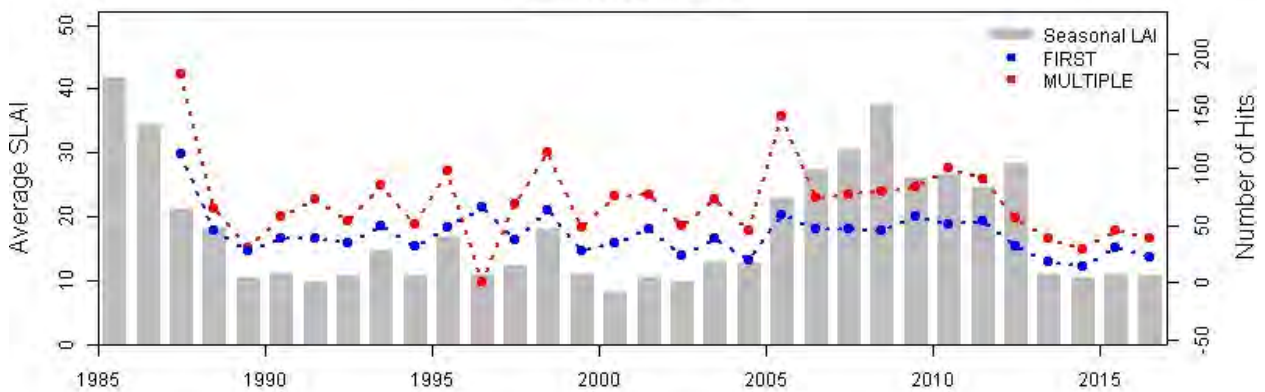

Chart above shows the trend of average Seasonal LAI of all the pixels (black polygon) and MULTIPLE Hit DWP Line Point Field dataset

APPENDIX C

TM 8.3.1 – EVAPOTRANSPIRATION MAPPING

TECHNICAL MEMORANDUM

Title: TM 8.3.1 – Evapotranspiration Mapping

Project: Task Order 008 – Remote Sensing Pilot Project Implementation

Client: Los Angeles Department of Water and Power

Date: May 2017

TABLE OF CONTENTS

LIST OF FIGURES

LIST OF TABLES

ACRONYMS / ABBREVIATIONS

CIMIS	California Irrigation Management Information System
DWR	California Department of Water Resources
EC	Eddy Covariance
ET	Evapotranspiration
ETa	Actual Evapotranspiration
ETo	Reference Evapotranspiration
GIS	Geographical Information System
ICWD	Inyo County Water Department
LADWP	Los Angeles Department of Water and Power
LAI	Leaf Area Index
METRIC	Mapping Evapotranspiration at High Resolution Using Internal Calibration
MODIS	Moderate Resolution Imaging Spectroradiometer
NASA	National Aeronautics and Space Administration
RS	Remote Sensing
SEBAL	Surface Energy Balance Algorithm for Land
SEBS	Surface Energy Balance System
TM	Technical Memorandum
TSM	Two Source Model
USGS	United States Geological Survey

EXECUTIVE SUMMARY

This Technical Memorandum (TM 8.3.1) has been prepared in support of the Remote Sensing Pilot Project Implementation for the Owens Valley area. TM 8.3.1 describes the steps involved in the development of remote sensing based actual evapotranspiration (ETa) dataset and its validation. Validation of spatial ETa estimates against eddy covariance data shows good agreement. Results suggest that the remote sensing based spatial ETa mapping has the potential to be developed as an operational tool for managing water resource and monitoring vegetation in the groundwater-dependent ecosystem of Owens Valley.

1.0 INTRODUCTION

This Technical Memorandum (TM) has been prepared in support of the Remote Sensing Pilot Project Implementation for the Owens Valley area and represents the deliverable for Subtask 8.3 of Task Order 008 of Agreement No. 47381-6. As conceived in the Remote Sensing Work Plan (MWH, 2016), key findings from the Pilot Project are documented in brief periodic TMs. These TMs are not intended to contain extensive introductory material, but instead are intended to focus on the results of specific portions of the work. A listing of the key TMs associated with this work is summarized in **Table 1**, with the highlighted TM 8.3.1 presented in this document. TM 8.3.1 describes the steps involved in the development of remote sensing based actual evapotranspiration (ETa) dataset and its validation.

Table 1
Summary of Technical Memoranda

Task	TM Number	Subject
1 - Imagery Download, Preparation, and Preprocessing	TM 8.1	Imagery, cloud screening results, and radiometrically corrected imagery
2 - Leaf Area Index Image Analysis	TM 8.2	Leaf area index (LAI) image analysis, comparison of LADWP and ICWD historical data with remote sensing results, sampling scheme for collecting ground truth data
3 - Evapotranspiration (ET) Mapping and Options for Integration	TM 8.3.1	Surface Energy Balance System (SEBS) ET delivery, SEBS ET development and validation
	TM 8.3.2	Integration of Spatial ETa into the Bishop/Laws groundwater model
	TM 8.3.3	Estimation of historical Eta from agriculture in the Chalfant, Hammil, and Benton Valleys

2.0   PURPOSE AND OBJECTIVES OF TM

As part of water resources and vegetation management related to the Inyo/LA Long-Term Water Agreement, both the Los Angeles Department of Water and Power (LADWP) and the Inyo County Water Department (ICWD) conduct vegetation monitoring in the Owens Valley. The "Green Book" provides the protocols to undertake this management and monitoring procedures. The Green Book acknowledges that Remote Sensing (RS) is a valuable tool for mapping and monitoring vegetation and endorses its development for Owens Valley. The overarching purpose of the current work is to evaluate the possibility of augmenting, or potentially replacing, some of the current methods of vegetation monitoring and ET estimation in the Owens Valley through the use of remote sensing technology.

The vegetation monitoring is translated into evapotranspiration (ET) estimates for comparison to available soil water and ultimately to projected plant-soil water balance. The Green Book defines the following five (5) vegetation classes (**Table 2**), which are primarily classified by water consumptive use.

Table 2
Green Book Vegetation Classes

Vegetation Class	Description
A	Average ET less than or equal to 5.76 inches
B	Scrub communities with annual ET greater than estimated average precipitation
C	Grass dominant vegetation with estimated annual ET greater than quadrangle-average precipitation. The quadrangle-average precipitation was computed from maps of isohyetal contours
D	Riparian vegetation with annual average ET greater than precipitation
E	All vegetation whose ET requirement is fulfilled by irrigation water

The goal of the vegetation monitoring as mandated in the Green Book and conducted by LADWP and ICWD was to assign vegetation types A through E by first calculating the average ET of each community. The relationship between Transpiration and Leaf Area Index (LAI) was developed for each species as a function of day of the year. Annual field measurements of LAI were used for calculating plant water requirement using the developed relationship.

In 2000, ICWD and LADWP began a cooperative study designed to compare methods of forecasting plant water requirements based on vegetation leaf area with independent micrometerological measurements of ET. Towers equipped with eddy covariance (EC) sensors to measure the vertical flux of heat and water vapor were installed at seven sites over four growing seasons (Harrington et. al., 2004). Data from this study was used to validate the ET estimates generated from the remote sensing-based full energy balance algorithm.

The specific objective of Subtask 8.3 was to: 1) develop remote-sensing based estimates of ET and 2) test the performance against eddy covariance measurements of ET.

3.0   SUMMARY OF WORK CONDUCTED

A summary of work conducted is described in this section.

3.1   Field Observation Data

In the Inyo/LA Cooperative Study (Harrington et. al., 2004) conducted during the 2000-2003 period, ET was measured extensively using EC. EC measurements were collected at seven (7) sites over four (4) years providing 12 site-year combinations (**Table 3**). This dataset provides an independent measurement of actual evapotranspiration (ETa) that can be compared to estimates from the remote sensing based algorithm. Four sets of observed/estimated data were available:

1) ET from eddy covariance measurement

2) ET from Green Book method

3) ET from crop coefficient method

4) ET from a fitted Fourier series (Note - more details on this dataset is included in Harrington et. al., 2004)

Table 3
Details of Eddy Covariance Measurements

Station Code	Veg Code & Type		Latitude	Longitude	Year			
					2000	2001	2002	2003
FSL138	AM2	Alkali Meadow	37.41	-118.42			Available	
PLC018	RBS	Rabbitbrush Scrub	37.36	-118.35			Available	
PLC074	SBM	Nevada Saltbush Meadow	37.32	-118.36			Available	Available
PLC045	SBS	Nevada Saltbush Scrub	37.33	-118.35		Available		
PLC185	DSS	Desert Sink Scrub	37.27	-118.33			Available	Available
BLK009	RBM	Rabbitbrush Meadow	36.98	-118.22		Available		
BLK100	AM1	Alkali Meadow	36.89	-118.23	Available	Available	Available	Available

3.2   Remote Sensing Method for ET Estimation

Remote sensing algorithms based on the equilibrium between the radiation balance and energy balance at the surface of the earth is recognized as the only viable means to map regional- and field-scale patterns of ETa. These algorithms provided a robust, economical, and efficient tool for ETa estimations at field and regional scales. Remote sensing based surface energy balance methods have been found to be a reliable method for determination of ET in regions with phreatophytic and riparian vegetation (Eamus et. al., 2015, Hoyos et. al., 2016).

Numerous remote sensing based ET models have been developed in the last three decades to make use of the visible, near-infrared (NIR), shortwave infrared (SWIR), and most importantly, thermal infrared data acquired by sensors onboard satellite platforms. The surface energy balance algorithm can be broadly classified into three widely used models: SEBAL (Surface Energy Balance Algorithm for Land), SEBS (Surface Energy Balance System) and TSM (Two Source Model). All of these algorithms utilize residual approaches of surface energy balance to estimate ET at different temporal and spatial scales. The energy coming from the sun and atmosphere in the form of short- and long-wave radiation is transformed and used for (a) heating the soil (soil heat flux into the ground), (b) heating the surface environment (sensible heat flux to the atmosphere), and (c) transforming water into vapor (latent heat flux from the crop/soil surfaces). All the energy involved in the soil-vegetation-atmosphere interface can be given as the Energy Balance (EB) equation:

$$R_n = G_o + H + LE$$

where, R_n is the net radiation, G_o is the soil heat flux, H is the sensible heat flux, and LE is the latent heat flux, with all units expressed in watt per square meter (Wm^{-2}). Latent heat is expressed as hourly ET (mm) (by dividing LE by the latent heat of vaporization and the density of water). A brief description of the SEBS algorithm used in this work is described in the following section.

3.3   Surface Energy Balance System (SEBS)

SEBS, developed by Bob Su (Su, 2002), is a peer reviewed extensively applied remote sensing-surface energy balance algorithms used in regional- and field-scale mapping of ETa. The SEBS model provides an improved and detailed parameterization for estimation of surface heat fluxes, producing robust ETa estimates over a wide range of land cover. In algorithms like SEBAL and METRIC, a process called 'hot and cold pixel' calibration is required to develop temperature gradient relationship; however, this process is subjective to analyst decision, thus producing variable results. Instead, SEBS uses a physically based temperature gradient-resistance model to automate this process in a robust, peer reviewed approach.

Surface Energy Balance System (SEBS) is a single source, land surface energy balance algorithm with a dynamic model for the thermal roughness and Monin-Obukhov Atmospheric Surface Layer (ASL) similarity for surface layer scaling. SEBS uses an excess resistance term that accounts for the fact that the roughness lengths for heat and momentum are different for canopy and soil surfaces. Primarily, three input data sets are utilized for executing the SEBS:

1) Albedo, emissivity, surface temperature and Normalized Difference Vegetation Index (NDVI) derived from remote sensing data

2) Air pressure, air temperature, relative humidity, and wind speed measurements from weather stations

3) Downward solar radiation

In satellite-based energy balance algorithms, the challenge is in the use of the radiometric temperature (*Ts;* derived from satellite sensor) in lieu of aerodynamic temperature (*To*) required in the sensible heat flux formulation (Harrington and Steinwand, 2003). SEBS uses an excess resistance parameter (kB^{-1}) as a correction factor to resolve this difference between '*To'* and '*Ts'*. SEBS has a detailed parameterization for kB^{-1} applicable over a wide range of land cover. Su (2002), have used analytical and experimental approaches to develop a relationship based on environmental variables, vegetation structural characteristics, multi-layer approach, and simulation results, and provided the formulation for excess resistance to heat transfer parameter:

3.4   Computing Framework for SEBS

A comprehensive image analysis framework was developed for spatially mapping daily actual evapotranspiration (ETa). The core of the framework includes satellite imagery, meteorological data, and a Surface Energy Balance Algorithm (SEBS). The satellite data was acquired from the NASA/USGS Landsat program which represents the world's longest continuously-acquired collection of space-based, moderate-resolution satellite imagery. Landsat provides accurate, routine, and repeated measurements of Earth's land cover and is available at an interval of approximately 8-16 days. All available imagery for path row 42-34 and 41-35 from Landsat satellites 5, 7, and 8 was used in the image analysis framework. Weather information was acquired from the California Irrigation Management Information System (CIMIS) Program. In addition, the daily reference ET (ETo) data for the entire state, resampled to 30m resolution (Spatial CIMIS), is used in the computing framework. The image analysis framework utilizes the weather information from the time of satellite overpass for computing various parameters of the SEBS algorithm. All the weather variables are quality checked and gaps are filled before it is ingested into the framework. A 30m interpolated surface of each weather variable is generated for the date of image acquisition. The image analysis framework includes automatic cloud screening to remove severely cloud-contaminated scenes. Smaller cloud patches in scenes are filtered through a temperature-driven algorithm and assigned 'null' values. Landsat 7 scan line error produces strips of null values in the dataset, these and any other gaps are filled through a spatial interpolation algorithm. Several refinements were performed to improve the accuracy and reliability of these sub-models for local conditions by including atmospheric correction algorithm; daily-reference ET-based extrapolation algorithm and a cloud-screening sub-module. Extensive testing and validation of the output dataset was performed using on-the-ground measurements collected by DWR, University of California, Ameriflux Stations, and several other sources (Paul et. al, 2017a, 2017b). The main output from the framework is an unprecedented, daily 30-meter spatial resolution, ETa dataset.
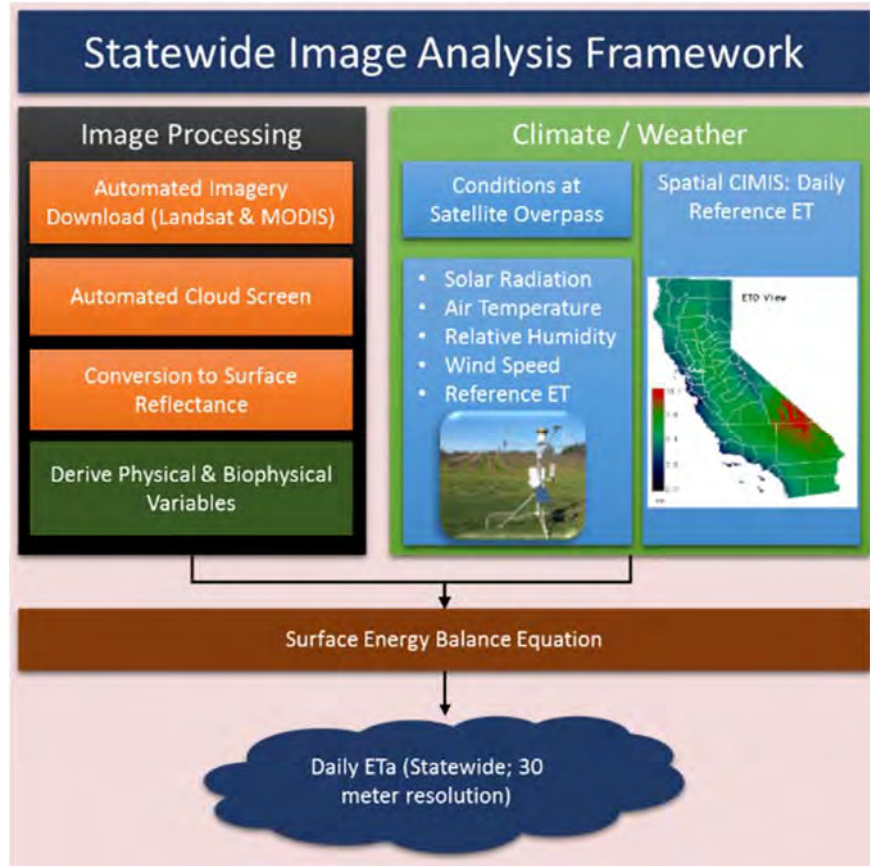
Figure 1
Image Analysis Framework Comprised of Surface Energy Balance Algorithms and Crop Classification Tools

3.5   Evaluation Statistics

The daily ETa estimates generated from the Remote Sensing Algorithm was validated against the measured and modeled dataset collected during the 2000-2003 time range (**Table 3**). Standard and regression statistics (mean, slope, intercept, and coefficient of determination), were used in conjunction with three error index statistics; MBE (mean bias error), MAE (mean absolute error), and RMSE (root mean square error), as well as with a dimensionless performance statistic, NSE (Nash-Sutcliffe efficiency) for a detailed validation. Description and formulation of these performance statistics and error indices follows. In equations described below, n is the number of observations points, O_i and M_i are the observed and model predicted values at each comparison point i, and $\bar{O}$ and $\bar{M}$ are the arithmetic means of the observed and modeled values.

Coefficient of determination (R^2): The coefficient of determination (R^2) describes the proportion of the variance in measured data explained by the model and ranges from 0 to 1 with the greater values indicating less error variance.

$$R^2 \; = \frac{\left(\sum_{i=1}^{n}(O_i - \bar{O})(M_i - \bar{M})\right)^2}{\sum_{i=1}^{n}(O_i - \bar{O})^2 \cdot \sum_{i=1}^{n}(M_i - \bar{M})^2}$$

Nash-Sutcliffe efficiency (NSE): Nash-Sutcliffe efficiency (NSE) is a dimensionless model evaluation statistics and indicates how well the plot of observed versus model estimated data fits the 1:1 line. NSE ranges between $-\infty$ and 1.0 (1 inclusive), with NSE=1 being the optimal value. Values between 0.0 and 1.0 are generally viewed as acceptable levels of performance, whereas values <0.0 indicates unacceptable model performance.

$$NSE = \frac{\sum_{i=1}^{n}(O_i - \bar{O})^2 - \sum_{i=1}^{n}(M_i - O_i)^2}{\sum(O_i - \bar{O})^2}$$

Mean bias error (MBE) and percent bias (PBIAS): In MBE, the individual differences between the modeled and corresponding observed values are averaged while retaining the sign. Positive values indicate model overestimation error, and negative values indicate model underestimation error. A value of zero or close to zero indicates good performance of the model. The optimal value of PBIAS is 0.0, with low-magnitude values indicating accurate model simulation.

$$MBE = \frac{1}{n}\sum_{i=1}^{n}(M_i - O_i)$$

$$PBIAS = \frac{\sum_{i=1}^{n}(M_i - O_i)}{\sum O_i} \times 100$$

Root mean square error (RMSE) and percentage root mean square error (%RMSE): RMSE is a quadratic scoring rule where the squared values of the differences are averaged over the sample. RMSE gives a relatively greater weight to larger errors, severely penalizing large deviations, and hence is most useful when large errors are particularly undesirable. Large differences between RMSE and MAE indicate high variance in the individual errors of the dataset. RMSE is a commonly used error index statistics with lower value range indicating better model performance.

$$RMSE = \sqrt{\frac{1}{n}\sum_{i=1}^{n}\{(M_i - O_i)\}^2}$$

$$Percent\ RMSE = \frac{RMSE}{\frac{\sum_{i=1}^{n}O_i}{n}} \times 100$$

Mean absolute error (MAE) and Mean absolute percent error (MAPD): MAE is a linear score whereby individual absolute differences are weighted equally in the average. MAE is the most natural and unambiguous measure of average error magnitude, and recommended for all dimensioned evaluations and inter-comparisons of average model performance.

$$MAE = \frac{1}{n}\sum_{i=1}^{n}|M_i - O_i|$$

$$MAPD = \frac{\sum_{i=1}^{n}|M_i - O_i|}{\sum_{i=1}^{n}O_i} \times 100$$

All three error indices provide errors in the constituent's unit and can also be expressed as relative error with respect to the mean. Each of them serve a unique purpose and should be used together to diagnose the performance of model. From the definition of these error indices, it follows that MBE ≤ MAE ≤ RMSE (Willmott and Matsuura, 2005). Willmott and Matsuura (2005) point out that RMSE is an inappropriate indicator of average error and that MAE is the most natural and unambiguous measure of average error magnitude. They recommend MAE for all dimensioned evaluations and inter-comparisons of average model performance. In this study MBE was used as an indicator of under/overestimation error, MAE was used as the primary indicator for average error, RMSE was reported as a conventional measure of error, and MAPD (mean absolute percent difference) was used as a relative error indicator expressed as percentage deviation.

4.0   RESULTS AND FINDINGS

Table 4 shows the performance statistics for each station-year compared at daily time scale. The correlation and trend plots for each station-year is given in **Appendix A**. All the performance statistics indicated very good agreement of the remote sensing ETa to the EC measurement of ETa. This evaluation, performed at daily time step, provides the most stringent validation and any time-aggregation (weekly or monthly) would result in higher agreement. The positive value of NSE (Nash-Sutcliffe efficiency) for all station-years indicates good predictive accuracy of the model. All the observed data was used in the validation, and no analysis was performed to remove any outliers. In general, the percentage error (MAPD) ranged between 20 to 30% which is same as the typical error reported in an eddy covariance measurement (Allen et al., 2011). Eddy Covariance ETa data for station-year BLK100-2003, PLC185-2002 and PLC185-2003 appears anomalous and requires further data processing, which is beyond the current scope of the study. The time series plot of LAI and ETa for station BLK100 (**Figure 2**) shows similar trend indicating collinearity between these variables. Overall, the satellite-derived ETa estimates using surface energy balance algorithm compares well with ground observation data and has great potential for monitoring vegetation in the groundwater dependent ecosystem of Owens Valley.

In conclusion, validation of spatial ETa estimates against eddy covariance data shows good agreement. Results suggest that the remote sensing based spatial ETa mapping has the potential to be developed as an operational tool for managing water resource and monitoring vegetation in the groundwater dependent ecosystem of Owens Valley.
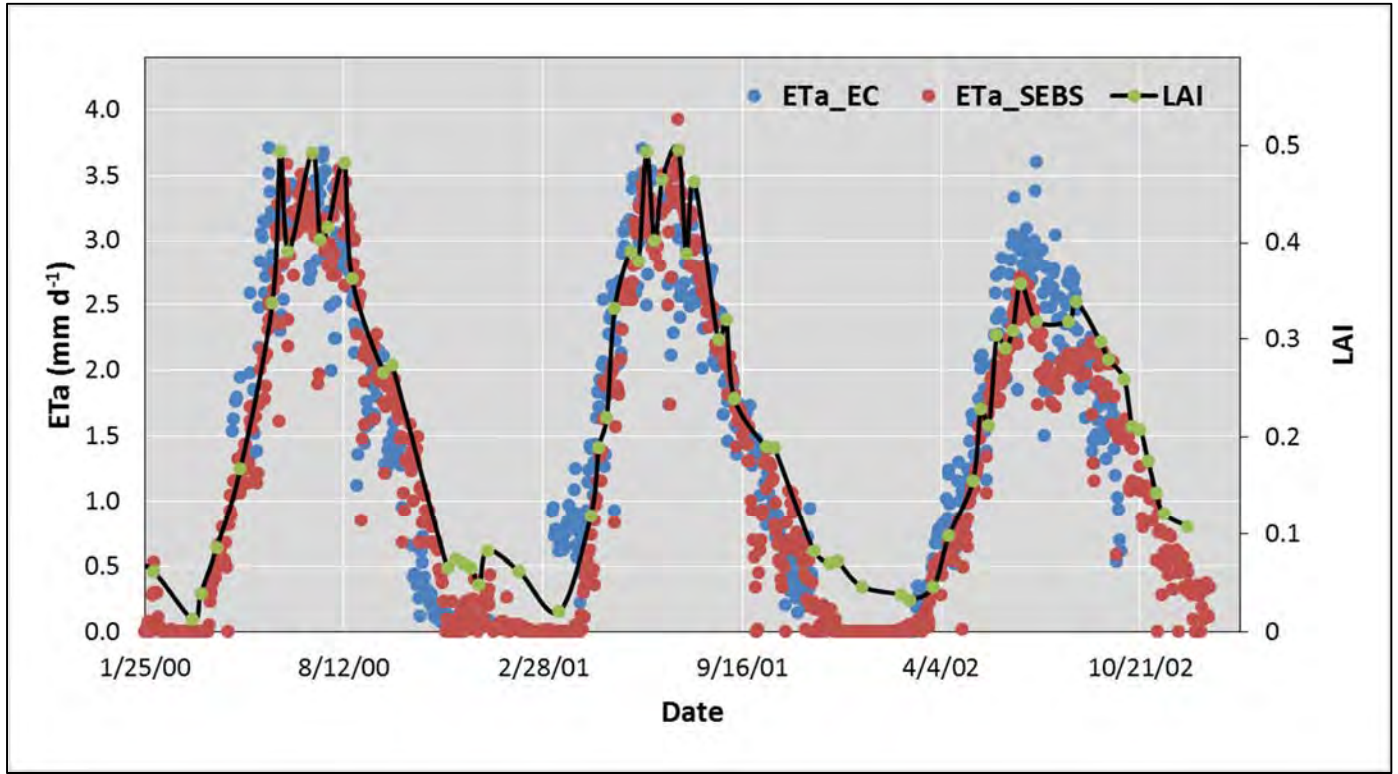
Figure 2
ETa and LAI for Station BLK100 (AM1) from 2000 to 2002

Table 4
Validation Results: Daily ETa from EC Compared to Daily ETa from SEBS

Station_Year	Number of Obs.	Mean (Obs)	Mean (Est)	MBE	PBIAS (%)	RMSE	RMSE (%)	MAE	MAPD (%)	NSE	R^2
		mm d^{-1}	mm d^{-1}	mm d^{-1}	%	mm d^{-1}	%	mm d^{-1}	%	unitless	unitless
BLK100_2000	206	1.63	1.72	0.09	5.38	0.50	30.38	0.39	23.81	0.84	0.84
BLK100_2001	255	1.70	1.57	-0.14	-8.02	0.51	29.71	0.41	23.80	0.74	0.82
BLK100_2002	212	1.64	1.44	-0.20	-11.97	0.42	25.78	0.33	20.16	0.81	0.85
BLK100_2003*											
BLK009_2001	187	1.12	1.19	0.08	6.80	0.28	25.22	0.23	20.94	0.77	0.82
PLC045_2001	199	0.40	0.41	0.02	3.81	0.10	25.96	0.08	20.15	0.81	0.83
PLC074_2002	119	0.89	0.80	-0.10	-10.96	0.24	26.43	0.18	20.42	0.18	0.32
PLC074_2003	155	1.61	2.08	0.47	29.03	0.58	35.83	0.50	30.80	0.01	0.66
FSL138_2002	115	3.90	4.67	0.77	19.72	0.90	23.13	0.79	20.34	0.03	0.78
PLC018_2002	150	0.26	0.27	0.004	1.66	0.08	31.88	0.07	26.82	0.005	0.23
PLC185_2002†	137	0.59									
PLC185_2003†	186	0.83									

*The received EC data range is out of bound.
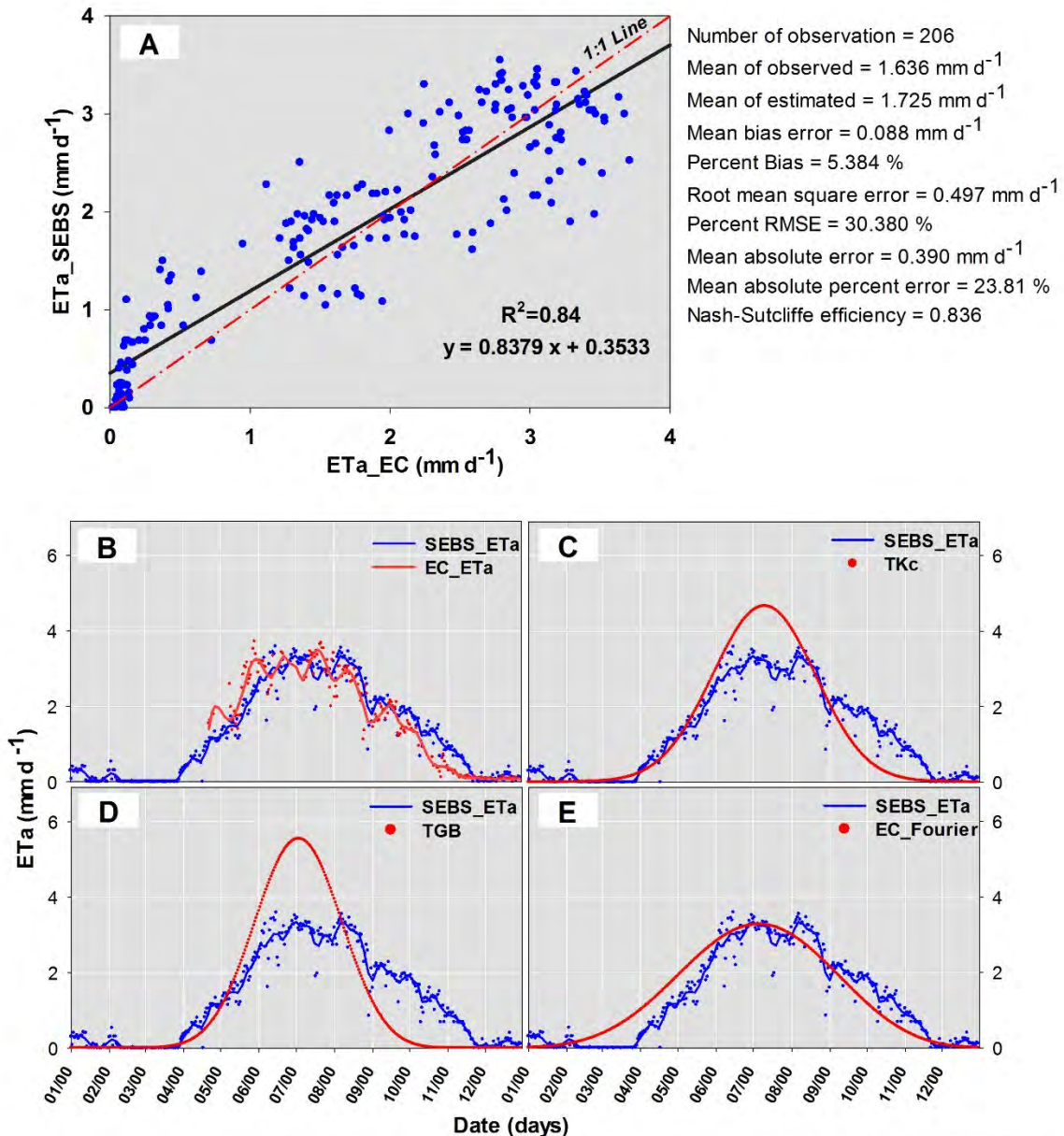† Some anomalies seen in the data, further investigation needed in future scope of the study.

5.0 REFERENCES

Allen, R.G., Pereira, L.S., Howell, T.A., Jensen, M.E., 2011. Evapotranspiration information reporting: I. Factors governing measurement accuracy. Agric. Water Manage., 98, 899–920.

Eamus, D., Zolfaghar, S., Villalobos-Vega, R., Cleverly, J., and Huete, A., 2015. Groundwater-dependent ecosystems: recent insights from satellite and field-based studies. Hydrol. Earth Syst. Sci. 19, 4229-4256, 2015.

Harrington, R., and Steinwand, A., 2003. Development of hydrologic and vadose models to improve groundwater management in the Owens Valley. Final report prepared by the County of Inyo Water Department.

MWH, 2016. Final Work Plan: Remote Sensing Pilot Project (Task Order 002 of Agreement 47381-6). September 2016.

Paul, G., Townsend, P., Schmid, B., Chong, C.S., Roberson, M., Hawkins, T., Smith, A., Williams, D., Kellar, C., 2017a, California Actual Evapotranspiration (CalETa) Mapping Program. California Water and Environmental Modeling Forum 2017 Annual Meeting, March 20–22, 2017, Folsom, CA.

Paul, G., Schmid, B., Chong, C.S., Roberson, M., Hawkins, T., Smith, A., Williams, D., Kellar, C., 2017b, California Actual Evapotranspiration (CalETa) Mapping Program: A Crucial Component for the development of Water Budgets. Groundwater Resources Association of California SGMA conference- Tools for developing Groundwater Sustainability Plans, May 3–4, 2017, Modesto, CA.

Pérez-Hoyos, I.C., Krakauer, N.Y., Khanbilvardi, R., Armstrong, R.A., 2016. A Review of Advances in the Identification and Characterization of Groundwater Dependent Ecosystems Using Geospatial Technologies. Geosciences, 2016, 6,17.

Harrington, R., Steinwand, A., Hubbard, P., and Martin, D., 2004. Evapotranspiration from Groundwater Dependent Plant Communities: Comparison of Micrometeorological and Vegetation-Based Measurements. A cooperative study final report prepared by the county of Inyo Water Department and Los Angeles Department of Water and Power.

Steinwand, A.L., Harrington, R.F., Or, D., 2006. Water balance for Great Basin phreatophytes derived from eddy covariance, soil water, and water table measurements. Journal of Hydrology, 329:595-605.

Su, Z., 2002. The Surface Energy Balance System (SEBS) for estimation of turbulent heat fluxes. Hydrology and Earth System Sciences, 6:85-99.

Willmott, C.J., & Matsuura, K., 2005. Advantages of the mean absolute error (MAE) over the root mean square error (RMSE) in assessing average model performance. Clim. Res. 30, 79–82.
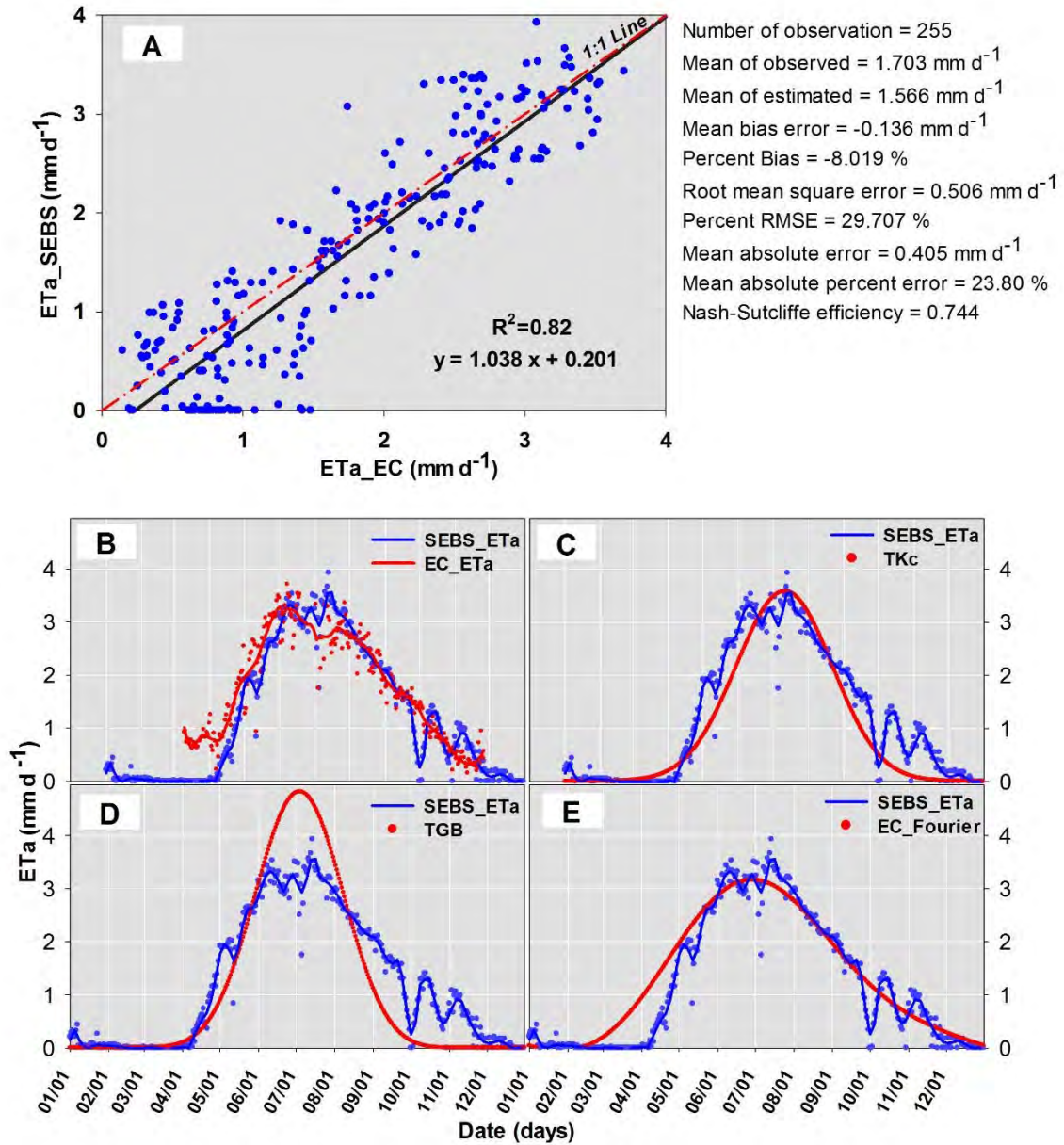
APPENDIX-A

EC_ETa is the measured ETa using Eddy Covariance and SEBS_ETa is the remote sensing based ETa. Tkc is ETa developed using crop coefficient concept, TGB is ETa computed using Green Book Method and EC_Fourier is a fitted series.

BLK100- YEAR 2000

Number of observation = 206
Mean of observed = 1.636 mm d^{-1}
Mean of estimated = 1.725 mm d^{-1}
Mean bias error = 0.088 mm d^{-1}
Percent Bias = 5.384 %
Root mean square error = 0.497 mm d^{-1}
Percent RMSE = 30.380 %
Mean absolute error = 0.390 mm d^{-1}
Mean absolute percent error = 23.81 %
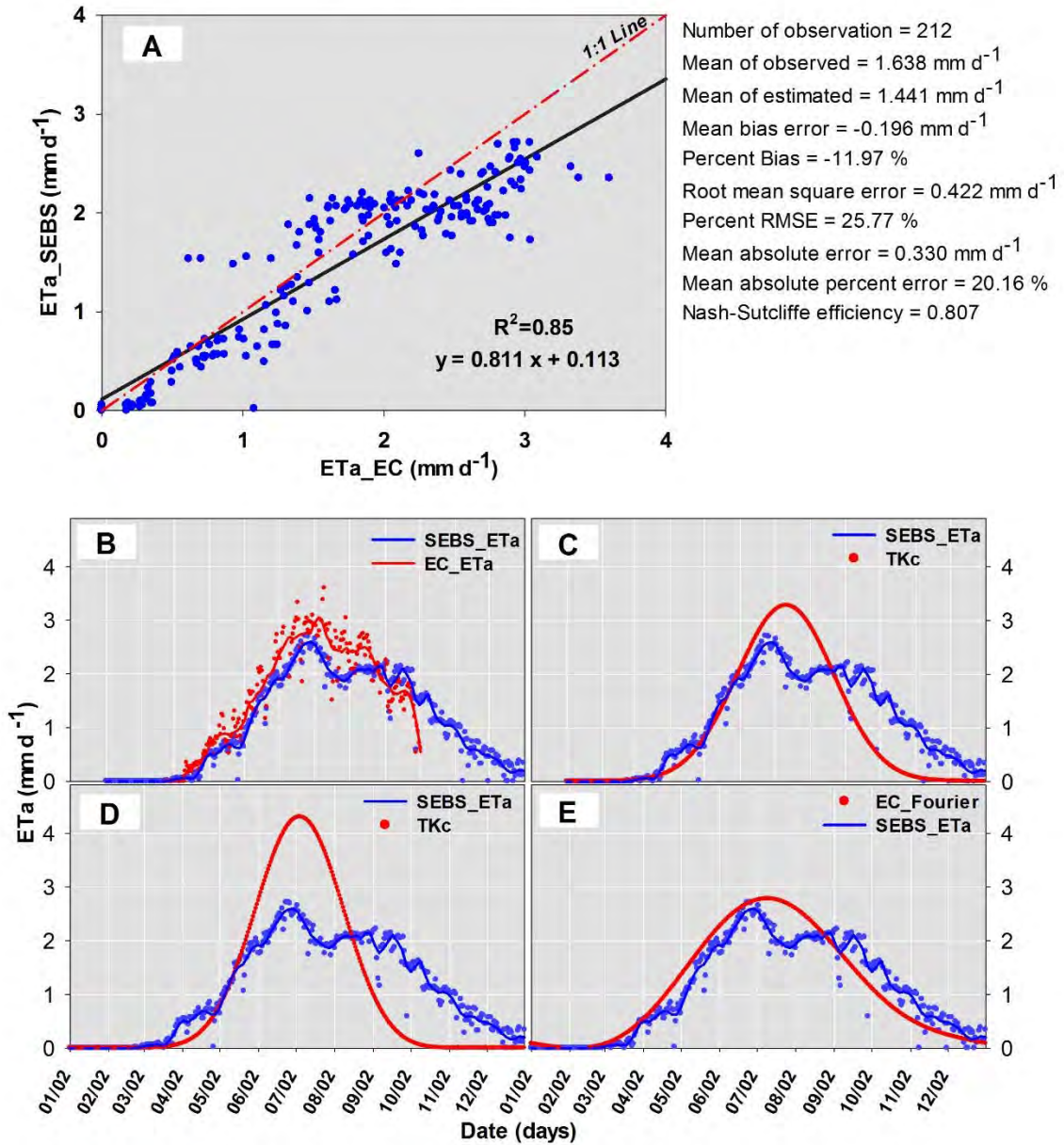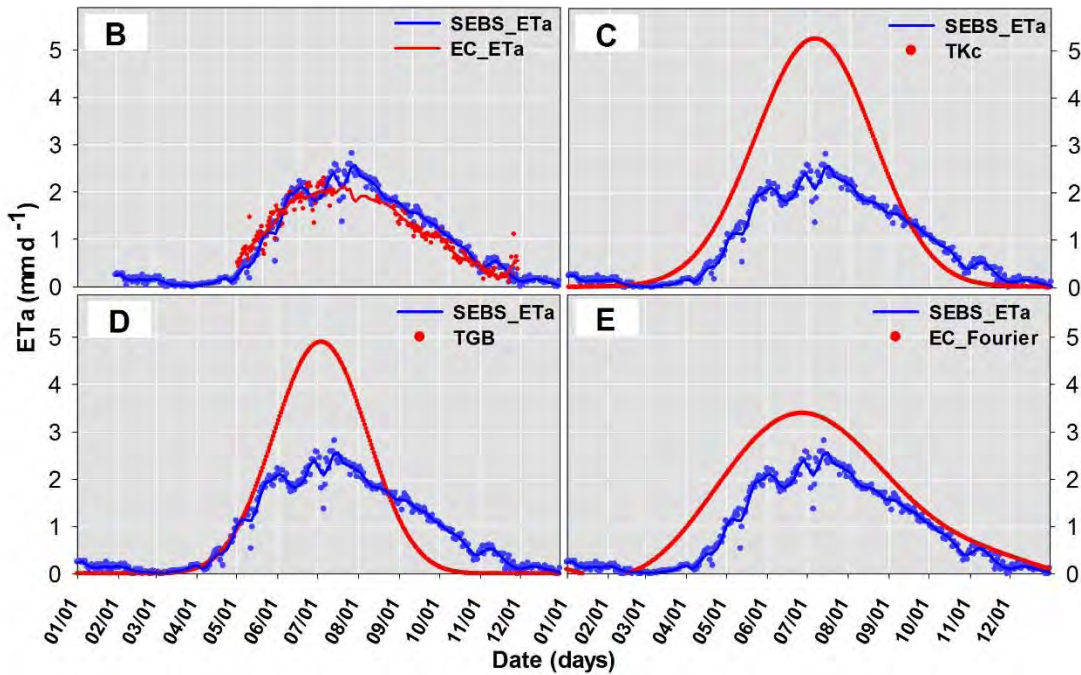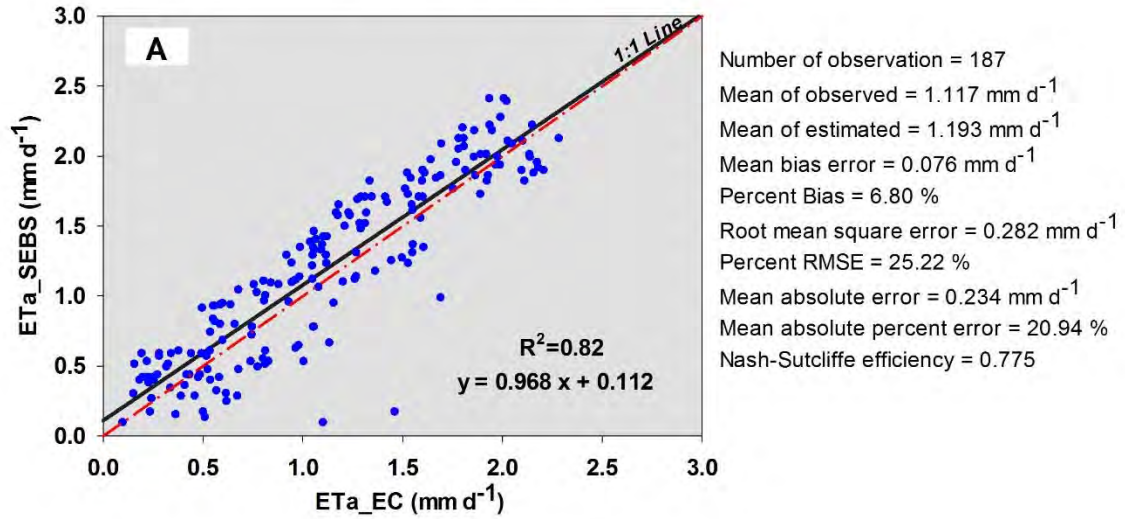Nash-Sutcliffe efficiency = 0.836

R^2=0.84
y = 0.8379 x + 0.3533

[A] Scatter plot of observed (ETa_EC) versus estimated (ETa_SEBS) daily ETa, [B] Trend plot of EC_ETa and SEBS_ETa
[C] Trend plot of TKc and SEBS_ETa, [D] Trend plot of TGB and SEBS _ETa and [E] Trend plot of EC_fourier and SEBS_ETa

BLK100- YEAR 2001

A

Number of observation = 255
Mean of observed = 1.703 mm d^{-1}
Mean of estimated = 1.566 mm d^{-1}
Mean bias error = -0.136 mm d^{-1}
Percent Bias = -8.019 %
Root mean square error = 0.506 mm d^{-1}
Percent RMSE = 29.707 %
Mean absolute error = 0.405 mm d^{-1}
Mean absolute percent error = 23.80 %
Nash-Sutcliffe efficiency = 0.744

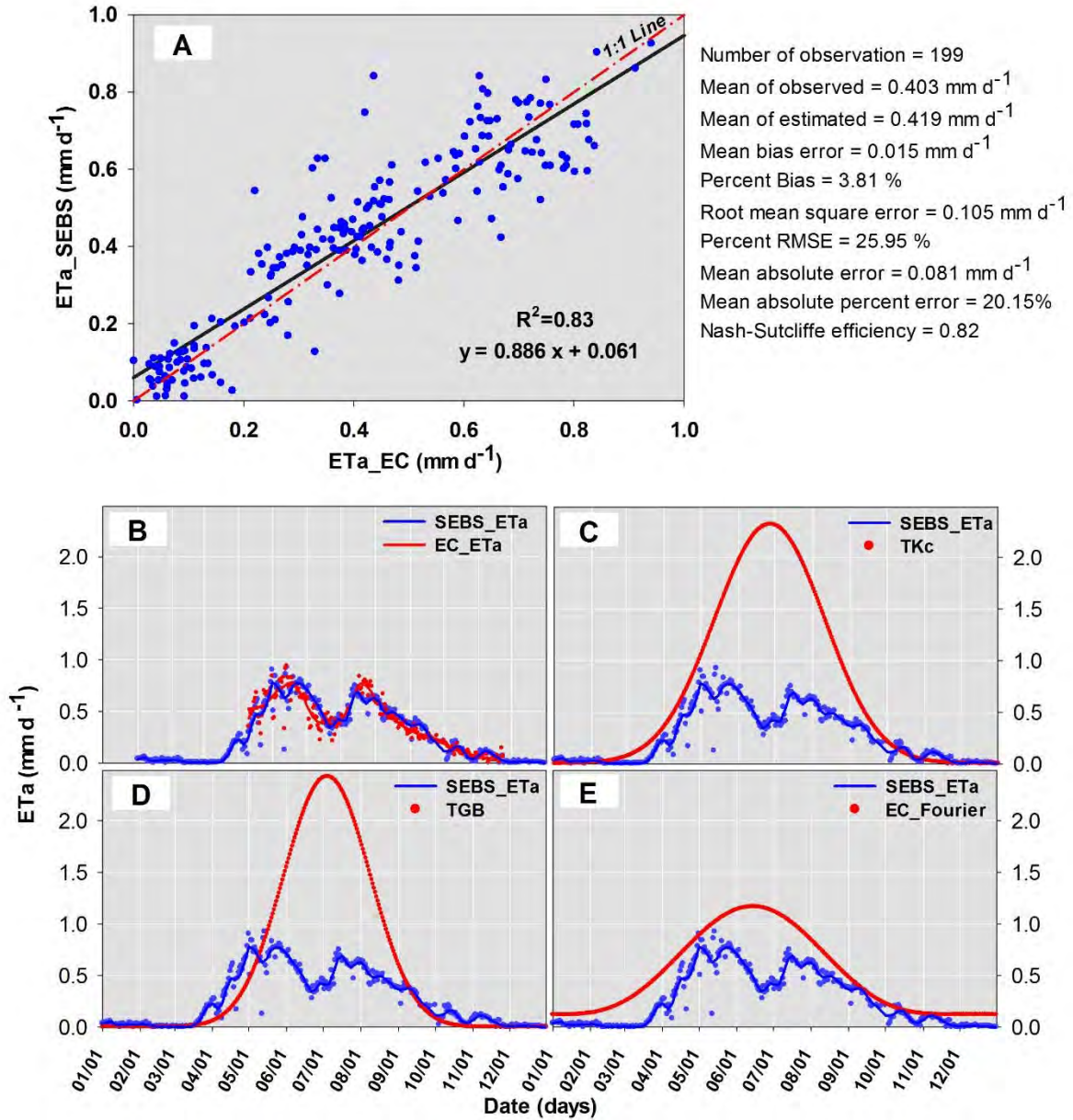$R^2 = 0.82$
$y = 1.038 x + 0.201$

[A] Scatter plot of observed (ETa_EC) versus estimated (ETa_SEBS) daily ETa, [B] Trend plot of EC_ETa and SEBS_ETa
[C] Trend plot of TKc and SEBS_ETa, [D] Trend plot of TGB and SEBS _ETa and [E] Trend plot of EC_fourier and SEBS_ETa
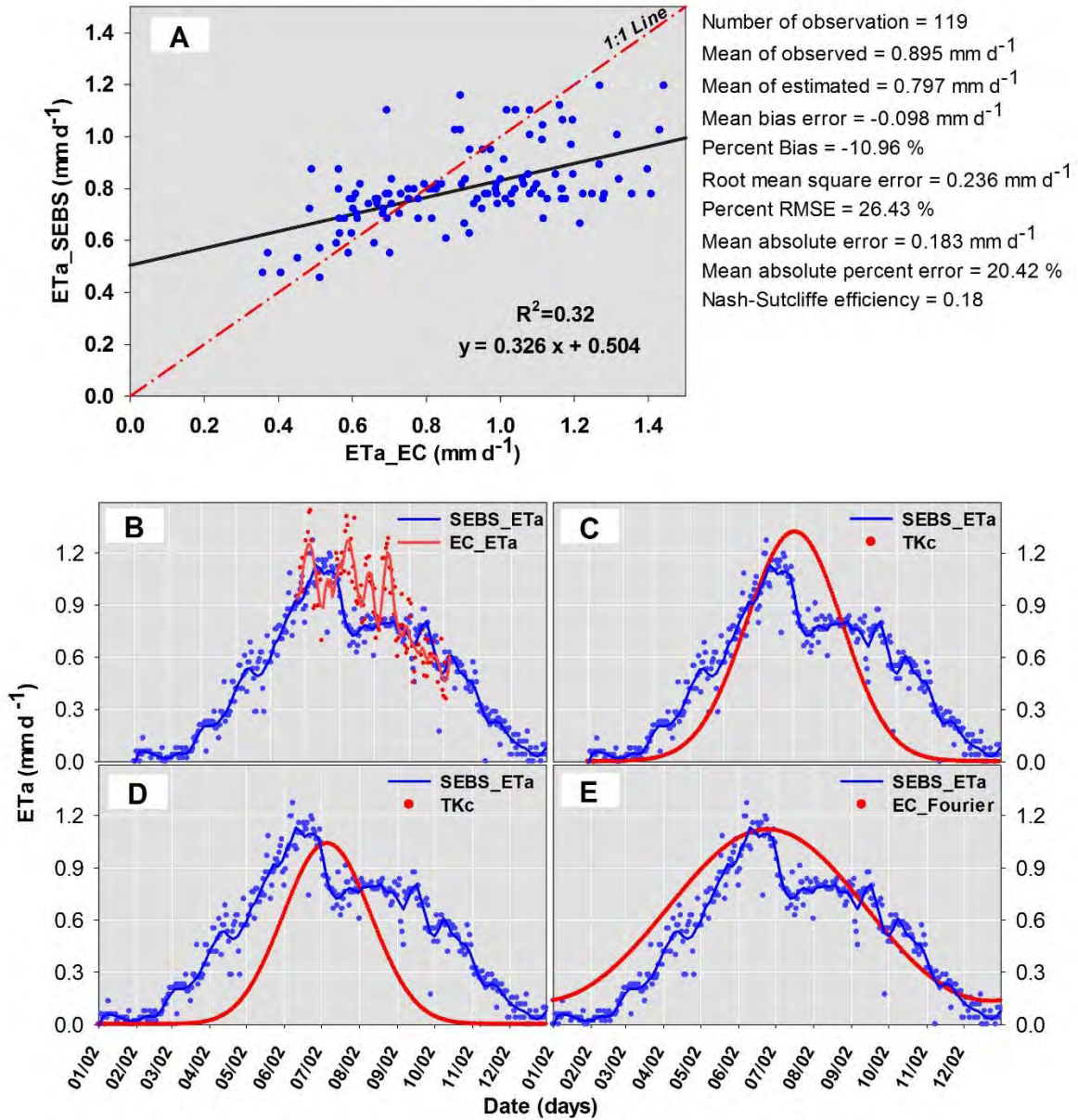
BLK100- YEAR 2002

[A] Scatter plot of observed (ETa_EC) versus estimated (ETa_SEBS) daily ETa, [B] Trend plot of EC_ETa and SEBS_ETa
[C] Trend plot of TKc and SEBS_ETa, [D] Trend plot of TGB and SEBS _ETa and [E] Trend plot of EC_fourier and SEBS_ETa

BLK009- YEAR 2001

Number of observation = 187
Mean of observed = 1.117 mm d^{-1}
Mean of estimated = 1.193 mm d^{-1}
Mean bias error = 0.076 mm d^{-1}
Percent Bias = 6.80 %
Root mean square error = 0.282 mm d^{-1}
Percent RMSE = 25.22 %
Mean absolute error = 0.234 mm d^{-1}
Mean absolute percent error = 20.94 %
Nash-Sutcliffe efficiency = 0.775
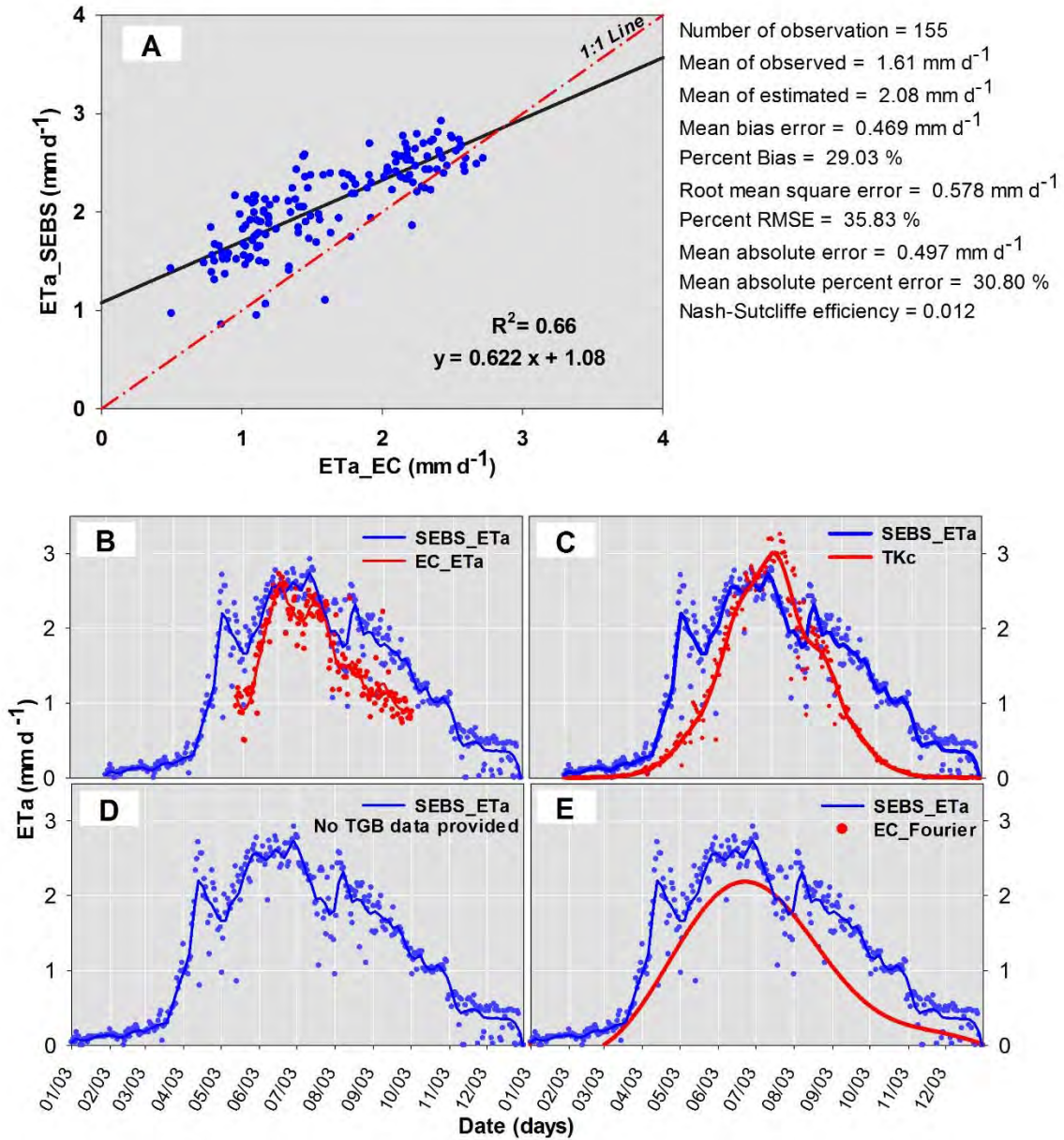
$R^2 = 0.82$
$y = 0.968 x + 0.112$

[A] Scatter plot of observed (ETa_EC) versus estimated (ETa_SEBS) daily ETa, [B] Trend plot of EC_ETa and SEBS_ETa
[C] Trend plot of TKc and SEBS_ETa, [D] Trend plot of TGB and SEBS _ETa and [E] Trend plot of EC_fourier and SEBS_ETa
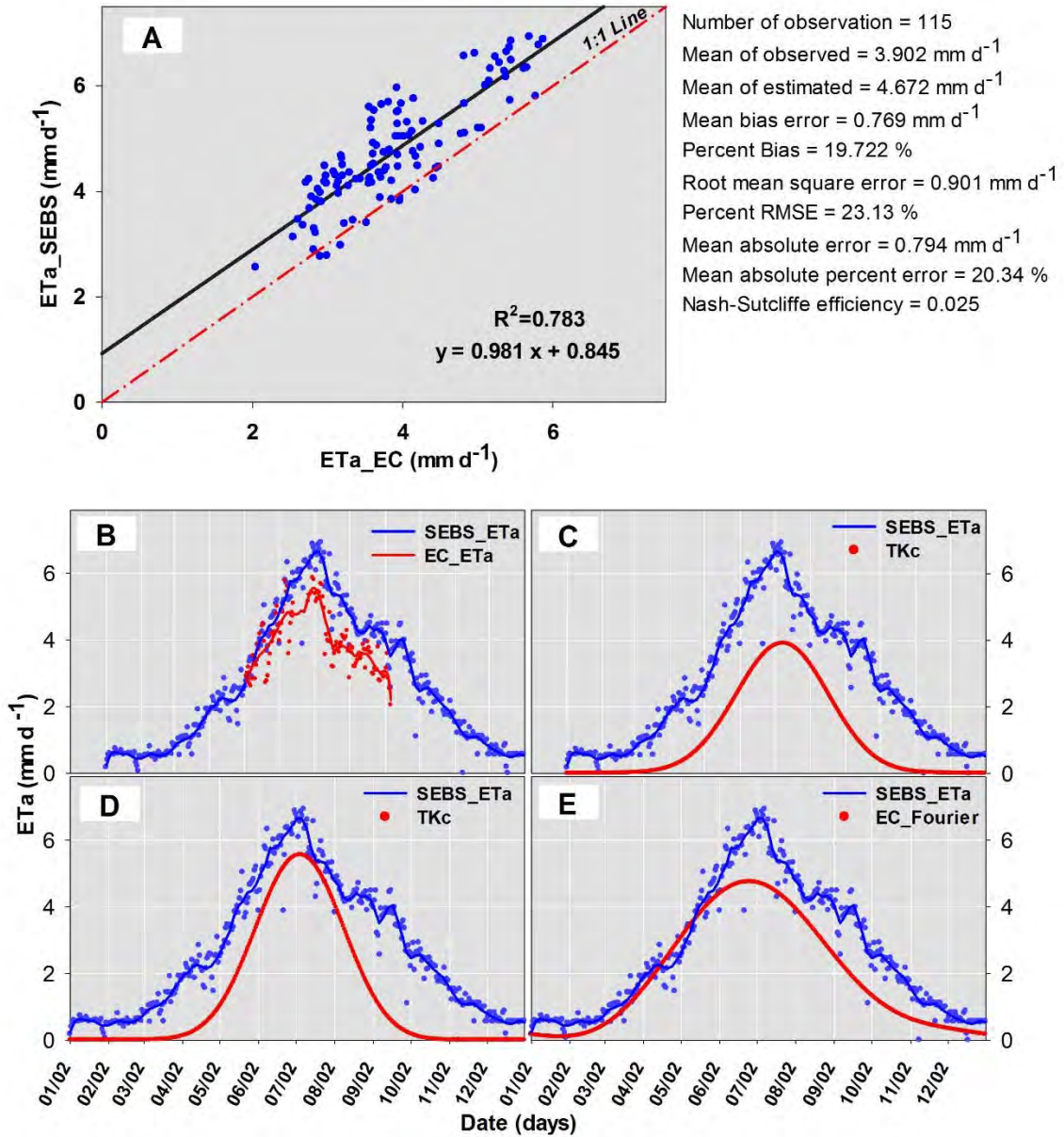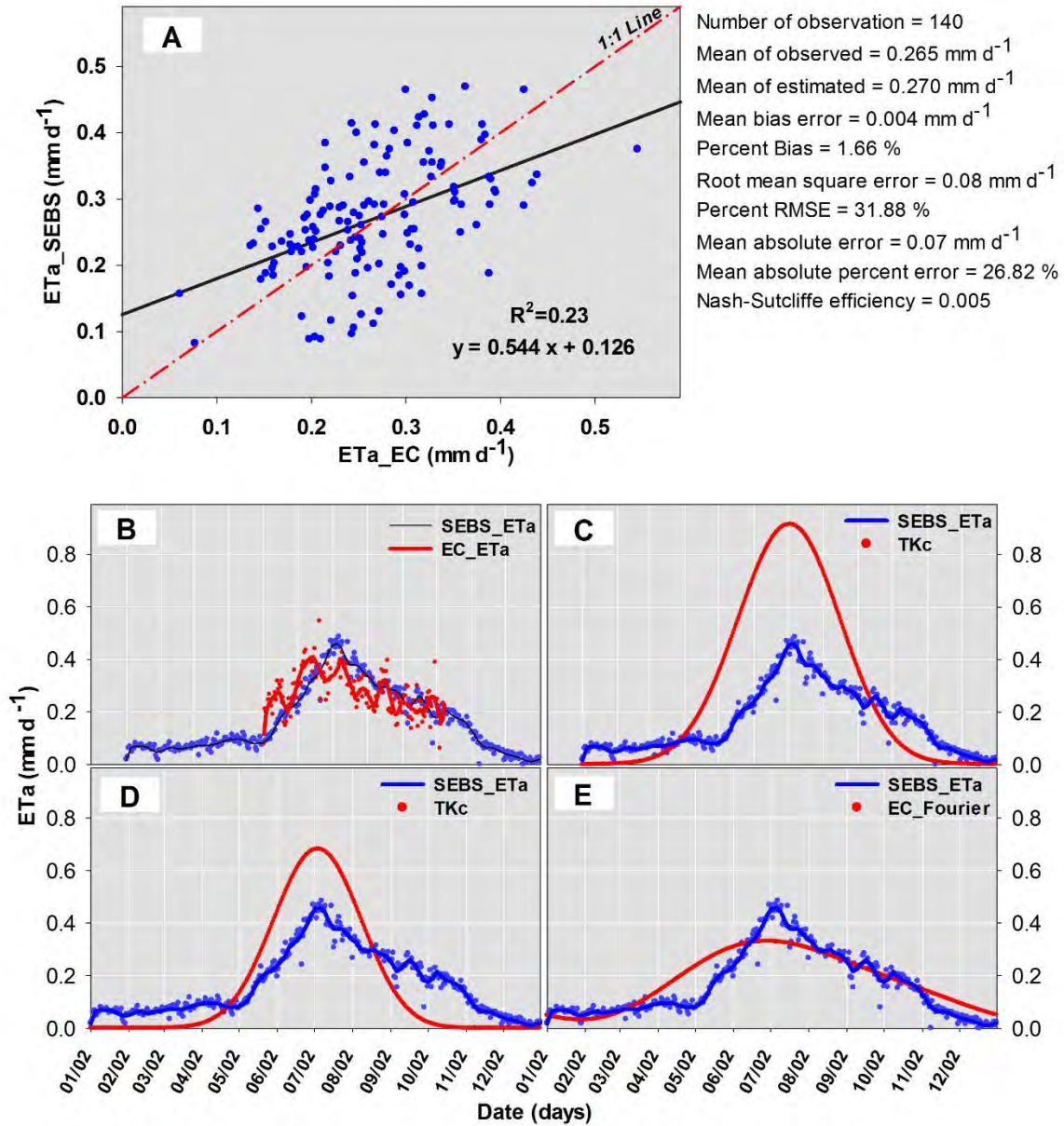
PLC045- YEAR 2001

[A] Scatter plot of observed (ETa_EC) versus estimated (ETa_SEBS) daily ETa, [B] Trend plot of EC_ETa and SEBS_ETa
[C] Trend plot of TKc and SEBS_ETa, [D] Trend plot of TGB and SEBS _ETa and [E] Trend plot of EC_fourier and SEBS_ETa

PLC074- YEAR 2002

Number of observation = 119
Mean of observed = 0.895 mm d^{-1}
Mean of estimated = 0.797 mm d^{-1}
Mean bias error = -0.098 mm d^{-1}
Percent Bias = -10.96 %
Root mean square error = 0.236 mm d^{-1}
Percent RMSE = 26.43 %
Mean absolute error = 0.183 mm d^{-1}
Mean absolute percent error = 20.42 %
Nash-Sutcliffe efficiency = 0.18

[A] Scatter plot of observed (ETa_EC) versus estimated (ETa_SEBS) daily ETa, [B] Trend plot of EC_ETa and SEBS_ETa
[C] Trend plot of TKc and SEBS_ETa, [D] Trend plot of TGB and SEBS _ETa and [E] Trend plot of EC_fourier and SEBS_ETa

PLC074- YEAR 2003

Figure A statistics:

Number of observation = 155
Mean of observed = 1.61 mm d^{-1}
Mean of estimated = 2.08 mm d^{-1}
Mean bias error = 0.469 mm d^{-1}
Percent Bias = 29.03 %
Root mean square error = 0.578 mm d^{-1}
Percent RMSE = 35.83 %
Mean absolute error = 0.497 mm d^{-1}
Mean absolute percent error = 30.80 %
Nash-Sutcliffe efficiency = 0.012

$R^2 = 0.66$
$y = 0.622 x + 1.08$

[A] Scatter plot of observed (ETa_EC) versus estimated (ETa_SEBS) daily ETa, [B] Trend plot of EC_ETa and SEBS_ETa
[C] Trend plot of TKc and SEBS_ETa, [D] Trend plot of TGB and SEBS _ETa and [E] Trend plot of EC_fourier and SEBS_ETa

FSL138- YEAR 2002

Number of observation = 115
Mean of observed = 3.902 mm d^{-1}
Mean of estimated = 4.672 mm d^{-1}
Mean bias error = 0.769 mm d^{-1}
Percent Bias = 19.722 %
Root mean square error = 0.901 mm d^{-1}
Percent RMSE = 23.13 %
Mean absolute error = 0.794 mm d^{-1}
Mean absolute percent error = 20.34 %
Nash-Sutcliffe efficiency = 0.025

R^2=0.783
y = 0.981 x + 0.845

[A] Scatter plot of observed (ETa_EC) versus estimated (ETa_SEBS) daily ETa, [B] Trend plot of EC_ETa and SEBS_ETa
[C] Trend plot of TKc and SEBS_ETa, [D] Trend plot of TGB and SEBS _ETa and [E] Trend plot of EC_fourier and SEBS_ETa

PLC018- YEAR 2002

Number of observation = 140
Mean of observed = 0.265 mm d^{-1}
Mean of estimated = 0.270 mm d^{-1}
Mean bias error = 0.004 mm d^{-1}
Percent Bias = 1.66 %
Root mean square error = 0.08 mm d^{-1}
Percent RMSE = 31.88 %
Mean absolute error = 0.07 mm d^{-1}
Mean absolute percent error = 26.82 %
Nash-Sutcliffe efficiency = 0.005

[A] Scatter plot of observed (ETa_EC) versus estimated (ETa_SEBS) daily ETa, [B] Trend plot of EC_ETa and SEBS_ETa
[C] Trend plot of TKc and SEBS_ETa, [D] Trend plot of TGB and SEBS _ETa and [E] Trend plot of EC_fourier and SEBS_ETa

APPENDIX D

TM 8.3.2 – INTEGRATION OF SPATIAL EVAPOTRANSPIRATION INTO
THE BISHOP/LAWS GROUNDWATER MODEL

TECHNICAL MEMORANDUM

Title: TM 8.3.2 – Integration of Spatial Evapotranspiration into Groundwater Model

Project: Task Order 008 – Remote Sensing Pilot Project Implementation

Client: Los Angeles Department of Water and Power

Date: March 2018

TABLE OF CONTENTS

LIST OF FIGURES

LIST OF TABLES

EXECUTIVE SUMMARY

Actual Spatial Evapotranspiration (Spatial ETa) estimated from the surface energy balance system using satellite imagery throughout the growing season within the Bishop/Laws model domain shows variable trends with measured depth to groundwater. In total, 34 wells and ETa for the surrounding 100-meter radius circular area were examined. Results from this work demonstrate that the strength and behavior of the trend is dependent on complex interactions. This includes (but is not limited to) well location, groundwater depth, plant community composition, soil profile characteristics, precipitation, runoff, as well as adjacency to irrigated land, rivers, intermittent streams, and irrigation ditches. Results from this work indicate the following apparent time series trends:

- **Connected Trends:** A connected trend was defined (for this analysis) as a consistent qualitative relationship where ETa was connected to summer depth to groundwater measurements. Specifically, as groundwater depth decreases, there is a corresponding increase in ETa and vice versa. This trend was apparent for 14 of the 34 (41%) wells evaluated.

- **Disconnected Trends:** A disconnected trend was defined as a relationship where ETa was inversely related to summer depth to groundwater measurements. Specifically, as groundwater depth increased, there was a corresponding increase or stabilization of ETa and plant biomass. This relationship was most prevalent for wells near irrigated agriculture and irrigated urban areas, and occurred in 5 of the 34 wells (15%) with valid time series. In these conditions, vegetation growth and ETa is unaffected (due to irrigation) from changes in depth to groundwater.

- **No Trends:** Several wells exhibited no relationship with depth to groundwater and ETa. These wells were located in barren or sparsely-vegetated upland areas where the depth to groundwater was greater than 25 feet (outside of the root zone). Seasonal summer ETa was generally 2 inches or less, indicating minimal vegetation on the landscape.

Factors, such as plant communities, soil profile characteristics, precipitation events, runoff magnitude and proximity to streams are some of the external factor besides the well characteristics, impacting the ETa and groundwater trends.

A more quantitative relationship between ETa and groundwater depth was studied for 34 wells in the Bishop/Laws model domain using regression analysis. The analysis shows apparent relationship between ETa and groundwater depth; however, the relationship is by no means consistent. A method of analyzing the regression of monthly ETa data was developed in order to provide suggestions for the variables of maximum ET, maximum ET elevation, and extinction depth using the MODFLOW ET package. It is recommended that modeling in the Bishop/Laws area be initiated using these variables, modifying them as necessary during calibration efforts. Future studies focusing on quantifying this relationship should use a high-resolution dataset and further investigate the interactions of various factors. Recommendations from the present study are:

1. The spatial ETa information is a rich dataset that should be used in assisting the management of groundwater pumping in areas of phreatophytic vegetation. Options could be explored to integrate spatial ETa information in groundwater models, and the existing 11 years of ETa dataset could be expanded to cover the 30-year modeling period (1986 – Present).

2. Quantification of the relationship between ETa and groundwater depth could be carried out using a high-resolution dataset to better understand the intrinsic relationship and to study the factors that drive this relationship. The present study looked into this relationship from a regional scale; however, the processes that drive the ETa versus depth-to-groundwater relationship is very localized, and therefore concerted studies focused on specific wells could be undertaken to further explore this relationship.

3. Once a more robust dataset is available, select more refined depth-to-groundwater/ ETa comparison locations that are free from external factors such as applied water, grazing, fire or unusual precipitation events.

4. The ET analysis could be expanded to evaluate species-specific, or vegetation type-specific (A, B, C, D, or E-type vegetation) for depth-to-groundwater/ETa comparisons.

1.0   BACKGROUND AND WORK SUMMARY

This TM represents the deliverable for Subtask 8.3.2 of Task Order 008 of Agreement No. 47381-6. As conceived in the Work Plan for this effort (MWH, 2016), key findings from the Pilot Project are documented in brief periodic TMs. These TMs are not intended to contain extensive introductory material, but are instead focused on results from individual work areas. A listing of the key TMs delivered is summarized in **Table 1**, with the highlighted TM 8.3.2 presented in this document.

The specific purpose of this task (and associated TM) was to evaluate the relationship between time series actual evapotranspiration (Eta) and depth to groundwater in selected locations in the Bishop/Laws model domain. Figure 1 shows the modeling domain and the 49 monitoring wells in the area. Of the 49 wells, 15 wells had depth-to-groundwater data that was irregular or missing and judged not suitable for ETa correlation. Spatial ETa data for a 100-meter (m) buffer around each of the 34 remaining monitoring wells was extracted for the period 2000 through 2003 (4 years) and 2010 through 2016 (7 years). This represents the timeframes where Spatial ETa has been developed in previous work. Under task 8.3, the spatial ETa dataset was developed for the time period 2000-2003 (4 years) for evaluation against ET measurement collected during the Inyo/LA Cooperative Study (Harrington et. al., 2004[1]). The 2010 through 2016 spatial ETa was an existing dataset developed by the task team and delivered as part of this task.

Depth-to-groundwater information were plotted, and the resulting hydrographs were quality checked. **Table 2** lists the details of the monitoring wells. The frequency of measurements from the monitoring wells varied between 12 readings per year (1 per month) to 4 readings per year. Daily Spatial ETa data were aggregated to monthly and bi-annual time steps for the analysis. April through September, and October through March were the time ranges used for aggregating ETa into bi-annual values.

Table 1
Summary of Technical Memoranda

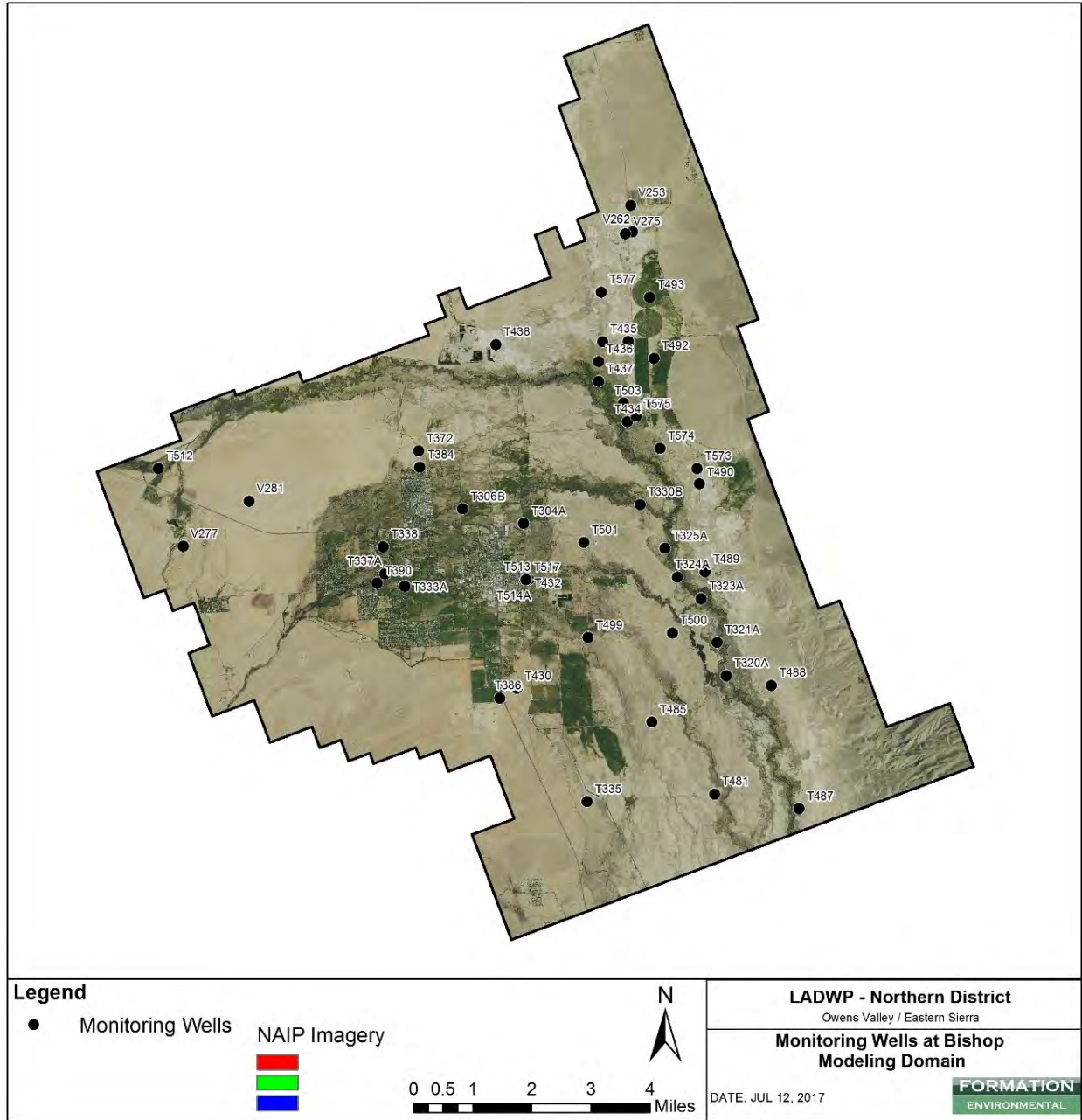| Task	TM Number	Subject
1 - Imagery Download, Preparation, and Preprocessing	TM 8.1	Imagery, cloud screening results, and radiometrically corrected imagery
2 - Leaf Area Index Image Analysis	TM 8.2	Leaf area index (LAI) image analysis, comparison of LADWP and ICWD historical data with remote sensing results, sampling scheme for collecting ground truth data
3 - Evapotranspiration (ET) Mapping and Options for Integration	TM 8.3.1	Surface Energy Balance System (SEBS) ET delivery, SEBS ET development and validation
	TM 8.3.2	Integration of Spatial ETa into the Bishop/Laws groundwater model
	TM 8.3.3	Estimation of historical Eta from agriculture in the Chalfant, Hammil, and Benton Valleys

Figure 1
Bishop/Laws Model Domain Showing Monitoring Well Locations

Table 2
Bishop/Laws Model Domain Monitoring Well Information

NO.	WELL ID	START DATE	END DATE	AVG.DEPTH TO GROUNDWATER (FEET)	READINGS PER YEAR
1.	T304A	05-02-1978	11-21-2016	6.94	12
2.	T306B	05-04-1978	11-21-2016	7.21	12
3.	T320A	02-08-1978	10-13-2016	5.17	3
4.	T321A	02-08-1978	10-13-2016	6.98	3
5.	T324A	02-07-1978	10-13-2016	5.01	3
6.	T325A	05-08-1978	10-13-2016	1.82	3
7.	T384	07-06-1973	10-25-2016	10.81	10
8.	T390	08-07-1973	10-05-2016	5.23	4
9.	T430	10-03-1973	10-03-2016	24.61	4
10.	T434	10-03-1973	10-24-2016	10.22	5
11.	T435	06-04-1974	10-19-2016	13.06	9
12.	T436	10-03-1973	11-01-2016	11.50	15
13.	T438	10-03-1973	11-21-2016	11.51	17
14.	T481	03-20-1974	10-20-2016	14.12	4
15.	T485	03-20-1974	10-24-2016	14.48	4
16.	T487	03-20-1974	10-24-2016	7.47	4
17.	T488	10-07-1974	11-21-2016	21.14	4
18.	T490	03-20-1974	11-01-2016	13.88	12
19.	T492	10-04-1974	11-01-2016	35.58	14
20.	T500	10-07-1974	10-24-2016	25.29	3
21.	T501	03-20-1974	10-24-2016	20.15	6
22.	T503	05-04-1978	11-21-2016	12.91	10
23.	T512	09-06-1978	10-25-2016	4.33	6
24.	T513	01-08-1979	10-24-2016	5.19	7
25.	T573	08-22-1985	11-21-2016	25.19	13
26.	T574	08-22-1985	10-19-2016	16.18	11
27.	T575	08-22-1985	11-21-2016	16.63	13
28.	T577	08-22-1985	10-19-2016	18.47	11
29.	V001G	09-03-1985	11-21-2016	21.06	13
30.	V253	10-04-1971	10-20-2016	42.22	5
31.	V262	10-04-1971	10-20-2016	29.99	6
32.	V275	10-04-1971	10-20-2016	31.04	5
33.	V277	10-26-1971	10-25-2016	68.99	6
34.	V281	10-01-1971	10-25-2016	124.29	6
35.	T323A	02-07-1978	04-21-1992	*	
36.	T330B	05-08-1978	04-21-1992	*	
37.	T333A	03-16-1984	07-19-2016	*	
38.	T335	10-01-1971	10-24-2016	*	
39.	T337A	01-13-1978	07-19-2016	*	
40.	T338	10-06-1971	10-24-2003	*	
41.	T372	10-17-1972	10-03-2016	*	
42.	T386	07-06-1973	10-20-2016	*	
43.	T432	10-03-1973	10-24-2016	*	
44.	T437	10-03-1973	10-20-2016	*	
45.	T489	-	-	No Data	
46.	T493	10-04-1974	03-23-2005	*	
47.	T499	03-20-1974	10-24-2016	*	
48.	T514A	12-05-1985	10-24-2016	*	
49.	T517	01-08-1979	10-24-2016	*	

*Possible issue with data quality

2.0   QUALITATIVE REVIEW OF RESULTS

The spatial and temporal variability in ETa across the Bishop/Laws model domain is depicted in **Figure 2**. This data show that for the 11 years that ETa data are available, ETa across the entire model domain varied from approximately 30,000 to 39,000 acre-feet/year (AFY). The biospheric demand and the availability of moisture drives the annual variability in plant consumptive use. The monthly and bi-annual ETa were plotted against depth to groundwater for each well and are provided in **Appendix A**. Out of 49 wells in the Bishop/Laws model domain, 14 were not included in the analysis due to potential inconsistency in the well data. Well number T489 did not have any data. Hydrographs of these 14 wells (not included in the analysis) are provided in **Appendix B**.

Appendix A contains hydrographs and Spatial ETa comparisons for the remaining 34 wells used in the analysis. The plots reveal the seasonal cycle of depth to groundwater and its qualitative relationship to ETa. The top left panel of each plot shows the spatial ETa for summer 2016 (this provides an example of low and high ET during the time periods with available data, as previously described), while the top right shows the location of the well (outlined in the hydrograph) in the Bishop/Laws model domain. The bottom left panel is a high-resolution imagery from 2016 National Agricultural Imagery Program (NAIP) showing the 100-m buffer region where ETa was summarized for the well. The two graphs on the bottom left panel show the depth to groundwater on the y-axis and monthly ETa on secondary y-axis while the other graph is very similar except the secondary y-axis is bi-annual ETa in inches. The bi-annual ETa is defined as summer ET (April through September) and Winter ET (October through March).
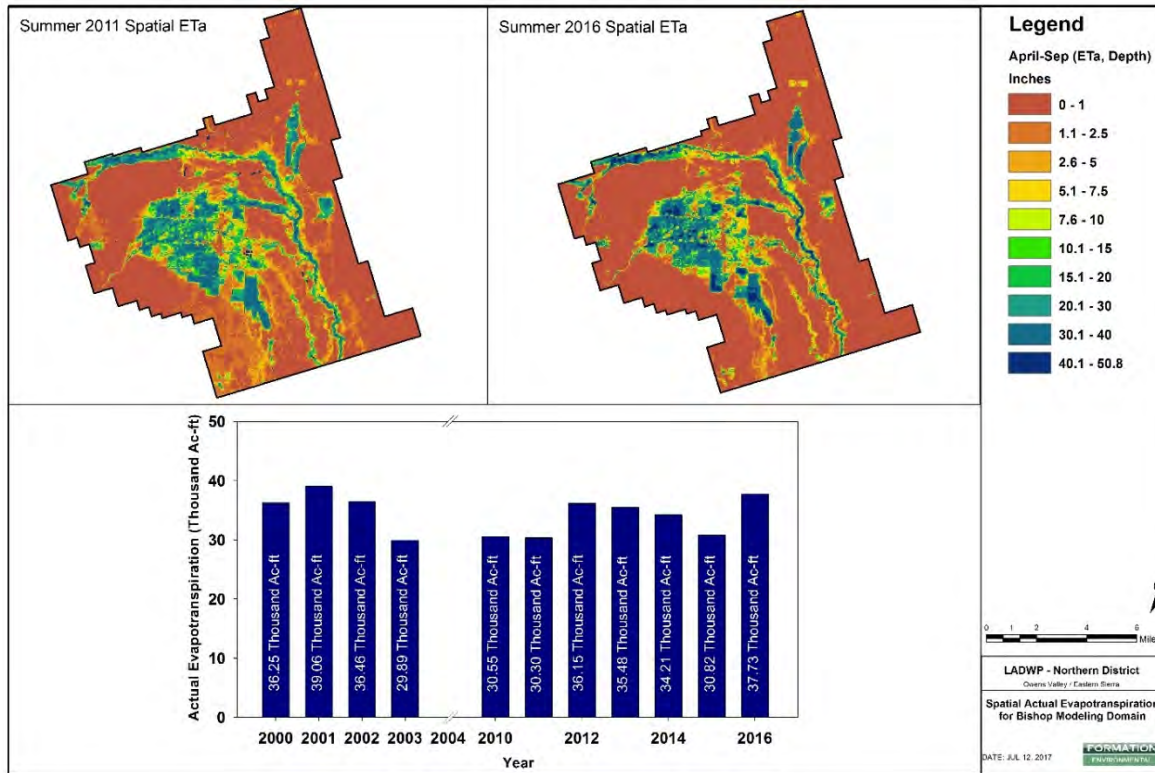
Figure 2
Annual Evapotranspiration for Bishop/Laws Model Domain.

A review of the plots in **Appendix A** reveals the complex relationships that exist between ETa and depth to groundwater. The interaction of several factors determines the strength and behavior of this relationship. Factors such as plant communities, underlying soil profile, precipitation events, runoff magnitude, as well as proximity to streams and irrigated land are some of the external factors besides the well characteristics that impact the ETa and groundwater relationship. Based on the strength and trend of the relationship seen in the 34 wells plotted in the model domain, the wells were grouped into three classes:

- **Connected Trends:** A connected trend is defined (for this analysis) as a consistent qualitative relationship where ETa was connected to summer depth-to-groundwater measurements. This trend is best demonstrated by wells T321A and T324A. Specifically, as groundwater depth decreases in these wells, there is a corresponding increase in ETa and vice versa. This trend was apparent for 14 of the 34 (41%) wells with valid time-series data and is intuitive for groundwater-dependent vegetation systems. It was most prevalent in wells with shallow groundwater, typically 5 to 10 feet. However, the strength of the trend was a function of groundwater well location, adjacency to other land uses, and conditions that affect spatial ETa estimates (e.g., changes in plant community composition, steams, irrigation canals, etc.). For example, a weak connected trend was identified in Wells T384 and T390, where surrounding irrigated land use impacts the Spatial ETa estimates and mutes the relationship with depth to groundwater.

- **Disconnected Trends:** A disconnected trend is defined as a relationship where ETa was inversely related to summer depth-to-groundwater measurements. Specifically, as groundwater depth increased in these wells, there was a corresponding increase or stabilization of ETa and plant biomass. This relationship was most prevalent for wells near irrigated agriculture and irrigated urban areas, and occurred in 5 of the 34 wells (15%) with valid time series. This trend is best demonstrated by wells T492, T434, and T575. In these conditions, vegetation growth and ETa is unaffected (due to irrigation) from changes in depth to groundwater.

- **No Trends:** Several wells exhibited no relationship with depth to groundwater and ETa. This lack of a trend was observed in 15 of the 34 wells (44%). These wells are located in barren or sparsely-vegetated upland areas where the depth to groundwater was greater than 25 feet. This trend is best demonstrated by wells T485, T488, and V262. Seasonal summer ETa was generally 2 inches or less for the area surrounding these wells, indicating minimal or no groundwater-dependent vegetation on the landscape.

A tabulated summary of these relationships for each of the 34 wells is provided in **Table 3**.

Table 3
Apparent Relationship of Depth to Groundwater and ETa for 34 Wells in Bishop/Laws Modeling Domain

Well	Avg. Depth to Groundwater (feet)	Monitoring Duration (years)	Apparent Groundwater vs. ETa Relationship	Qualitative Relationship	Notes on ETa and Well Locations
T304A	6.9	38.6	Connected Trend	Weak	Well within 30 meters of irrigation ditch
T306B	7.2	38.6	Connected Trend	Weak	Well within 30 meters of creek / intermittent stream. Clear early spring spike in GW levels each year.
T384	10.8	43.3	Connected Trend	Weak	Well located on the boundary between upland vegetation and irrigated urban land use. ETa impacted by urban land use
T390	5.2	43.2	Connected Trend	Weak	Well located in irrigated park setting, surrounded by urban land use
T435	13.1	42.4	Connected Trend	Weak	Well located in upland area; measurements flat line in 2015 to 2017
V277	69.0	45.0	Connected Trend	Weak	ETa estimate impacted by urban / commercial land use. Well located in a wash
T320A	5.2	38.7	Connected Trend	Moderate	Well within 30 to 50 meters of Owens River
T325A	1.8	38.5	Connected Trend	Moderate	Well within 50 to 75 meters of Owens River; Well appears to be located on boundary between upland and groundwater dependent habitats
T436	11.5	43.1	Connected Trend	Moderate	Upland Area, ETa >4 inches per season.
T487	7.5	42.6	Connected Trend	Moderate	Well on boundary between upland and groundwater dependent vegetation. ETa estimate impacted by this boundary
T513	5.2	37.8	Connected Trend	Moderate	Well located on boundary with urban land use, also within distance of irrigation ditch
T574	16.2	31.2	Connected Trend	Moderate	Upland vegetation
T321A	7.0	38.7	Connected Trend	Strong	Well within 50 to 75 meters of Owens River
T324A	5.0	38.7	Connected Trend	Strong	Well within 50 to 75 meters of Owens River

Well	Avg. Depth to Groundwater (feet)	Monitoring Duration (years)	Apparent Groundwater vs. ETa Relationship	Qualitative Relationship	Notes on ETa and Well Locations
T434	10.2	43.1	Disconnected Trend	Moderate	Well located in upland area; ETa measurements impacted by road and other nearby features
T492	35.6	42.1	Disconnected Trend	Moderate	Well on boundary between upland and irrigated vegetation. ETa estimate impacted by this boundary
T575	16.6	31.3	Disconnected Trend	Strong	ETa estimate impacted by irrigated agriculture
V253	42.2	45.1	Disconnected Trend	Strong	ETa estimate impacted by irrigated agriculture
T503	12.9	38.6	Disconnected Trend	NA	ETa very minimal (less than 4 inches per year)
T430	24.6	43.0	No Trend	NA	ETa very minimal (less than 10 inches per year)
T438	11.5	43.2	No Trend	NA	Barren landscape, ETa very minimal (>1.5 inches). ETa might be affected by small ponds nearby
T481	14.1	42.6	No Trend	NA	No relationship. ETa might be affected by nearby boundary of groundwater dependent vegetation
T485	14.5	42.6	No Trend	NA	Upland Area, ETa >2 inches per season.
T488	21.1	42.2	No Trend	NA	Upland Area, ETa >2 inches per season.
T490	13.9	42.6	No Trend	NA	Upland Area, ETa >2 inches per season.
T500	25.3	42.1	No Trend	NA	Upland Area, ETa >2 inches per season.
T501	20.2	42.6	No Trend	NA	Upland Area on boundary with commercial land use, ETa >4 inches per season.
T512	4.3	38.2	No Trend	NA	Shallow GW area, No relationship with ETa
T573	25.2	31.3	No Trend	NA	Upland Area, ETa >2 inches per season.
T577	18.5	31.2	No Trend	NA	Upland Area, ETa >2 inches per season.
V001G	21.1	31.2	No Trend	NA	Barren Area, ETa >1 inches per season.
V262	30.0	45.1	No Trend	NA	Barren Area, ETa >1 inches per season.
V275	31.0	45.1	No Trend	NA	Barren Area, ETa >1 inches per season.
V281	124.3	45.1	No Trend	NA	Barren Area, ETa >1 inches per season.

3.0   SUMMARY OF PREVIOUS WORK

In addition to previous modeling by LADWP that utilized the Ecological Dynamics Simulation (EDYS) model, the ET package of MODFLOW has been used by others in the Owens Valley and similar environments. A summary of this work is provided below.

3.1 Ecological Dynamics Simulation Model

Use of the EDYS model to evaluate evapotranspiration is fundamentally different than traditional use of the ET package of MODFLOW. EDYS is a mechanistic model that calculates use of water by vegetation and evaporation based on rooting depth, plant biomass, soil type, and depth to groundwater, precipitation, and other factors. Although an entirely different method is proposed with future work, it is of interest to review what EDYS calculated for the Bishop/Laws model domain. **Figure 3** shows the monthly measurement of ETa from remote sensing data for the time periods in which it is available. It is clear from this data that ETa is much higher in the growing season and is at a relatively low and relatively constant in the winter.
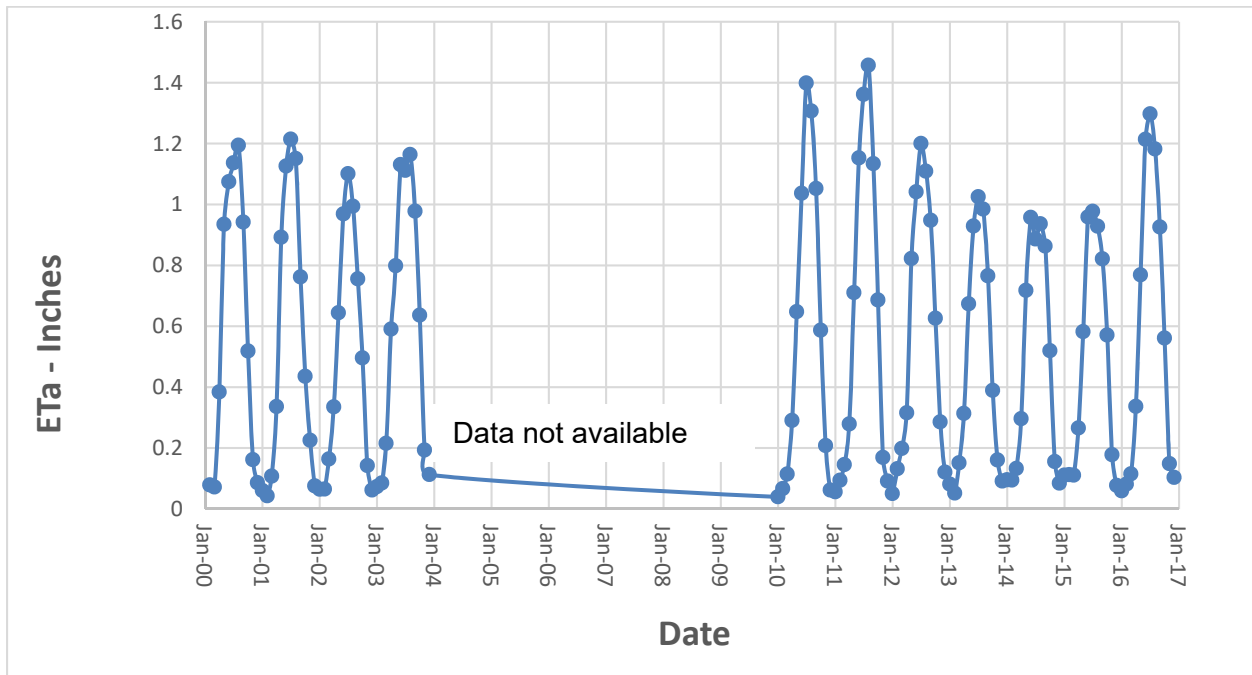
Figure 3
Monthly ETa Data for Time Periods When It is Available

Figure 4 shows a comparison of the EDYS data to ETa data from remote sensing. It is important to note that the initial (1985 to 1993) ET values based on EDYS are probably not realistic, but represent the EDYS equilibrating after setting initial conditions. A similar pattern of low winter values and higher growing season values is evident, and the overall values are comparable, although it is evident that the ETa values are generally higher, particularly in the winter. This might be expected in that EDYS calculated ET losses from the groundwater body (and not the ground surface), whereas remote sensing calculates total ET from the ground surface. Thus, ET derived from precipitation is accounted for in the ETa values, but not the EDYS values. Another difference with the use of the EDYS data is although the EDYS data were entered into the ET package of MODFLOW for calculation purposes, the ET values were not dynamic in that they were "hard coded" into the ET package by setting a very deep extinction depth, effectively negating the extinction depth function of the MODFLOW ET package.
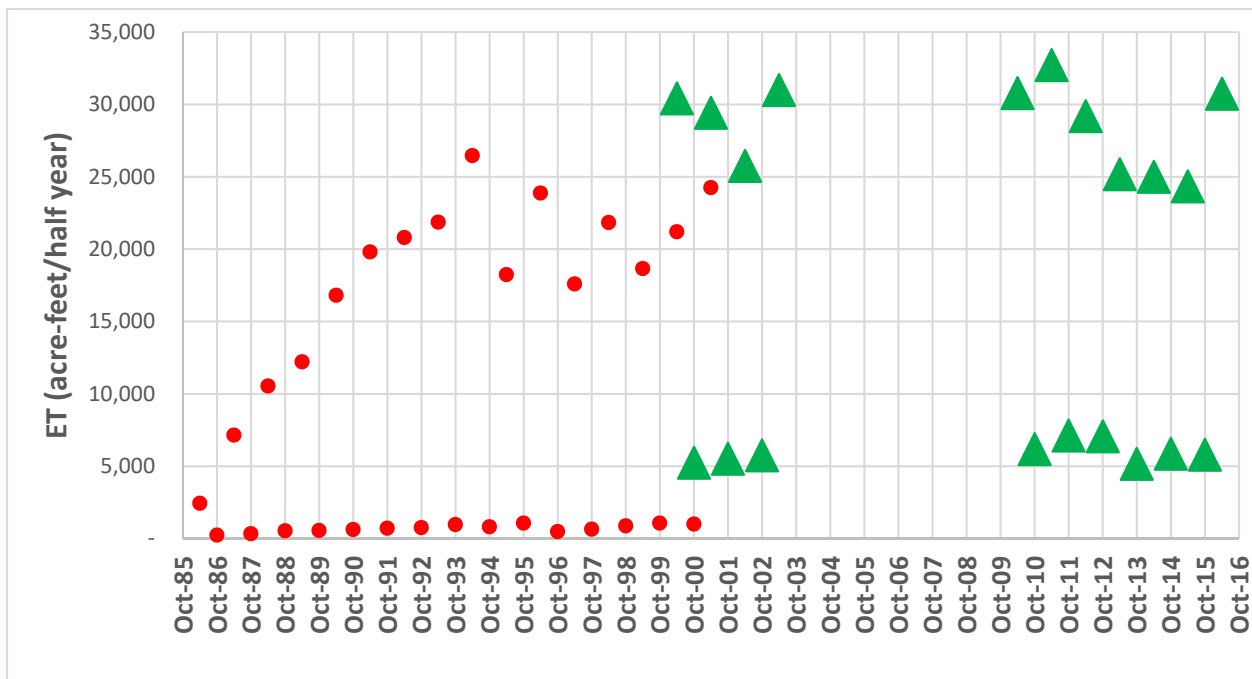
Figure 4
Comparison of EDYS ET Calculations (Red Dots) to Remote Sensing ETa Data (Green Triangles for Both Winter (Low Values) and Summer (High Values) – Total Model Domain

3.2 Other Workers

The ET package of MODFLOW has been used by other workers for modeling in the Owens Valley and similar areas. Duell (1990) estimated ET at seven representative sites in the Owens Valley from December 1983 through October 1985, using the Bowen-ratio, eddy-correlation, and Penman combination methods. Estimates of annual ET range from 1.0 feet at a low-density scrub site to 3.7 feet at high-density meadow site. Duell found that ET can be correlated to air temperature, vapor-density deficit, and net radiation. His data also show a crude correlation of ET to depth to groundwater as shown in **Figure 5**. Duell also noted that 74 percent of the ET occurs in the months of April through September.
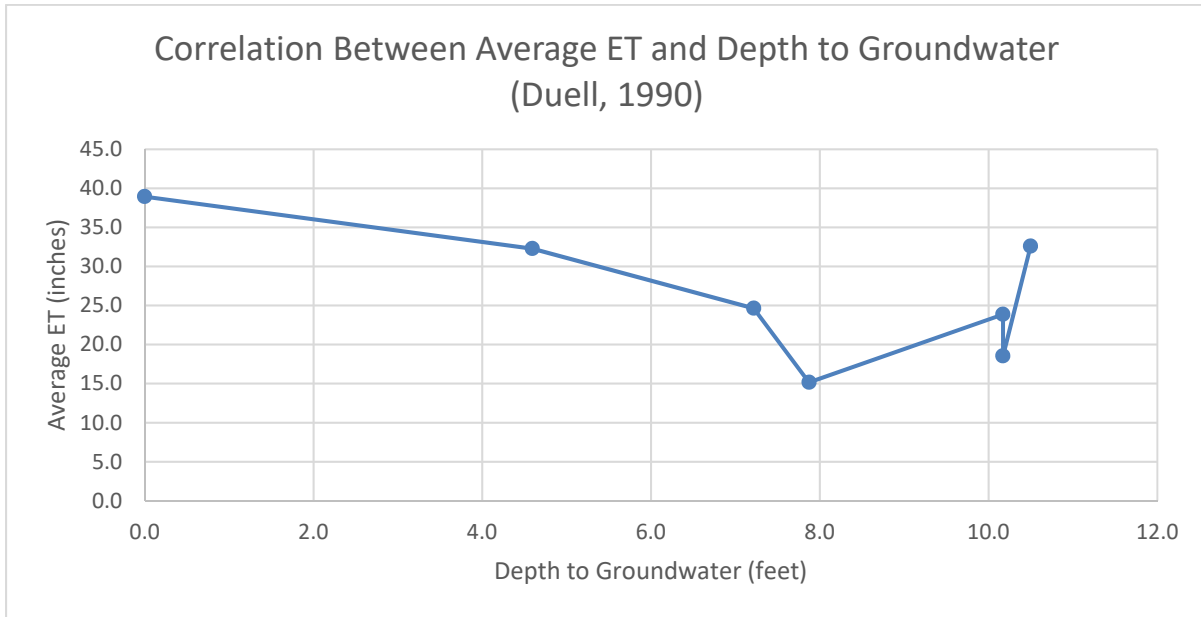
Figure 5
Correlation Between Average ET and Depth to Groundwater

In his Owens Valley-Wide model developed by the U.S. Geological Survey, Danskin (1998) utilized maximum ET rates of 24 inches per year prior to 1978, and 18 inches per year thereafter, with the rationale the groundwater pumping after 1978 reduced ET rates from vegetation. Danskin found that the model was relatively insensitive to the extinction depth, except that values less than 10 feet made the model unstable. Danskin utilized an extinction depth of 15 feet.

Nichols (2000) studied regional groundwater evapotranspiration and groundwater budgets using data from the Great Basin in Nevada and the Owens Valley of California. He found correlations between ET from the groundwater body and depth to groundwater (DTW), as well as percent cover. He described ET as a linear function of DTW (for DTW<10 feet) as follows:

ET=A+B (DTW)

Where:
ET= evapotranspiration in feet per day
A and B = coefficients shown below
DTW = depth to groundwater in feet

	A	B	r^2
May-September, feet per day	0.0125	-0.00078	0.505
October-April, feet per day	0.00276	-0.000121	0.415

Extrapolating these values to a zero ET rate results in an extinction depth of 16 feet during the summer growing season, and 23 feet in the winter, and maximum ET rates of 0.0125 and 0.00276 feet per day in the summer and winter, respectively.

Harrington (2007) assigned ET zones based on LADWP's maps of vegetation types and by digitizing areas of phreatophytes from aerial photographs in his model of the Bishop area. A maximum ET rate of 5 ft/year (equal to the potential ET rate for Bishop) was used for all ET zones. An extinction depth of 23 feet was used for all ET zones. Harrington notes that this extinction depth is somewhat deeper than the nominal root zone of phreatophytic grasses (6.6 feet) and shrubs (13.1 feet), but is comparable to root zones for larger phreatophytes such as cottonwoods and willow trees.

Moreo and others (2017) measured evapotranspiration at six eddy-correlation sites for a 1-year period between September 1, 2005 and August 31, 2006. Five sites were in phreatophytic shrubland dominated by greasewood, and one site was in a grassland meadow. The measured annual evapotranspiration ranged from 10.02 to 12.77 inches at the shrubland sites and 26.94 inches at the grassland site. Evapotranspiration rates were greater at sites with denser vegetation. Moreo and others reported that the primary water source supporting evapotranspiration was water derived from local precipitation at the shrubland sites and ground water at the grassland site. The amount of groundwater consumed by phreatophytes depends primarily on local precipitation and vegetation density. The groundwater contribution to local evapotranspiration ranged from 6 to 38 percent of total evapotranspiration at the shrubland sites, and 70 percent of total evapotranspiration at the grassland site. Average depth to groundwater ranged from 7.2 to 32.4 feet below land surface at the shrubland sites, and 3.9 feet at the grassland site.

4.0   REGESSION ANALYSIS OF ETa AND DEPTH TO GROUNDWATER DATA

In addition to the qualitative review of depth-to-groundwater and ETa measurements, a quantitative assessment of the relationship between measured ETa and depth-to groundwater (DTW) was performed using the following methods:

- The ETa for a given month from January 2000 to December 2003 and January 2010 to December 2016 was utilized on a pixel basis.

- The depth to groundwater in corresponding month at 34 locations was tabulated.

- Contouring software was utilized to extract ETa value at the 34 groundwater level monitoring locations.

- The ETa was assumed to be zero when depth to groundwater was greater than 20 feet to eliminate ETa occurring from sources other than the groundwater table.

- A series of linear regression equations was developed between ETa and depth to groundwater for each month from January through to December.

Figure 6 illustrates an example of this regression analysis for the month of November, and the concept of deriving maximum ET rates and extinction depth for these regression equations for each month, whereby the maximum ET rate is set at the zero depth intercept, and the extinction depth is set at the zero ETa intercept. A Summary of the regression analysis is provided in **Table 4**.
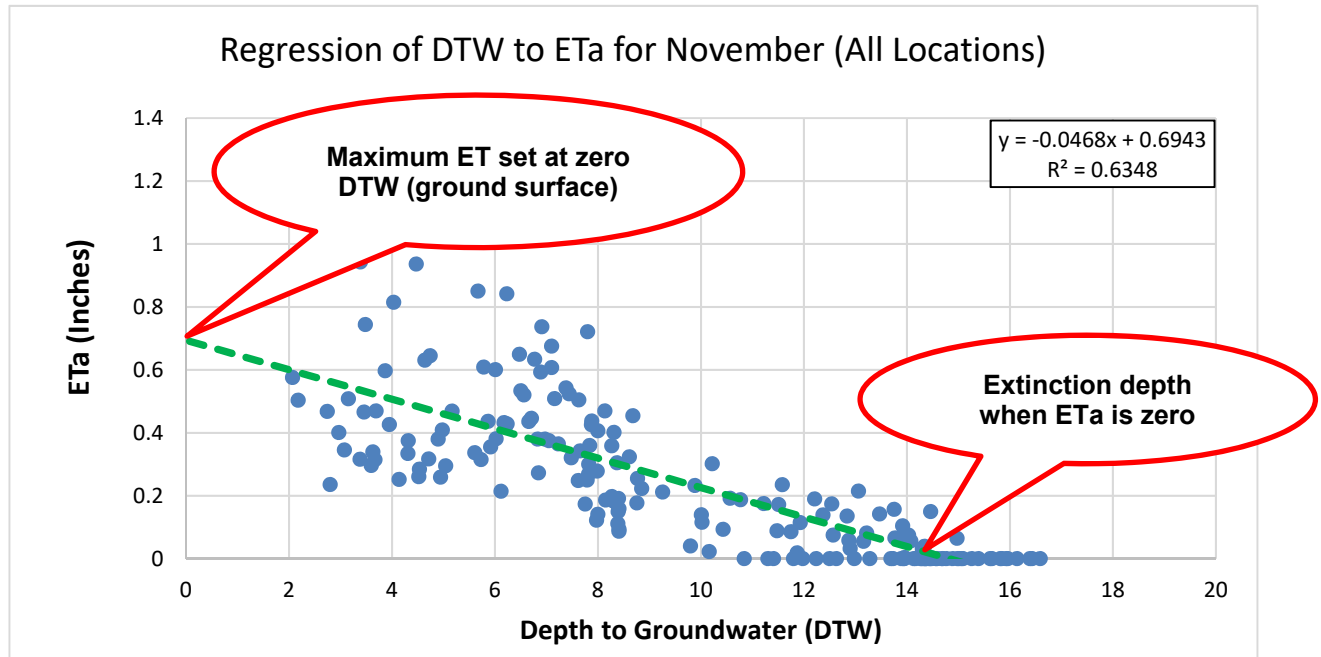
Figure 6
Example Regression Equation for November (All Locations)

Table 4
Summary of Results from Regression Analysis

Stress Period	Month	Extinction Depth (Feet)	ET maximum (Inches)
Winter	January	15.1	0.31
Winter	February	14.4	0.27
Winter	March	15.0	0.36
Summer	April	15.3	0.91
Summer	May	15.4	4.08
Summer	June	14.4	8.50
Summer	July	15.4	10.20
Summer	August	16.3	9.26
Summer	September	16.5	6.23
Winter	October	15.1	2.45
Winter	November	14.8	0.69
Winter	December	15.1	0.34
Maximum ET Rate			
Stress Period Total	**Inches/6 months**	**Feet/6 months**	**Feet/Day**
Summer	39.18	3.27	0.0181
Winter	4.42	0.37	0.0020
Average Extinction Depth	**Feet**		
Summer	15.6		
Winter	14.9		

Key conclusions of this analysis are:

- Winter ETa rates are much lower in the winter months, regardless of the depth to groundwater. This becomes a very significant finding when stress periods are 6 months or shorter, because winter ET is typically an order of magnitude lower than summer ET. A year-around constant maximum ET rate in the MODFLOW package is clearly not appropriate.

- Comparison of ETa to DTW consistently suggests an extinction depth of ~15 feet, in both winter and summer.

- Average maximum ET rates during summer are on the order of 0.02 feet per day

- Average maximum ET rates during winter are on the order of 0.002 feet per day.

5.0   RECOMMENDATIONS

The relationship between ETa and groundwater depth was studied for 34 wells in the Bishop/Laws model domain. The analysis shows the apparent relationship between ETa and groundwater depth based on regression analysis. This relationship is by no means consistent, with coefficients of determination (R^2) in the 0.4 to 0.6 range, but a general pattern does exist.

Further quantification of the relationship between DTW and ET is warranted, but it is recommended that until further work is completed, groundwater modeling continue using the average winter and summer MODFLOW ET package variables summarized in **Table 4**. Initial calibration efforts should focus on varying maximum ET rates using array multipliers during the summer months, especially where wide variations in seasonal groundwater elevations are noted.

Future studies focusing on quantifying this relationship should use a high-resolution dataset and further investigate the interactions of various factors. Recommendations from the present study are:

- The spatial ETa information is a rich dataset that should be used in assisting the management of groundwater pumping in areas of phreatohytic vegetation. Options could be explored to integrate spatial ETa information in groundwater models and the existing 11 years of ETa dataset could be expanded to cover the 30-year modeling period (1986 – Present).

- Quantification of the relationship between ETa and groundwater depth could be carried out using a high-resolution dataset to better understand the intrinsic relationship and to study the factors that drive this relationship. The present study looked into this relationship from a regional scale; however, the processes that drive the ETa versus depth-to-groundwater relationship is very localized, and therefore concerted studies focused on specific wells could be undertaken to further explore this relationship.

- Once a more robust dataset is available, more refined DTW/ ETa comparison locations should be selected that are free from external factors such as applied water, grazing, fire or unusual precipitation events.

- Evaluate species-specific, or type-specific (A, B, C, D, or E-type vegetation) for DTW/ETa comparisons.

6.0   REFERENCES

Danskin, W.R., 1998. Evaluation of the hydrologic system and selected water-management alternatives in the Owens Valley, California. Prepared in cooperation with Inyo County and the Los Angeles Department of Water and Power. U.S. Geological Survey Water-Supply Paper 2370-H.

Duell, L.F.W., Jr., 1990. Estimates of evapotranspiration in alkaline scrub and meadow communities of Owens Valley, California, using the Bowen-ratio, eddy-correlation, and Penman-combination methods: U.S. Geological Survey Water-Supply Paper 2370-E, 39 p.

Harrington, R., 2007, Development of a Groundwater Flow Model for the Bishop/Laws Area, Final Report for Local Groundwater Assistance Grant Agreement, No. 4600004129.

Moreo, M.T., Andraski, B.J., and Garcia, C.A., 2017, Groundwater discharge by evapotranspiration, flow of water in unsaturated soil, and stable isotope water sourcing in areas of sparse vegetation, Amargosa Desert, Nye County, Nevada: U.S. Geological Survey Scientific Investigations Report 2017–5079, 55 p., https://doi.org/10.3133/ sir20175079.

MWH, 2016. Final Work Plan: Remote Sensing Pilot Project (Task Order 002 of Agreement 47381-6). September

Nichols, W. D., 2000. Regional groundwater evapotranspiration and groundwater budgets, Great Basin, Nevada; prepared in cooperation with the Las Vegas Valley Water District and the Nevada Division of Water Resources. U.S. Geological Survey Professional Paper 1628.

Steinwand, A.L., Harrington, R.F., Or, D., 2006. Water balance for Great Basin phreatophytes derived from eddy covariance, soil water, and water table measurements. Journal of Hydrology, 329:595-605.

APPENDIX-A

Well # T304A
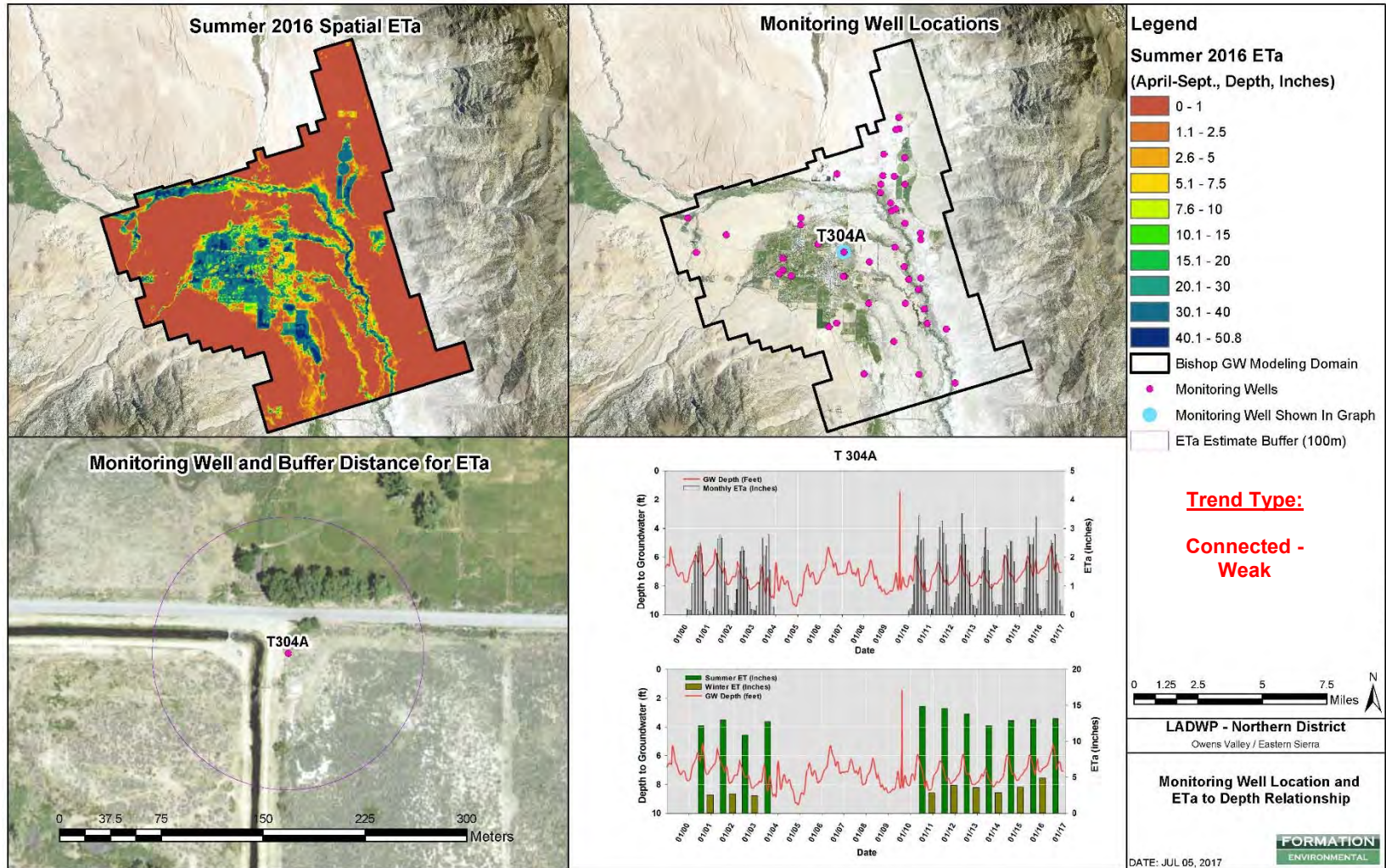
Well # T306B
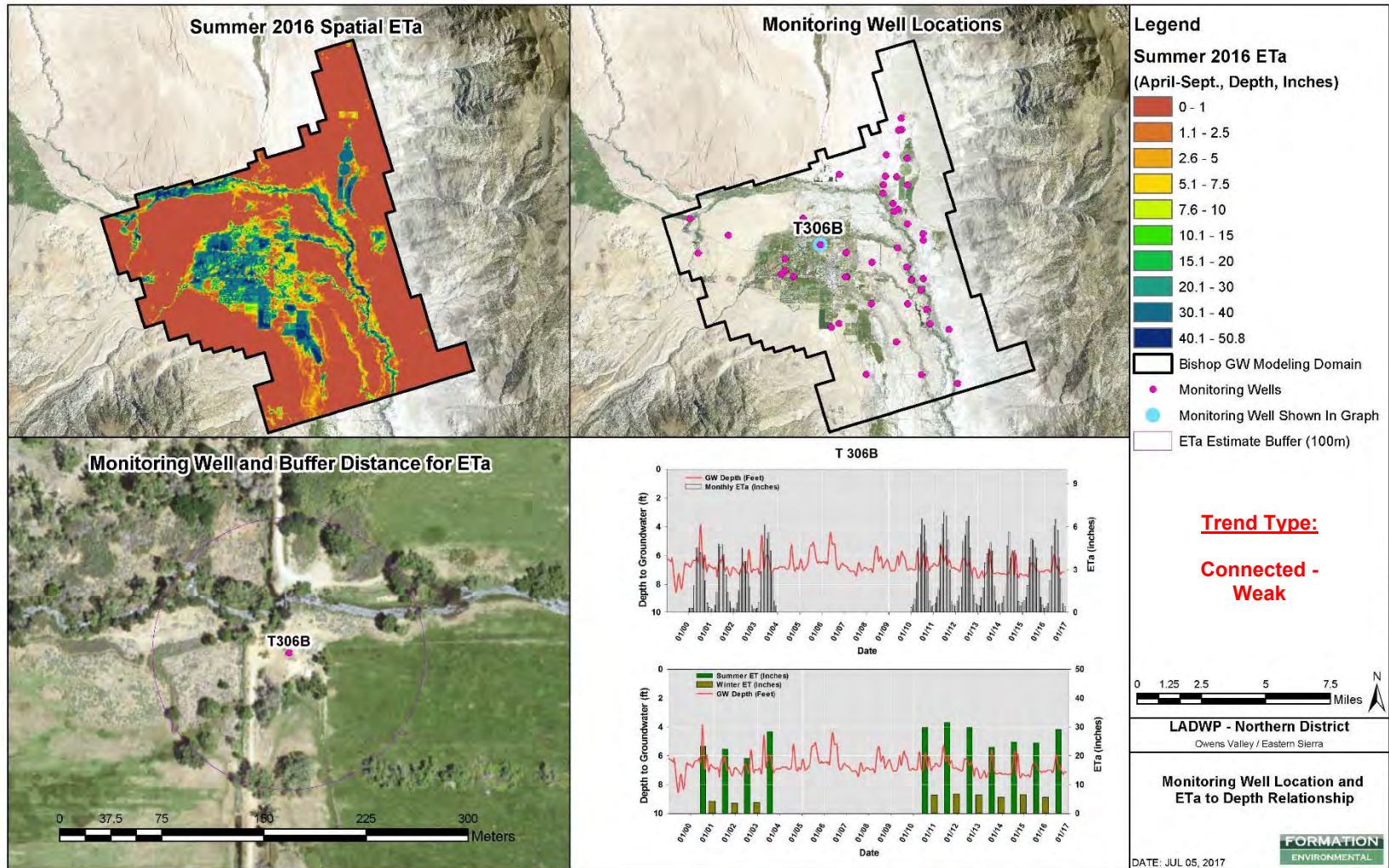
Well # T320A
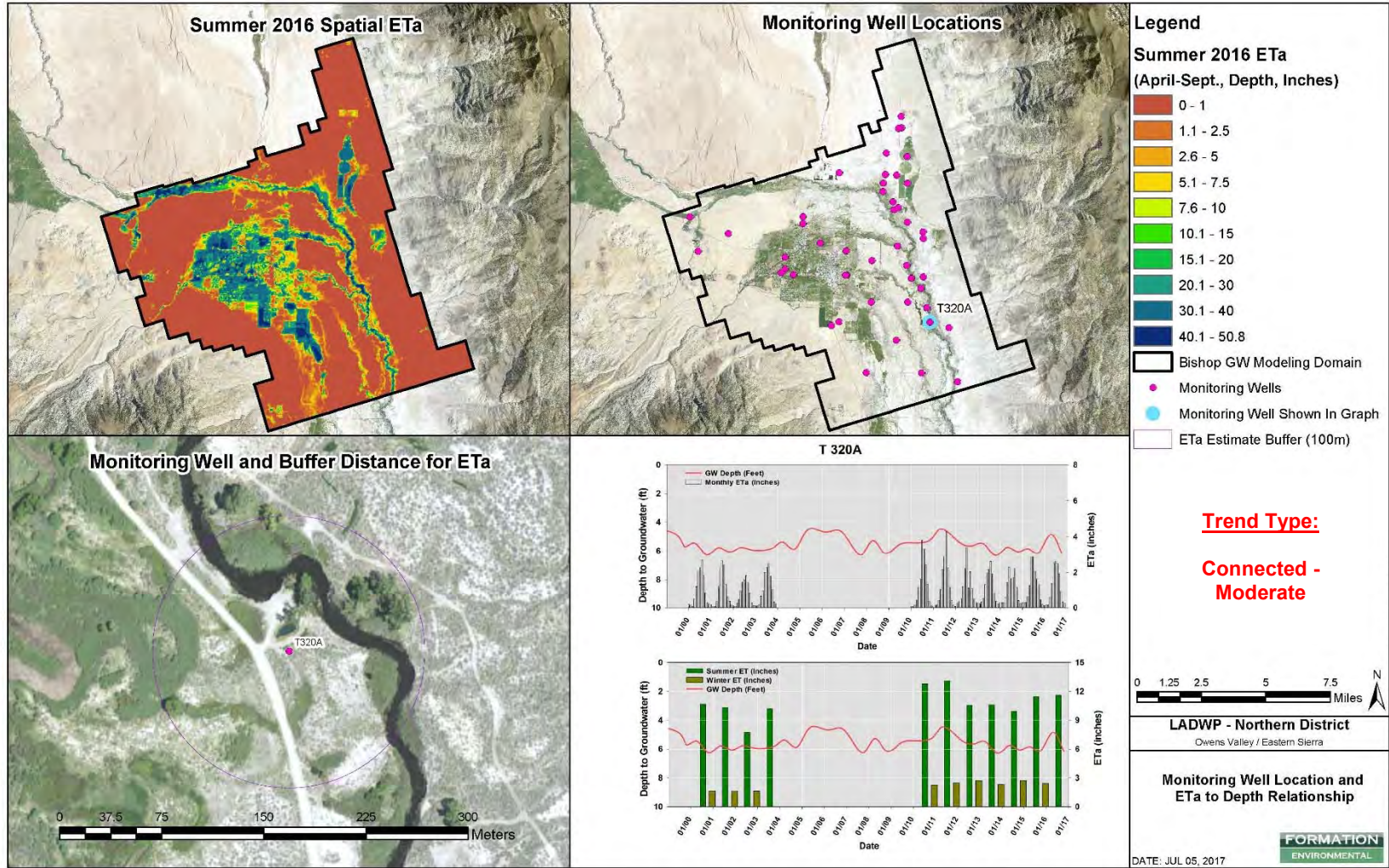
Well # T321A
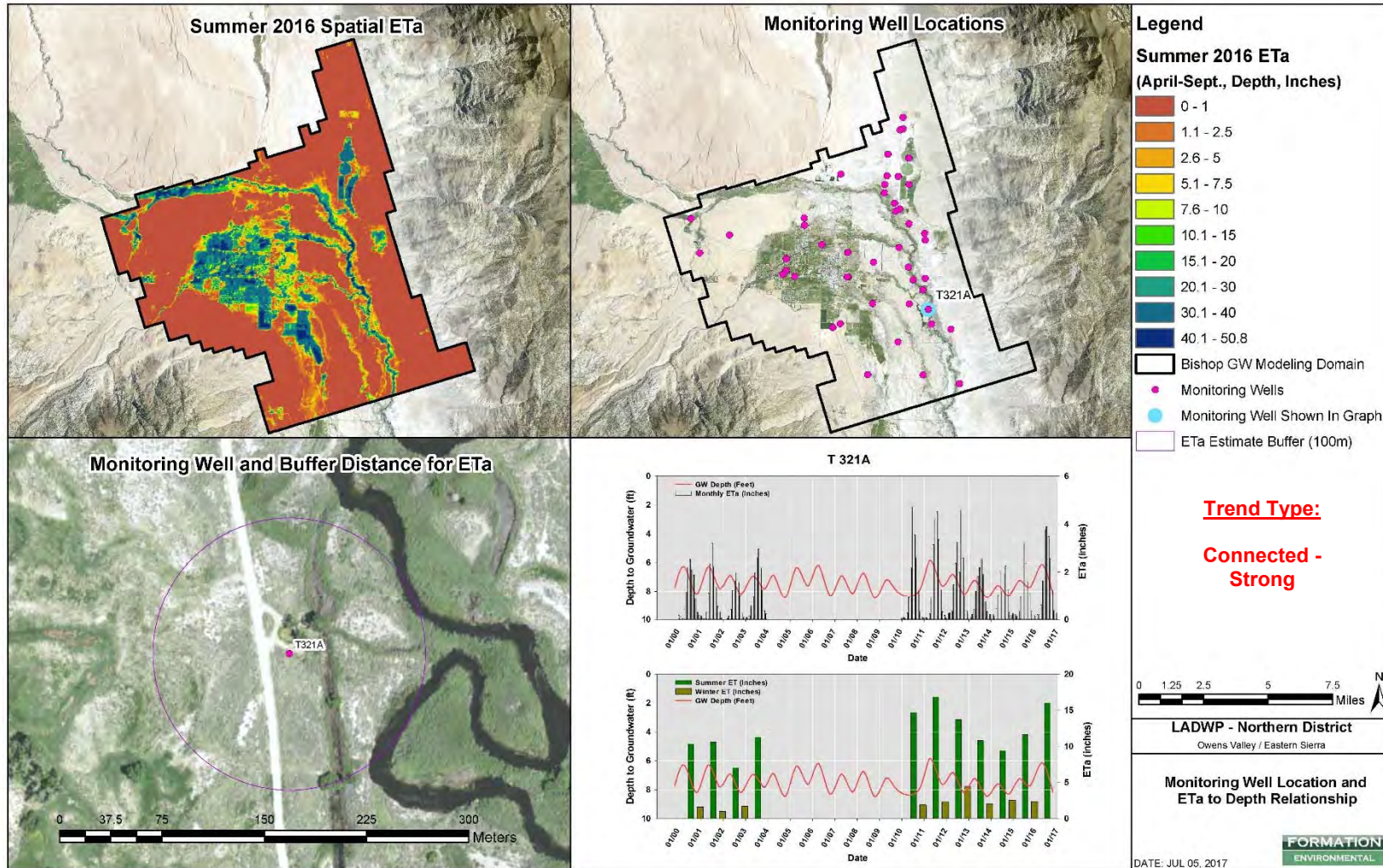
Well # T324A
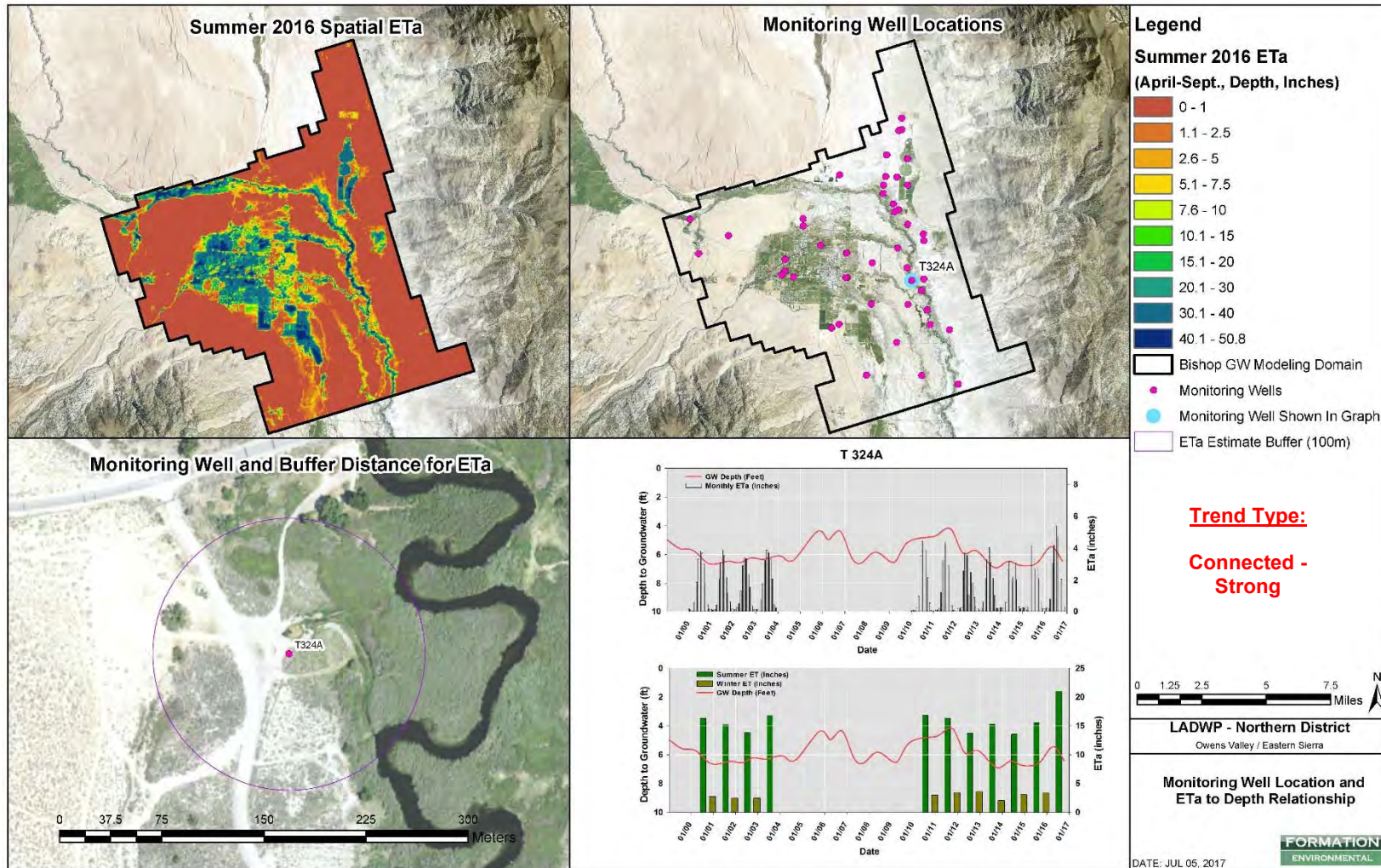
Well # T325A
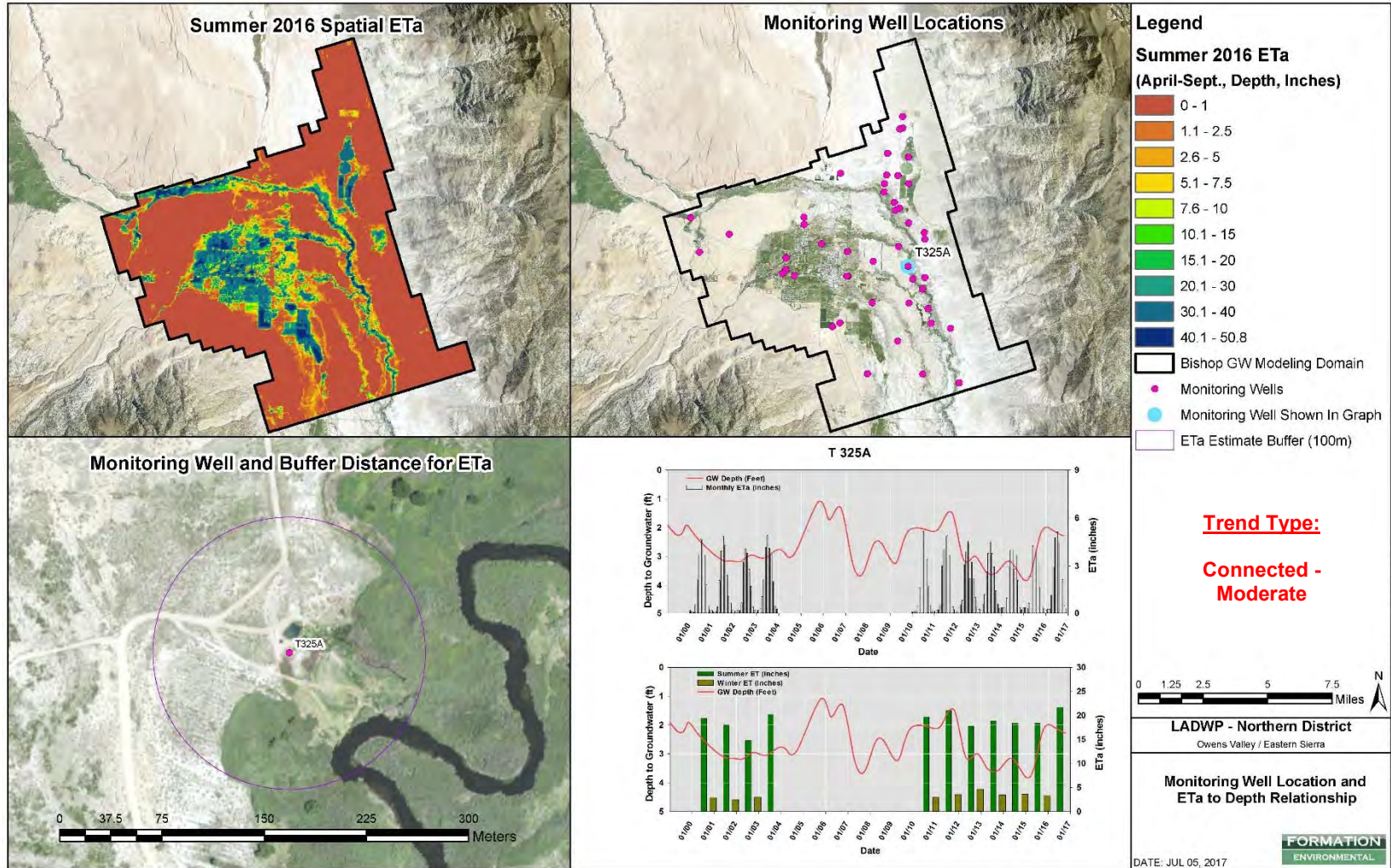
Well # T384
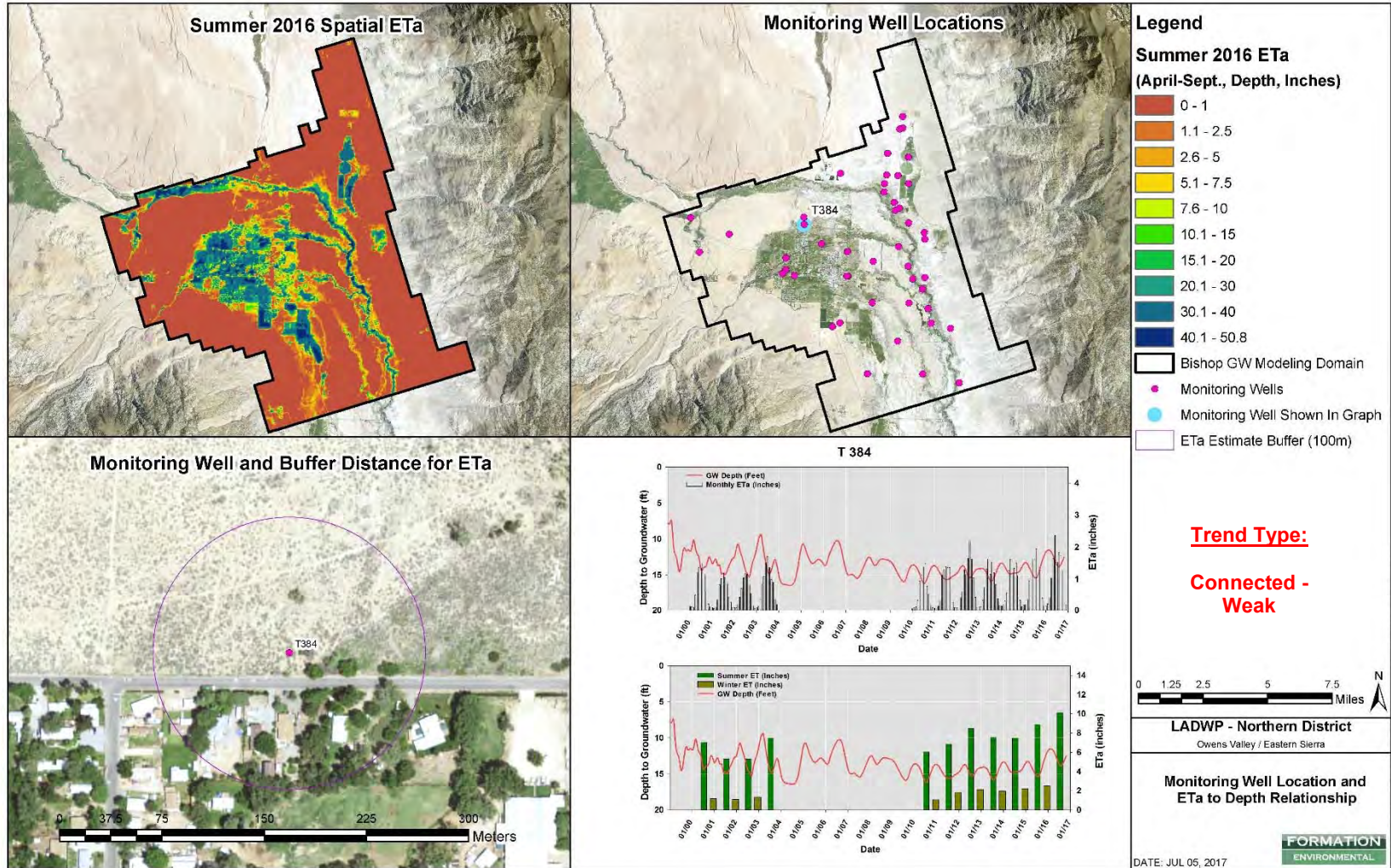
Well # T390
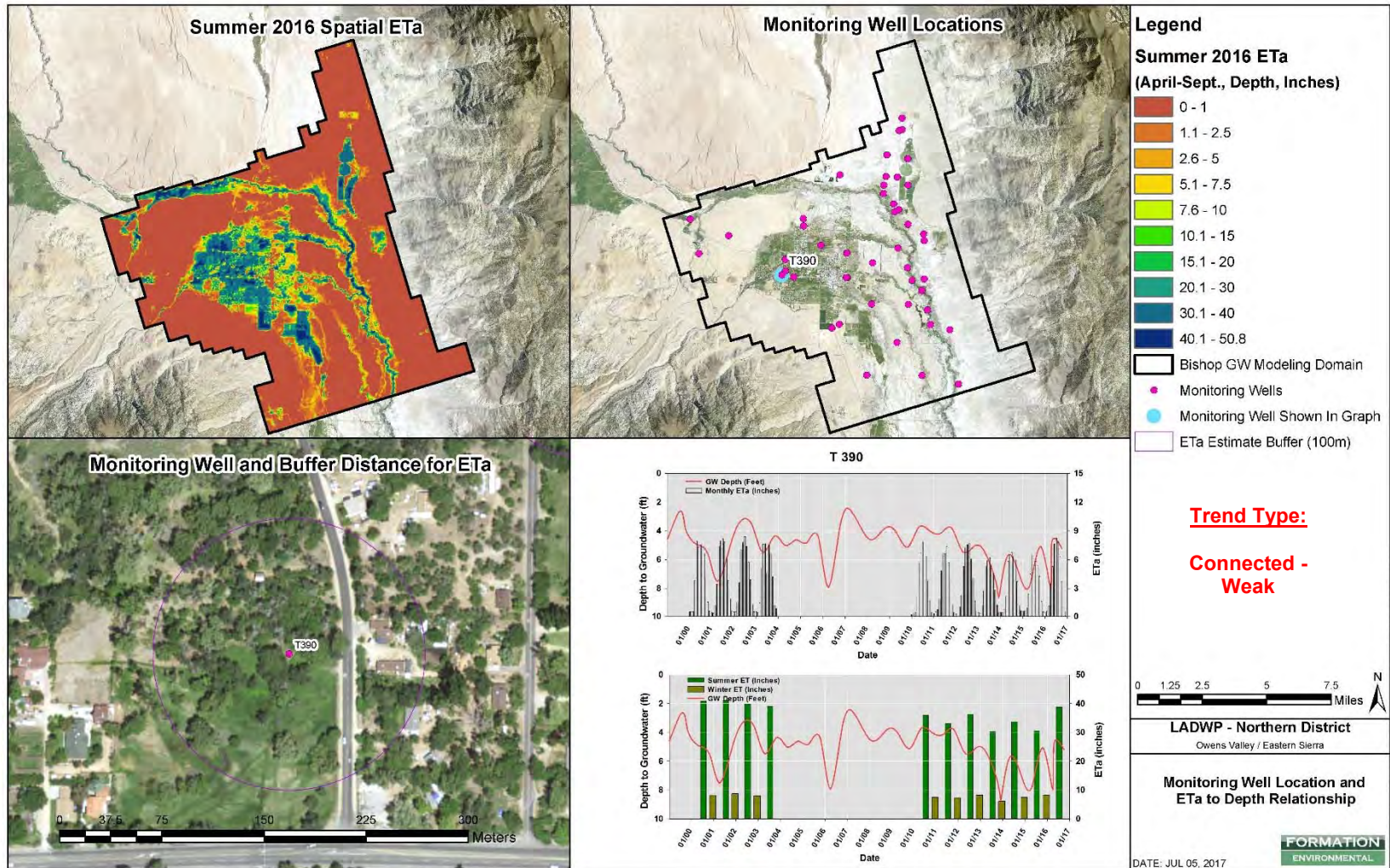
Well # T430
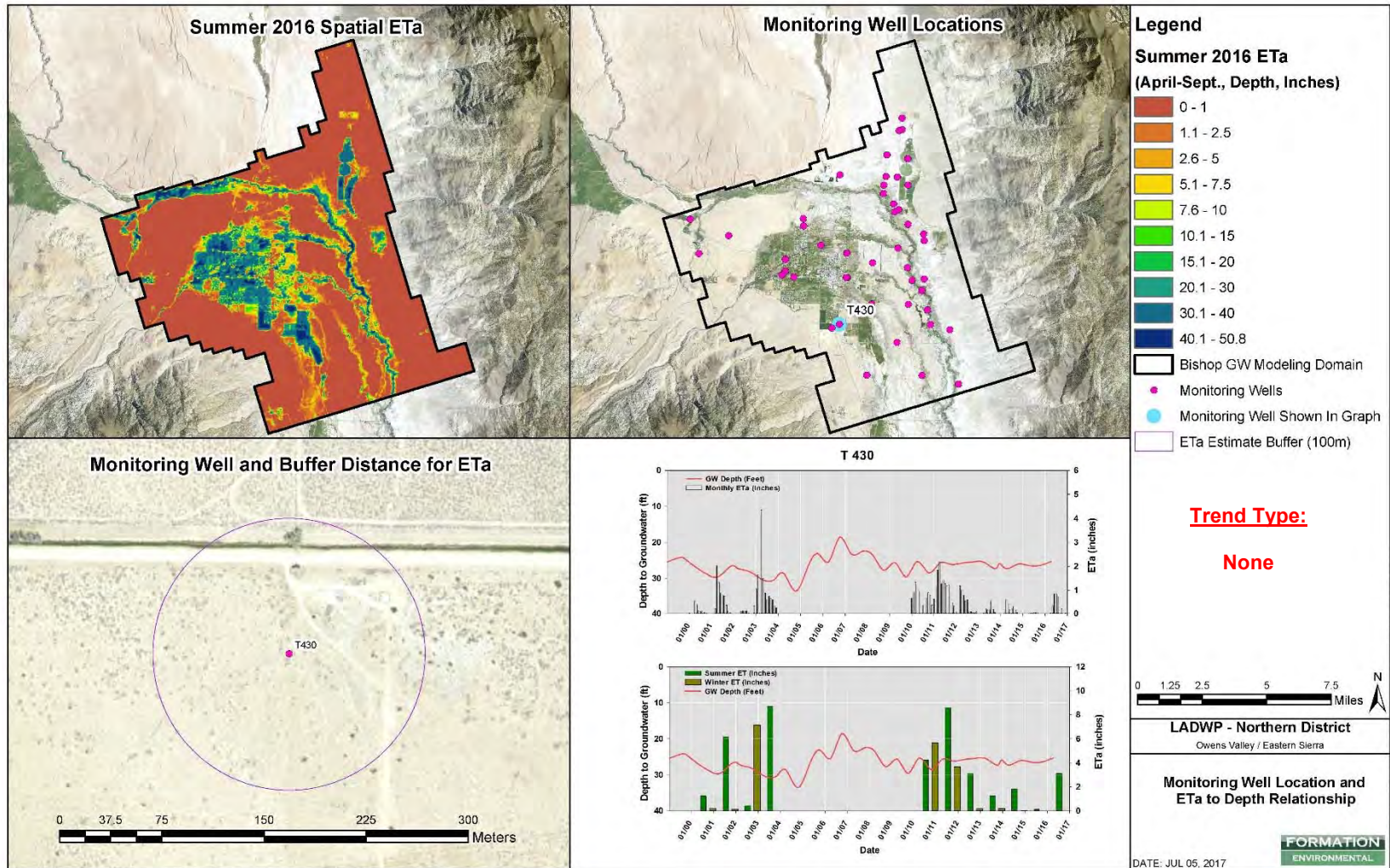
Well # T434
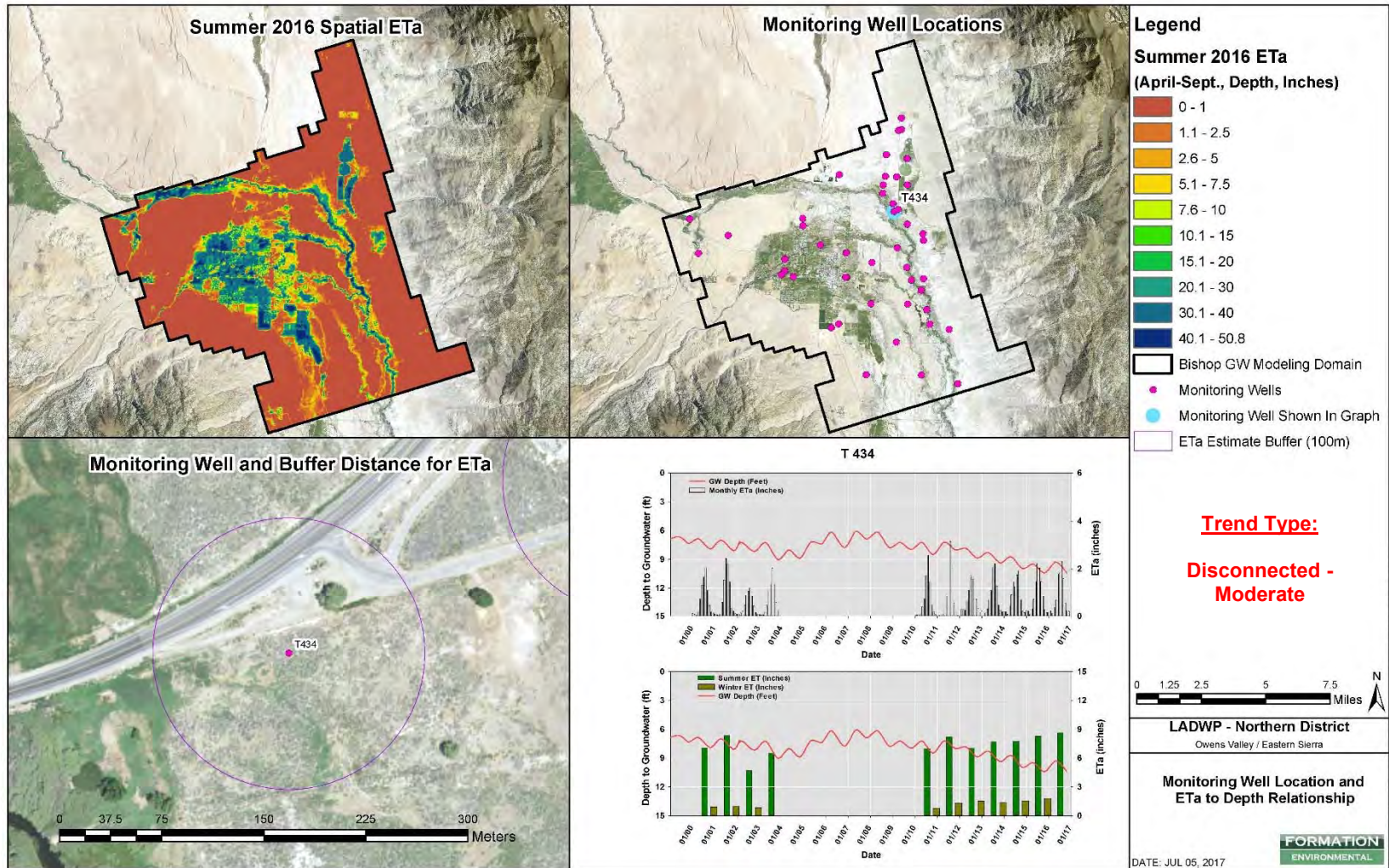
Well # T435
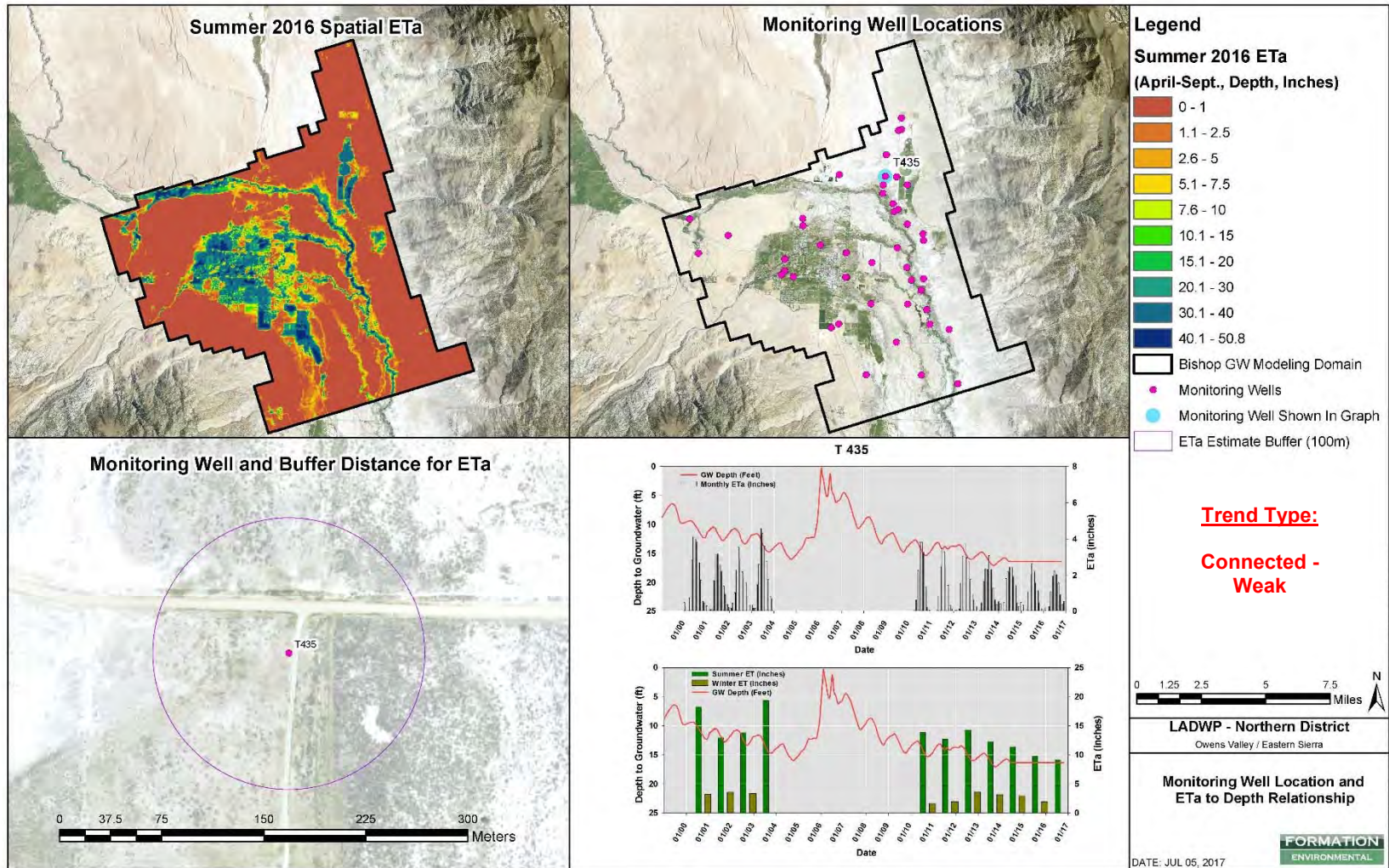
Well # T436
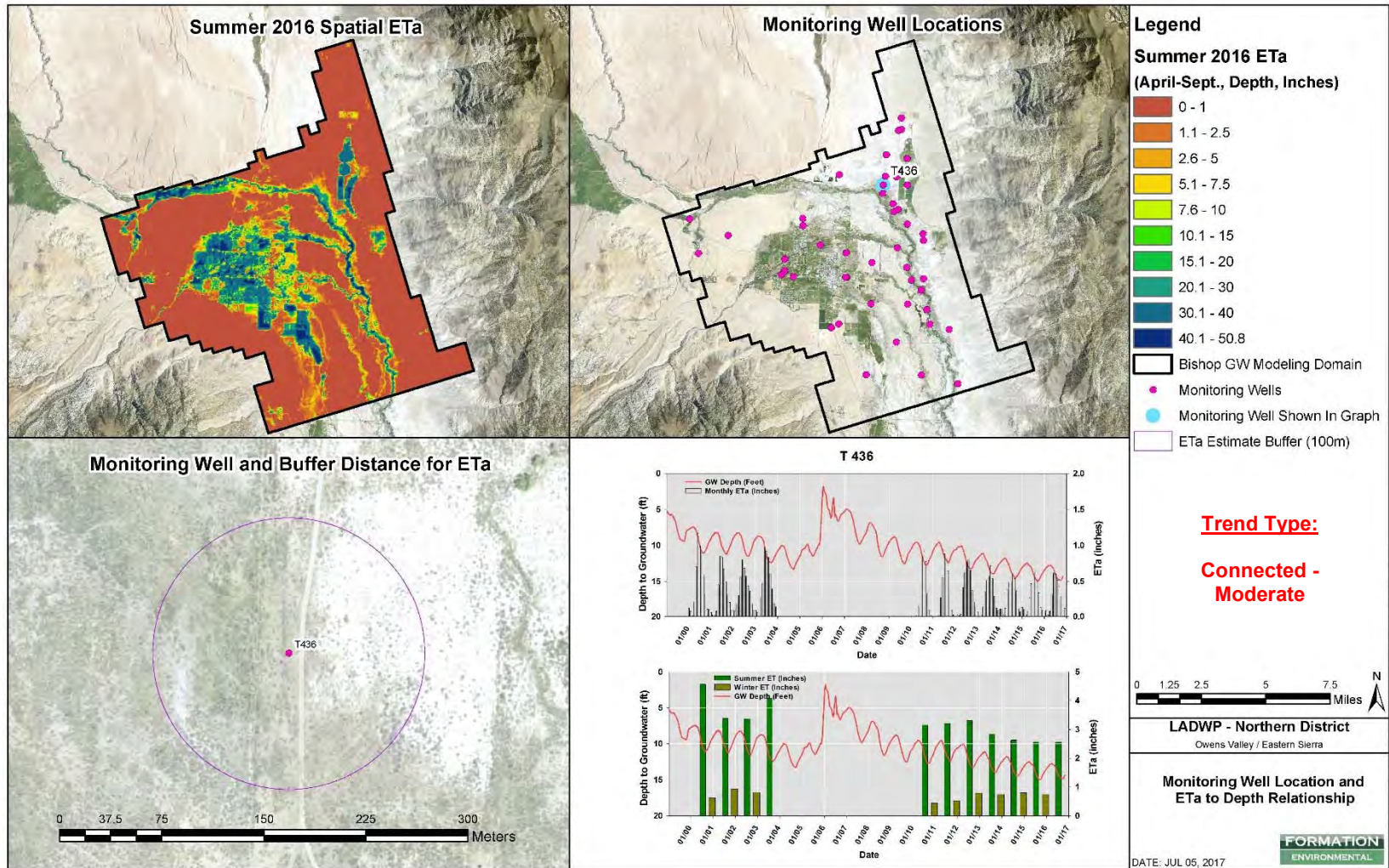
Well # T438
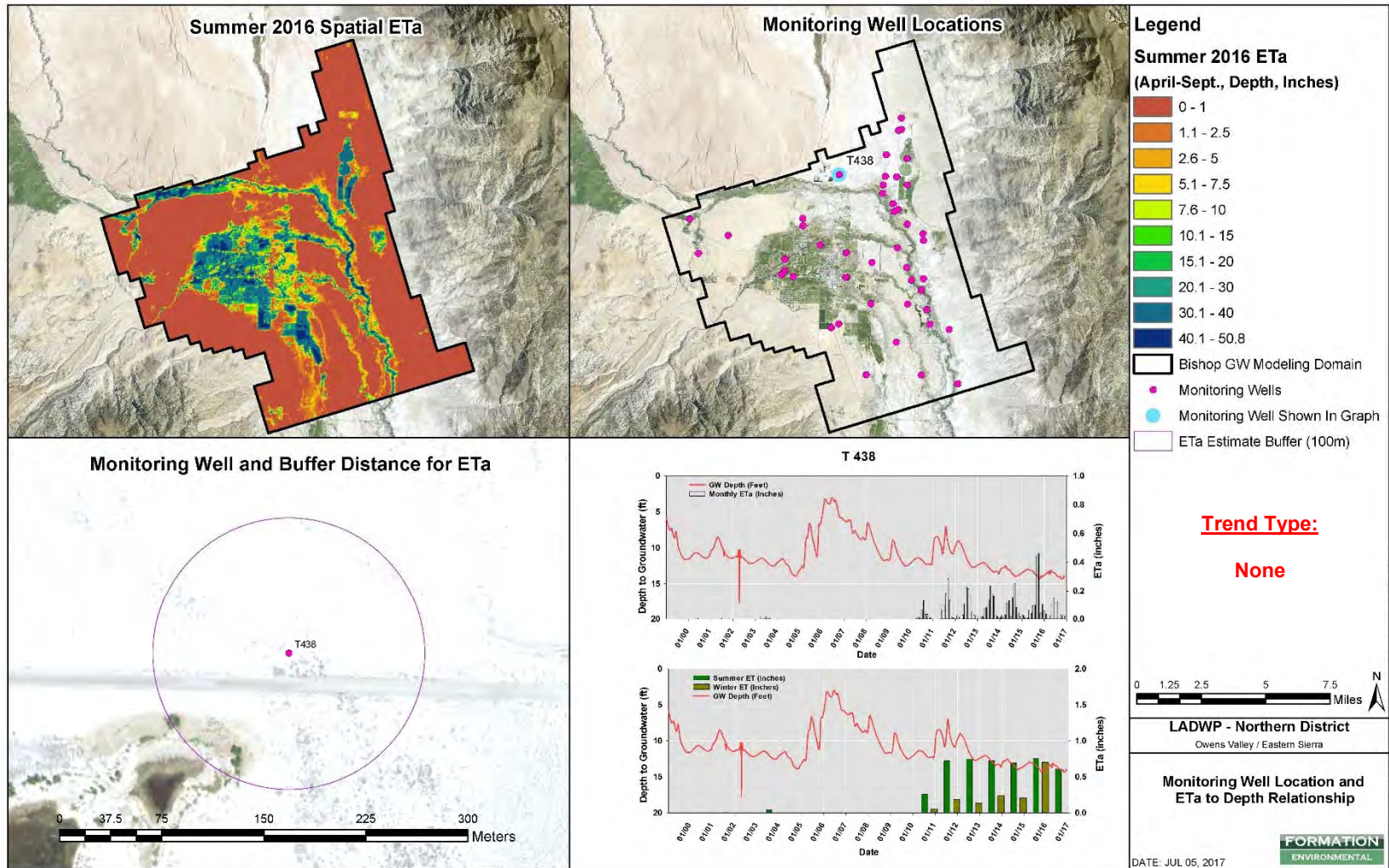
Well # T481
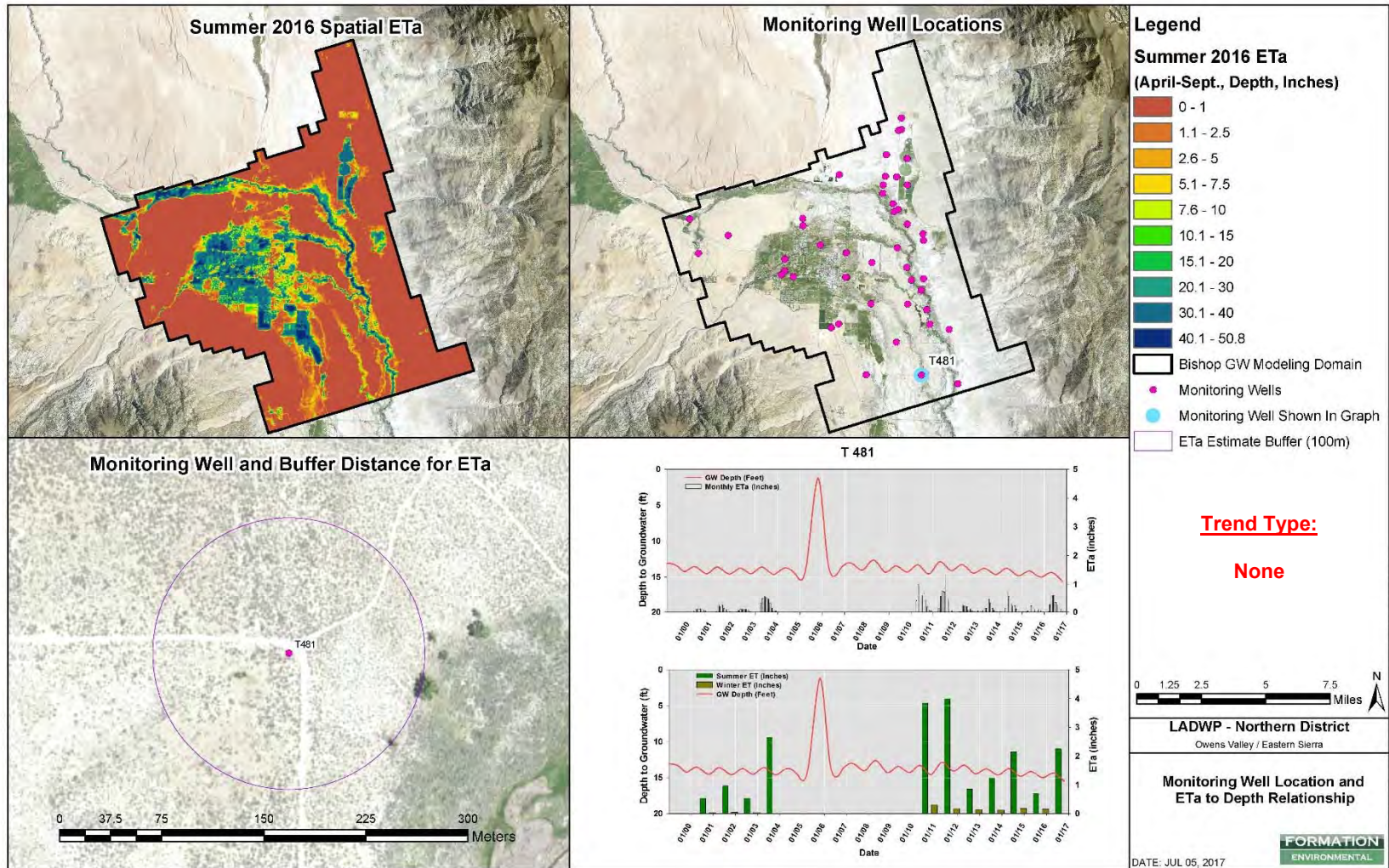
Well # T485
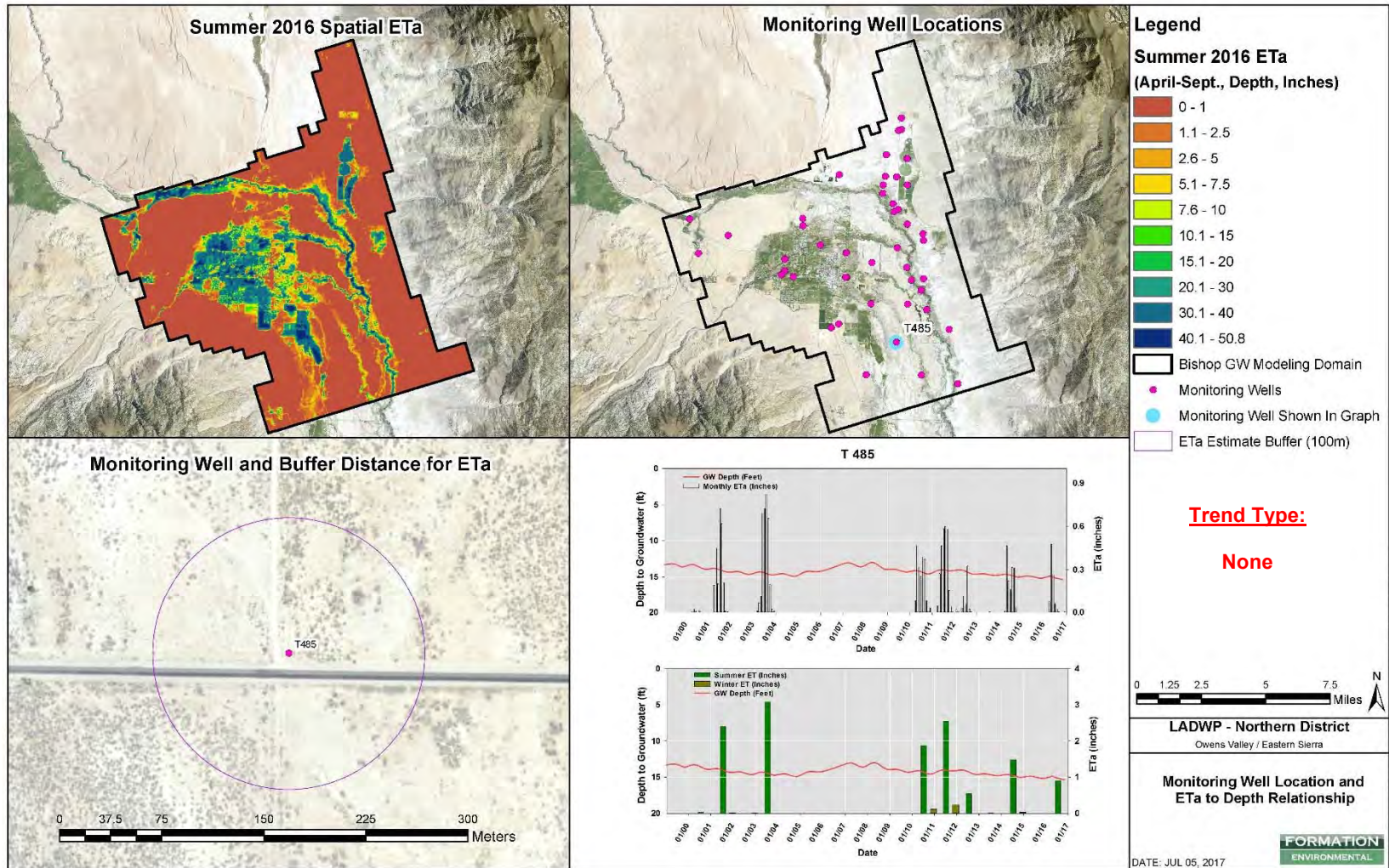
Well # T487
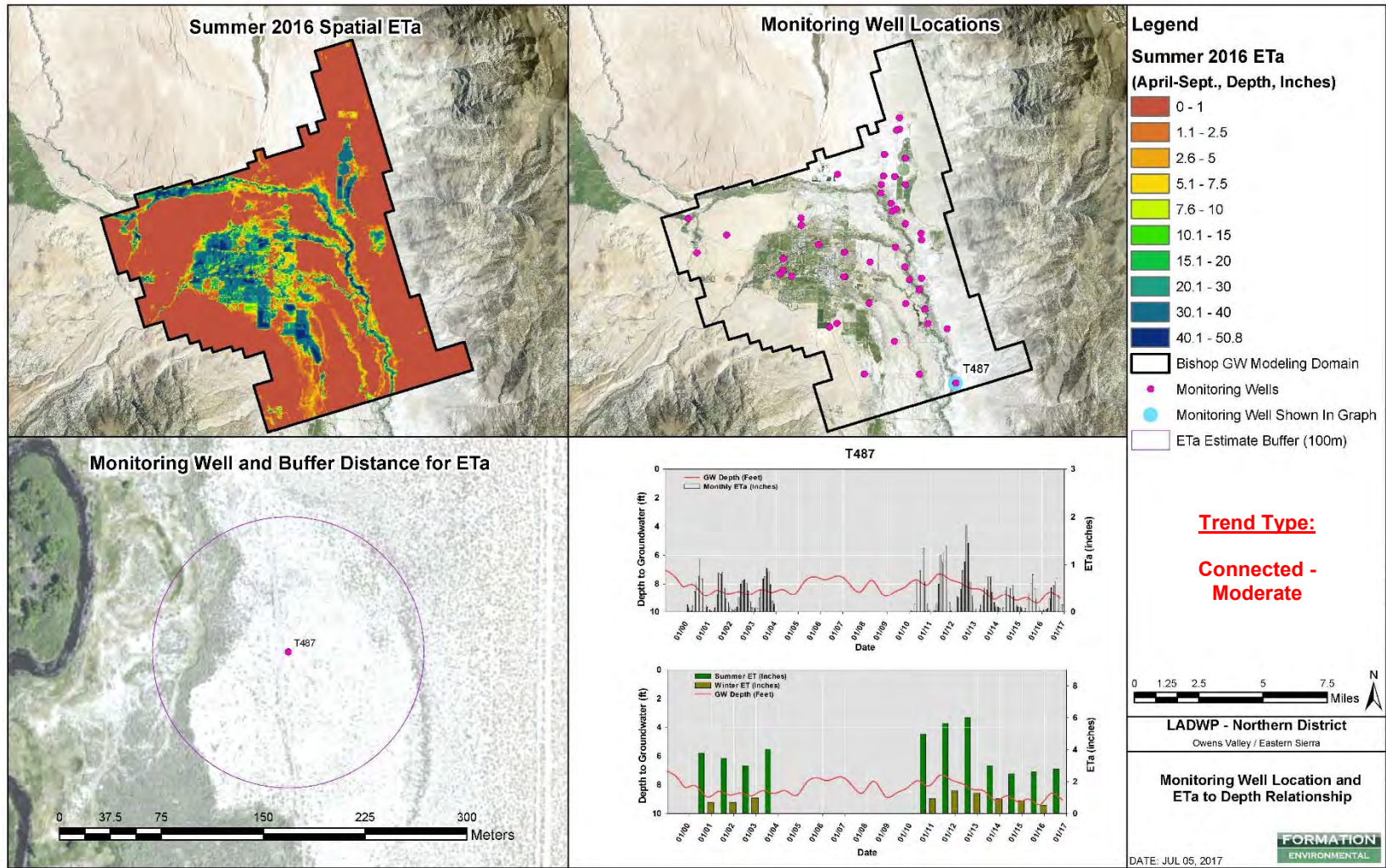
Well # T488
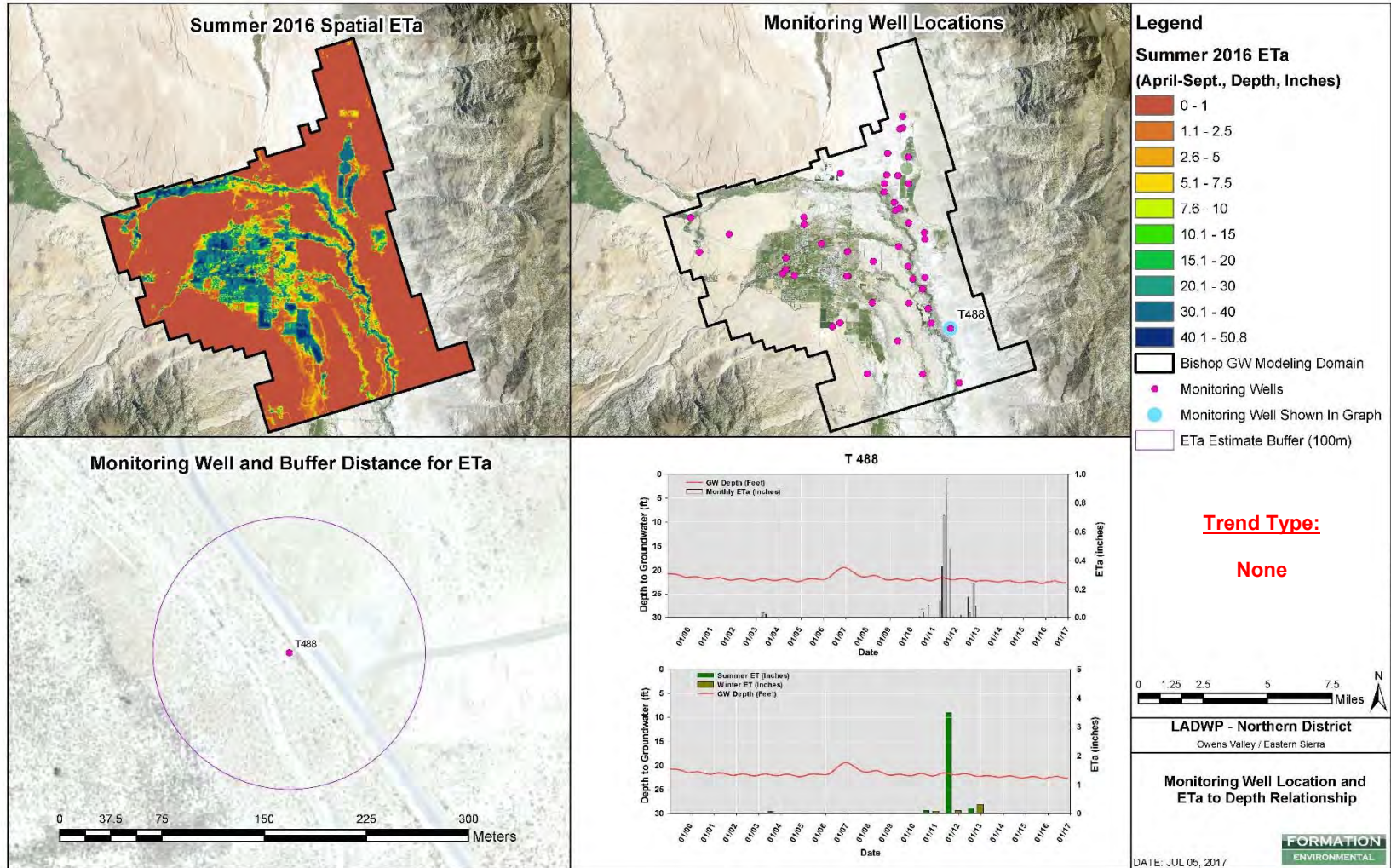
Well # T490
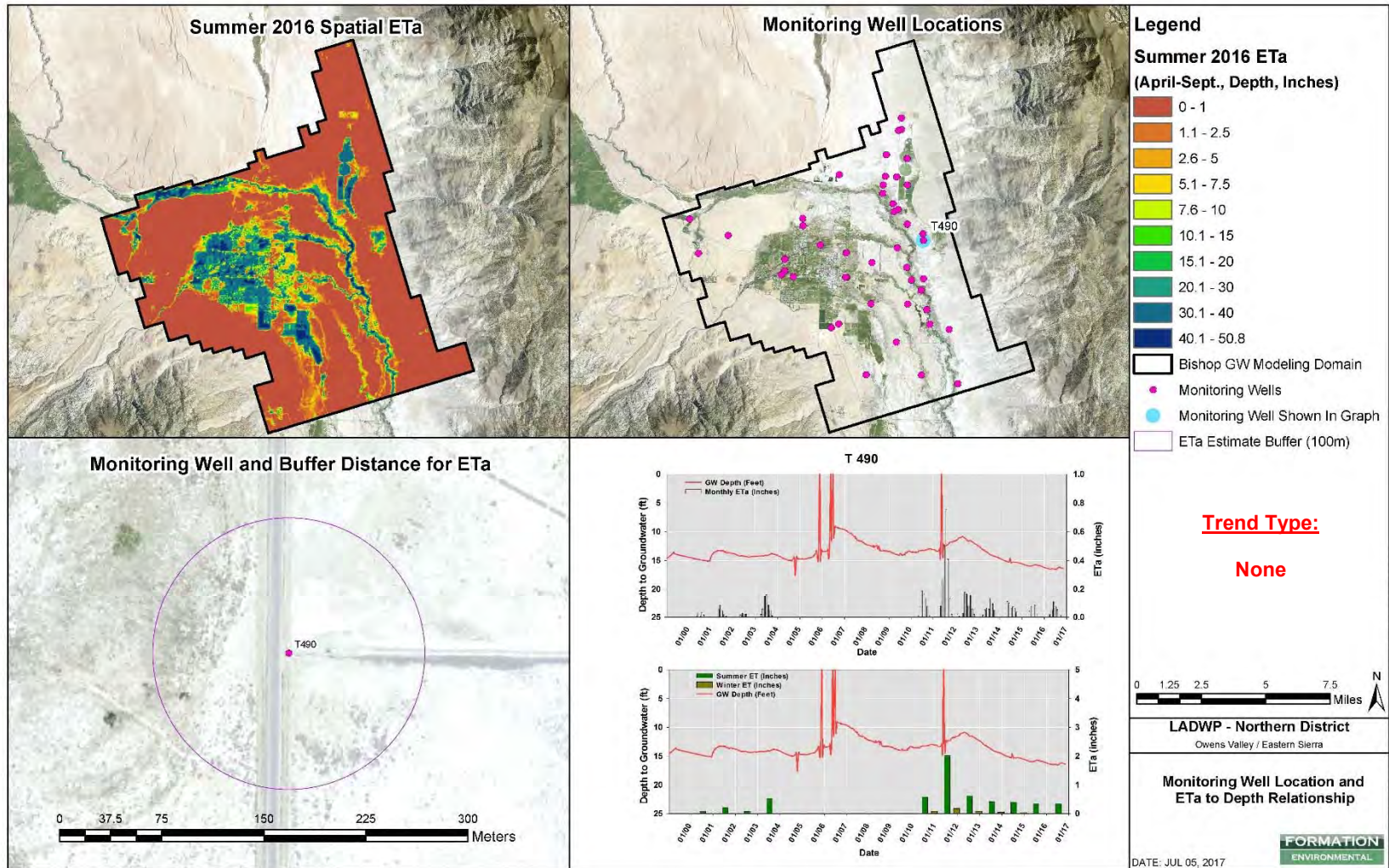
Well # T492
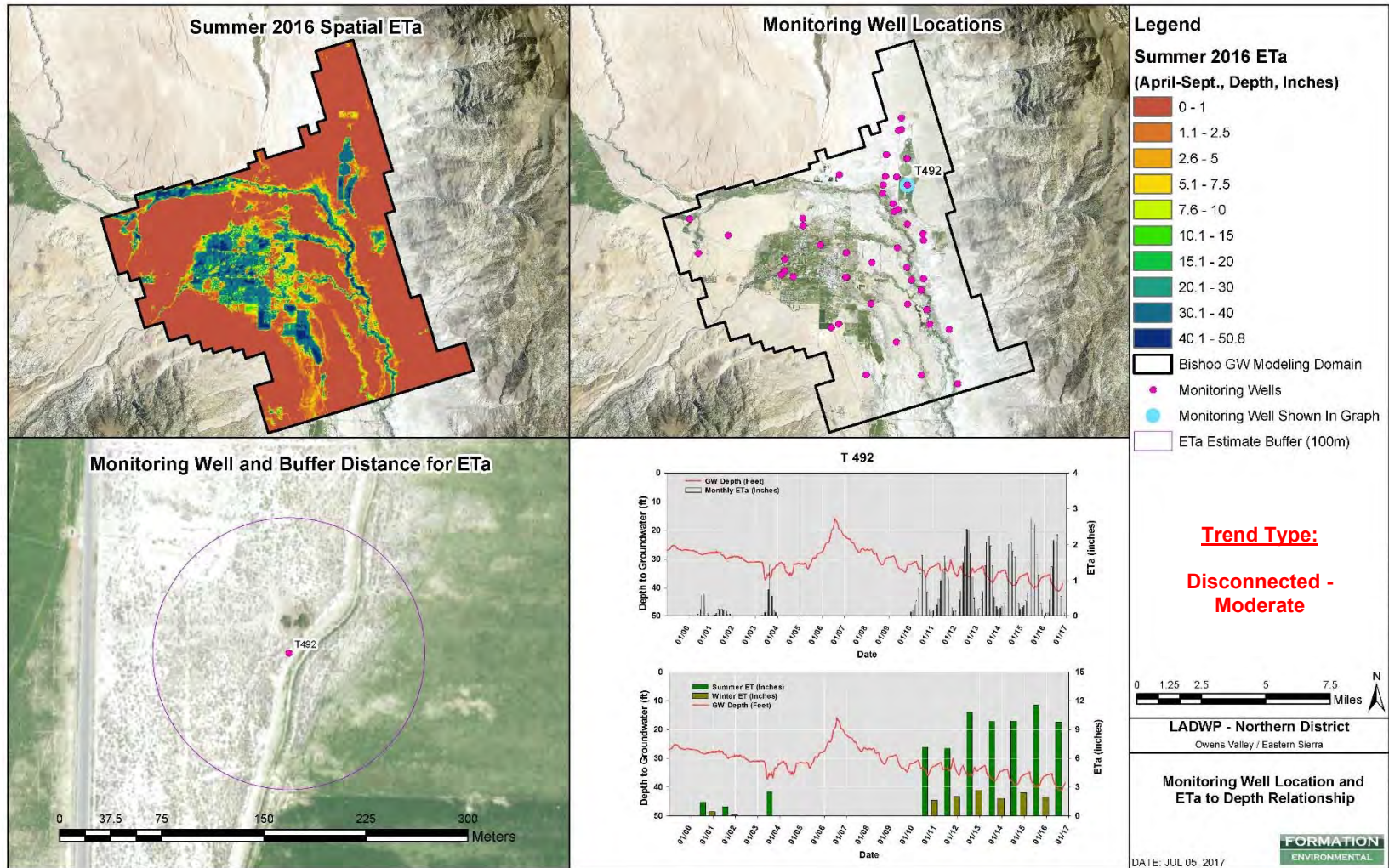
Well # T500
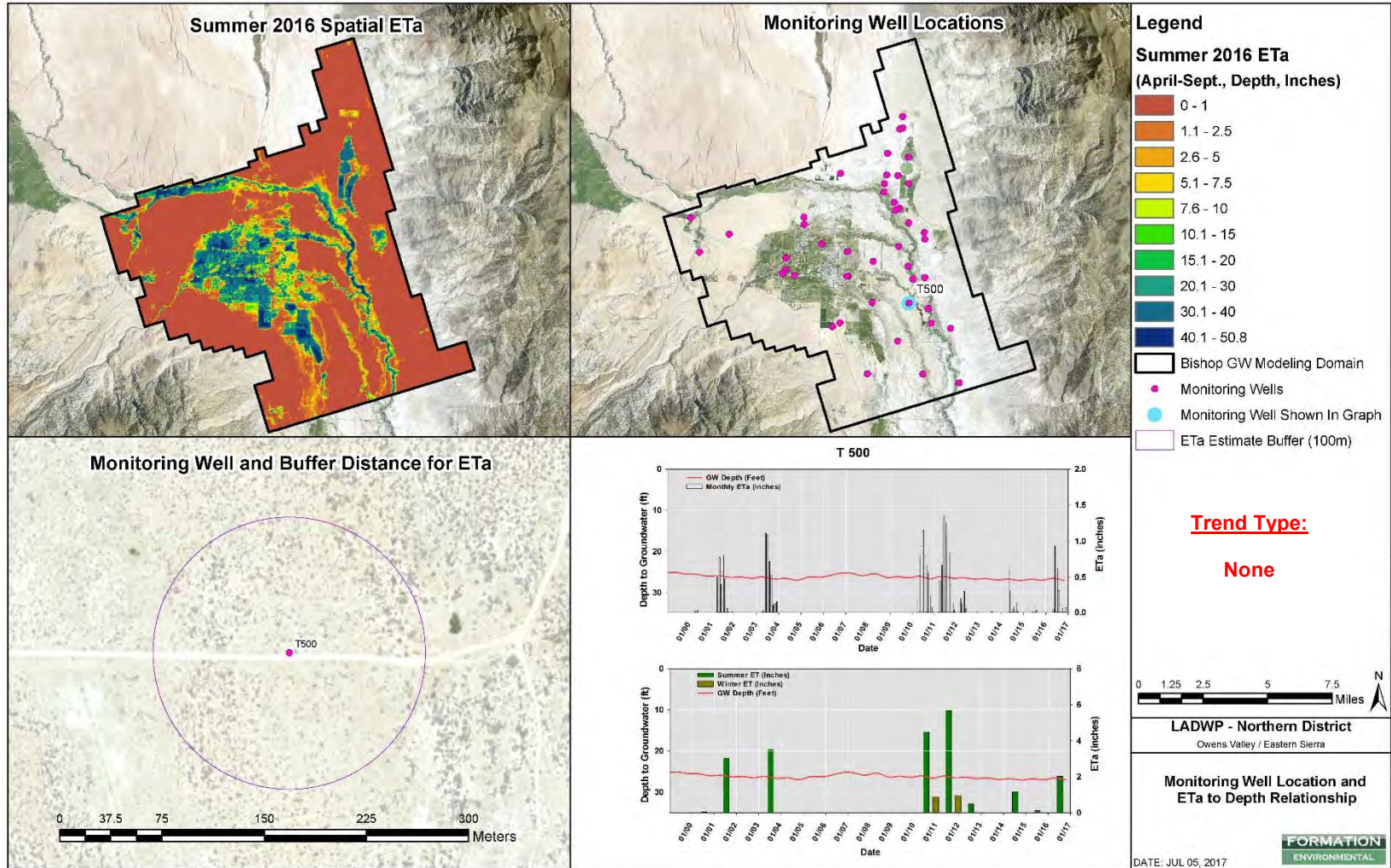
Well # T501
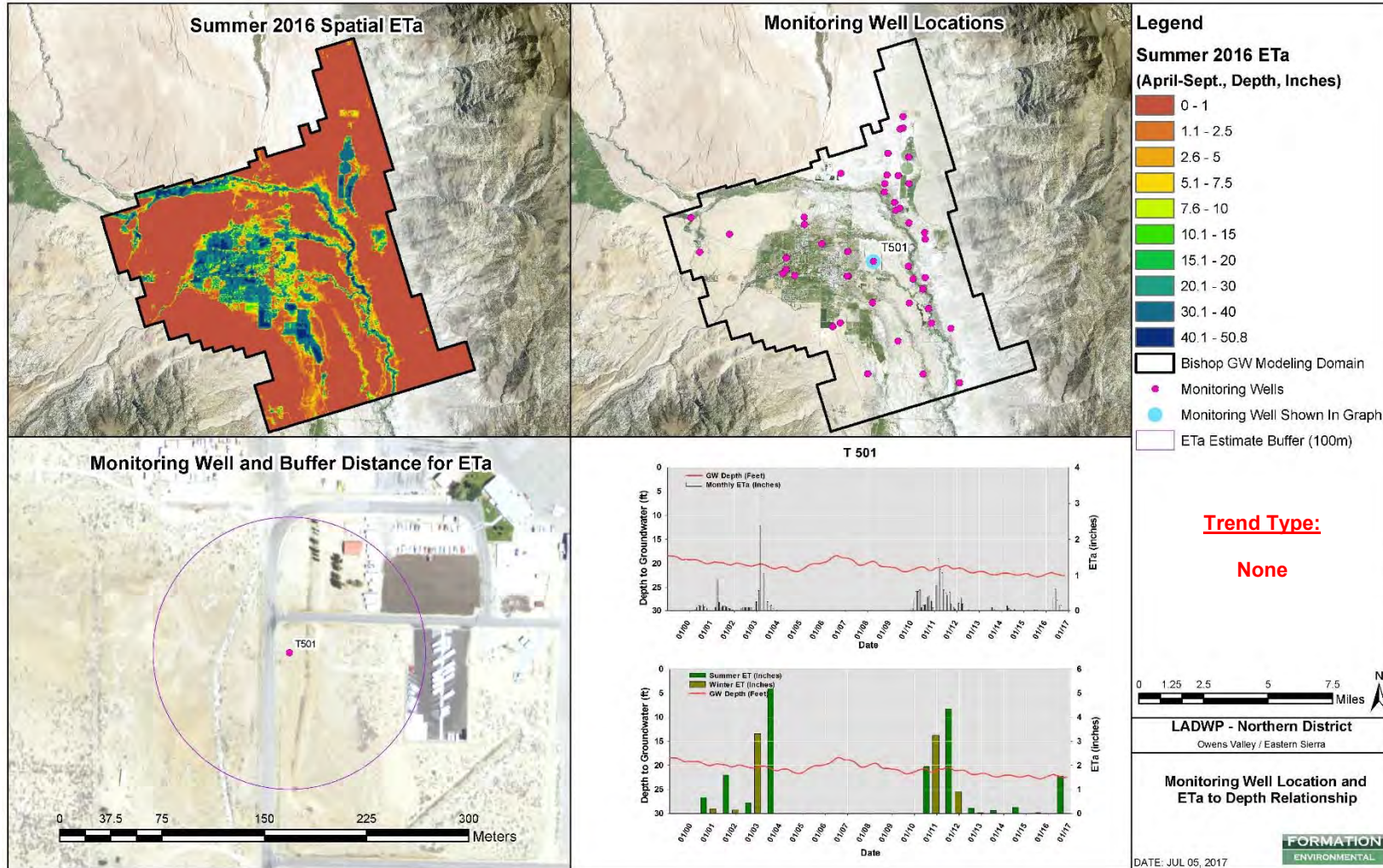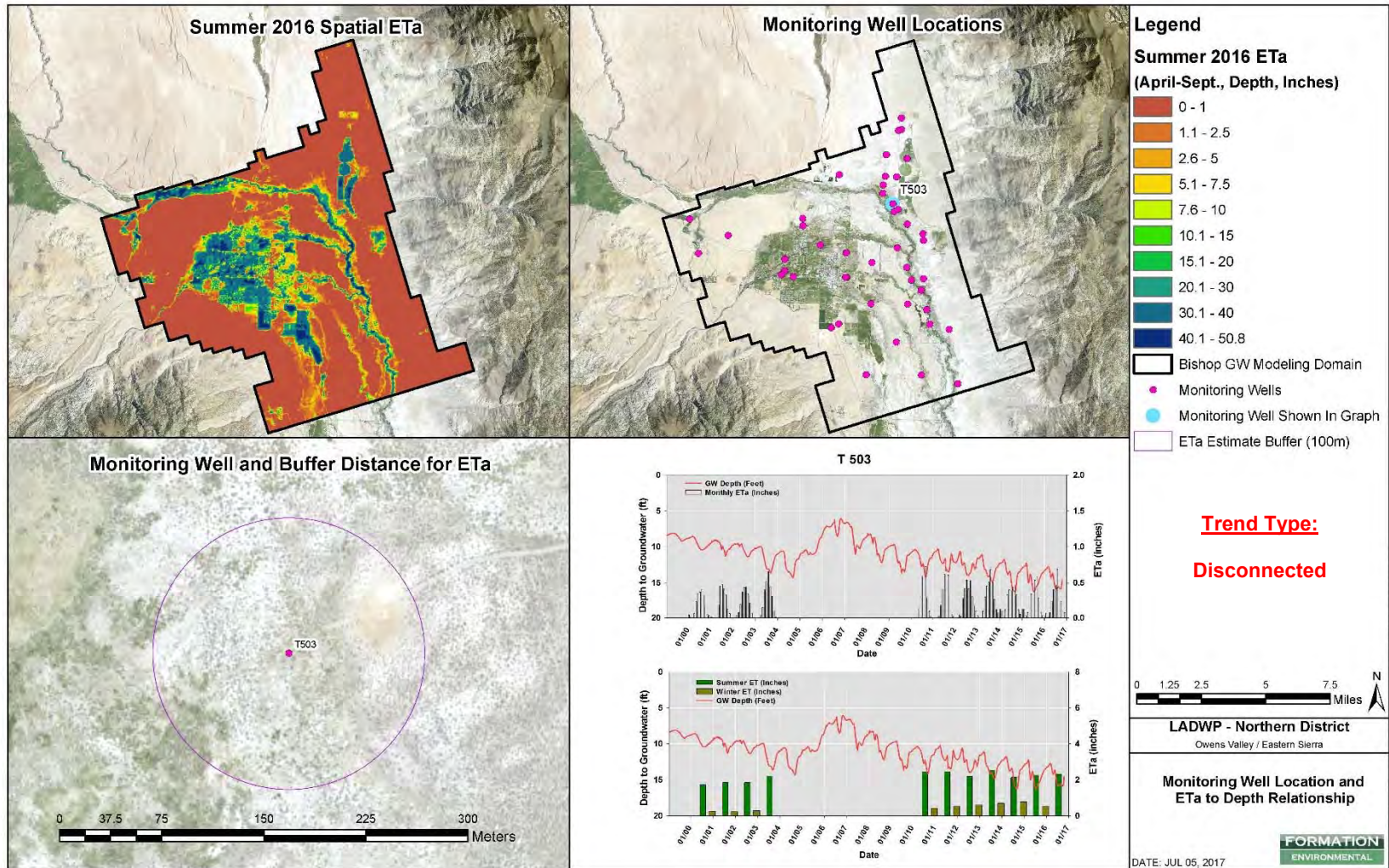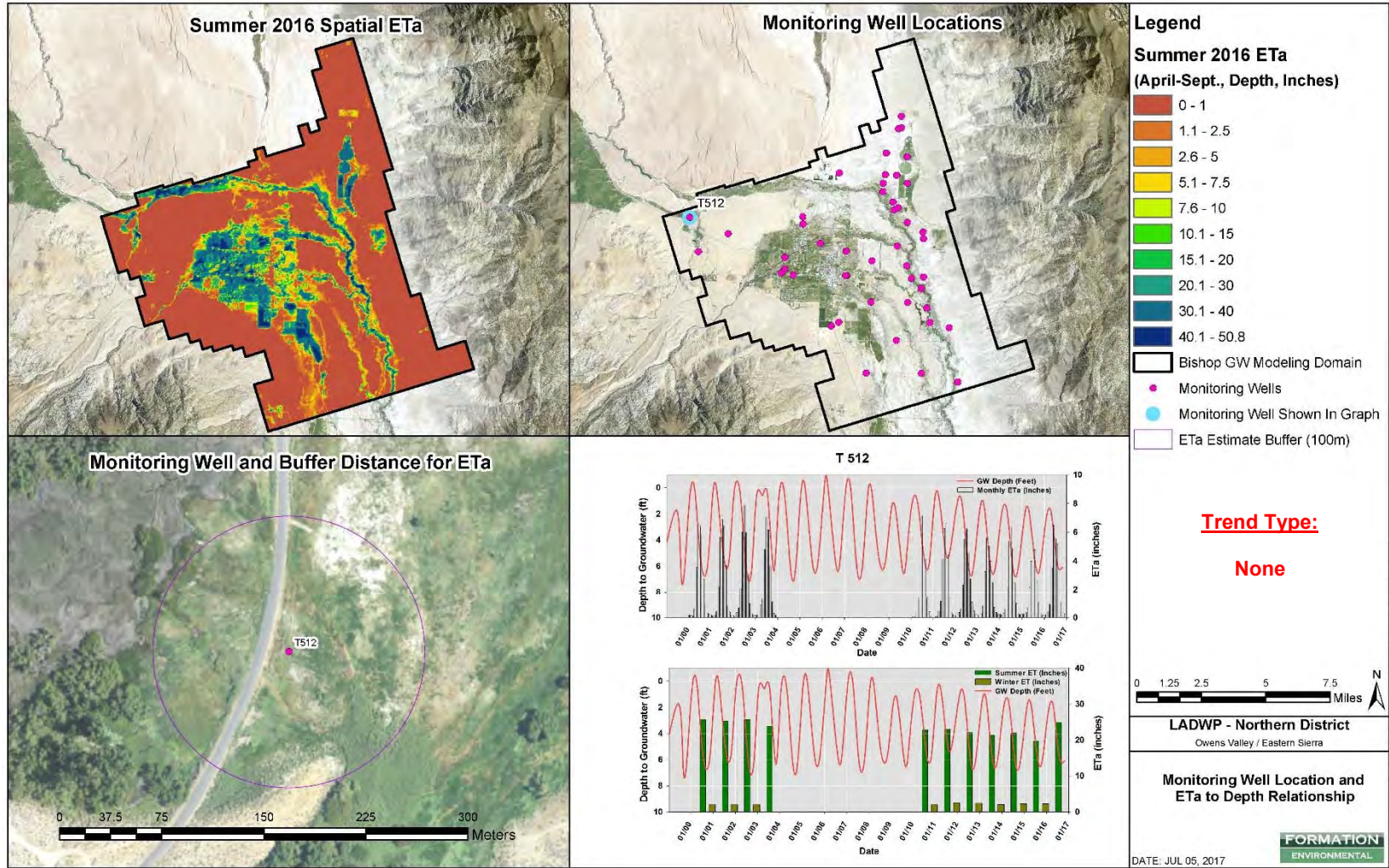
Well # T503

Well # T512

Well # T513
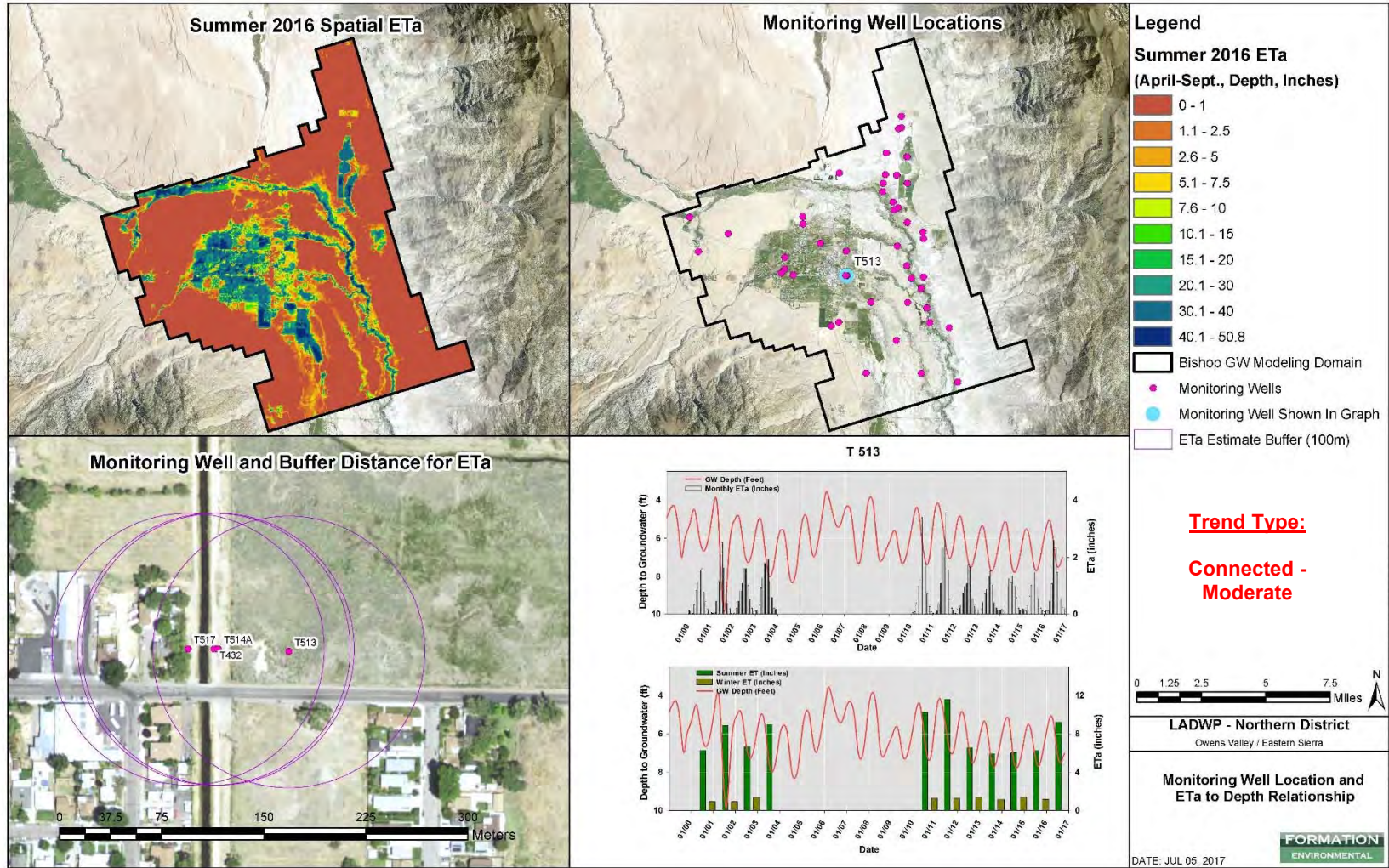
Well # T573
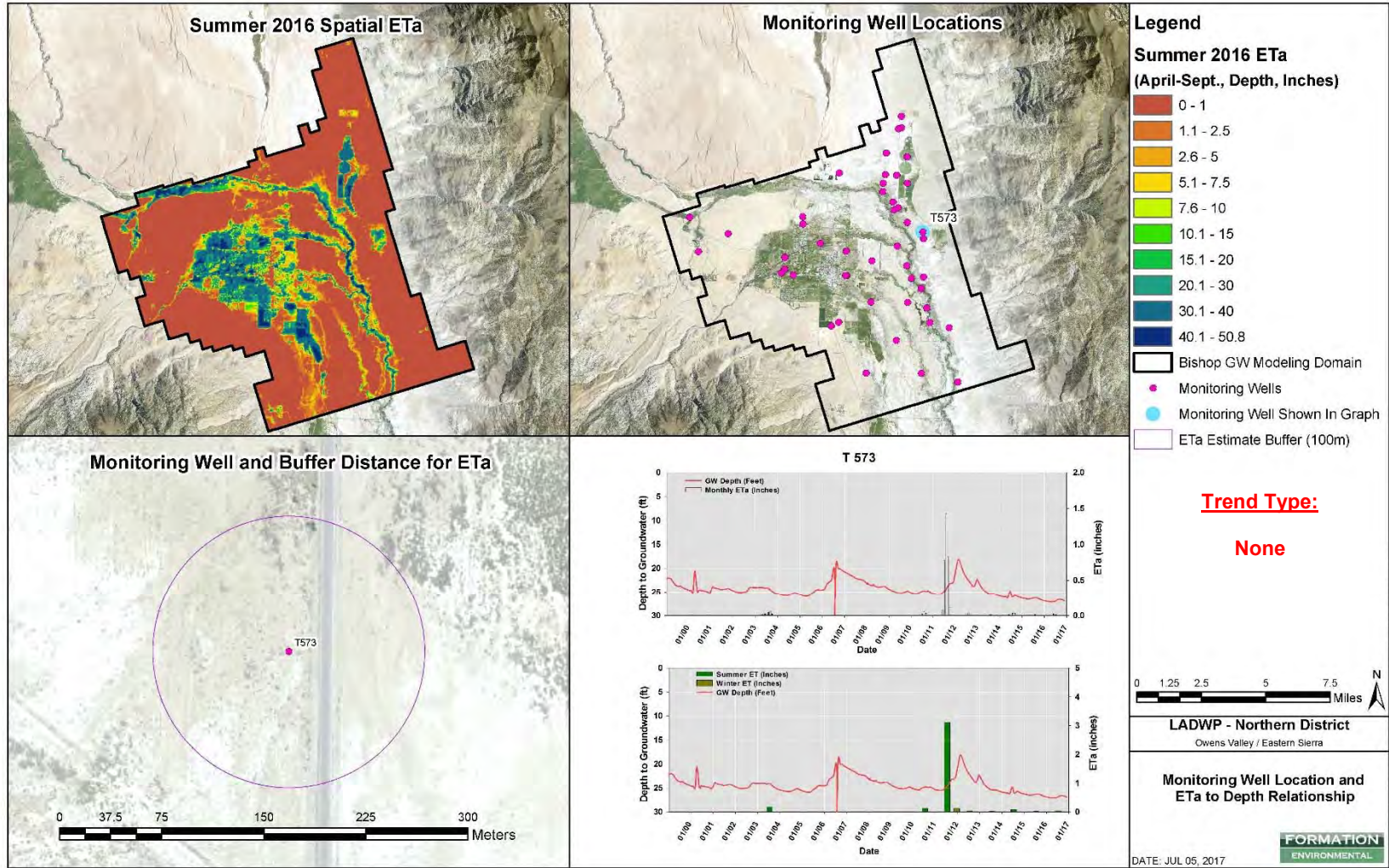
Well # T574
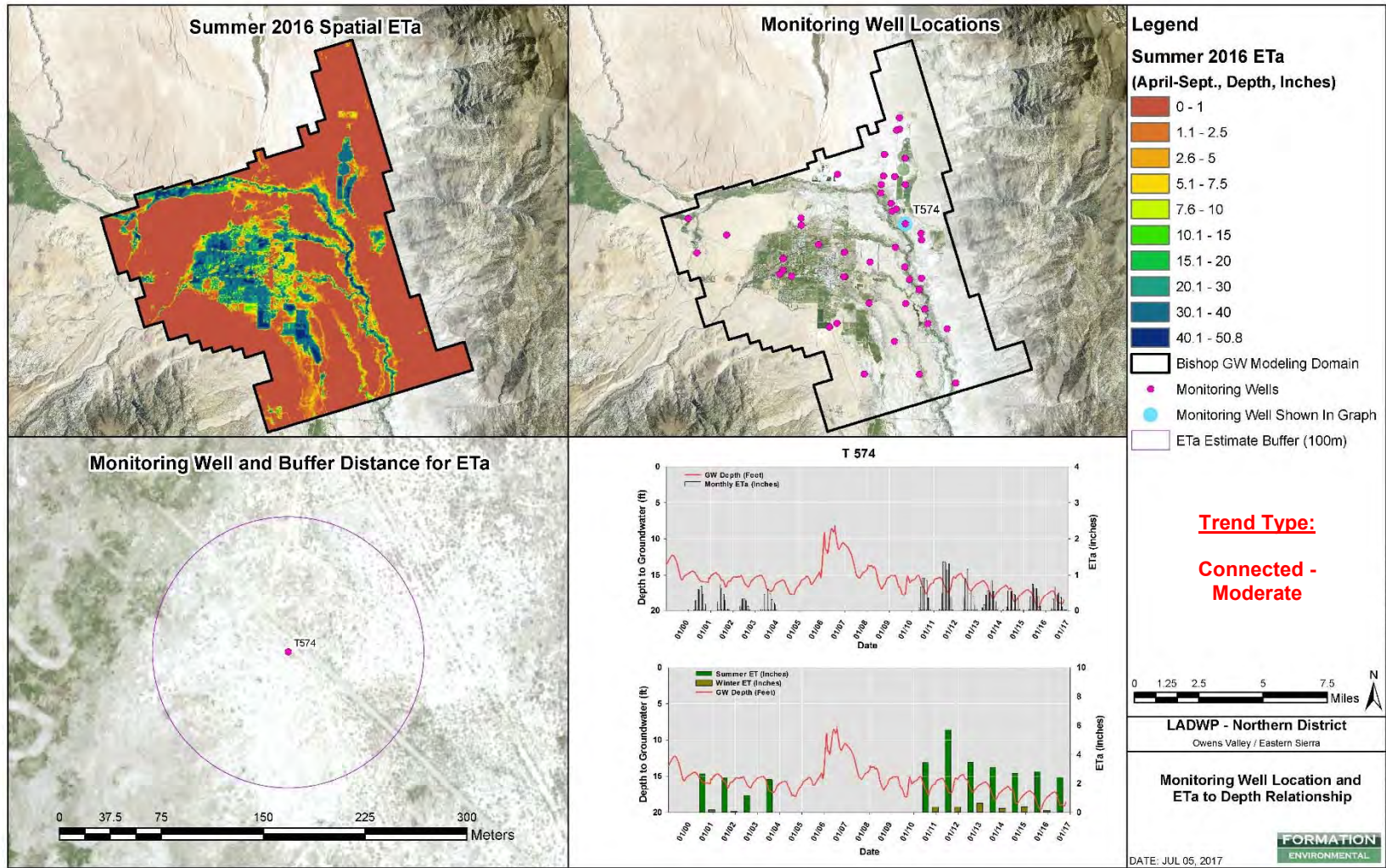
Well # T575
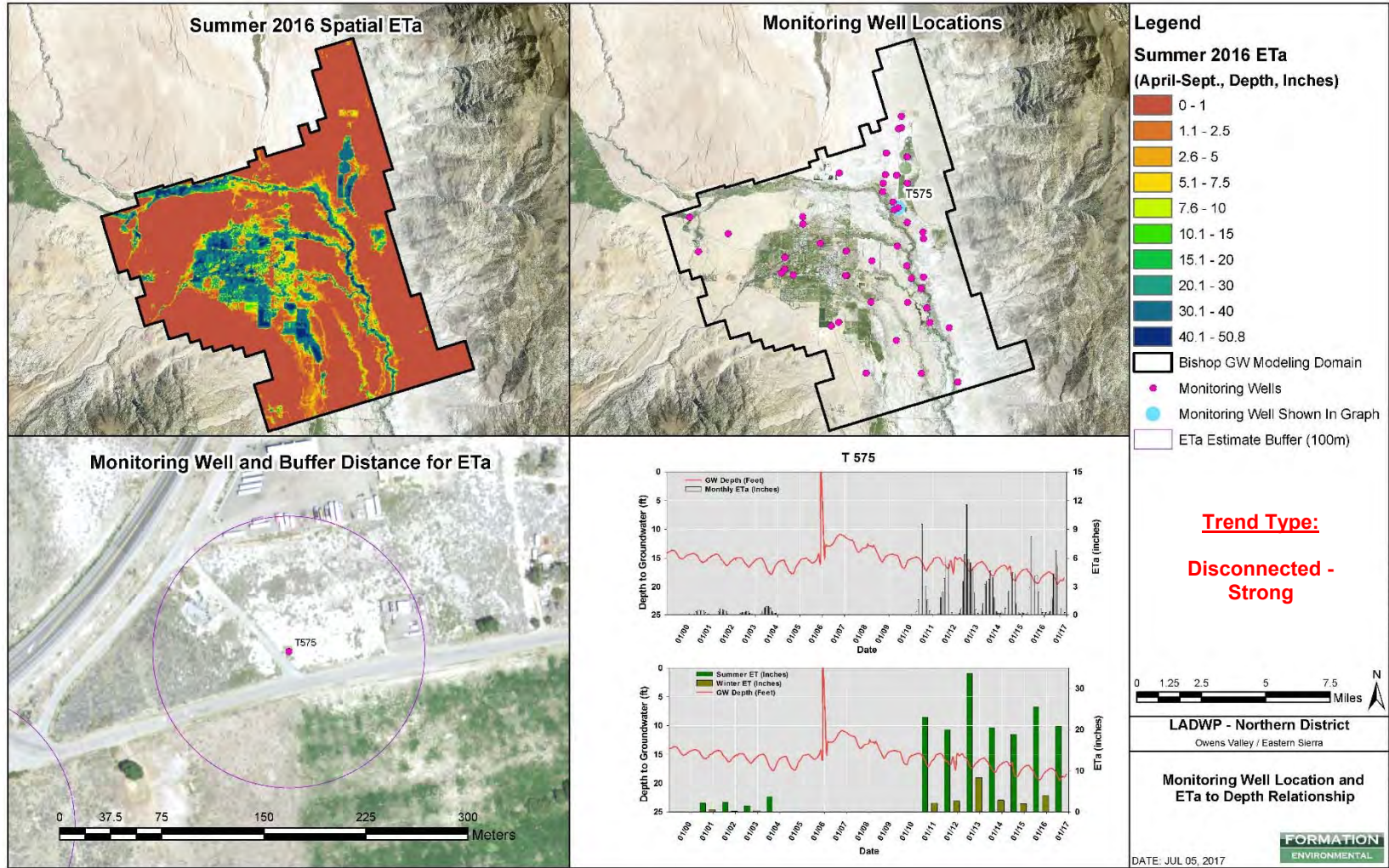
Well # T577
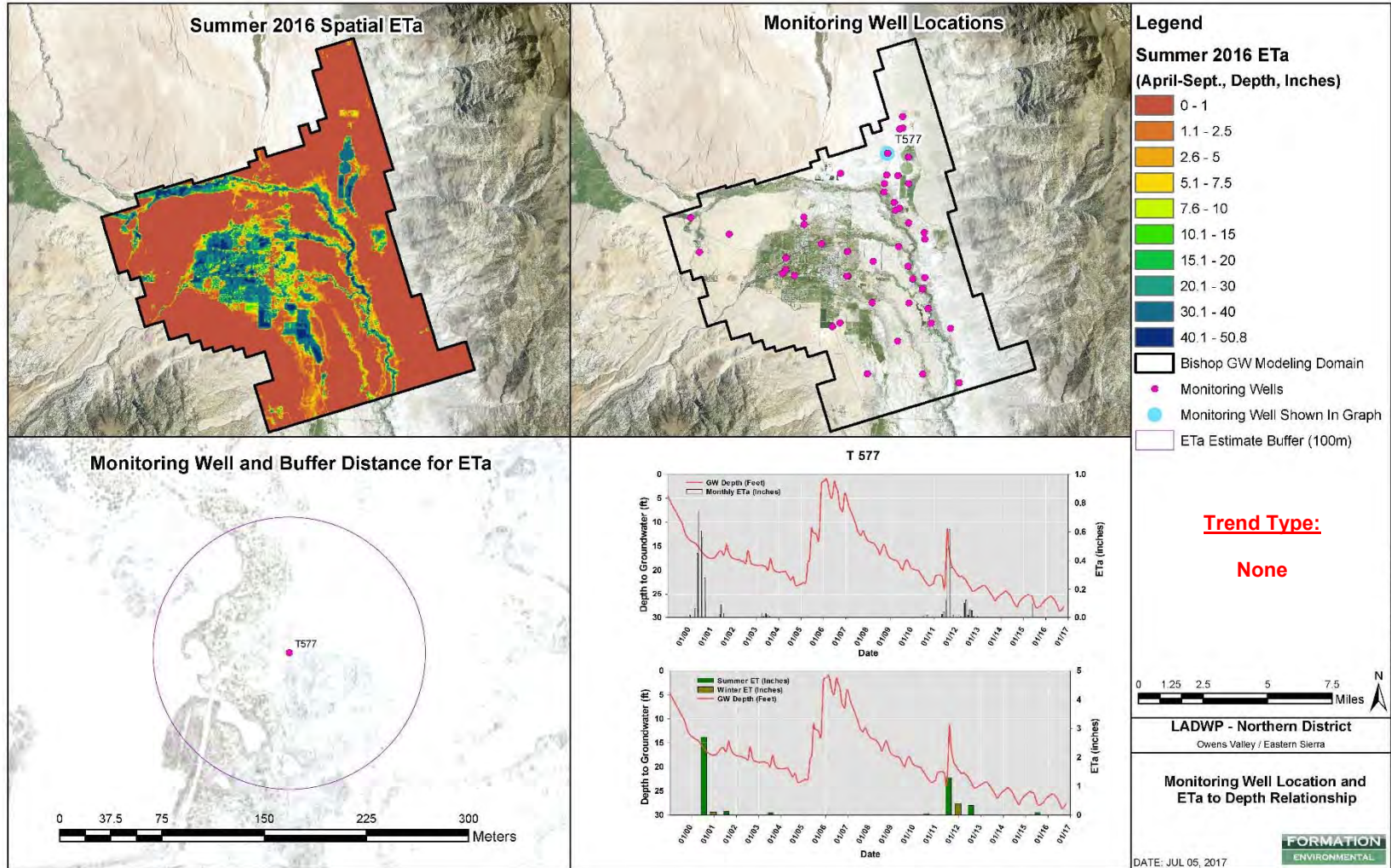
Well # V001G
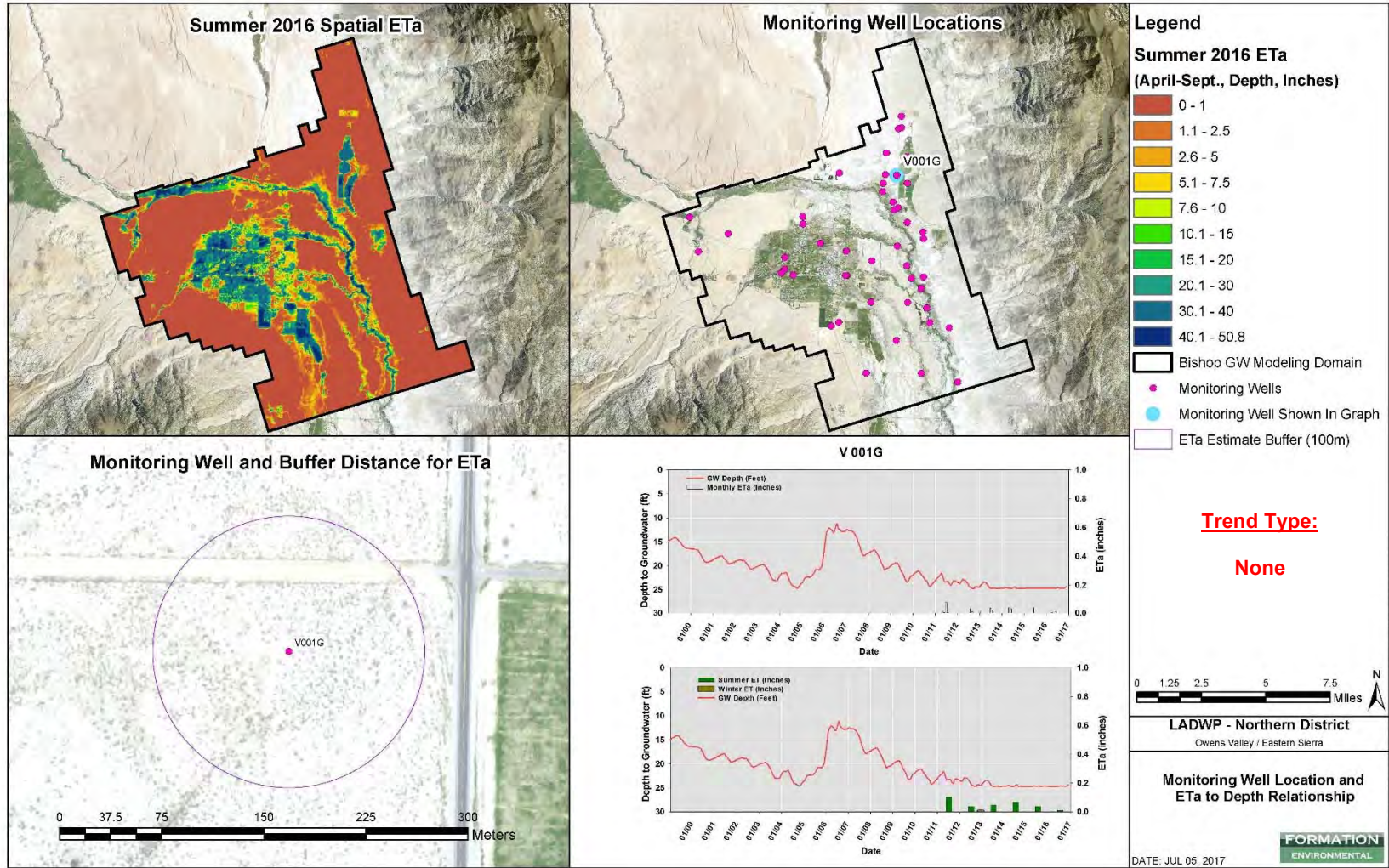
Well # V253
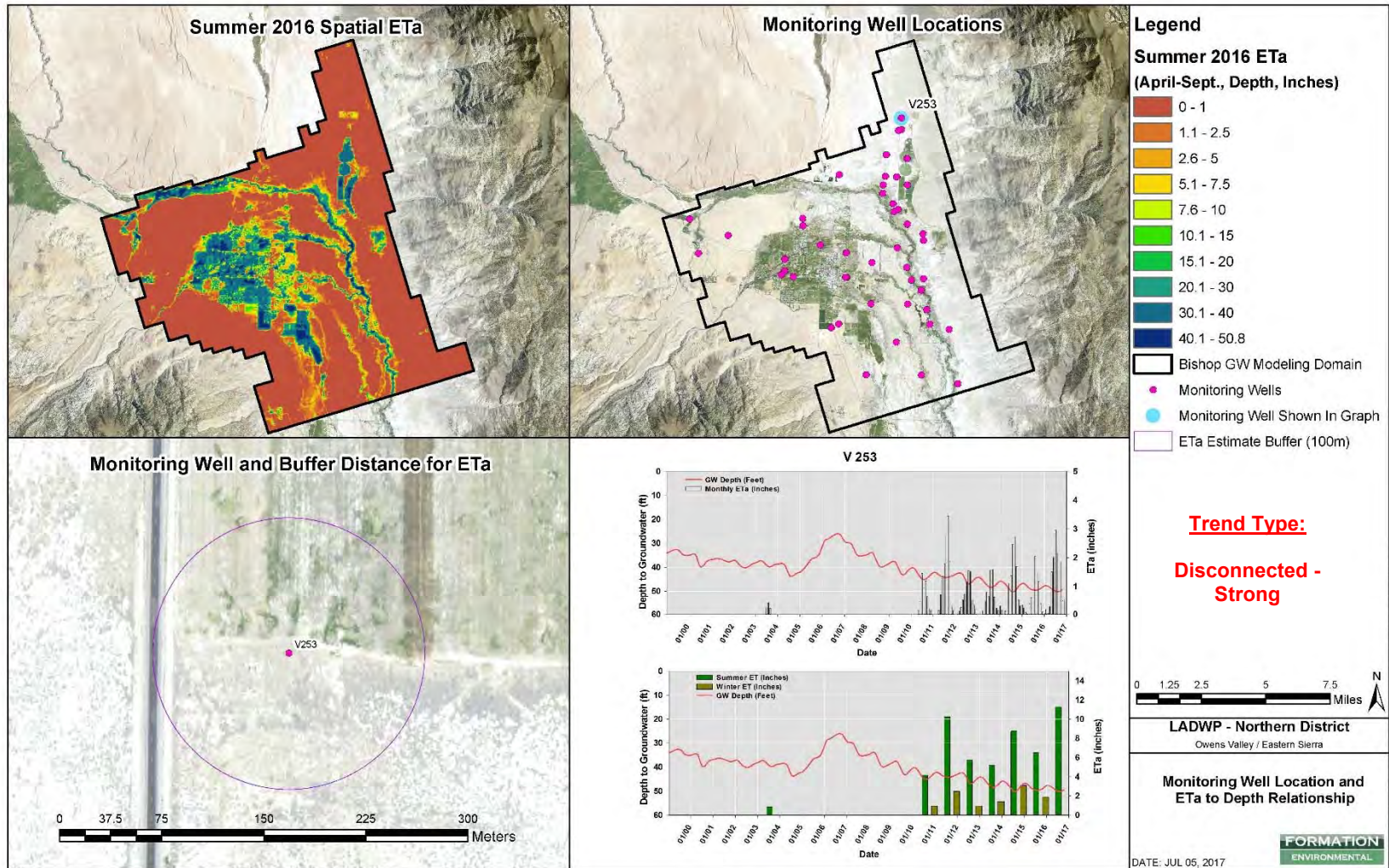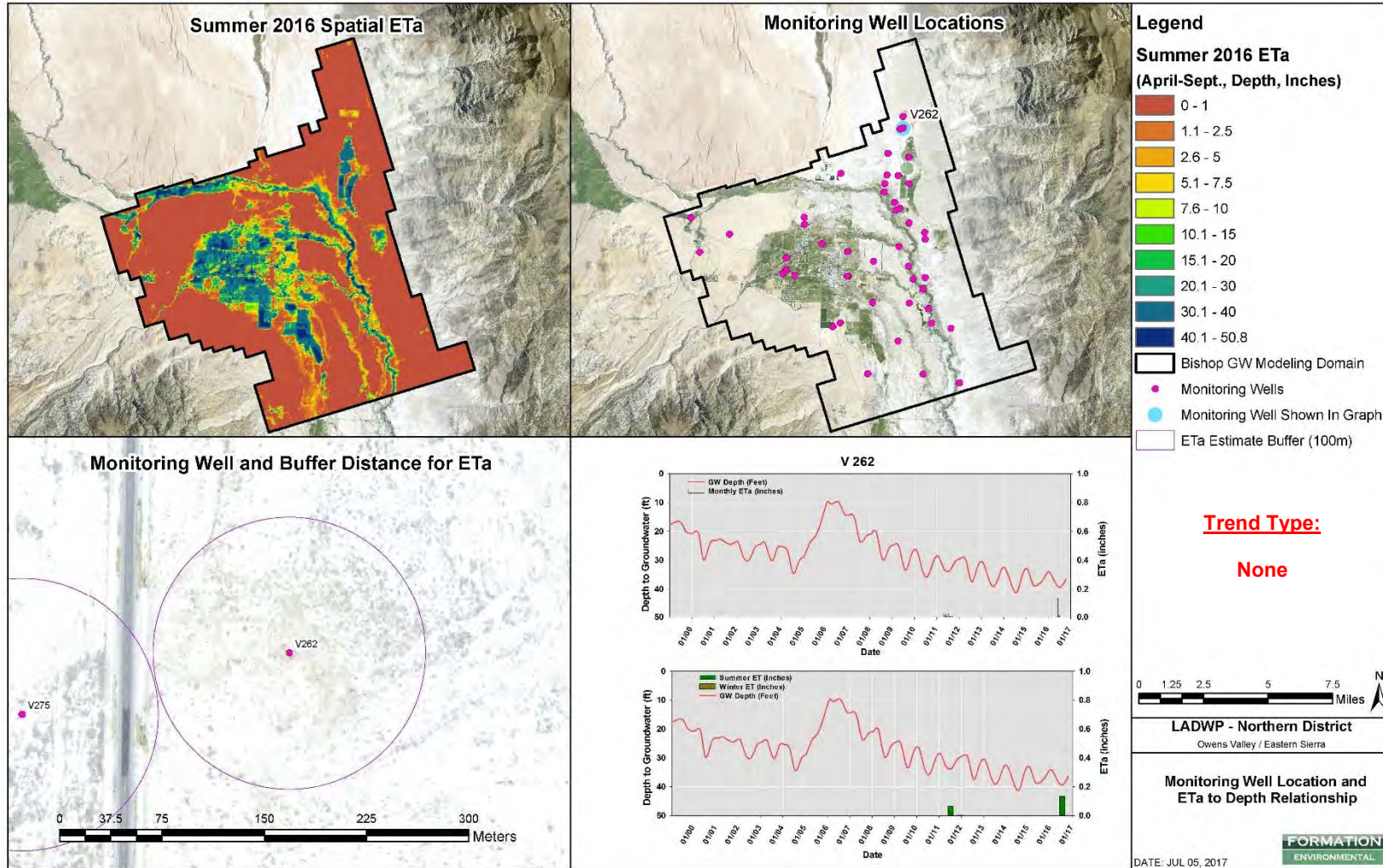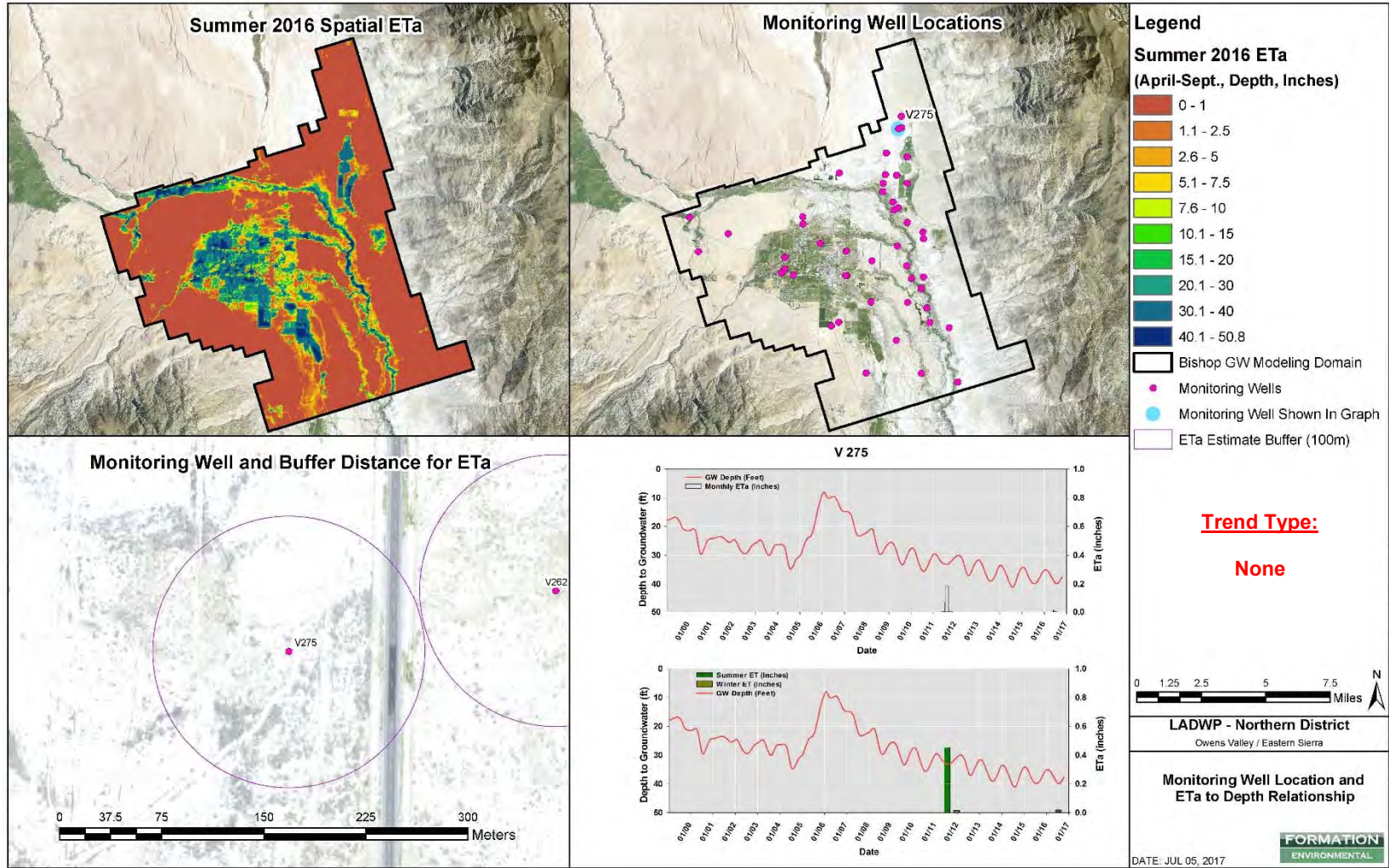
Well # V262

Well # V275

Well # V277
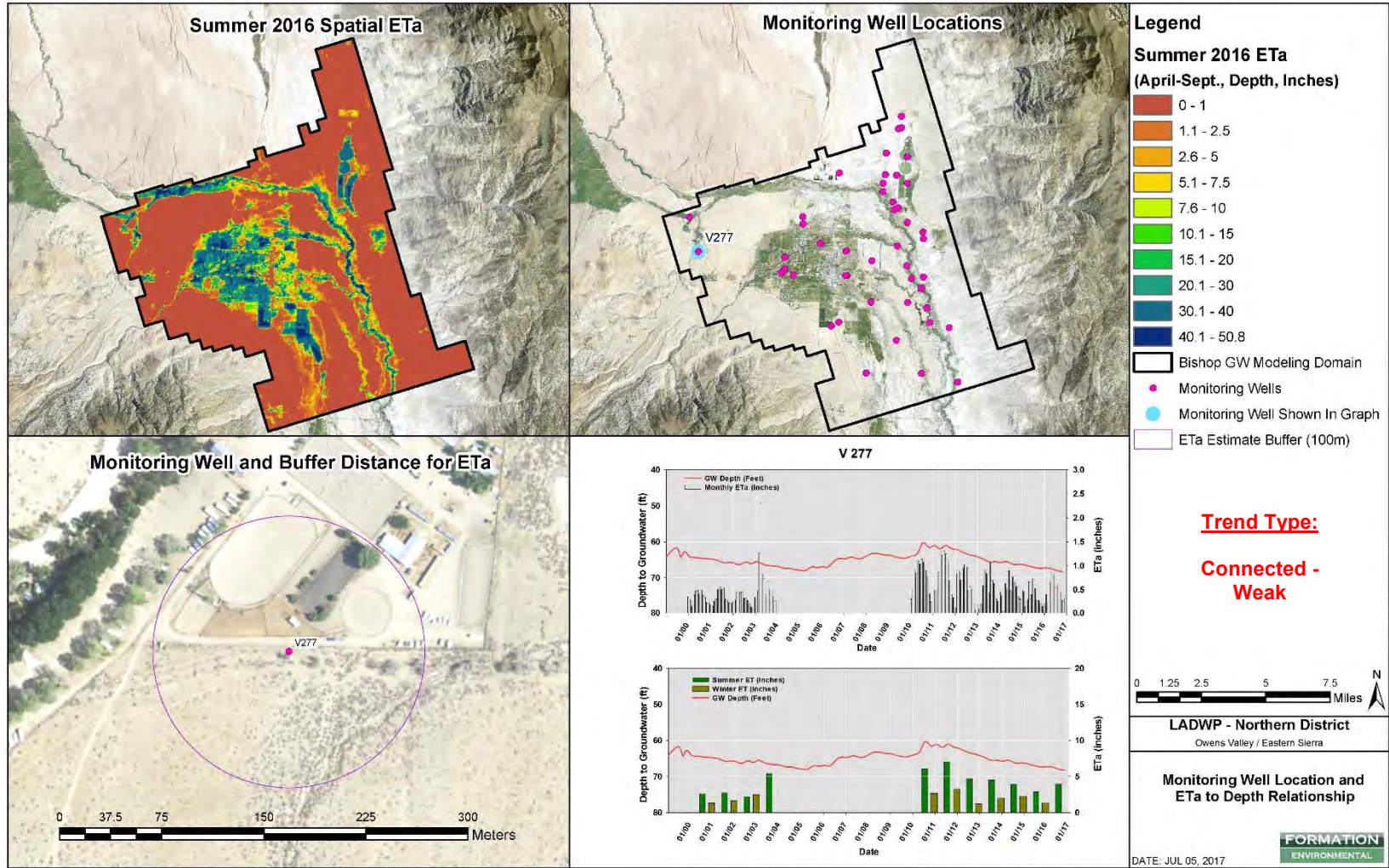
Well # V281
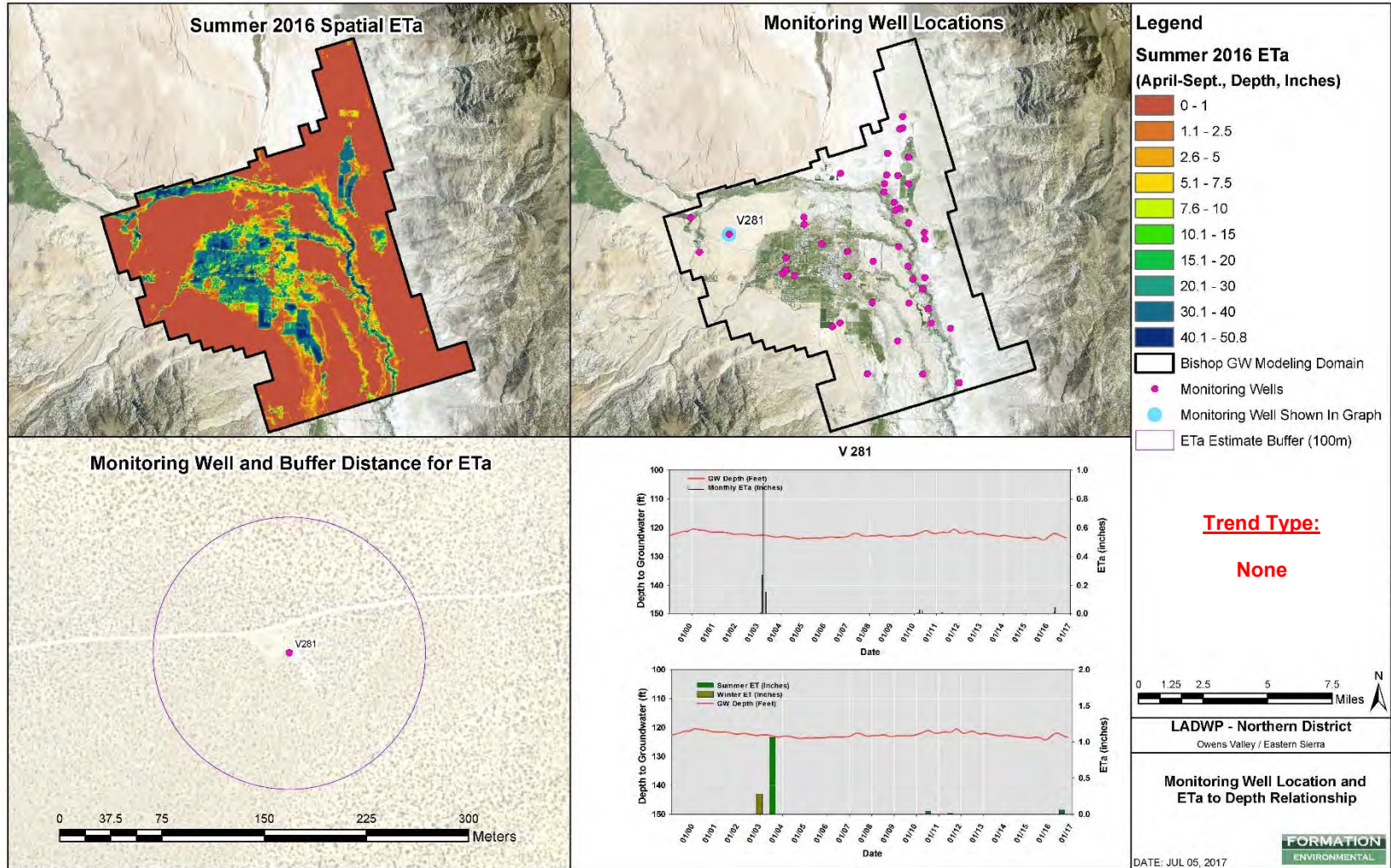
APPENDIX-B

Of the 49 monitoring wells in the Bishop Groundwater modeling domain, one well did not have any data and 14 wells had some kind of inconsistency in the data. Hydrographs of 14 wells are presented here with x-axis showing the time period and y-axis depth to groundwater (ft). Some of the reasons for inconsistent data were (1) well becoming a flowing well (2) Outlier due to equipment malfunction (3) Well inactive or destroyed (4) highly variable record and/or (5) No data after certain period.
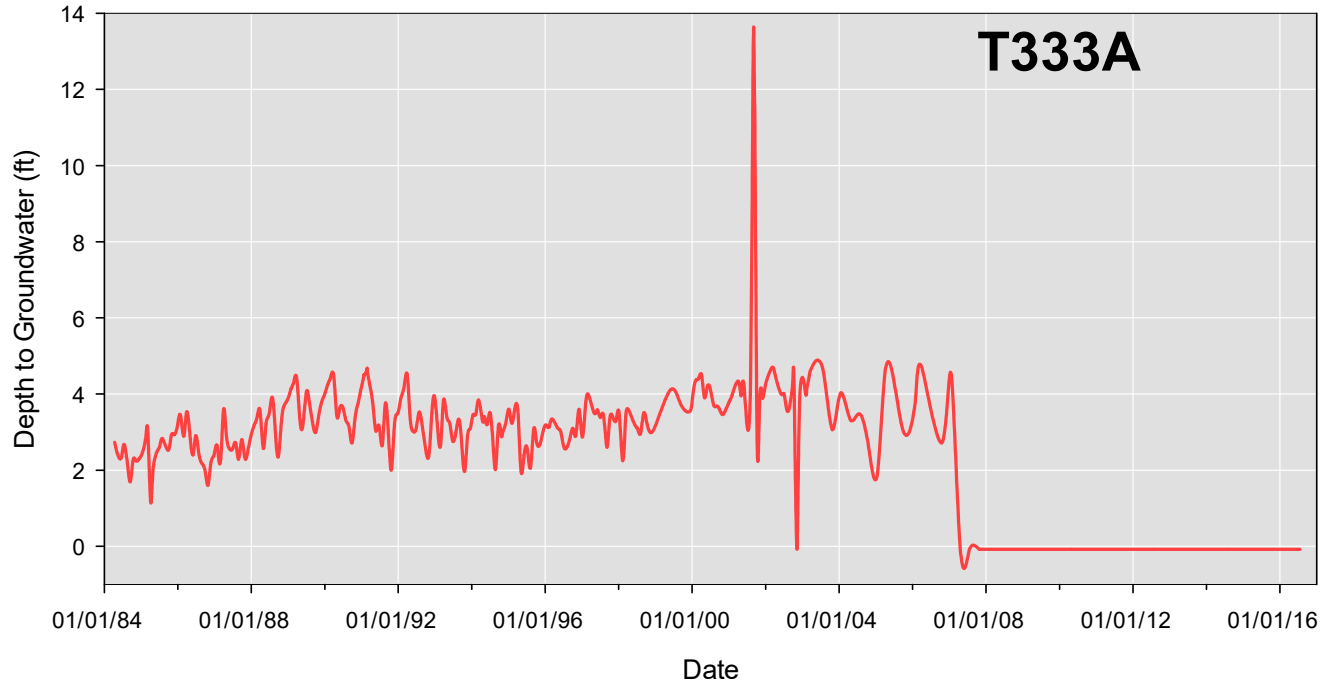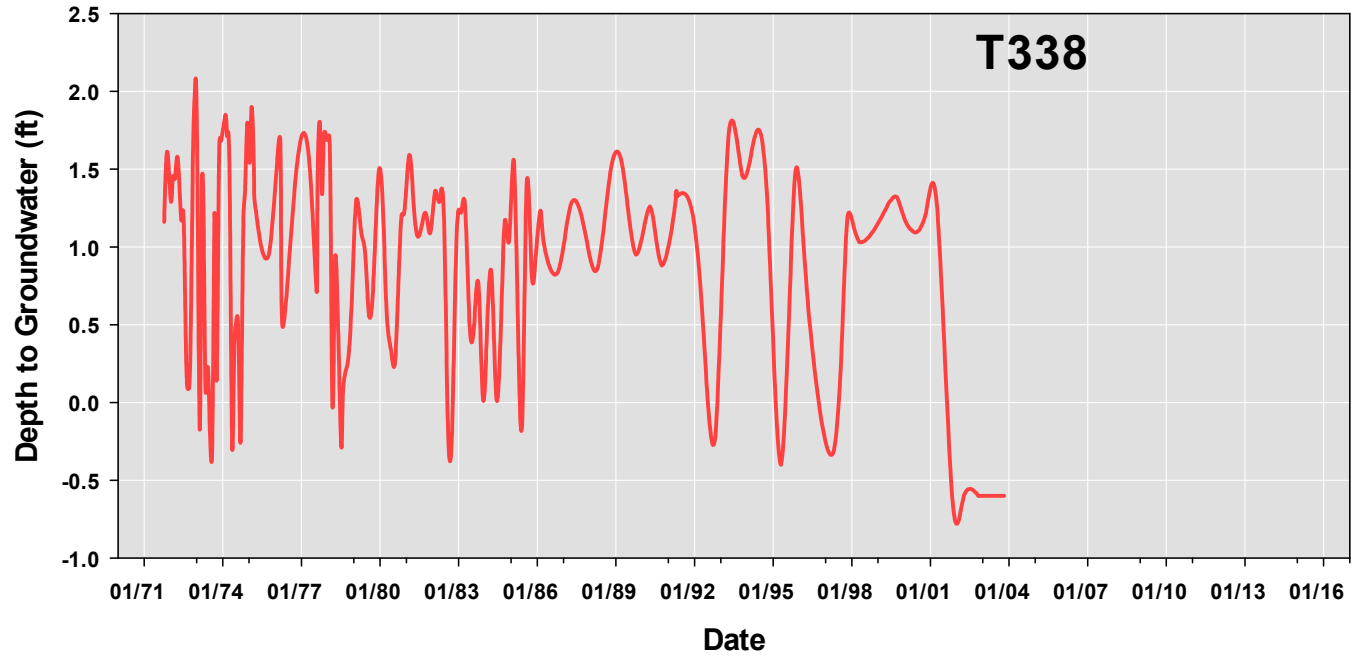

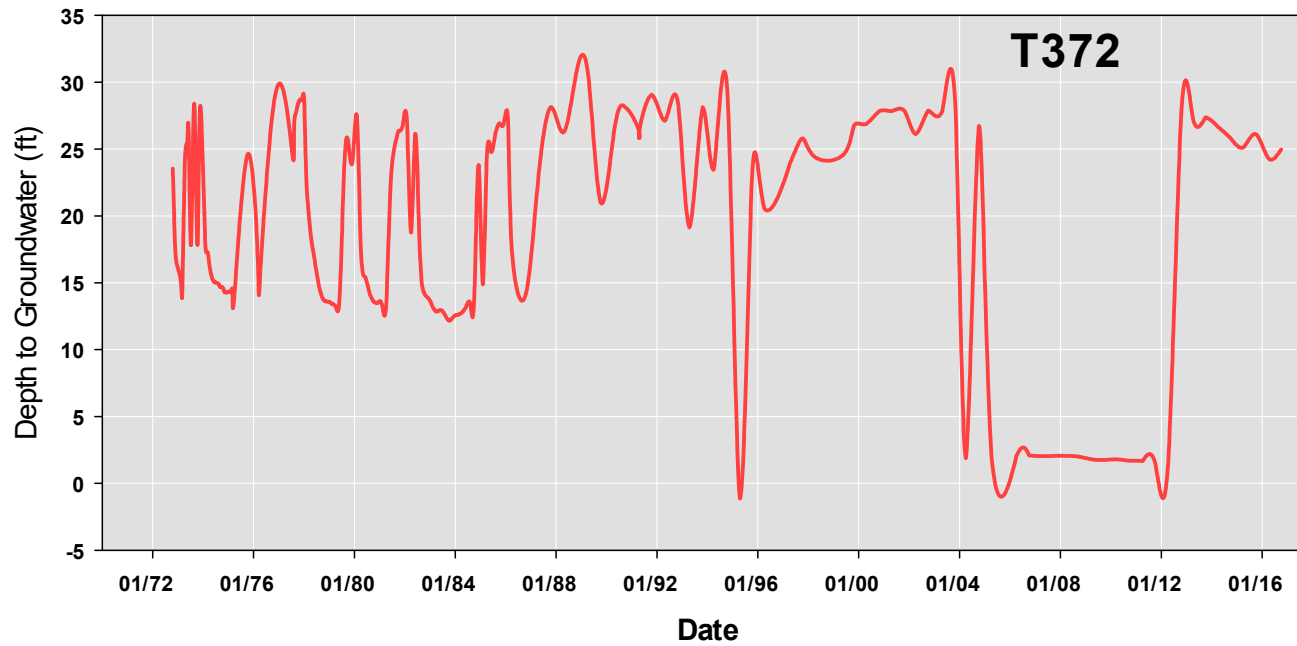**Well # T 333A: Data after 2006 seems to have some inconsistency**
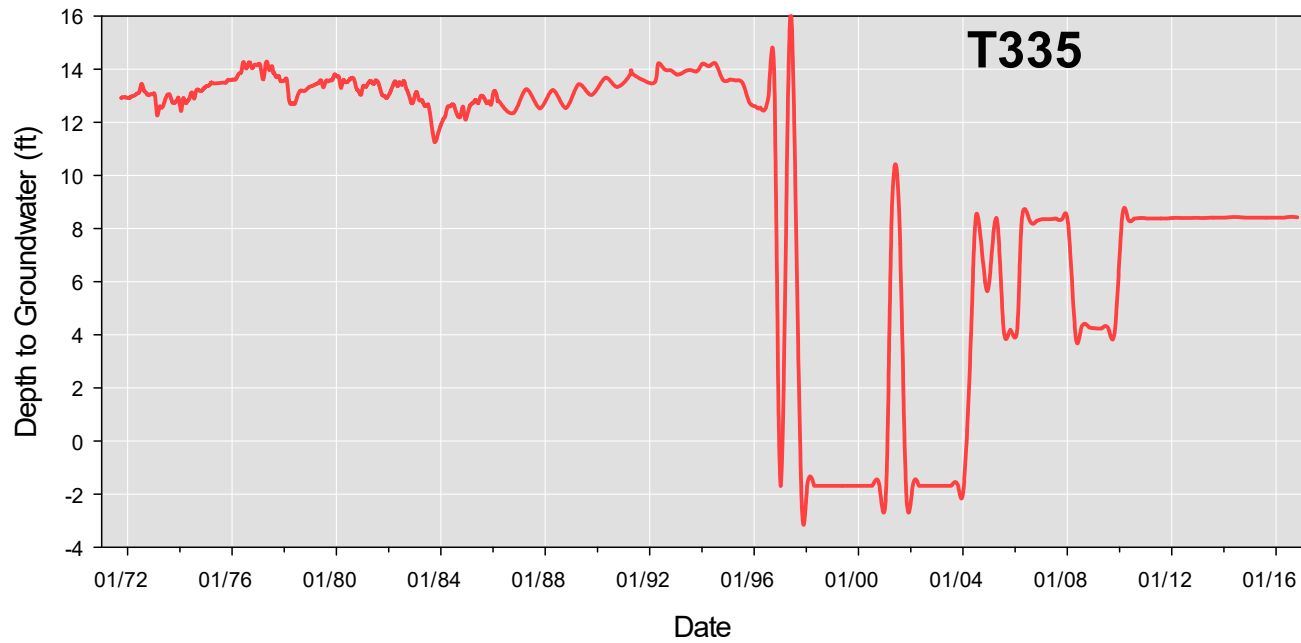
Well # T 335: Data after 1996 seems to have some inconsistency
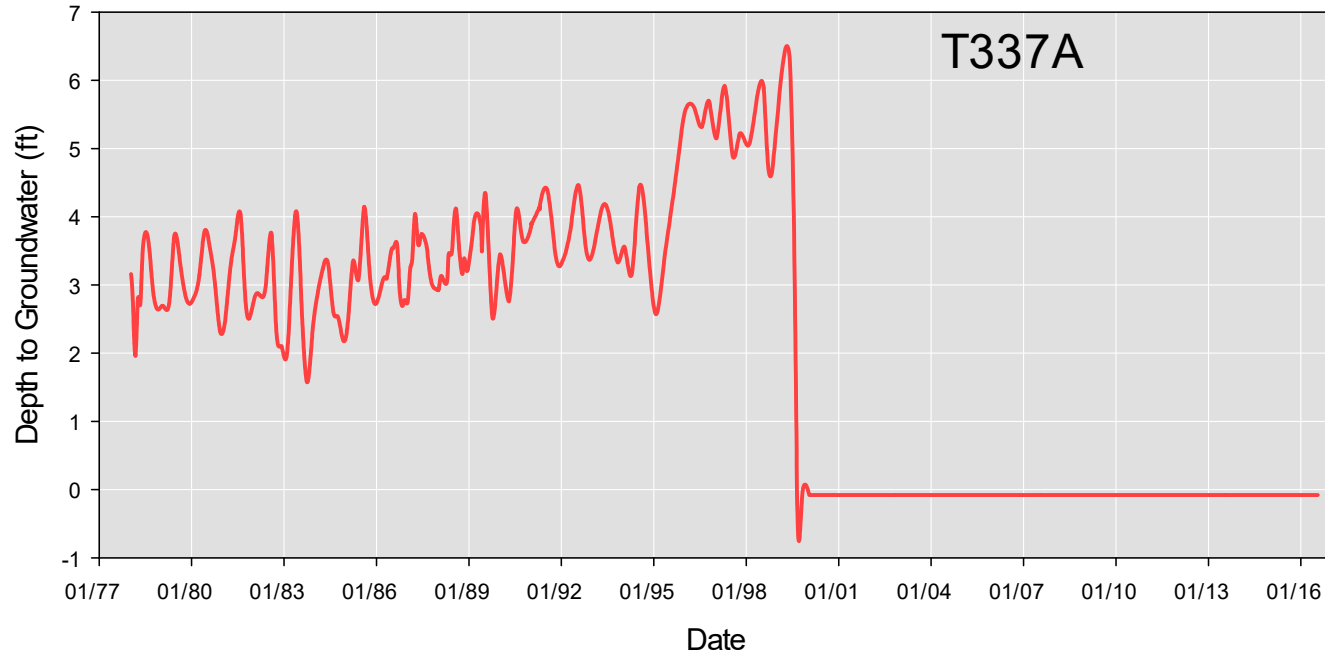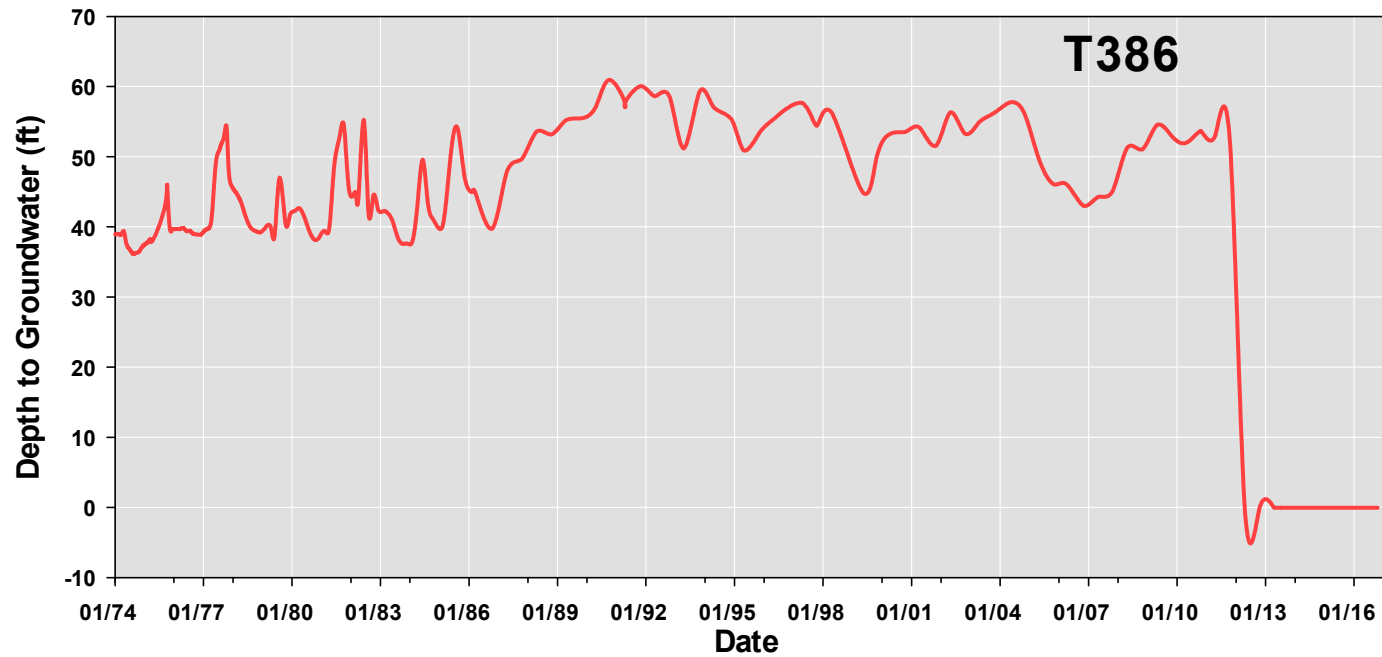
Well # T 337A: Data after 1999 seems to have some inconsistency
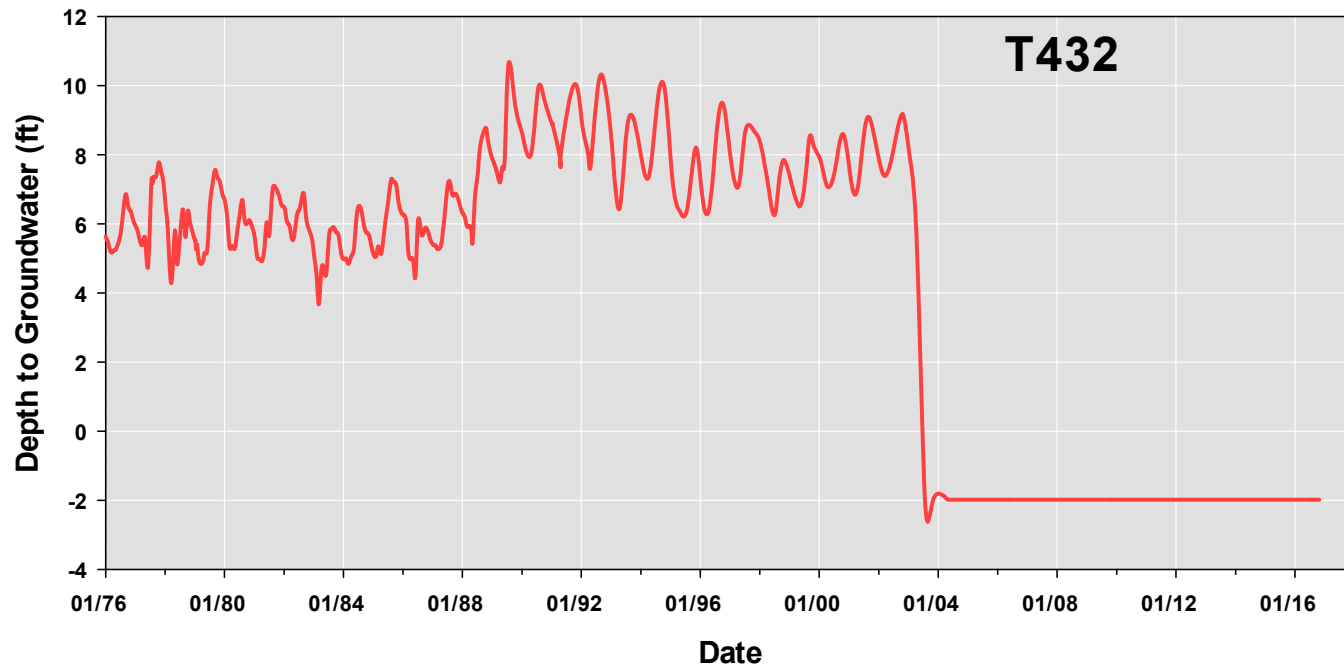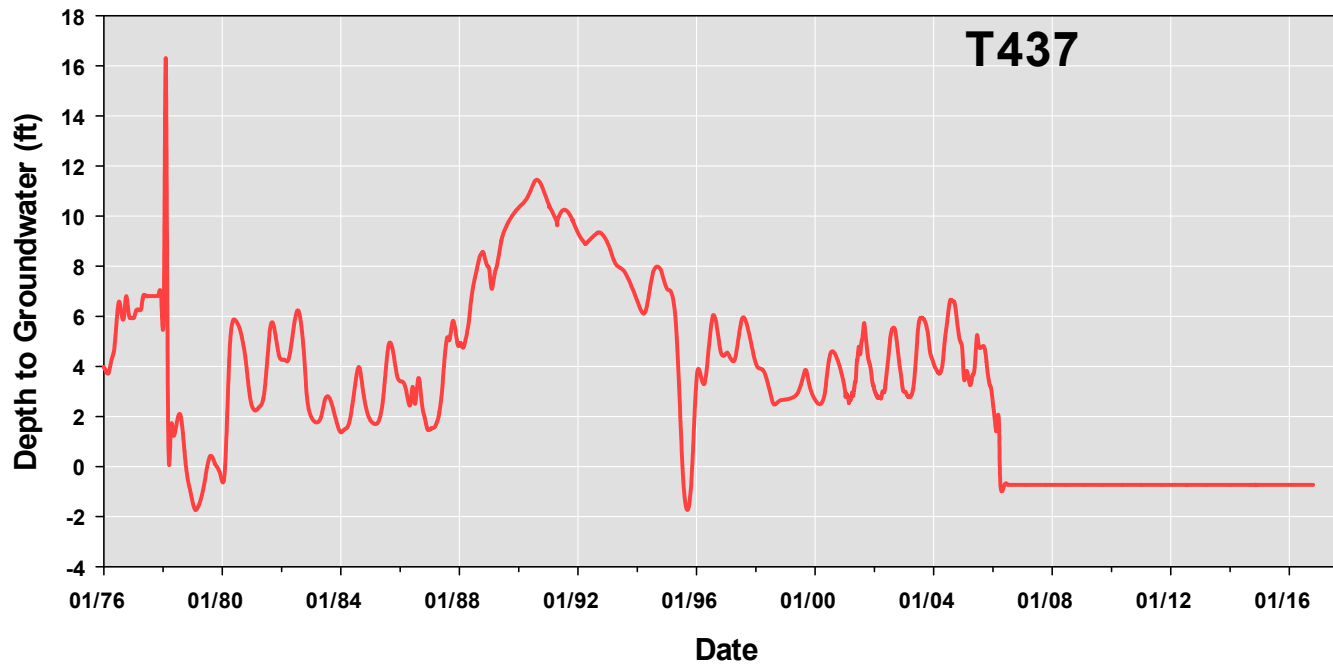
Well # T 338: Data missing after 2003

Well # T 372: Data after 2003 seems to have some inconsistency
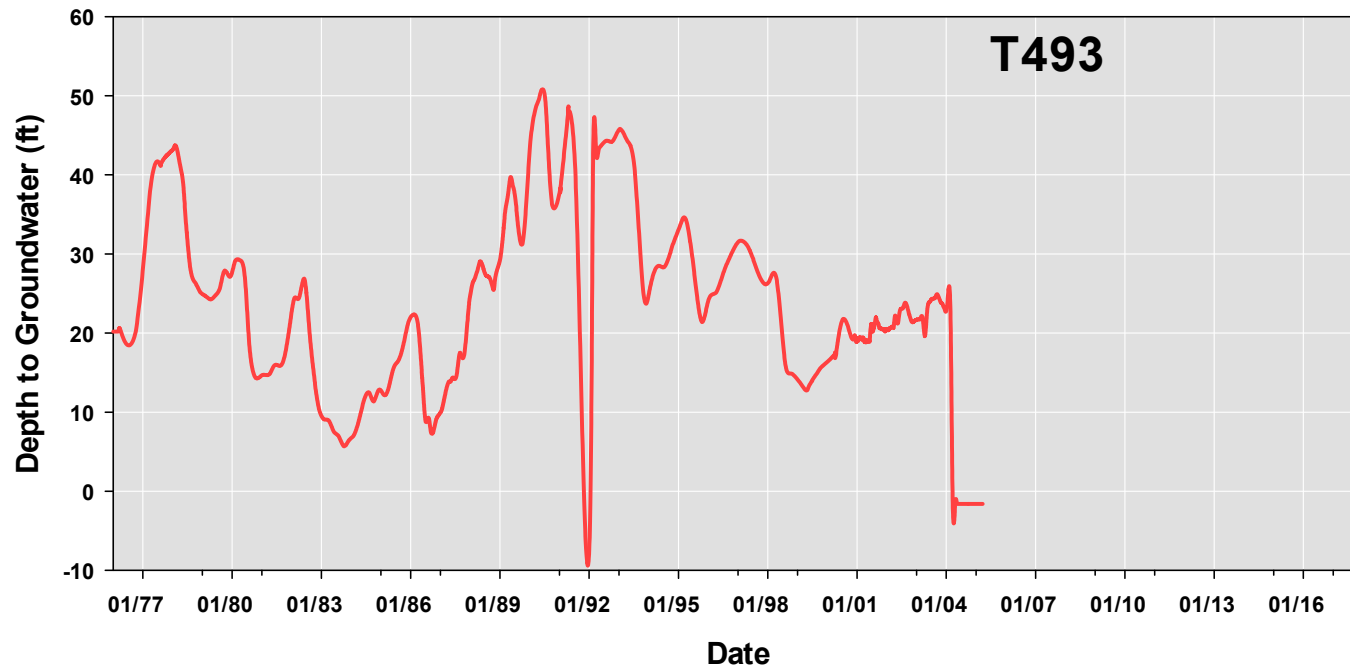
Well # T 386: Data after 2012 seems to have some inconsistency

Well # T 432: Data after 2003 seems to have some inconsistency

Well # T 437: Data after 2005 seems to have some inconsistency
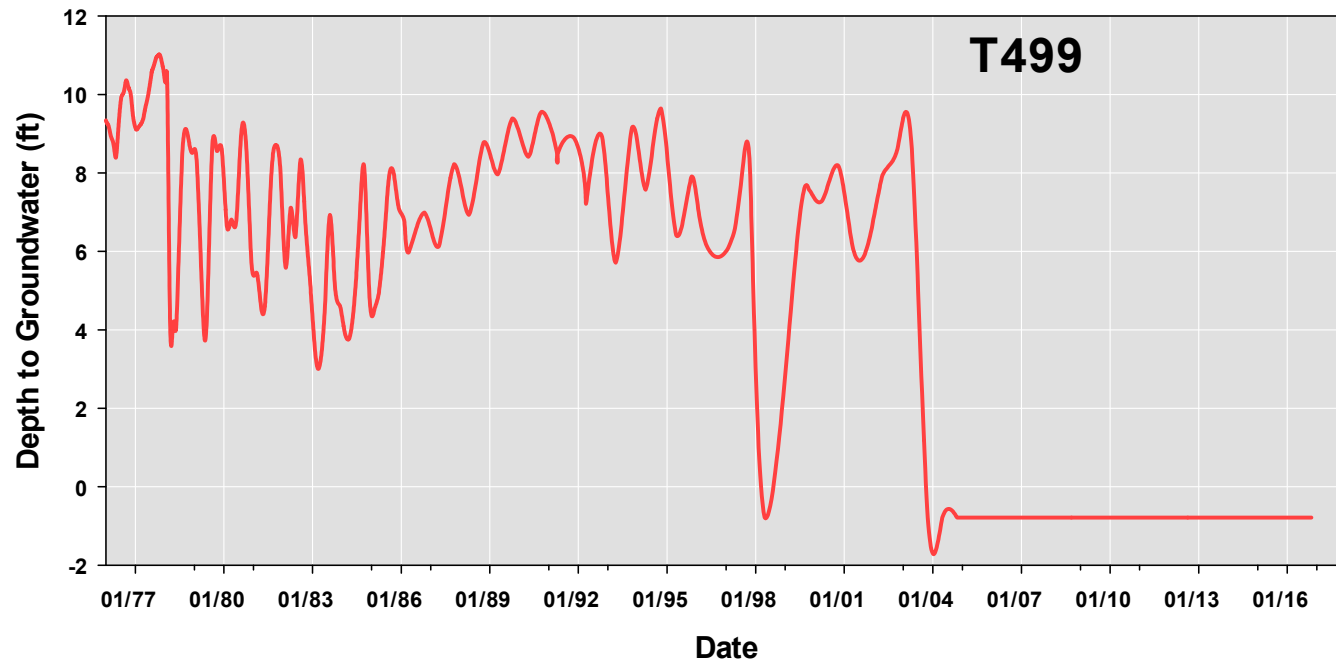
Well # T 493: Data missing after 2004

Well # T 499: Data after 2003 seems to have some inconsistency

Well # T 514A: Data after 2003 seems to have some inconsistency

Well # T 517: Data after 1997 seems to have some inconsistency
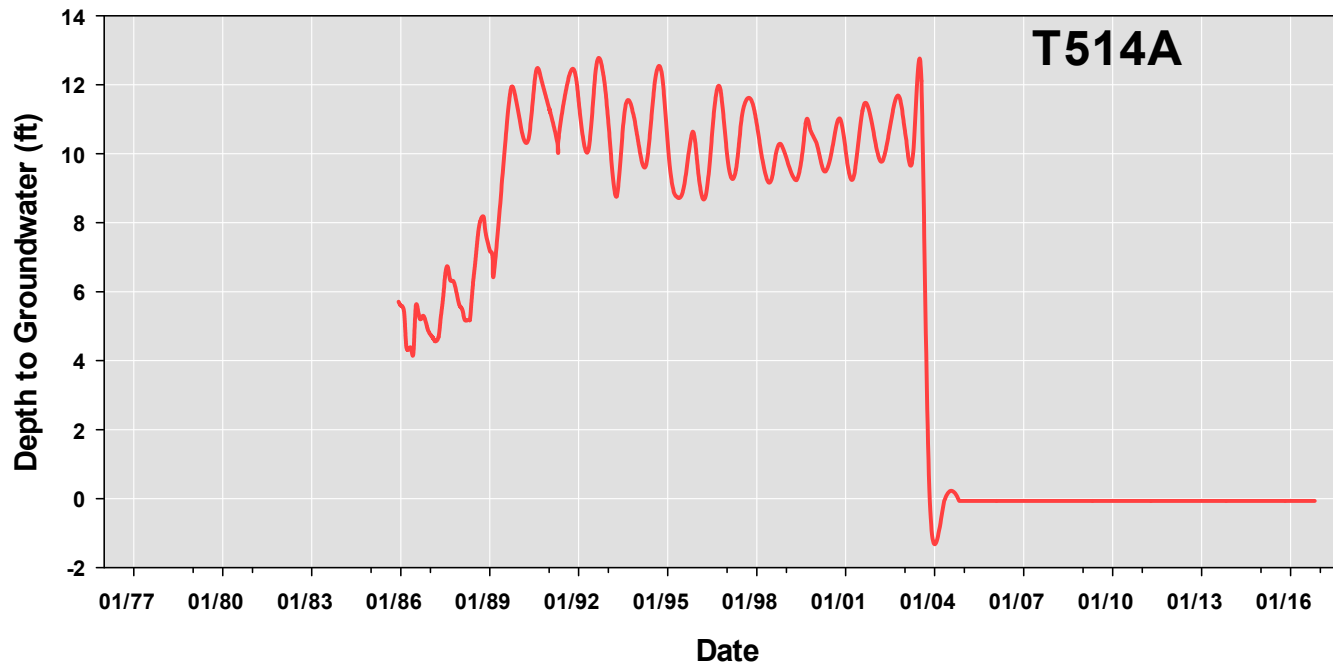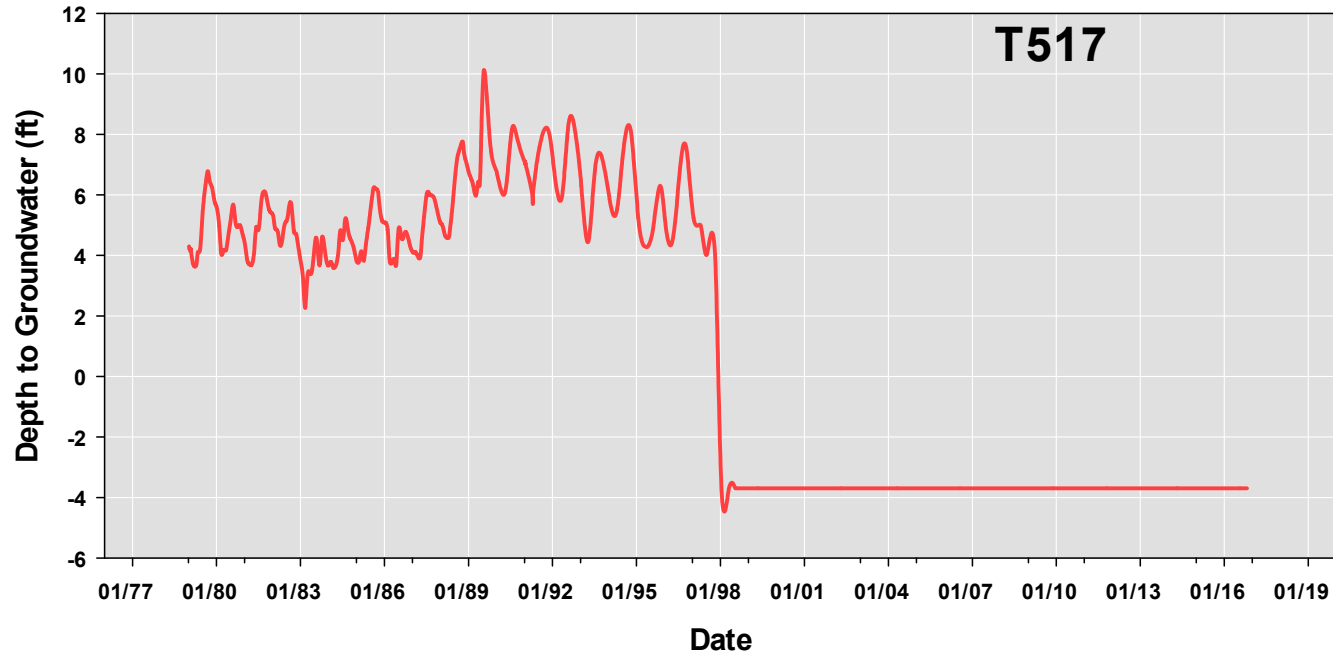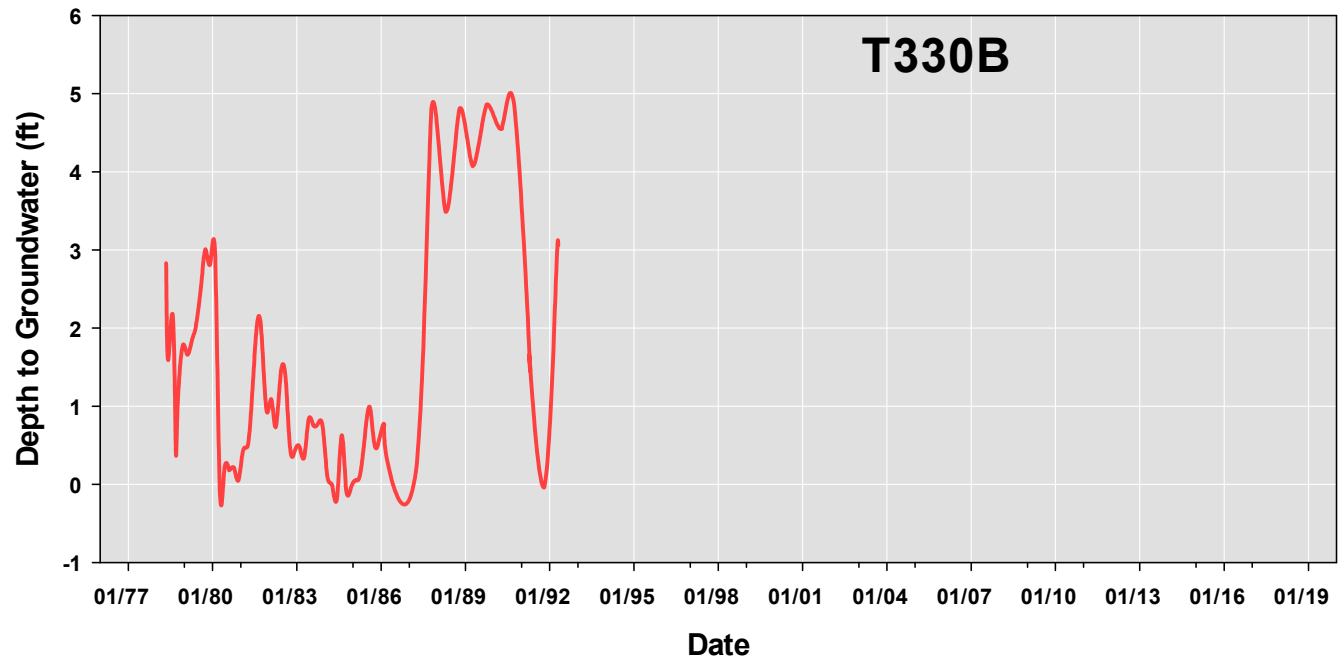
Date
Well # T 330B: Data missing after 1992
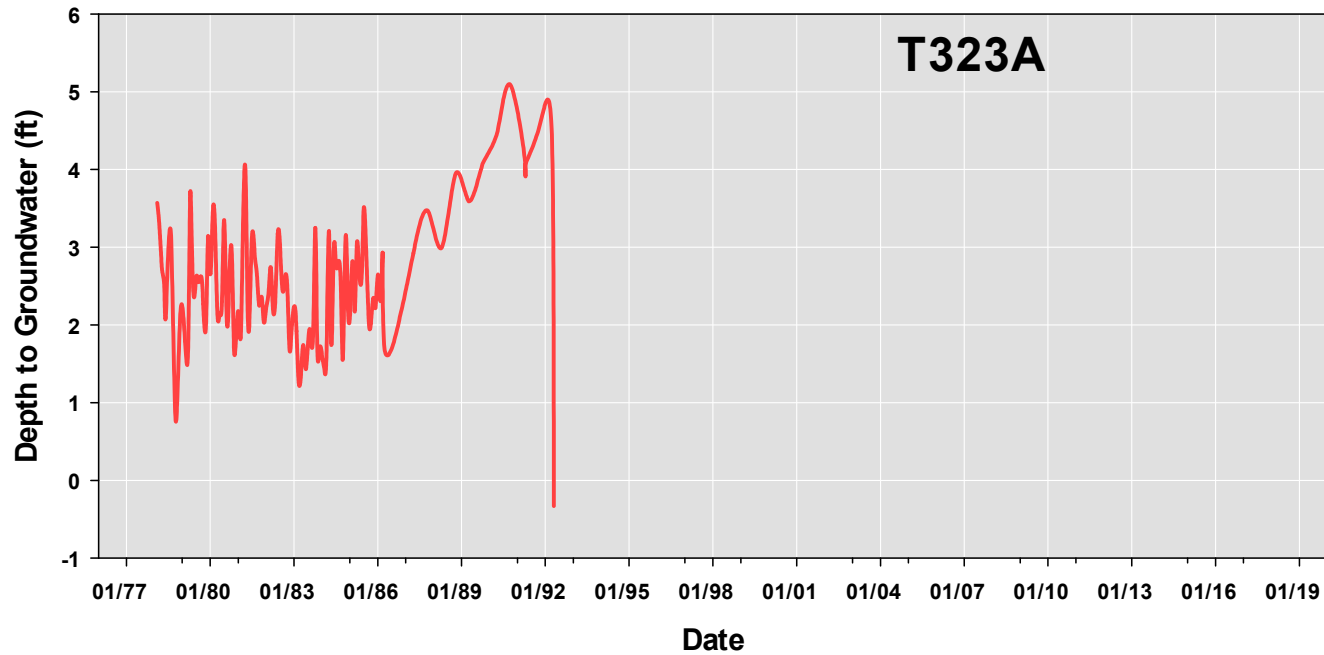
Well # T 323A: Data missing after 1991

Well # T 489 did not have any data

APPENDIX E

TM 8.3.3 – ESTIMATION OF HISTORICAL ETA FROM AGRICULTURE IN
THE CHALFRANT AND BENTON VALLEYS

TECHNICAL MEMORANDUM

Title: TM 8.3.3 – Estimation of Historic ETa from Agriculture in the Chalfant and Benton Valleys

Project: Task Order 008 – Remote Sensing Pilot Project Implementation

Client: Los Angeles Department of Water and Power

Date: March 2018

Chalfant-Benton Valley Agricultural Water Demand

DATE: MAY 24, 2017
BY: GP,CSC,BS FOR: LADWP

TABLE OF CONTENTS

LIST OF FIGURES

LIST OF TABLES

EXECUTIVE SUMMARY

Remote sensing (Landsat) was used to estimate the total agricultural demands in the Chalfant and Benton Valleys (**Figure ES-1**) during the times in which ETa are currently available from Landsat da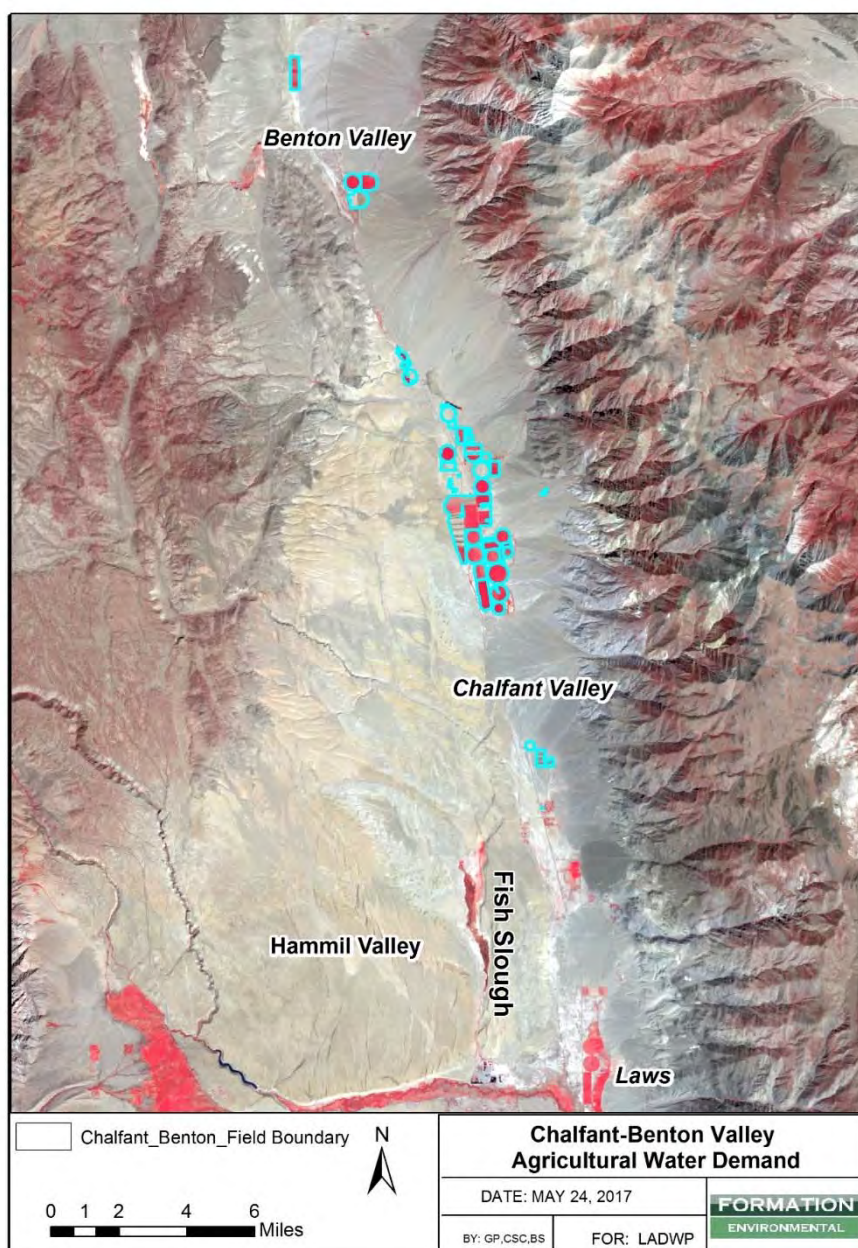ta. These data were compared to flow data from Fish Slough to evaluate a potential relationship between pumping in Chalfant/Benton Valleys, and the observed decrease in flows over time.

Fish Slough, located to the north of the Bishop/Laws model boundary, southwest of Chalfant Valley, and east of Hammil Valley (**Figure ES-1**), is an area of groundwater discharge with sensitive habitat and critical environmental concern. There has been a long-term reduction in flow at Fish Slough from 6,000 – 7,000 acre-feet per year (AF/yr) in the 1960's to 3,000 AF/yr currently. As a result, there is a need to identify the reason for reduced flows (i.e., pumping from the Bishop/Laws area, pumping in the Chalfant area, or some other factor).

The purpose of this subtask was to investigate one potential reason for reduced flows at Fish Slough through time in support of the Bishop/Laws model update being performed for LADWP. It is hypothesized that the groundwater withdrawal in Chalfant and Benton Valleys for agriculture consumptive use has contributed to the reduction in flow at Fish Slough.

This analysis shows that consumptive use by agriculture is a significant and increasing component of the water budget in the Chalfant/Benton Valleys, which could easily result in decreased flows to Fish Slough. It also suggests that groundwater flow through the alluvium north of Laws into the Owens Valley has decreased through time. Results of this analysis are being incorporated into the Bishop/Laws model update, such that flow on the northern boundary of the model is not necessarily fixed, but may also decrease with time.
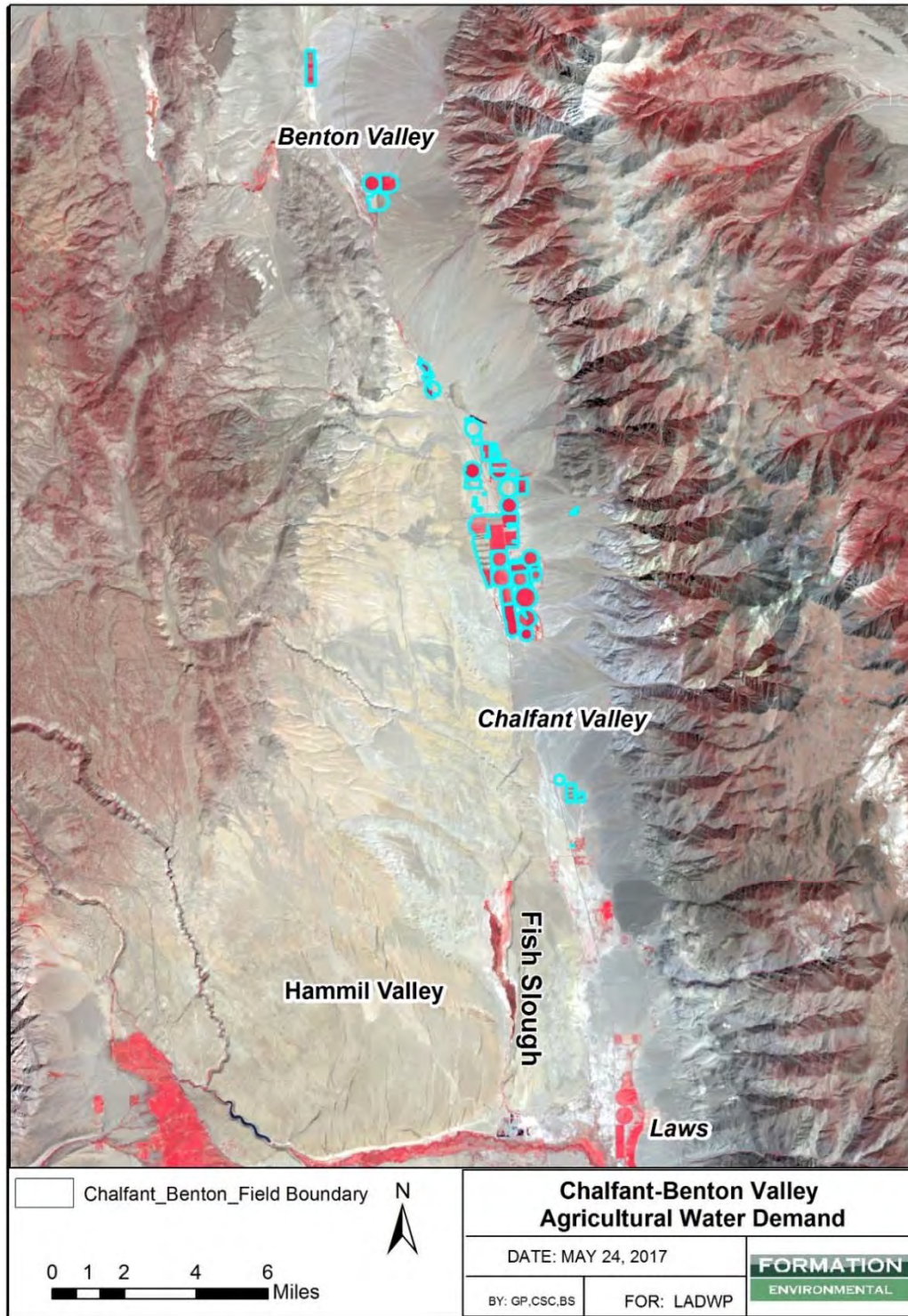
Figure ES-1 – Study Area of Chalfant and Benton Valleys

1.0   INTRODUCTION

This TM represents the deliverable for Subtask 8.3.3 of Task Order 008 of Agreement No. 47381-6. As conceived in the Work Plan for this effort (MWH, 2016), key findings from the Pilot Project are documented in brief periodic TMs. These TMs are not intended to contain extensive introductory material, but are instead focused on results from individual work areas. A listing of the key TMs delivered is summarized in **Table 1**, with the highlighted TM 8.3.3 presented in this document.

In this substak, remote sensing (Landsat) was used to estimate the total agricultural demands in the Chalfant and Benton Valleys (**Figure 1**) during the times in which ETa are currently available from Landsat data. The methods used to estimate ETa are detailed in previous memoranda (Stantec, 2017). These data were compared to flow data from Fish Slough to evaluate a potential relationship between pumping in Chalfant/Benton Valleys, and the observed decrease in flows over time.

Fish Slough, located to the north of the Bishop/Laws model boundary, southwest of Chalfant Valley, and east of Hammil Valley (**Figure 1**), is an area of groundwater discharge with sensitive habitat and critical environmental concern. There has been a long-term reduction in flow at Fish Slough from 6,000 – 7,000 acre-feet per year (AF/yr) in the 1960's to 3,000 AF/yr currently. As a result, there is a need to identify the reason for reduced flows (i.e., pumping from the Bishop/Laws area, pumping in the Chalfant area, or some other factor).

The purpose of this subtask was to investigate one potential reason for reduced flows at Fish Slough through time in support of the Bishop/Laws model update being performed for LADWP. It is hypothesized that the groundwater withdrawal in Chalfant and Benton Valleys for agriculture consumptive use has contributed to the reduction in flow at Fish Slough.

Table 1
Summary of Technical Memoranda

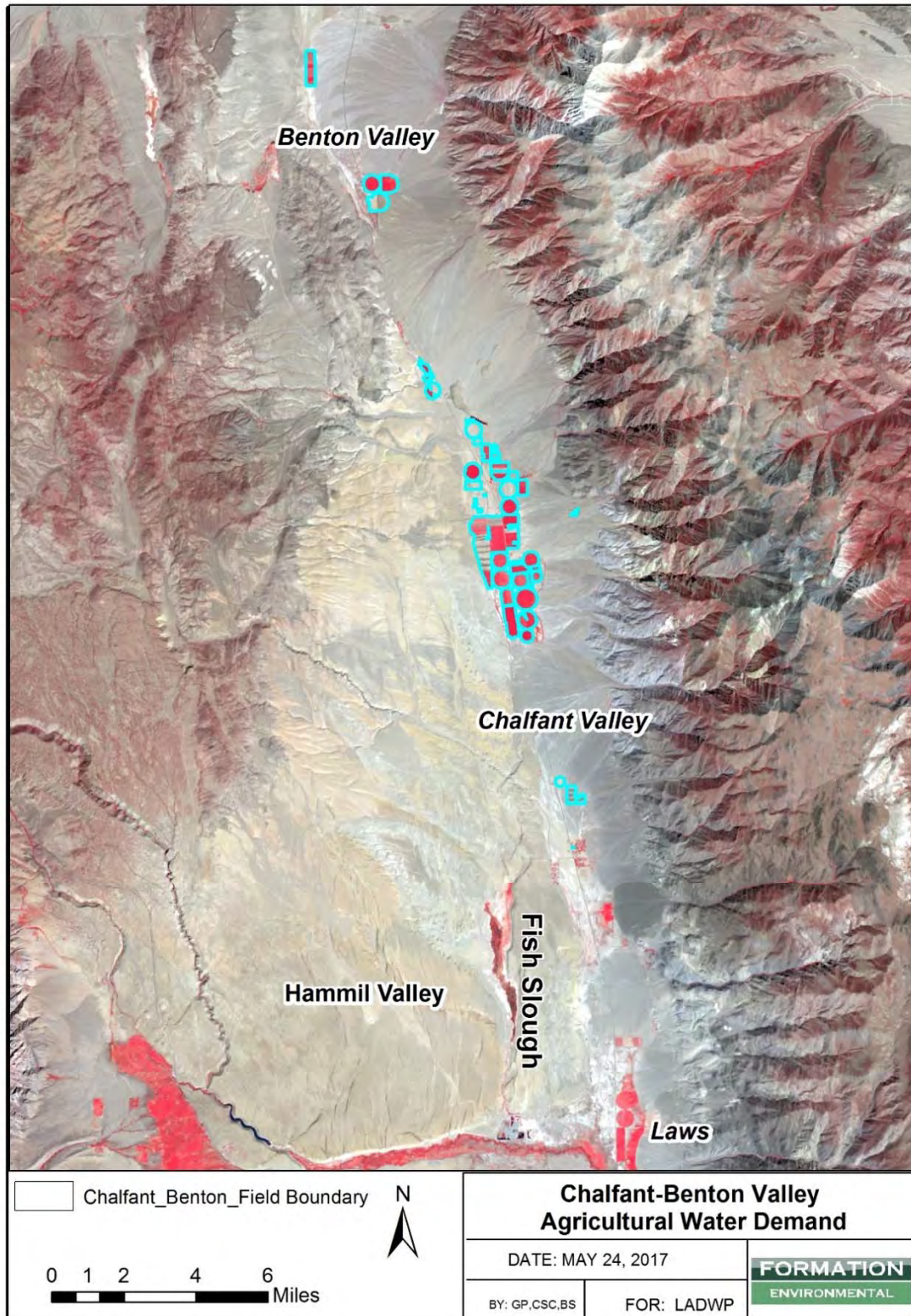| Task	TM Number	Subject
1 - Imagery Download, Preparation, and Preprocessing	TM 8.1	Imagery, cloud screening results, and radiometrically corrected imagery
2 - Leaf Area Index Image Analysis	TM 8.2	Leaf area index (LAI) image analysis, comparison of LADWP and ICWD historical data with remote sensing results, sampling scheme for collecting ground truth data
3 - Evapotranspiration (ET) Mapping and Options for Integration	TM 8.3.1	Surface Energy Balance System (SEBS) ET delivery, SEBS ET development and validation
	TM 8.3.2	Integration of Spatial ETa into the Bishop/Laws groundwater model
	TM 8.3.3	Estimation of historical Eta from agriculture in the Chalfant, and Benton Valleys

Figure 1: Study Area of Chalfant and Benton Valleys

Note - Image is a Landsat 8 data from September 2016. Note the location of field borders used in extraction of ETa information; agricultural fields in the Laws region were not included.

2.0   SUMMARY OF AGRICULTURAL WATER DEMAND FROM CHALFANT AND BENTON VALLEYS

Actual Evapotranspiration (ETa) represents the total evapotransporation from an area from all sources (precipitation, applied water, or vegetation). Because precipitation in the area is sparse, and there is no source of imported water, high rates of ETa generally represent total water use from irrigated agriculture. Because no groundwater pumping infromation is available in the Chalfant area, a remote sensing algorithm was used to estimate ETa, and this information was further used to study the trend of agricultural water demand in the valley.

The ETa dataset developed for two discrete time steps- 2000-2003 (4 years) and 2010-2016 (7 years), were used in this investigation. ETa data from 2000 through 2003 was developed as part of the validation study under Remote Sensing Pilot Project Implementation for the Owens Valley area (Agreement No. 47381-6; MWH,2016). This study showed good performance of remote sensing algorithm in estimating ETa in Owens Valley. The other set of ETa data (2010-2016) was developed through the same framework and made avaialble for Remote Sensing Pilot Project.

Figure 1 shows the study area and the irrigated field borders used to extract the ETa information. All agricultural field boundaries were qulaity checked and updated before using it for extraction of ETa information. Only the agricultural fields north of Laws region were used in the study. There are currently 53 fields in the study area covering 4,007 acres.

Figure 2 shows the plot of annual ETa for the two time periods. A rising trend in agricultural water demand is evident from the plot. **Table 1** provides the monthly ETa aggregated for all the fields in acre-feet.

This analysis shows that there is an increase in ETa over the time remote sensing data is available (2000-2016). Agricultural demand in the Chalfant and Bentron Valleys increased from as low as 7,300 AF in 2002, to approximately 11,500 in 2016, a 58 percent increase in water use by agriculture. It is unknown when large-scale agriculture began in the Chalfant/Benton area, but aerial photos indicate that much of the agriculture was in place prior to 1984, although some agricultural area is relatively new. For example, 150 acres of agriculture 3 miles northwest of the northern portion of Fish Slough (10 miles north of Laws – southernmost field shown on **Figure 1**) began between 1998 and 2005.

This analysis shows that consumptive use by agriculture is a significant and increasing component of the water budget in the Chalfant/Benton Valleys, which could easily result in decreased flows to Fish Slough. It also suggests that groundwater flow through the alluvium north of Laws into the Owens Valley has decreased through time. Results of this analysis are being incorporated into the Bishop/Laws model update, such that flow on the northern boundary of the model is not necessarily fixed, but may also decrease with time.

3.0   REFERENCES

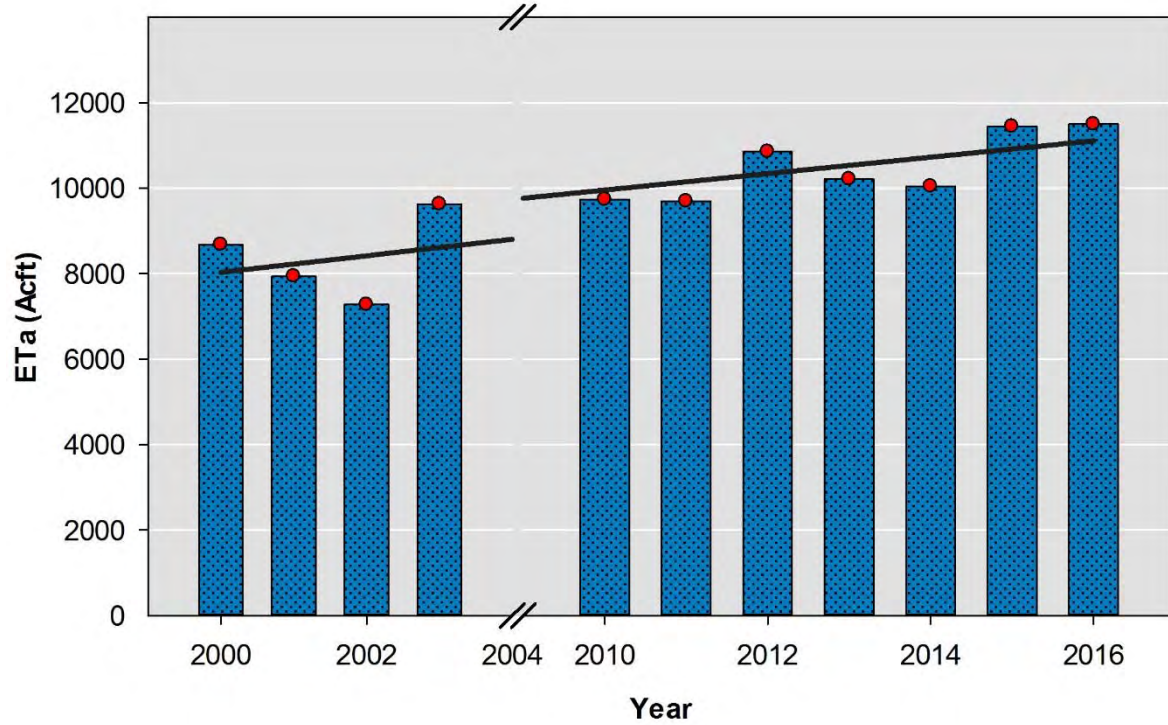Stantec, 2017. TM 8.2 - Leaf Area Index-Image Analysis. May.

Figure 2: Annual ETa from Agricultural Fields in Chalfant-Benton Valleys

Table 2: Monthly Aggregated ETa (acre-feet) for all Fields in the Study Area

Month	2000	2001	2002	2003	2010	2011	2012	2013	2014	2015	2016
Jan	66.50	49.58	65.76	105.11	17.93	38.98	33.82	81.46	84.23	166.69	117.89
Feb	78.42	34.07	46.09	117.10	30.27	65.99	138.31	124.73	107.64	251.70	133.52
Mar	127.81	170.25	197.20	390.21	160.05	211.48	466.32	587.99	235.76	434.06	698.20
Apr	738.12	600.93	570.47	748.91	866.29	819.83	1,014.69	1,091.47	1,068.51	1,147.26	1,175.42
May	1,329.93	1,428.42	1,077.67	1,090.74	1,374.08	1,117.94	1,811.11	1,351.39	1,514.25	1,465.05	1,417.13
Jun	1,178.16	1,260.42	1,106.48	1,275.94	1,628.22	1,535.05	1,501.36	1,538.04	1,545.49	1,606.45	1,787.39
Jul	1,184.95	1,133.07	1,132.42	1,692.42	1,724.40	1,722.93	1,476.82	1,648.62	1,489.18	1,616.72	1,729.26
Aug	1,482.70	1,269.09	1,191.08	1,617.44	1,560.95	1,729.08	1,630.09	1,388.33	1,257.08	1,627.38	1,689.69
Sep	1,339.53	1,083.82	975.60	1,343.82	1,250.70	1,268.84	1,371.58	1,209.05	1,269.27	1,457.56	1,304.99
Oct	811.13	585.22	588.64	865.57	732.39	873.15	875.49	744.78	994.86	1,106.57	865.72
Nov	254.81	228.80	220.53	249.31	331.85	230.28	381.98	336.86	359.64	390.88	390.92
Dec	87.34	96.44	107.55	134.07	61.37	81.93	156.96	112.43	119.81	174.25	188.22
Total	8,679.42	7,940.13	7,279.48	9,630.65	9,738.51	9,695.49	10,858.54	10,215.14	10,045.72	11,444.56	11,498.34